Clinical and Imaging Assessment of Metal on Metal Hip Patients

A dissertation submitted to University College London in partial fulfillment of the requirements for the degree of

Doctor of Philosophy, PhD

Reshid Berber

Institute of Orthopaedics and Musculoskeletal Sciences:
Division of Surgery and Interventional Science

2019

Signed Declaration

I, Reshid Berber, confirm that the work presented in this thesis is my own. Where information has been derived from other sources, I confirm that this has been indicated in the thesis.

ABSTRACT

A high failure rate of metal-on-metal (MoM) hip implants prompted regulatory authorities to issue worldwide product recalls. The cause for their failure and decisions surrounding the need for revision is complex due to poor understanding of the toxic effects of metal debris. In addition to local soft tissue destruction, circulating cobalt can cause rare but fatal cardiotoxicity.

This thesis describes the detection of metal cobalt-chromium within the liver of a patient with highly elevated blood cobalt (587ppb) using novel MRI imaging techniques, validated by liver biopsy and micro x-ray fluorescence. The prevalence of tissue metal deposition and potential cardiotoxic effects were assessed through a prospective case controlled cohort study. Ninety patients were recruited into three age and gender-matched groups according to blood metal levels. All underwent detailed cardiovascular and liver phenotyping using MRI (for myocardial volumes and function, T2*, T1 and Extra-Cellular Volume mapping), echocardiography, and blood biomarker sampling. T2* is a novel MRI biomarker of tissue metal deposition.

Blood cobalt levels among the cohort ranged 0.1 to 118ppb, which is still seen in patients presenting for clinical follow-up. No significant between-group differences were found for cardiac volume or function, nor was there any difference in tissue characterization using T1, T2* and ECV. Higher blood cobalt levels did not translate to increased metal deposition within the heart or liver.

The application of these results were analsyed through a multi-disciplianary team setting designed to aid complex decisions of who, when and how to treat MoM

patients surgically. By analysis of MDT recommendations compared to the treatment undertaken it was demonstrated that an MDT approach is an acceptable evidence-based aid to decision-making.

This thesis concludes that cobalt tissue deposition can be detected using non-invasive MRI techniques, however metal deposition is not commonly seen with blood cobalt levels upto 118ppb with reassuringly little cardiotoxic effects. These results help reassure clinicians managing MoM patients through an MDT approach.

IMPACT STATEMENT

The content and conclusions from this thesis are likely to have wide reaching impact in both a clinical and academic standpoint.

Clinically, over 1 million patients worldwide continue to have a metal on metal hip in situ and remain under clinical review. These patients will have ongoing concern regarding metal debris disease. Reports continue to surface regarding suspected systemic toxicity, which includes neurological, endocrine and in some cases fatal cardiomyopathy. This is not just related to metal on metal hips but other more traditional joint bearing surfaces where metal can be released from trunionosis or following ceramic fracture and third body wear.

Clinicians themselves are advised to question patients with regards to potential metal toxicity and their symptoms that may indicate this process. However, clinicians do not currently have robust non-invasive techniques to assess for potential metal diseae.

This thesis offers reassurance to patients and clinicians that metal deposition has not been demonstrated within the heart or the liver, and additionally that cardiac function is not adversely affected. This applies to patients with metal levels upto 118ppb, which will include the vast majority of patients currently with metal hip implants. The reason for this is that those with early failure and extremely elevated metal levels tend to have been revised already.

From an academic point of view, this thesis has brought together orthopaedic surgeons, cardiology physicians and imaging scientists to apply established and

new techniques to a new concern. It has demonstrated that current MRI techniques can identify cobalt and chromium deposition within liver tissues. This has not been done before. It offers hope that a non-invasive technique is now possible for the detection of metal debris within systemic organs. Exposure to metals occurs in all walks of life, in particular medicines, surgical implants and industrial cases, which widen the scope of the results presented within this thesis.

On publication of the results from this thesis, we were featured in the headline news from the American Academy of Orthopaedic Surgeons, and also asked to comment for a feature within the Orthopaedic Today News journal, which has international readership.

Most importantly the results have also been discussed at the committee meetings held by the Medicines and Healthcare Products Regulatory Agency (MHRA) when preparing the latest guidance for orthopaedic surgeons and industry for the management of patients with metal hip implants.

ACKNOWLEDGEMENTS

First and foremost, I am greatly indebted to Professor Alister Hart for his mentorship, guidance and supervision throughout my research. I would also like to thank Professor Jia Hua for his guidance. Special thanks are extended to Professor John Skinner for his valuable advice and support during my research.

Furthermore I would like to acknowledge Professor James Moon, Dr Charlotte Manisty, Dr Amna Abdel-gadir and the rest of the Cardiology Team at the Heart Hosptial, without their support this project would not have been possible.

I would like to thank the Reaseach and Development team at the Royal National Orthopaedic Hospital for their sponsorship and support for this study, with particular thanks for Iva Hauptmannova, Ufedo Miachi, Avril Power, Nicky Saunders, Harry Hothi, Anna Di Laura and Luigi Palla.

I would also like to acknowledge the Gwen Fish Trust, the Royal National Orthopaedic Hospital Charity and the Heart Hospital Imaging Centre for their generous financial support.

Finally, I would like to thank my family and in particular I extend my deepest gratitude to my wife Derya, who has been steadfast in her support and guidance. None of this would have been possible without her unremitting patience.

To my Wife, Derya

CONTENTS

FIGURES

TABLES

ABBREVIATIONS

ALVAL	Aseptic Lymphocytic Vasculitis-Associated Lesion
ASR XL	Articular Surface Replacement XL
ATN	Acute Tubular Necrosis
AVN	Avascular Necrosis
BHR	Birmingham Hip resurfacing
BMI	Body Mass Index
BNP	B-type Natriuretic Peptide
CMR	Cardiac Magnetic Resonance
CoC	Ceramic on Ceramic
Cr	Chromium
Co	Cobalt
CT	Computed Tomography
DNA	Deoxyribonucleic Acid
DCM	Dilated Cardiomyopathy
Dmax	Feret Diameter
ECHO	Echocardiography
ECG	Electrocardiogram
ECM	Extracellular Matrix
ECV	Extracellular Volume
EDD	End Diastolic Diameter
EDV	End Diastolic Volume
ESD	End Systolic Diameter
ESV	End Systolic Volume
EXAFS	Extended Xray Absorption Fine Structure
FDA	Food and Drug Administration
Fe	Iron
GPLS	Global Peak Longitudinal Strain
HH	Hereditary Haemochromatosis
HIV	Human Immunodeficiency Virus
HLA	Horizontal Long Axis

HRA	Hip Resurfacing Arthroplasty
ICLH	Imperial College London Hospital
ICP-MS	Inductively Coupled Plasma Mass Sptectrometry
IR	Inversion Recovery
IVS	Interventricular Septum
LGE	Late Gadolinium Enhancement
LA	Left Atrium
LAV	Left Atrial Volume
LV	Left Ventricle
LVEDD	Left Ventricular End Diastolic Diameter
LVESD	Left Ventricular End Systolic Diameter
LVEF	Left Ventricular Ejection Fraction
MAPSE	Mitral annular plane systolic excursion
MARS	Metal Artefact Reduction Sequence
MDT	Multi-Disciplinary Team
MHRA	Medicines and Healthcare Products Regulatory Agency
MoC	Metal on Ceramic
MoM	Metal on Metal
MoP	Metal on Polyethylene
MOLLI	Modified Look and Locker Inversion recovery sequence
MRI	Magnetic Resonance Imaging
NJR	National Joint Registry
OA	Osteoarthritis
PPB	Parts per Billion
RA	Right Atrium
RF	Radiofrequency
RNOH	Royal National Orthopaedic Hospital
ROI	Region Of Interest
RV	Right Ventricle
ShMOLLI	Shortened Modified Look and Locker Inversion recovery sequence
SV	Stroke Volume
TAPSE	Tricuspid Annular Plane Systolic Excursion
TDI	Tissue Doppler Imaging

TE	Echo Time
THA	Total Hip Arthroplasty
TR	Repetition Time
T1	Longitudinal relaxation time
T2	Transverse relaxation time
VLA	Ventricular Long Axis
XAS	Xray Absorption Spectroscopy
XRF	Xray Fluorescence

PUBLICATIONS FROM THIS THESIS

Assessing for Cardiotoxicity from Metal-on-Metal Hip Implants with Advanced Multimodality Imaging Techniques

Journal of Bone and Joint Surgery (American), 2017 Nov 1;99 (21):1827-35

Berber R, Abdel-Gadir A, Rosmini S, Captur G, Nordin S, Culotta V, Palla L, Kellman P, Lloyd G, Skinner J, Moon JC, Manisty C, Hart A

Detection of metallic cobalt and chromium liver deposition following failed hip replacement using T2* and R2 magnetic resonance.

Journal Cardiovascular Magnetic Resonance, 2016 May 6;18(1):29

Berber R, Abdel-Gadir A*, Porter JB, Quinn PD, Suri D, Kellman P, Hart AJ, Moon JC, Manisty C, Skinner JA

Management of metal-on-metal hip implant patients: Who, when and how to revise?

World Orthopaedic Journal, 2016 May 18;7(5):272-9.

Berber R, Skinner J, Hart A

A New Approach to Managing Patients with Problematic Metal Hip implants: The use of an Internet enhanced Multidisciplinary Team Meeting.

Journal of Bone & Joint Surgery (American), 2015 Feb 18;97 (4):e20.

Berber R, Khoo M, Miles J, Carrington R, Skinner JA, Hart AJ

SCIENTIFIC MEETING PRESENTATIONS FROM THIS THESIS

American Academy of Orthopaedic Surgeons

'Assessing for Cardiotoxicity from MoM Hip Implants using Advanced Multi-modality Imaging: A Prospective Cross Sectional Study'

AAOS, San Diego, March 2017, Poster

'**A New Approach to Managing Patients with Problematic Metal Hip implants: The use of an Internet enhanced Multidisciplinary Team Meeting'**

AAOS**,** New Orleans USA, March 2014, Scientific Exhibit

Society for Cardiovascular Magnetic Resonance

'Non-invasive Assessment for Cardiotoxicity from Metal-on-Metal Hip Implants using CMR'

SCMR, Washington, February 2017, Podium

European Federation of National Associations of Orthopaedics and Traumatology

'The use of an Internet enhanced Multidisciplinary Team Meeting'

EFORT, London, June 2014, Podium

British Hip Society

'Cardiac Toxicity from Metal Hip Implants'

BHS, London, March 2017, Podium

'Management of patients using MDT teams: RNOH experience'

BHS, Exeter, March 2014, Podium

CHAPTER 1

CHAPTER 1 INTRODUCTION AND LITERATURE REVIEW

1.1 Background and Aims

Hip prostheses are implanted as a surgical treatment for osteoarthritis. Over one million patients worldwide have implanted metal-on-metal (MoM) hip prostheses, predominantly composed of cobalt chromium alloy [1]. Release of nano-particulate debris and metal ions from implants can cause harm [2]. Local soft tissue deposition adjacent to the joint [3-5] can result in high failure rates of MoM hip implants and has led to regulatory agency safety alerts against their use [6-8]. As a consequence, necessitated surveillance includes serial measurement of blood metal ion levels to guide revision surgery [9]. Figure 1.1a and 1.1b. These figures demonstrate high failure rates for both cemented and uncemented hip prosthesis.

Figure 1.1a: *Comparison of cumulative probability of revision (Kaplan-Meier estimates) for uncemented primary hip replacements with different bearing surfaces (Source: NJR)* [10]

Figure 1.1b: *Comparison of cumulative probability of revision for Cemented primary hip replacements with different bearing surfaces, blue line represents MoM bearings (Source: NJR)* [10]

The relationship between MoM hip implants and systemic toxicity is less clear. Elevated levels of circulating cobalt and chromium are linked with cardiac, thyroid and neuro-ocular pathology in case reports and case series, but causation and prevalence remain to be established [11-18]. In addition, widespread dissemination of metal debris has been demonstrated within the liver, spleen and abdominal lymph nodes, albeit without clinical morbidity [19].

For cardiotoxicity, diagnosis requires invasive myocardial biopsy or post-mortem, with no available non-invasive methods for measuring cardiac metal deposition. Heart failure is common in the patient population most likely to undergo hip replacement [20], so concern exists that an association between MoM hips and heart failure may be missed: one echocardiography study found a 7% reduction in left ventricular ejection fraction (LVEF) in MoM recipients [21] (although all values were within the normal range). More recently, epidemiological data compared 87 subjects with one type of MoM hip prosthesis

(ASR XL) to 2,028 subjects with metal-on-plastic (MoP) prostheses, and found the age-adjusted rate of hospitalization for heart failure to be almost double, translating into one excess heart failure hospitalization for every 10 patients [22].

Cardiac MRI (magnetic resonance imaging) is the gold standard technique for measuring cardiac volumes and function. In addition, the MRI T2* method for assessing cardiac iron in patients suffering haemochromatosis is histologically validated, and has become a routine measure, having transformed the management of these patients at risk of iron cardiomyopathy [23,24]. As cobalt and chromium exhibit similar magnetic properties to iron, the T2* method has the potential to play a role in the non-invasive detection of metal ion deposition in failing MoM hip implants.

Study Aims

The aim of this thesis has been designed to seek evidence of tissue metal ion deposition in a population of patients with metal hip implants using non-invasive imaging techniques, with particular focus on hepatic and cardiac tissues. In addition, our aim is to assess the relationship between elevated blood metal ion levels and cardiac function. Lastly, given the multi-disciplinary management of patients with MoM hip implants and the multi-disciplinary nature of this thesis, the use of MDT meetings that utilize evidence based medicine in clinical decision making will be analysed.

1.2 Hip Arthroplasty

Hip arthroplasty, particularly as a treatment for hip osteoarthritis, is one of the most successful procedures in terms of patient satisfaction and cost-effectiveness, and was called the "operation of the century" by the Lancet [25 26]. In 2014, a total of 83,125 hip arthroplasties were registered with the National Joint Registry (UK NJR) for England, Wales and Northern Ireland, compared to 67,804 hips in 2009, a rise of 22% over 5 years [10].

1.2.1 Indications for Hip Arthroplasty

Various disease processes can affect the hip joint such that the hip no longer functions effectively to allow a person to fulfil their activities of daily living, or the individual experiences sufficient enough pain that their quality of life is poor and seeks treatment. Depending on the aetiology, patients may be able to seek conservative non-surgical treatments, however often the end result is hip arthroplasty. The UK NJR summarises the common indications for hip arthroplasty. These include osteoarthritis, fractured neck of femur, avascular necrosis, hip dysplasia and inflammatory arthropathy [10].

Osteoarthritis

Osteoarthritis (OA) is a common condition that affects patients of all ages, particularly older adults. OA can be a debilitating illness affecting all joints of the body. The principle symptom of OA is pain, with associated stiffness and in

advanced cases deformity, all of which may affect a person's gait. Symptoms may vary depending on activity levels, body habitus or even climate.

OA has many risk factors, including age, gender, family history, obesity, metabolic factors, occupation, injury and joint morphology [27]. It can be considered to be a disorder of cartilage homeostasis, where chondrocyte led repair mechanisms fail and lead to degradation through inflammation and cartilage degeneration. This process is progressive and cannot be reversed. It leads to subchondral bone remodeling, which includes sclerosis and osteophyte formation. Figure 1.2a.

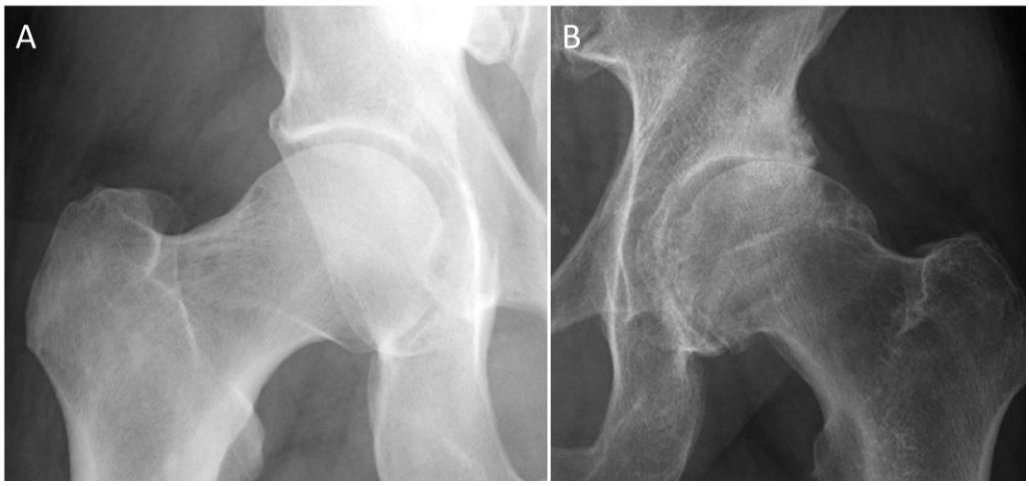

Figure 1.2a: *Radiographs to demonstrate a healthy normal hip (A) compared to a hip with radiographic evidence of osteoarthritis (B - Loss of joint space, subchondral sclerosis, marginal osteophytes and subchondral cysts)*

Estimates of prevalence in the hip joint vary depending on which diagnostic criteria are used [28]. Radiographic prevalence is as high as 43% in over 75 year-olds, and symptomatic OA is seen in up to 17% of patients [29]. Radiographic

severity does not always correlate with patient's symptoms, where severe end stage arthritis on radiographs can be seen in an asymptomatic patient. Whilst in most people, symptoms are well managed; end stage OA requiring hip replacement is increasingly common.

Fracture

Fractures that require a hip replacement tend to involve the head or the neck of the femur. In the adult hip, the main blood supply to the femoral head arises from branches of the medial and lateral femoral circumflex arteries that form an extra-capsular arterial ring at the base of the femoral neck. Superior and inferior gluteal arteries and the artery of the ligamentum teres contribute a small proportion blood supply also. Branches from the extra-capsular arterial ring give rise to ascending retinacular vessels that run along the femoral neck and form the subsynovial intra-articular ring – the main blood supply to the femoral head. Figure 1.2b.

Figure 1.2b: *Image to demonstrate the blood supply to the femoral head. 1) Profunda Femoris artery, 2) Lateral Femoral Circumflex artery, 3) Vessels within the Ligamentum Teres, 4) Medial Femoral Circumflex artery. Vessels 2 and 4 give rise to an extra-capsular arterial ring at the base of the femoral neck that forms the main blood supply to the femoral head (source AOsurgery)*

Fractures through the neck of the femur disrupt these vessels and therefore increase the risk of non-union or avascular necrosis; as a result fractures through the neck of the femur are commonly managed with hip arthroplasty. Hip arthroplasty for fracture can be either a hemi-arthroplasty (femur replacement alone) or a total hip replacement (both femur and acetabular replacement).

The National Institute for Health and Clinical Excellence produced guidance in 2011 that recommended the use of total hip replacements in patients with a displaced intra-capsular fracture who:

- were able to walk independently out of doors with no more than a stick and
- are not cognitively impaired and
- are medically fit for anaesthesia and the procedure.

Approximately 75,000 hip fractures occur annually in the UK. The average age of patients requiring treatment for a hip fracture is 83 years of age with a strong preponderance for females [30].

Avascular Necrosis

Avascular necrosis (AVN) of the femoral head results from a disruption of the blood supply. Inciting causes of AVN include trauma as above, systemic steroid use, underlying blood coagulopathy (Factor V Leiden disease), alcohol abuse, diabetes mellitus, sickle cell anaemia and Gaucher's disease [31] [32]. In general, patients with confirmed AVN have a 70-80% chance of femoral head collapse after 3 years [32]. Femoral head collapse results in an incongruent hip joint causing

pain and advanced degenerative changes requiring total hip arthroplasty. AVN accounts for approximately 10% of total hip arthroplasties performed [10].

Hip Dysplasia

Hip dysplasia is a disorder of abnormal development of the hip secondary to capsular laxity or mechanical factors in early childhood. Untreated hip dysplasia can progress to early hip degenerative changes and arthritis. Hip dysplasia accounts for 2% of all patients (all ages) undergoing total hip replacement, however it accounts for 26% of cases having a total hip replacement less than 30 years of age [10].

Inflammatory Arthropathy

Inflammatory arthropathy arises due to a chronic systemic auto-immune disorder with a genetic pre-disposition, this includes rheumatoid arthritis. It accounts for approximately 1% of all cases of total hip arthroplasty on the UK NJR [10]. The pathophysiology underlying the condition results in a destructive cell-mediated immune response against soft tissues and cartilage. It most commonly affects the small joints of the hands and feet in a symmetrical pattern, but can affect the hip and knee joints.

1.2.2 History of hip arthroplasty

"Arthroplasty is an operative procedure undertaken for the purpose of creating a joint. Such a joint, if it is going to stand up under the wear and tear of function, must be mechanically as nearly perfect as possible" (Quote: M. N. Smith-

Petersen) [33]. The hip joint is a fulcrum exposed to the power of the strongest muscles in the body and to the repetitive trauma of weight bearing. A joint exposed to such stresses with every step must be mechanically perfect, almost without friction, if it is going to have lasting function [33].

The earliest recorded attempts at prosthetic hip replacement occurred in Germany in 1891, with the use of ivory to replace femoral heads of patients whose hip joints had been destroyed by tuberculosis. This was on a background of crude attempts at improving symptoms from degenerate joints when surgeons experimented with inter-positional arthroplasty, which involved placing various tissues (fascia lata, skin, pig bladder submucosa) between articulating hip surfaces during the late 1800's [26]. These procedures continued into the 1920's, however they were largely unsuccessful and alternative methods were sought.

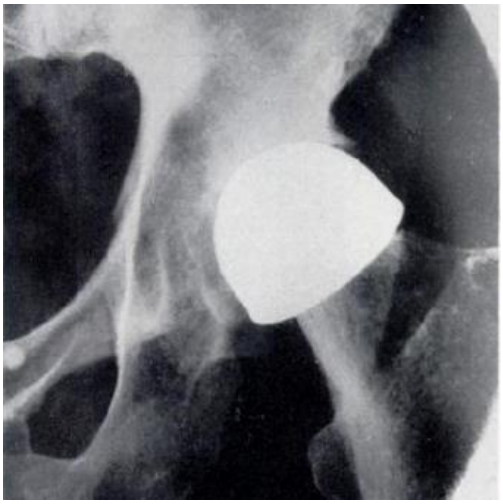

Figure 1.3: *The Mould Arthroplasty, 1925* [33]

Subsequently in 1925, the American surgeon Marius Smith-Petersen developed the *Mould Arthroplasty*. This hollow hemisphere cup design was manufactured from glass, and designed to sit between the femoral head and acetabulum as an inter-positional implant. The glass surface was intended to provide a smooth

surface for painless articulation [33]. This was, in essence, the first successful widely used hip implant and the most impressive illustration of this was a published report of a well functioning mould in situ for over 45 years [34]. However, despite the biocompatibility of glass, it failed to withstand the forces applied through it and would frequently shatter. With time this evolved through viscaloid, pyrex and lastly, vitallium in 1938 [33]. However, problems remained, instability of the cup or resorption of the femoral neck were reported [35].

Surgeons continued to search for an improved method for treating the osteoarthritic hip and the emphasis changed from re-fashioning the joint to replacing it. The Judet brothers, of Paris, ushered in the 'resection-reconstruction' in the 1940's. They removed the femoral head and replaced it with a new head constructed from acrylic resin. Jean and Robert Judet likened the design to a 'mushroom with a rounded head and long stem' [36]. Figure 1.4.

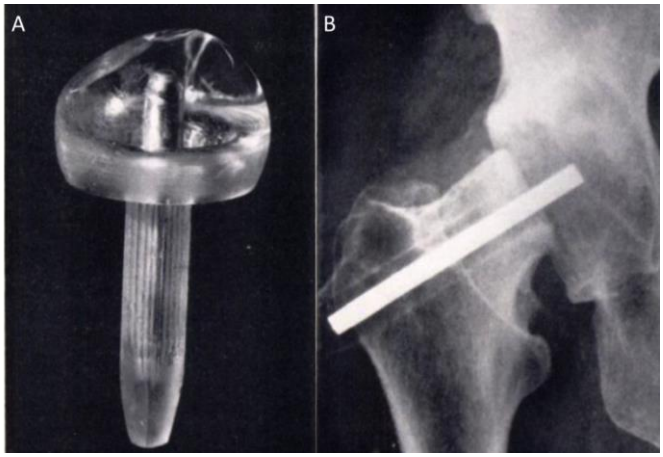

Figure 1.4: *(A) The Judet hip implant with signs of wear, (B) Radiograph demonstrating an implanted Judet hip with a central steel core for prevention of stem fractures, 1940s*

The Judet hip had a polished articulating surface and a stem designed to penetrate the lateral cortex of the femur, thus imparting stability. Stem fractures necessitated the introduction of a reinforcing central steel core. Excellent early

results led to a rapid and widespread increase in its use, however because of increasing numbers of subsequent failures their use was eventually abandoned [37]. Devas reviewed 110 cases of Mould or Judet replacement arthroplasties, and found positive outcomes in only half of those reviewed, noting favourable outcomes of the Mould replacement over and above the Judet replacement [38]. A larger survey conducted by Margaret Shepherd on behalf of the British Orthopaedic Association, reported poor outcomes at 5 years in 30% of patients with the Mould Arthroplasty [39].

Philip Wiles performed the first true total hip arthroplasty in 1938, in which he used a bolt to attach a stainless steel ball to the femur and pins to attach a stainless steel acetabular liner into the acetabulum. Heterotopic ossification, joint stiffness and bone resorption troubled early cases and Philip Wiles himself doubted the longevity of the device [35]. Figure 1.5.

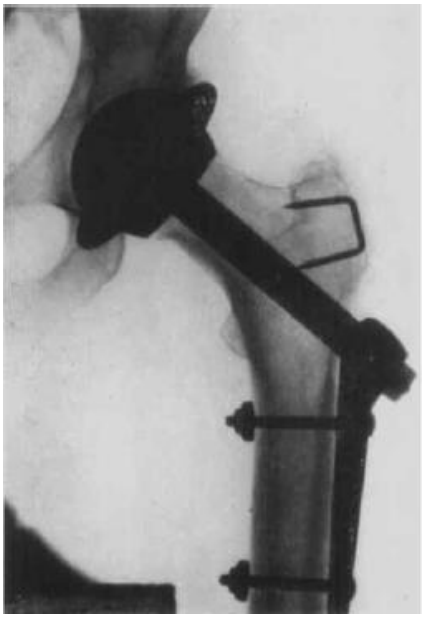

Figure 1.5: *Radiograph demonstrating the ball and cup replacement as designed by Philip Wiles in 1938* [35]

1.2.3 Introduction to Metal on Metal hip arthroplasty

The first use of a metal-on-metal prosthesis on a regular basis was an evolution of the Wiles design, introduced in 1951 by G.K. McKee and J. Watson-Farrar. They initially used a stainless steel acetabular cup with a long femoral stem, however poor corrosion resistance of the cup component led to a change in the design to use a cobalt-chromium alloy, which proved to be a lot more successful at reducing the failure rate [40].

The introduction of polymethylmethacrylate bone cement as a fixation method in total hip arthroplasty was found to significantly reduce rates of loosening of hip replacements [41] [42]. McKee and Watson-Farrar subsequently incorporated bone cement into their designs [40], Figure 1.6.

Figure 1.6: *The McKee Watson-Farrar Hip implant, 1951. A stainless steel femoral stem is coupled with a cobalt chrome acetabular cup implant. Bone cement was used to achieve fixation [40]*

Despite these successes the introduction of the Charnley low friction arthroplasty in 1962 largely abolished the idea of metal on metal hip and

resurfacing (Mould) designs. John Charnley himself had experimented with his own versions of resurfacing arthroplasty before settling on his final total hip prosthesis that was seen as the way forward up until 1975 [43].

Based on the idea of the Mould arthroplasty, coined by Smith-Petersen, the first attempt at total hip resurfacing was undertaken by John Charnley in the early 1950s. Charnley investigated the coefficient of friction between various bearing surfaces of the femoral head and the acetabulum using articular cartilage as the benchmark. He found that polytetrafluorethylene (Teflon) had a coefficient nearing that of articular cartilage. His idea behind the use of a low-friction substance to replicate that of cartilage was not solely driven by the need to reduce wear, but that reduced friction at the bearing surface would decrease the forces transferred between the implant and the living bone thus improving the mechanical bond and stability of the implant [44]. Based on this premise, Charnley lined the acetabulum with a thin shell of Teflon, while the femur was similarly covered with a hollow sphere made of the same material, to create a slippery bearing surface. Despite encouraging early results, high wear rates and early failures were frequent and the idea abandoned. Figure 1.7.

Figure 1.7: *Charnley Total Hip Resurfacing, manufactured from Teflon, 1950s*

Various resurfacing designs were trialled throughout the 1960's and 70's, including Müller in 1968, Gerard in 1970, Furuya in 1970 and Trentani in 1971 [45]. In 1972, Freeman introduced the first version of the cemented ICLH resurfacing prosthesis. This consisted of a high-density polyethylene femoral component and a metallic acetabular component. By 1978, 40% of the first 36 hips implanted had failed [46]. High wear rates and frequent implant loosening were reported as the reasons for failure. These failures necessitated change in the design, which were employed in 1975 and consisted of a reverse of the bearing surface to a metallic femoral component and a high-density polyethylene acetabular component [45]. However both of these were fraught with problems of massive polyethylene wear and associated inflammation with soft tissue collections [47].

Further metal on polyethylene designs followed, however none were able to mitigate high levels of polyethylene wear and the associated osteolysis that ensued from polyethylene wear debris. The subsequent high rates of cup

loosening and early clinical failures of the implant meant an alternative to high-density polyethylene was desired.

In 1986 metal-on-metal hips enjoyed a renaissance following the publication of the long-term follow up results of the then obsolete McKee Watson-Farrar total hip replacement [48]. 84% of hips were found to be functioning after 15 years of implantation of which 90% were satisfied with their replacement.

This paper showed that metal-on-metal was a feasible bearing over the long term, but the need for bone conservation and reduction in the volume of metal being implanted into an individual was considered important. Despite the problems of resurfacing designs previously reported, this data paved the way for the modern hip resurfacing implant.

1.2.4 Modern Hip Resurfacing Arthroplasty

The current generation of MoM hip resurfacing arthroplasty results from the longevity of the McKee Watson-Farrar prosthesis with the additional advantage of femoral bone conservation that is advantageous in future revision surgery [49]. Other advantages include improved wear properties of MoM over MoP bearings [50] [51], absence of polyethylene wear debris, enhanced stability [52] and improved range of motion compared to a total hip arthroplasty [53] [54].

The Birmingham Hip Resurfacing (BHR; originally Midlands Medical Technology, now Smith and Nephew, Memphis, Tennesee) was the first of the current generation of hip resurfacings to be developed and was introduced in 1997. This was a hybrid design (cemented femoral head with an uncemented

hydroxyapatite coated acetabular component) constructed of Cobalt-Chromium-Molybdenum alloy. Early results using the BHR were excellent with reported 99.8% cumulative survival at 4 years [55], and subsequently 95.5% at ten years with aseptic revision as the endpoint [56]. Figure 1.8.

Figure 1.8: *Birmingham Hip resurfacing implant*

Several implant manufacturers followed suit with their own hip resurfacing designs, with many variations appearing on the market. See figure 1.9. Due to the perceived advantages of improved hip stability when using a large femoral head, manufacturers also designed modular large head metal-on-metal bearings to couple with femoral stems (MoM Large Head Total Hip Arthroplasty). Manufacturers portfolios rapidly expanded and unsurprisingly the use of Metal-on-Metal hip implants flourished in the 1990s and subsequently accounted for approximately a third of all hip replacements being implanted in the United States in 2008 [1].

Figure 1.9: *National Joint Registry data demonstrating the top five resurfacing head brands used between 2003-2011, the market leader has been the BHR*

However, despite the reported excellent early results, problems surfaced in the literature. Complications included unexplained pain, femoral neck fracture, osteonecrosis of the femoral head, femoral neck thinning, soft tissue reactions and elevated blood cobalt and chromium levels [2 3 57-59].

Hip resurfacing is a technically demanding procedure and notching of the femoral neck when preparing the proximal femur must be avoided due to the associated risk of neck fracture [60]. In addition, the external acetabular diameter in a BHR is a minimum of 6 mm greater than the external diameter of the prosthetic femoral head in order to provide a sufficiently rigid construct. The increased size of the femoral component necessitates over-reaming of the acetabulum, meaning the hip resurfacing may not be as bone preserving as initially described [61].

The information on failures of Metal on Metal implants was revealed through Joint registry data in Australia (figure 1.10) and the UK (figure 1.1 and 1.11), where certain implants were identified as performing significantly less well than others used to replace painful arthritic hip joints.

Figure 1.10: *Australian National Joint Registry data demonstrating markedly raised revision rates for MoM bearings (yellow) compared to conventional bearings*

The British Orthopaedic Association brought this to the attention of the MHRA between 2008 and 2010 and helped provide senior and expert clinical input into the Expert Advisory Group on Metal on Metal Implants. The Expert Advisory Group triggered the first MHRA alert in 2010 [6]. An additional advisory statement followed from the Food and Drug Administration (FDA) recommending post market surveillance of patients with MoM implants [9]. See figure 1.1 and 1.11.

Figure 1.11: *Green line depicts the rise and subsequent decline in use of Metal on Metal Bearings, source NJR Annual report 2011*

Several MoM hip implant designs have since been withdrawn from the market and are no longer considered safe for use. Certain hip implants fared much worse

than others, as illustrated by the published poor results of the Articular Surface Replacement [62] (ASR; DePuy Synthes, Warsaw, IN), which suffered a worldwide recall from the market amongst others [7]. See Table 1.1. Metal debris from MoM hip implants is thought to be the driving force behind the complications seen and for the early failure of MoM hip implants.

Risk	Hip Resurfacing Arthroplasty	Total Hip Arthroplasty
Low	Birmingham Hip Resurfacing[a]	Small head THA
	ReCap[b]	(< 36mm head diameter)
Medium	Cormet[c]	Birmingham Mid-Head
	Magnum[b]	Resection[a]
	Conserve Plus[d]	
High	Adept[e]	All large head THA
	Durom[f]	(≥ 36mm head diameter)
	Mitch[g]	ASR XL[h]
	ASR[h]	

Table 1.1: *Implant specific risk stratification, based on current registry data and regulatory/manufacturer recall data. [(a) Smith and Nephew, London, UK (b) Biomet, Indiana, USA, (c) Corin, Cirencester, UK (d) Wright Medical, Tennessee, USA, (e) MatOrtho, Leatherhead, UK, (f) Zimmer, Indiana, USA, (g) Stryker Michigan USA, (h) DePuy Synthes, Indiana, USA]*

1.3 Metal Debris: A cause for concern?

Metal implants are manufactured using a variety of metal alloys, the majority of which contain cobalt and chromium. Hip arthroplasties are subject to significant mechanical loading that requires both mechanical and material stability, but also biocompatibility and long term wear resistance. Cobalt chromium alloys were found to have excellent biomechanical features including high material toughness, resistance to deformation and breakage, ductility, hardness, wear and corrosion resistance and compatibility with other materials [63]. Conversely,

stainless steel is also used, particularly in femoral head or stem components, but contains very little cobalt in comparison.

Metal particulate and ionic wear debris from the hip is released into the peri-prosthetic tissues and haematologically transported throughout the body [5] [64]. Blood cobalt and chromium ion levels in patients with unexplained painful MoM hips are double those of well functioning MoM hips [2]. Metal implants are considered biologically inert, however wear debris is not and is thought to evoke an immune response [65].

Cobalt

Cobalt is a trace metal element that is essential for normal cellular metabolism. Diet is the main source of cobalt in the general population, conversely in industry, exposure can occur during hard metal production and diamond polishing.

Cobalt exists as either the bi-valent or tri-valent form in vivo, which can complex with other extra or intra-cellular molecules, forming cobalt oxides, organophosphates and chlorides [66]. Cobalt is essential in the formation of vitamin B12, however excessive intake has been shown to lead to hypothyroidism and goitre formation [67]. On a cellular level, excessive exposure can lead to cellular apoptosis [68] [69], necrosis [66] [70] [71], and oxidative DNA damage [71] [72]. "Beer Drinkers" cardiomyopathy surfaced in 1966, in Quebec City, Canada, as a result of cobalt salts used to stabilize beer foam for aesthetic purposes [73]. Pericardial effusion, elevated haemoglobin levels and congestive heart failure

characterized this syndrome. It has also been associated with contact dermatitis, and occupational asthma [74].

Chromium

Chromium exists either as a trivalent or hexavalant variant. The latter of these is not used in the manufacture of metal hip implants, however the corrosion and subsequent dissolution of the ions has been shown to release hexavalant chromium ions [64].

The concern is that the hexavalant form is more biologically active and can have implications for local and systemic effects, however it is thought that it is rapidly oxidized to its trivalent form within cells. It has been shown that hexavalant chromium can accumulate in red blood cells [64], whereas the trivalent form is essential in glucose metabolism and has no reported toxicity at high oral doses in nutritional studies [75] [76].

Environmentally, hexavalant chromium is of main concern in inhalational exposure where it is associated with respiratory tract carcinogenesis [76]. Hexavalant chromium is also a skin and mucous membrane irritant, and some are corrosive agents. In addition, they have been shown to produce an allergic contact dermatitis characterized by eczema [76].

1.3.1 Mechanisms of Metal Ion Release

Scales et al published the first report of raised levels of cobalt and chromium in the blood and urine of patients with MoM hip implants versus MoP implants in 1973 [77]. Since the start of the modern MoM era, several authors have also

reported metal ion release, describing elevated blood and urine levels of cobalt and chromium in patients with MoM hips [2 4 57 59 78-84].

Studies have demonstrated a peak in blood cobalt levels at 6-months post implantation and chromium levels at 9-months, followed by a steady decline over time [85 86]. Following revision of a MoM implant to an alternative bearing, blood ion levels reduce but do not normalise in the post-operative period [87 88]. Figure 1.12.

Figure 1.12: *Temporal changes in blood cobalt following implantation of a MoM hip implant, demonstrating a rise to peak between upto 6 months after implantation followed by a plateau [89]*

The release of material from metallic implants occurs by corrosion, wear and mechanical factors such as fretting and third body wear. Ultimately corrosion is the leading cause of ion release. It occurs due to oxidation-reduction reactions with the surrounding environment. Ion release occurs from the metal surface undergoing corrosion. Mechanical wear and the release of metal particulate debris occur through contact between articulating surfaces. See figure 1.13. This can be at the bearing surface, non-bearing surface or through third body wear (un-intended contaminant abrasive debris). Corrosion and wear can occur concurrently, giving rise to 'tribocorrosion' [90]. This arises in cases of fretting at

non-articulating junctions such as at modular metal-on-metal junctions in total hip arthroplasty (taper junction of head and neck), but also in degradation of MoM bearing surfaces.

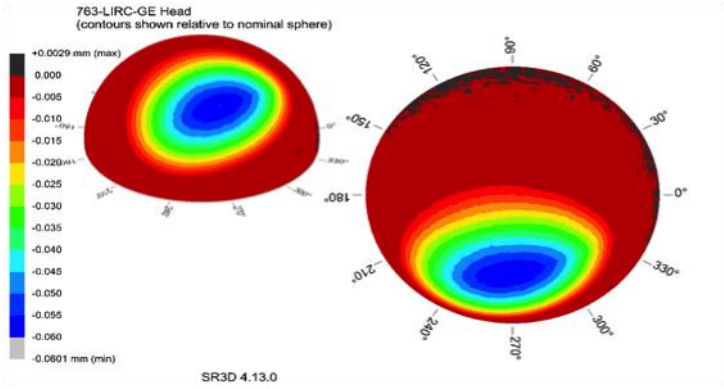

Figure 1.13: *Head wear profile of an explanted hip resurfacing. Areas of blue demonstrate increased wear compared to surrounding surface, likely to represent the contact zone between the head and cup (image courtesy of LIRC)*

Component design and positioning has been shown to be associated with increased wear and as a result raised metal ion levels [57 83 91-94]. A cup inclination angle of more than 55^{o} is associated with higher serum cobalt and chromium levels when compared to controls [2 57]. The optimal cup position being reported as 40^{o} inclination and 25^{o} anteversion [94]. This is partly due to the risk of edge loading, particularly in cups designed with less head coverage [95]. Secondly, implants with a small head size (<44mm), particularly common in female patients, were 5 times more likely to require revision compared to patients with large heads (>55mm) [96].

Micromotion at unintended bearing surfaces can also occur, particularly at the taper junction, such that the motion can initiate a loss of the protective surface oxide layers with subsequent corrosion and metal ion release [97-99]. This is a particular problem in MoM total hip arthroplasties where a large diameter

femoral head is used. The torque force created at the taper is such that micromotion arises and drives this form of wear [100-102]. Figure 1.14.

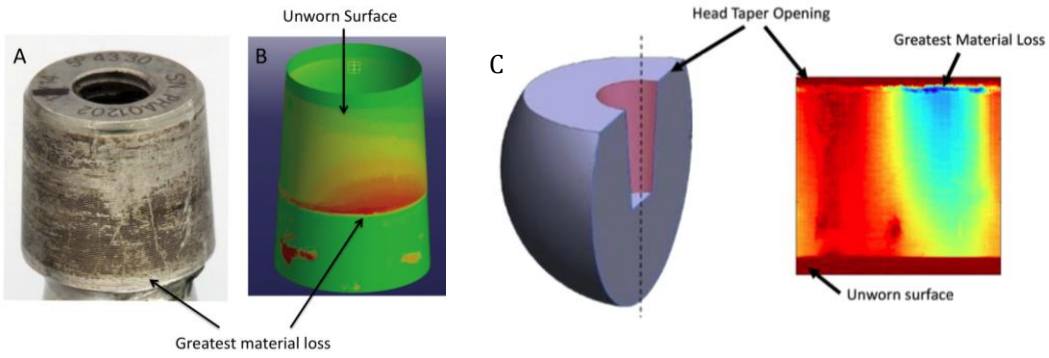

Figure 1.14: *(A) Stem trunnion from a retrieved MoM hip replacement; (B) Associated wear map of the trunnion – area in Red suggests increased wear which corresponds to the black deposits seen on the image in A – representing corrosion deposits; (C) Reciprocal image of the female taper of the head component where blue demonstrates increased material loss (images courtesy of Hothi et al, LIRC)*

The underlying reasons for elevated blood metal levels are believed to be multi-factorial from a combination of component size and orientation, activity levels and implant design.

1.3.2 Metal Ion Distribution

Metal wear particles from whichever mechanism of release are smaller than the debris generated from other THA bearing surfaces, such as polyethylene (measured in nanometers not micrometers) [103]. Being similar in size to typical cellular components and proteins, such metallic nanoparticles can become intra-cellular without difficulty and therefore have an impact on cell function, such as DNA metabolism and gene transcription [104 105].

Recent work by Newton et al, demonstrated that cobalt is distributed equally between blood cells and plasma, whereas chromium is mainly in the plasma,

suggesting differences in the physiological handling of each. They also demonstrated that chromium is in the less toxic trivalent form [106]. They established that renal excretion of cobalt is much greater than chromium, and in particular urinary concentrations were greater than that in blood [106]. Post mortem studies have identified metal wear product accumulation in regional lymph-nodes, the liver and the spleen [5] [19]. Afolaranmi et al demonstrated the systemic distribution of metal wear debris. Wear debris was colleted from a hip simulator and injected into subdermal air pouches in mice. The team sacrificed the mice at different temporal stages after injection, removed the organs and determined the metal content within. They demonstrated high levels in the liver, kidney, spleen, lung, heart, brain, and testes [107].

1.3.3 Pathophysiology of Cobalt Toxicity

Early studies examining the in vitro effects of the metals used in orthopaedic implants demonstrated that cobalt and vanadium were toxic, while chromium, nickel, titanium and molybdenum was not. Morphological changes were seen after exposure to cobalt and nickel, however the solubility of nickel meant that toxic levels were not reached. The authors concluded that the only combination of materials likely to give rise to toxic levels of metal under clinical conditions is cobalt-chromium alloy articulating with cobalt-chromium [108]. It has been demonstrated that cobalt could induce gross tissue necrosis and macrophage toxicity through DNA fragmentation and cell apoptosis [108] [109].

This cytotoxic effect can concern the function of macrophages, fibroblasts and osteoblasts through free radical formation and aneuploidy [110-113]. The extent of

toxicity is dependent on dose, size and shape of the metal released from the articular surface by wear or by ionic dissolution [108] [114]. The smaller the particulate debris, the greater infiltration achievable, and as such particles that infiltrate mitochondria and macrophages may undergo intra-cellular corrosion, producing soluble cobalt ions that activate both intrinsic and extrinsic apoptotic pathways. Generation of reactive oxygen species in the presence of cobalt chloride has been described [115]. Interestingly, higher doses also see the initiation of inflammatory cascades where exposure to cobalt triggers transcriptional changes that mimic the hypoxic response [115].

Such cytotoxic effects have been reported both locally and systemically, through adverse soft tissue reactions to cardiac, thyroid and neuro-ocular pathology, respectively, as described in case reports and series, but causation and prevalence remain to be established[11-18] [116].

1.3.4 Local Effects of Metal Debris

Wear debris can accumulate locally as seen by studies of joint fluid surrounding MoM hip implants [117-119]. The level of chromium is greater in joint fluid compared to cobalt, whereas the converse is true for blood analysis [119]. However, it is believed that cobalt is the species with greatest reactivity causing local tissue inflammatory reactions due to its ready solubility [120-122].

The role of Diagnostic Imaging

The MHRA advise Metal Artefact Reduction Sequence MRI (MARS MRI) or Ultrasound scan as part of the investigation algorithm [6]. MARS MRI has been

optimised for viewing the soft tissues surrounding metal hip implants by reducing the signal to noise ratio seen if higher receiver bandwidths and matrix sizes are used [123]. MARS MRI has been shown to have excellent sensitivity and specificity for detection of both superficial and deep lesions [124-126], and also muscle atrophy. Ultrasound is a satisfactory modality for identifying tendon abnormalities [125]. Current MARS MRI techniques do suffer from metal artefact that limits the diagnosis of osteolysis, however, improved techniques are being developed [127]. CT scanning is ideal for visualising osteolysis if it is suspected on plain radiographs [128].

Pseudotumours

Abnormal peri-prosthetic masses termed pseudotumours have been reported in the presence of MoM hip resurfacings, first by Pandit et al, and subsequently by various groups with incidences varying from 0.1% to 61% [3 129-132]. It is important to note that similar soft tissue masses were first reported by Freeman et al, who observed such reactions to polyethylene debris arising from the early ICLH implants [45]. Pseudotumours can be locally destructive and warrant revision surgery, particularly if symptomatic or consisting of solid tissue [2 58]. Figure 1.15.

Recent evidence regarding the natural history of soft tissues abnormalities is conflicting. Studies report varying degrees of progression in size and grade of pseudotumours, however limitations in sample size, implant type and imaging modality do not readily allow the generalisability of the results [133-135]. It appears that when disease progression does occur, it is slow and therefore serial imaging annually is sufficient to identify change. The potential to cause local pressure

effects causing necrosis and compression of nearby structures such as the iliac vessels, femoral vessels and the sciatic nerve is also a concern.

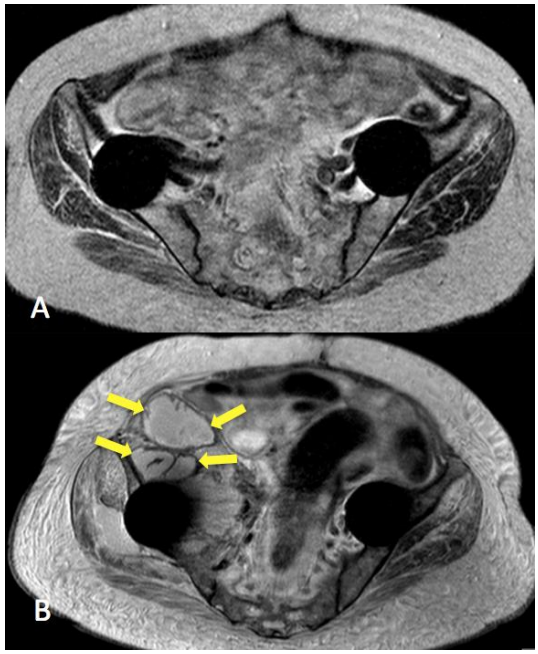

Figure 1.15: *Example of new pseudotumour (not seen in image A, but marked by yellow arrows in image B) formation in a patient with bilateral Birmingham hip resurfacings. T2 weighted axial MRI images. Date of implantation - January 2007, Time post-op to first MRI (A) was 69 months, and time post-op to second MRI (B) was 84 months.*

The precise aetiology is not known, however the term aseptic lymphocytic vasculitis-associated lesion (ALVAL) is used to describe the histological features associated with metal hip reactions [136]. The typical appearance of pseudotumour material is that of necrotic dense fibrous tissue containing metal wear particles. These areas are surrounded by connective tissue with pseudotuberculoid macrophages, a giant cell granulomatous reaction and diffuse inflammatory infiltrate [3]. Figure 1.16. Due to the various descriptions that exist for the soft tissue abnormalities described, the term Adverse Reaction to Metal Debris (ARMD) is preferred.

Figure 1.16: *(A) In situ pseudotumour identified during revision surgery for a MoM hip implant and (B) Histological analysis of the excised pseudotumour tissue: Atypical lymphocytic vasculitis-associated lesion (ALVAL) with typical appearance of a perivascular infiltrate of lymphocytes and accumulation of macrophages containing metal particles* [137]

It has been suggested that a delayed type IV hypersensitivity reaction to cobalt and chromium ions is the potential cause, however Kwon et al refuted this argument [138]. Pseudotumours were, however, shown to correlate with elevated blood and hip aspirate metal ion levels suggesting a relation to excessive implant wear [130 138]. Despite this, their presence in non-MoM articulations leaves the true aetiology to remain unknown [45 139].

Bone

In 2007, Hing et al reported femoral neck narrowing after hip resurfacing, who observed this phenomenon in 77% of the patients reviewed. In 27.6% the narrowing exceeded 10% of the diameter of the neck [140]. The reasons behind this observation are unknown, however it may be related to stress shielding, remodeling, avascularity, or a response to wear debris.

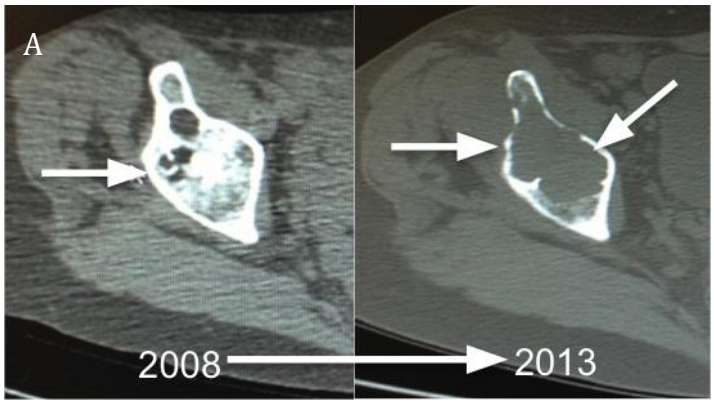

Figure 1.17: (A) Left image *Axial CT scans demonstrating the progression of osteolysis within the ilium of a patient with a MoM hip implant,* ***(B) Right image*** *Radiograph demonstrating thinning of the femoral neck beneath a hip resurfacing (image from Chen et al [141])*

Combined with the immune response demonstrated by Wooley et al [65], findings of in vitro studies demonstrated the inhibition of osteoblastic activity by cobalt and chromium ions [113], induction of osteocytic apoptosis [142], and stimulation of osteoclast cell activity [143]. It is therefore believed that raised ion levels potentially lead to bone resorption and aseptic implant loosening. Figure 1.17.

Muscle

Muscle atrophy is now becoming an increasing concern, and is driving the debate regarding the timing of revision surgery in order to prevent irreversible damage. The outcome after revision surgery of a MoM hip is worse than after a non-MoM hip because of the potential soft tissue destruction [144]. It may be possible to improve the outcome through early investigation and management of patients at risk of soft tissue destruction. Several studies have reported the frequency of muscle atrophy as ranging from 22% to 90% [145-147]. Figure 1.18.

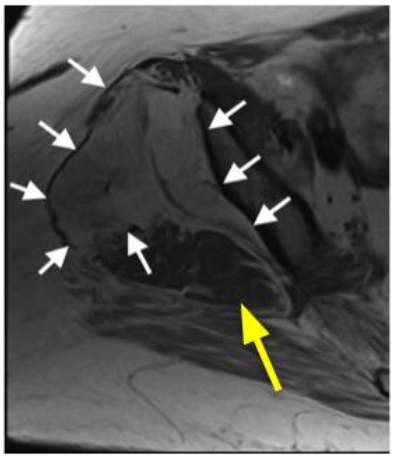

Figure 1.18: *Axial T1 weighted MRI scan demonstrating advanced muscle atrophy (white arrows) of the glutei muscles in a patient with a MoM hip implant (Yellow arrow highlights normal muscle for comparison)*

A recent publication demonstrated progressive muscle atrophy using serial MARS MRI scanning in a mixed cohort of patients with MoM hip implants in situ [148]. Little is known about the underlying aetiology of muscle atrophy and whether it can be attributed to exposure to metal debris, especially in the knowledge that muscle atrophy can be associated with joint pathology such as osteoarthritis [149].

1.3.5 Systemic Effects of Metal Debris

A variety of systemic effects have been reported in the literature. These include cases reported within healthcare, industry or occupational exposure to cobalt and chromium. Figure 1.19.

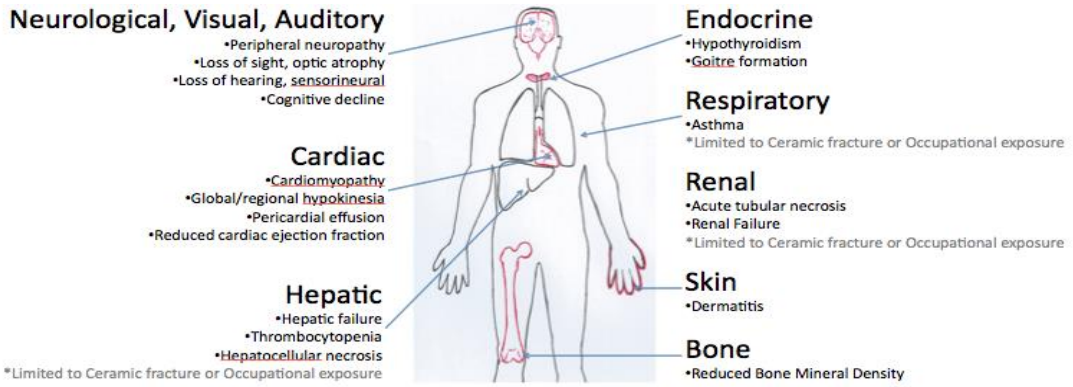

Figure 1.19: *Illustration of reported systemic effects attributed to cobalt toxicity*

Table 1.2 summarizes all published clinical cases of cobalt systemic toxicity in relation to metal hip arthroplasties.

Case	Age	Implant	Symptoms	Diagnosis	Objective Assessment	Co	Cr	Post-revision Symptoms	Co	Cr
1[150]	61	MoM	Numbness below the neck	Central demyelinating neuropathy	Nerve conduction studies	254.3	91	Improved	10	35
2[13]	52	MoP (Ceramic Fracture)	Fatigue, Anorexia, Weight loss, Dyspnoea	Hypothyroid, DCM, Pericardial effusion, Polycythaemia, Hepatic Failure and Multiorgan failure	LVEF (ECHO) = 30%, Autopsy confirmed	6521	23.6	Multi-organ failure and Death	2618	n/a
3[151]	53	MoC (Ceramic Fracture)	Visual and Hearing impairment, Parasthesia	Optic Atrophy and Retinopathy	Ophthamological and Audiometry	398	56	Improved	1	12.2
4[152]	49	MoM	Mental Fog, Memory loss, Vertigo, Hearing Loss, Groin pain and Breathlessness			23		Improved	11	n/a
5[153]	49	MoM	Cognitive, Behavioural and Mood disturbances, Dyspnoea, Tinnitus	High Frequency Hearing loss, Sleep Apnoea, Optic Atrophy	Audiometry, ECHO (Diastolic Dysfunction)	122	63	Improved	1.2	7.5
6[154]	58	MoP (Ceramic Fracture)	Impaired Vision and Hearing, Marked Sensori-motor peripheral neuropathy	Lower limb nerve amplitude reduction, absence of central acoustic responses and irregular visual repsonses, Hypothyroidism	Nerve Conduction Studies, Brain MRI showed hyper-intensity of optic nerves and tracts	549	54	Improved (except vision)	n/a	n/a
7[155]	56	MoP (Ceramic Fracture)	Painful neuropathy	Hypothyroid, Painful distal sensory neuropathy, Sensori-neural hearing loss	Nerve conduction studies	>400	22	Improved	39	19
8[156]	57	MoP (Ceramic Fracture)	Fatigue, Poor concentration, Headaches, Seizures, Hearing loss, Weight loss, Tachycardia	Hypothyroid, Peripheral Neuropathy, Cardiomyopathy	Nerve conduction studies (distal sensory latency and decreased conduction velocity), ECHO, Myocardial Biopsy (Concentric hypertrophy & fibrosis)	625	81	Improved (except neurology)	34	13
9[157]	59	MoP (Ceramic Fracture)	Distal parasthesia of both legs, Weight loss, Hearing loss, Fatigue	Hypothyroid, Pericardial effusion, Cardiomegally, Sensori-motor polyneuropathy, Hearing loss		506	14.3	Improved (except hearing)	270	25.8
10[158]	65	CoM (Ceramic Fracture)	Declining visual acuity, Poor colour vision, Malaise	DCM, Bulbar Palsy, Hypothyroid, Motor Axonopathy.	Retinogram	446.4	46	Improved (except colour vision)	n/a	n/a

11[159]	39	MoM	Unilateral paracentral scotoma, Bilateral ocular discomfort, Nausea, Metallic Taste	Patchy retinal pigment epithelium lesions	Retinogram	44.7	30.9	Not revised	-	-
12[11]	47	MoP (Ceramic Fracture)	Neuropathy	Sensori-motor peripheral neuropathy, Hypothyroidism	Sural nerve biopsy, Skin tests	n/a	n/a	Not revised	-	-
13[12]	75	MoM	Dyspnoea and Chest tightness	Dilated Cardiomyopathy	ECHO (LVEF = 21%)	13.6	4.1	Improved	4.5	n/a
14[160]	73	MoM	Cognitive decline, Memory loss, Depression, Anorexia, Weight loss, Metallic taste	-	-	24.2	12.5	Improved	3.5	n/a
15[160]	60	MoM	Muscle fatigue, Cramp, Dyspnoea, Cognitive decline	-	-	15.2	4.6	Improved	2.5	n/a
16[161]	75	MoM (Ceramic Fracture)	Weakness	Dilated Cardiomyopathy and Heart Failure	Thyroid function test, Electromyogram, ECHO (LVEF = 32%)	352.6	67.9	Improved	24	n/a
17[162]	59	MoM	Cough, Exertional Dyspnoea	Heart Failure, Hypothyroidism	ECHO (LVEF = 25%, Global Hypokinesia, Pericardial Effusion)	398.6	n/a	Improved	11.8	n/a
18[163]	55	MoP (Ceramic Fracture)	Heart Failure, Deafness, Visual Loss	Heart Failure, Hypothyroidism, Deafness	ECHO (LVEF = 25%)	885	49	Improved (except vision)	86.1	n/a
19[164]	54	MoM	Chest tightness, Exertional dyspnoea, Fatigue, Numbness to both feet	Heart Failure, Myocarditis, Cobalt Cardiomyopathy	ECHO (LVEF = 30%, Diastolic Dysfunction), CMR (Myocarditis), Myocardial Biopsy	189	109	Cardiac decline requiring Transplant	16	n/a
20[17]	69	MoM	Symptoms of Heart Failure	Congestive Heart Failure, Cobalt Cardiomyopathy	ECHO (LVEF = 25%), Coronary Angiogram normal, Cardiac MRI (LVEF = 14%), Myocardial Biopsy	300	80.3	Complicated, Died	n/a	n/a
21[165]	60	MoP (Ceramic Fracture)	Tachycardia, Tachypnea, Weight loss, Hearing Loss, Fatigue, Weakness	DCM, Mitral Regurgitation, Heart Failure, Respiratory Failure	ECHO (LVEF = 15%), Autopsy	817	60.5	Complicated, Died	n/a	n/a

Table 1.2: *Summary of reported cases of systemic toxicity. LVEF normal range = 55-70%. Co = Cobalt (in PPB), Cr = Chromium (in PPB) - MHRA threshold for concern = 7ppb.*

Cardiac Effects

The most profound recent published report describes a patient treated initially with a ceramic-on-ceramic bearing, which was revised to metal-on-polyethylene coupling due to ceramic bearing fracture. See case 2 illustrated in Table 1.2. Subsequently, this patient died secondary to multi-organ failure including cardiomyopathy with left ventricular ejection fraction (LVEF) of 30%, global cardiac muscle hypokinesis and significant pericardial effusion. Cardiac biopsy demonstrated dilated cardiomyopathy with deposits of electron-dense material, consistent with cobalt. Autopsy revealed cobalt saturation of cardiac, liver, and thyroid tissue [13].

Similar cases of cardiomyopathy secondary to elevated cobalt ion levels as a result of revision of a fractured CoC articulation to MoP bearings have also been reported [18 156 157].

Tower SS, presented the first cases of systemic cardiac toxicity secondary to primary MoM articulations. In this report two cases presented with a multitude of systemic symptoms one-year post implantation of large diameter MoM hip replacements, and were found to have highly elevated serum cobalt levels (upto 122ppb). The cases suffered diastolic dysfunction on echocardiography, suggestive of early cardiomyopathy. In total Tower has reported three cases of early cardiomyopathy, two of which required increased medication for hypertension, in patients with MoM hips [152 153]. Symptoms improved following removal of the implant.

Machado et al, report a case of severe global systolic dysfunction (LVEF 21%) in a patient 6 years following implantation of a MoM hip. Echocardiogram demonstrated a severely dilated left atrium. Cobalt levels were recorded at 13.57 ppb. Four weeks following revision surgery, the patient demonstrated marked symptomatic improvement, and an LVEF of 45% [12].

Van Lingen et al selected 10 patients with high cobalt levels (18-153ppb) from a cohort of 643 patients with stemmed large diameter MoM hip replacements, with mean follow-up of 4.2 years. Cardiac assessment included history, physical examination, electrocardiography, echocardiography and nuclear ventriculography. No obvious cardiac abnormalities were noted in the selected patients, where mean left ventricular end diastolic dimension (LVEDD) was 45 ± 4mm and mean LVEF equaled 58 ± 8% [166].

A recent health screen study undertaken by Wilkinson et al, selected age and sex matched patients from a single surgeon series of patients implanted with either a MoM resurfacing (n=36) or a non-MoM total hip arthroplasty (n=36). The index procedures took place greater than 5 years prior to the study period. Cardiac function was assessed by echocardiography and electrocardiography. They demonstrated a 7% reduction in cardiac ejection fraction in the MoM group and a 6% larger LVEDD, although both results were not clinically significant and lay within the normal range expected for patients of that age. It is also important to note that the patients had relatively low blood cobalt (median = 1.75ppb) and chromium (2.51ppb) levels when compared to the high levels seen in other case reports [167].

Of note accidental and occupational studies support the hypothesis that cobalt accumulation in the myocardium could affect its function. Linna et al demonstrated altered left ventricular relaxation and early filling in a series of 109 cobalt production workers who were exposed to an average of 0.40 mg/y, although clinically significant cardiac dysfunction was not seen [168]. The effect of cobalt accumulation on the myocardium was particularly evident following the 1966 episode of 'beer drinkers cardiomyopathy', a period when cobalt was used as a foam-stabilising agent in beer. Patients who drank large volumes of a particular brand of beer, presented with dilatative cardiomyopathy and systolic dysfunction, with associated pericardial effusions and polycythemia [73]. It was later seen that these patients were more susceptible to the effects of cobalt if their diet lacked in protein and overall nutrition [169]. There are several reports however, of occupational exposure to cobalt and development of cardiac disease, and it is possible to conclude that prior chronic exposure to alcohol and/or nutritional insufficiency can have a synergistic effect on the cardiotoxicity of cobalt.

Neurological, Visual and Auditory Systems Effects

Reports of neurological effects range from hearing loss, sight loss and peripheral neuropathy. Steens et al reported the case of a patient with a metal on ceramic (MoC) articulation (revised from a ceramic on ceramic (CoC) bearing for persistent pain) who developed increasing impairment in sight and sound 2 years following their revision surgery. This was associated with peripheral neuropathy affecting his feet and dermatitis of the head and neck, where hair

analysis demonstrated high cobalt deposits. Cobalt was 398ppb at the time of surgery (chromium 56ppb). The patients metal ions steadily declined after revision of the MoC bearing, in association with a steady improvement of his sight, hearing and peripheral neuropathy. Ophthalmological examination demonstrated toxic atrophy of the optical nerve and retinopathy with malfunction of the macula [151].

This was followed by a report from Rizzetti et al in 2009, of a patient who suffered a fractured CoC implant that was revised to a MoC bearing and later developed progressive visual and hearing loss. The patient also demonstrated new onset impairment of cranial nerves II and VIII bilaterally, and mild distal sensory motor disturbances progressing to hyposthenia declaring the patient wheelchair bound [116]. Cobalt levels were measured at 549ppb, and chromium 54ppb. Brain MRI demonstrated hyper intensity of optic nerves, electromyography demonstrated lower limb nerve amplitude reduction, and acoustic and visual evoked potentials demonstrated absence of brainstem acoustic and cortical visual responses. The patient was also seen to make progressive improvement following revision surgery.

Other cases of polyneuropathy following high cobalt and chromium levels exist in the literature, often following fracture of ceramic implants that were revised to metal bearings and suffered subsequent catastrophic abrasive wear [154-157]. Ikeda et al undertook detailed assessment of the neurotoxicity in this patient. Nerve conduction studies revealed absent sensory nerve action potential, yet normal motor conduction studies. They also performed a sural nerve biopsy, which revealed moderate axonal degeneration with no inflammatory changes,

however both cobalt and chromium levels where raised within the nerve tissue [155].

However more recently reports of similar symptoms have emerged in patients implanted with primary MoM bearings. Mao et al reported on two cases who had both received the DePuy Articular Surface Replacement (ASR) four and five years before the onset of symptoms, which included cognitive decline, memory difficulties and depression (Co levels of 15.2ppb) [160]. The report by Tower demonstrated symptoms of tinnitus and hearing loss, visual loss with optic nerve atrophy, hand tremor, cognitive decline and incoordination up to 3 years following DePuy ASR hip implants [152 153].

Similar presentations have been seen in patients with occupational exposure, supporting the hypothesis of a positive correlation of cobalt induced neurotoxicity. Memory loss, neuropathies and reduced visual acuity has been reported in hard metal workers exposed to cobalt dust [170 171]. Besides hip arthroplasty induced neurotoxicity, earlier reports of iatrogenic cobalt neurotoxicity were seen. Three particular reports described the toxic effects in patients treated with cobalt chloride for anaemia, where bilateral hearing loss, tinnitus, limb parasthesia, unsteady gait, optic atrophy and visual impairment developed after treatment, and improved after cessation of the agent [67 172 173].

The mechanism of action of cobalt-induced neurotoxicity has been extensively studied. The possibilities include cobalt interaction with mitochondria where reactive oxygen species formed by the presence of cobalt leads to loss of mitochondrial membrane potential and release of apoptogenic factors, thereby causing apoptosis and necrosis [172]. It has been suggested that neurotoxicity also

occurs by demyelination and axonal loss, both of which can be caused by reactive oxidative species formation as seen with cobalt [172]. Chromium has also been shown to induce oxidative stress on the brain by increased formation of reactive oxygen species in mice brain [174].

Endocrine and Reproductive Effects

Cobalt has been shown to affect thyroid function through its effects on inhibiting tyrosine iodinase, an enzyme that prevents the uptake of iodine into the hormone thyroxine, and therefore leads to the decrease in T3 and T4 production. The resultant increase in thyroid stimulating hormone release leads to thyroid hyperplasia, seen as goitre formation [175 176].

Recent case reports have implicated cobalt released from metal hip implants in the development of hypothyroidism in patients [13 153 156 157]. Historically it was first described in patients receiving cobalt therapy to treat anaemia [177]. Occupational exposure in a group of Danish pottery painters revealed no clinical effect on thyroid function however, despite normal thyroid metabolism being disturbed [178]. And more recently a cross sectional survey of cobalt workers in Belgium revealed no effect on thyroid function [179].

Chromium on the other hand has been shown experimentally to impact the anterior pituitary gland. Quinteros et al demonstrated that hexavalant chromium accumulates in the anterior pituitary gland of rats, and leads to endocrine dysfunction following prolonged oral intake [180]. They also demonstrated that chromium (VI) toxicity includes cell apoptosis and oxidative stress [181].

Experimental evidence exists to support a detrimental effect of chromium metal ions on reproductive function, with an impact on circulating hormone levels and cell formation (including reduced spermatogenesis, and impaired sperm and ova quality) [182]. However, confirmed reports in patients with MoM hip implants are lacking.

What has been reported however is the translocation of metal ions through materno-foetal circulation. Ziaee et al published evidence of transplacental transfer of cobalt and chromium [183], in this group no mothers had abnormally high metal ion levels. Fritzsche et al describe a 41 year old patient with bilateral MoM hip implants, with exceptionally high metal ions (Cobalt 138ppb, Chromium 39ppb), who gave birth to a male infant with elevated cord blood metal ion levels. The infant had persistent but reducing blood metal ion levels similar to that seen in the revised MoM hip patient, however no clinical signs of toxicity were evident [184]. Contrary to these studies, Brodner et al reported three women with MoM hip implants that gave birth to healthy infants without detectable metal ions in the cord blood [185]. Barceloux found no evidence of cobalt related teratogenicity in patients treated for pregnancy related anaemia [74], and there are no known reports of fetal malformations in patients with MoM hip implants [186]. There are however, studies that demonstrate teratogenicity in animals exposed to chromium and cobalt [187-190]. Given the evidence suggesting placental transfer, Delaunay et al and others, including the US FDA have recommended against the use of MoM hip implants in patients of childbearing age [137].

Renal Effects

Acute poisoning following excessive chromium ingestion has been shown to cause acute tubular necrosis (ATN), marked interstitial changes and renal failure [76]. Both trivalent and hexavalent chromium compounds are selectively accumulated in proximal convoluted tubules, where if in large doses they induce ATN [191]. Tubular proteinuria has been seen in chromium workers, suggesting prolonged exposure is related to chronic renal failure [191]. Contrary to this, Marker et al demonstrated that at 10-years follow up in 75 patients with Metasul MoM implants demonstrated no significant difference in renal function compared to pre-operative levels [192]. Corradi et al demonstrated similar findings in 31 patients with MoM implants at 10 years follow up [193]. Cobalt is rapidly excreted by the kidney and therefore has limited toxic effects [194].

Respiratory

Respiratory manifestations of exposure to cobalt and chromium are generally in association with occupational inhalational exposure to metal dust [74 76]. The effects can include asthma, inflammatory changes, interstitial fibrosis and emphysema. There are no reports of systemic respiratory effects attributable to metal ions released form MoM hip implants.

Hepatic

Fatal poisoning following ingestion of chromium resulted from significant hepatic damage and thrombocytopaenia, and resultant internal bleeding. Hepatic lesions included hepatocellular necrosis [195]. Dermal exposure to chromium with acute severe poisoning leading to multi-organ failure including

hepatic impairment was also recently reported [196]. Besides these reports of accidental exposure leading to hepatic dysfunction, no apparent studies demonstrating a causal link between MoM hip implants and hepatic impairment has been published.

Interestingly however, Urban et al demonstrated the widespread dissemination of metal debris including in the liver following metal hip implantation, although no apparent cell toxicity was seen on histological analysis [19].

Bone

Andrews et al demonstrated that hexavalent chromium can reduce osteoblast survival and function. Both cobalt and trivalent chromium are seen to increase osteoclast sensitivity, with a stimulatory effect, and the converse is seen with hexavalent chromium [143]. More recently the same group hypothesized that the demonstrated increased bone mineral density of a MoM hip resurfacing group over a conventional non-MoM group was a result of reduced osteoclast activity with secondary increased bone mineralization [167]. They also speculate that the stimulatory effect of chromium on insulin function leads indirectly to anabolic skeletal effects of insulin [167].

Dermatological

Dermatitis has been reported in association with a Metal on Metal hip (following revision for a failed ceramic on ceramic bearing implant 3 years earlier) affecting the head and neck of a patient [151]. Hallab et al described the prevalence of dermal sensitivity to cobalt to be greater in patients with an orthopaedic implant compared to the general population, and in particular in those with loose

implants [197]. The same group demonstrated methods for detecting and diagnosing metal sensitivity. These include lymphocyte transformation assay, lymphocyte migration inhibition assay and cytokine profiling of responding T cells. They demonstrated a dose dependent rise in lymphocyte reactivity to cobalt and chromium in patients with MoM hip implants compared with patients with conventional implants, suggesting metal hypersensitivity might increase with increased exposure [198]. More recently Mesinkovska et al have suggested that metal patch testing should be considered prior to implantation of metal implants in those with a clinical history of hypersensitivity, however the moderate predictive value of such tests would preclude its use in routine screening [199].

Genotoxicity and Interaction with the Immune System, and Cancer

The effect of cobalt and chromium wear particles is likely to be dependent on their ability to enter cells. Nanoparticle and metal ion entry into cells is partly dependent on their size. Very small particles are thought to enter by endocytosis and larger particles are phagocytosed by macrophages and the lysosomal pathway [200]. For instance the rate of uptake of cobalt nanoparticles was 80 times greater than the cellular uptake of cobalt metal ions [201]. Chromium ions on the other hand are thought to enter cells through anion channel mediated entry owing to their negative charge, leading to cytoplasmic accumulation [202]. Chromium accumulation within cytoplasm is thought to occur by conversion of hexavalent chromium to trivalent chromium [200].

Kwon et al report a dose dependent decline in macrophage viability with cobalt nanoparticles and ions, whereas no decline is seen with chromium products [114].

With regards to lymphocytes however, a significant reduction in cellular viability and increased apoptosis is seen in the presence of high concentrations of both cobalt and chromium metal ions [203]. This has relevance to the formation of pseudotumours as both these cell lines are thought to be integral in their aetiology.

Gill et al summarise the mutagenic and genotoxic effects of cobalt and chromium [200]. It is thought that cobalt is less genotoxic than chromium. Cobalt can cause single strand breaks, cross-linking, and inhibition of DNA repair mechanisms. Chromium on the other hand creates reactive oxygen species on cellular transformation from hexavalent to trivalent forms, and in addition it can cause DNA damage through cross-linking and induce strand breaks [200]. Ladon et al demonstrated aneuploidy and chromosomal translocations within lymphocytes studied in vivo in MoM patients [204]. A later study by the same group demonstrated that the rate of chromosome aberrations reduced once the MoM hip was revised to a MoP bearing [205].

1.4 Cardiomyopathy

One focus of this thesis will be the potential effects on cardiac function, namely the development of toxic cardiomyopathy and its detection.

Cardiomyopathy is a heart muscle disorder of which dilated cardiomyopathy (DCM) is a subset. It is defined as left ventricular dilatation and systolic dysfunction in the absence of coronary (ischaemic) artery disease or abnormal loading conditions (hypertension, valve disease) [206]. Figure 1.20. The heart walls

become thin and stretched, compromising cardiac contractility and ultimately resulting in poor left ventricular function.

DCM is a leading cause of heart failure, and predominantly affects younger adults between the ages of 20 and 50 years [207]. DCM is regarded as a non-specific phenotype in response to a cardiac insult, which can arise from any number of aetiologies. Genetically inherited forms of DCM contribute to approximately 30% of cases [208]. In cases where an underlying cause is not found – it is termed idiopathic DCM. The 5-year survival once diagnosis is made is 50% due to the progressive cardiac failure that is seen in these patients [209].

Figure 1.20: *Schematic demonstrating differences in wall thickness in a normal, hypertrophic and a DCM heart [210]*

1.4.1 Clinical Presentation

Patients typically present with signs and symptoms of reduced cardiac output and/or pulmonary congestion, often on a background of reduced exercise tolerance and fatigue. An inter-current illness or a cardiac event can precipitate an acute decompensation of cardiac output and lead to the diagnosis of DCM [207].

Symptoms include dyspnoea, fatigue, angina and ankle swelling. Symptoms may persist for several months, and often only surface when the disease has progressed to end-stage where significant cardiac scarring and fibrosis has developed [208].

Some patients present following a complication related to DCM, such as arrhythmias (atrial fibrillation) and thromboembolic events due to stasis of blood flow within dilated cardiac chambers [208].

Clinical examination can reveal physical findings of reduced cardiac output such as reduced arterial pressure, tachycardia and cool extremities. Pulmonary congestion may arise and is detected on auscultation due to pulmonary fluid accumulation. Ventricular dilatation can also lead to a shift in the cardiac apex to a more lateral position. Late changes such as mitral regurgitation may be detected on auscultation of the heart, revealing a murmur. Lastly, venous congestion may present itself as an elevated jugular venous pulse, ascites, hepatomegaly and pedal oedema [208].

1.4.2 Aetiology

Careful clinical history can reveal details pointing to a diagnosis of DCM and its underlying aetiology. Family history may reveal inherited causes, should two or more family members be affected within a single family. DCM can occur in certain X-linked inherited disorders such as Becker's and Duchenne's muscular dystrophy, or those with Mitochondrial DNA mutations and inherited metabolic disorders [206].

Nutritional deficiencies and endocrine disorders can present with cardiac failure, highlighting the need to review a patient's drug history, both prescription and recreational. Anthracycline (a chemotherapy agent) cardiotoxicity results principally from total cumulative dose and may only become apparent after several years of use. Regular alcohol consumption over several years has frequently been associated with left ventricular dilatation and cardiac dysfunction [211]. Cocaine abuse can present with acute cardiomyopathy, whereas HIV and Hepatitis C exposure can also be relevant.

Causes of DCM are summarised in table 1.3.

Cause	Example/s	Comment
Genetic	Haemochromatosis* Mitochondrial	Detailed family history Ferritin and Transferrin saturation levels*
Infectious	HIV	
Drug	Alcohol, Cocaine, Anthracycline, **Cobalt**, chloroquin	Detailed history of exposure
Metabolic	Hypocalcaemia, hypophosphataemia	Blood biochemistry
Endocrine	Cushing's disease, thyrotoxicity, acromegaly	Thyroid function, plasma glucose
Nutritional	Carnitine, Thiamine, Selenium	
Inflammatory	Eosinophilic Vasculitis (Churg Strauss Syndrome, Kawasaki Disease), Sarcoidosis	Autoantibody Screen
Neuromuscular	Duchenne / Becker muscular dystrophy	Raised Creatine Kinase, Skeletal muscle weakness, Family history
Other	Pregnancy, Tachyarrhythmia	

Table 1.3: *Causes of DCM [adapted from Japp et al [207]]*

Other conditions with characteristics similar to DCM can present in the same way and must be excluded. Ischaemic cardiomyopathy is diagnosed if over 75% stenosis is present within the left main coronary artery as seen on coronary angiography. Late gadolinium enhancement on cardiac MRI scanning can help characterise ischaemic changes in conjunction with angiography. Hypertensive cardiomyopathy demonstrates increased left ventricular wall thickness on a background of chronic poorly controlled hypertension. Hypertrophic cardiomyopathy patients demonstrate increased left ventricular wall thickness and myocardial fibrosis seen on gadolinium enhanced MRI imaging. Athlete's heart represents a patient without symptoms of heart failure with normal blood biomarkers, electrocardiogram features and left ventricular function. However physiological dilatation of the left ventricle has been reported in up to 15% of highly trained athletes, which can be associated with reduced LVEF at rest, thus mimicking DCM. Lastly cirrhotic cardiomyopathy can present in patients with advanced liver disease and is an important complication of liver cirrhosis from any cause. In such patients LVEF can be insufficient at times of physiological stress and lead to cardiac failure [207].

1.4.3 Clinical Assessment

Electrocardiogram

Electrocardiogram (ECG) assessment in patients with DCM can often be remarkably normal, however abnormalities ranging from isolated T wave changes, septal Q waves due to extensive fibrotic damage, prolonged

atrioventricular conduction and bundle branch block can be seen. The presence of persistent tachyarrhythmia and supraventricular arrhythmias are common and can lead to arrhythmogenic cardiomyopathy characterised by right ventricular dysfunction and regional wall abnormalities. Prolonged atrioventricular conduction is often seen in cases with genetic aetiology (e.g. myotonic dystrophy) or inflammatory disease (e.g. sarcoidosis) [206 207].

Echocardiography

The role of Echocardiography (ECHO) has become increasingly limited with the advent of cardiac MRI (CMR). However, certain features stand out, in particular its accessibility, and therefore remains the frontline investigation for estimation of LV volumes and LVEF. The diagnostic criteria for DCM uses parameters measured by 2D ECHO, such as left ventricular end diastolic dimension (LVEDD), fractional shortening and LVEF. ECHO can also demonstrate valvular function and anatomy, in particular mitral regurgitation secondary to ventricular dilatation. The finding of inferolateral LV hypokinesis relates to conditions such as muscular dystrophy or acute inflammatory myocarditis. Otherwise the role of ECHO in understanding DCM aetiology is rather limited [206 207].

Exercise testing

Exercise testing with blood gas analysis is useful in assessing disease severity and baseline exercise tolerance [208]. Its main use lies in disease progression and response to treatment.

Cardiac MRI

CMR is emerging as the gold standard for volume and function assessment in cardiac disease. It is invaluable in aetiological evaluation of DCM through detection of myocardial oedema (e.g. myocarditis) and determination of gadolinium enhancement to aid the diagnosis of muscular dystrophy, myocarditis and sarcoidosis [207].

Endomyocardial Biopsy

Tissue biopsy is used to differentiate certain underlying pathologies that can cause DCM such as sarcoidosis and haemochromatosis. However, complications are frequent, some severe, and include pneumothorax, air embolism, arrhythmias and cardiac tamponade [208].

1.4.4 Histopathology

To understand phenotype expressions of DCM, it is important to understand the underlying histopathological changes.

Macroscopic Appearance

The myocardium of patients suffering DCM can often weigh 2-3 times as much as normal as a result of the increased size and hypertrophied muscle fibres. A heart can appear spherical in shape, if both ventricles are affected, and when cut through the sagittal section the apex appears rounded (rather than pointed). If isolated left ventricular dilatation is seen, the inter-ventricular septum may be found bulging into the right ventricular cavity, figure 1.21.

Figure 1.21: *Pathological appearance of DCM. (A) Wall thinning and cavity dilatation of the left ventricle (asterisk), (B) extensive left ventricular mid-wall replacement fibrosis (white arrow)* [207]

Mitral and tricuspid valves can demonstrate changes consistent with regurgitation, as a result of deformation of the annulus secondary to progressive dilatation. Progressive dilatation also leads to fibrosis within the myocardial wall, and as a result there is reduced contractility [208].

Microscopic Appearance

Often, histological changes are non-specific and do not point to the underlying aetiology. Myocytes demonstrate changes consistent with hypertrophy as they appear thickened with enlarged nuclei. Interspersed with hypertrophied myocytes are other myocytes that appear elongated and thin with the nucleus inhabiting the full width of the cell. The number of intra-cellular contractile myofibrils are diminished. Myocyte death leads to degenerative change with interstitial fibrosis. Figure 1.22.

Figure 1.22: *Histology specimen of a patient with DCM. Myocyte hypertrophy (black arrow), myocyte atrophy (blue arrow), nuclear pleomorphism (arrowhead) and increased interstitial fibrosis (stained with Picrosirius Red)* [207]

The histology can vary depending on the underlying aetiology. For instance lymphocytic infiltration surrounding degenerate myocytes is seen in myocarditis, multinucleated giant cells surrounded by macrophages may be seen in sarcoidosis and areas of intra-myocellular iron deposition resulting in myocellular degeneration with iron staining is typical of haemochromatosis [208].

1.4.5 Assessment of Myocardial Change

A number of adverse phenotypes develop in DCM, which include LV dilatation, LV wall thinning, functional mitral regurgitation, myocardial fibrosis, asynchronous ventricular contraction and dilatation of other cardiac chambers. Various imaging techniques have been optimised to identify and monitor such events.

LV Size and Function

Two-dimensional ECHO is the frontline investigation for calculating ventricular volumes and LVEF. 2D imaging involves certain geometric assumptions, which can impede the accuracy of volume assessment, although this can be avoided by using contrast agents or 3D imaging [207].

Volume assessment is improved further with the use of CMR due to its improved delineation of the blood-muscle interface combined with high spatial resolution multi-planar imaging [207]. Refer to Figure 1.23. CMR is now the gold standard for assessment of ventricular volume and function.

Figure 1.23: *End Diastolic CMR images with blood-muscle delineation. Orange represents LV chamber blood, Purple represents RV chamber blood, brown demonstrates muscle wall* [207]

Remodelling of Cardiac Chambers

Left atrial (LA) dilatation can follow left ventricular cavity enlargement through diastolic dysfunction, mitral regurgitation or atrial fibrillation. LA volume is the

preferred measure of LA size, and is measured on CMR using a biplane area-length method. LA size is an independent predictor of outcomes from DCM [212].

Right ventricular (RV) remodelling results from pulmonary hypertension, or primary myocardial disease. Additional factors involved in the formation of RV dilatation is Tricuspid valve regurgitation and increased pulmonary artery pressure, both of which can be measured on ECHO. However, CMR provides the most accurate assessment of RV volume and ejection fraction [207]. Figure 1.23.

Mitral Regurgitation

Dysfunction of the mitral valve is a consequence of increasing LV dilatation. The increasing size and sphericity causes tethering of the mitral valve leaflets, which fail to meet on ventricular contraction leading to functional regurgitation. Mitral regurgitation can propagate LV dilatation and vice versa [207].

Mitral regurgitation can be measured on ECHO or CMR, however the most accessible currently is three-dimensional ECHO with colour Doppler flow assessments that allow direct measurement of regurgitation and the size of the defect.

Myocardial Fibrosis

One third of patients with DCM develop scarring ("fibrosis") as a consequence of myocyte injury. This typically arises within the mid wall and can be detected by late gadolinium enhancement (LGE) CMR. Figure 1.24.

Figure 1.24: *CMR (Left - 4 Chamber and Right - 2 Chamber view) with LGE. Arrows demonstrate detection of mid wall fibrosis through appearance of bright LGE compared to normal black appearance* [207]

Ventricular Dyssynchrony

Asynchronous ventricular contraction can develop in DCM and lead to poor outcomes. A key diagnostic criterion of ventricular dyssynchrony is a prolonged QRS interval (>150ms) on electocardiography. Left bundle branch block is also a key feature seen on ECG in DCM patients. ECHO techniques can detect dyssynchrony when ECG features are equivocal.

1.5 Cobalt Cardiomyopathy

A distinction needs to be made between idiopathic DCM and DCM as a consequence of toxicity. As discussed above, the histology can vary depending on the aetiology, as such idiopathic DCM demonstrates myocyte vacuolisation, myofibrillar loss, myocyte hypertrophy and interstitial fibrosis.

A historical study compared 12 cases of cobalt cardiomyopathy to 12 cases of idiopathic DCM using light microscopy of cardiac biopsy samples. They identified a distinction in the degree of myofibril loss and atrophy, both of which were prominent in the cobalt cardiomyopathy cases compared to the idiopathic

cases. There was also a documented absence of inflammatory infiltrates and fibrosis seen within the cobalt cases [213].

However, despite these findings, more recent cases of cardiomyopathy attributed to cobalt toxicity have demonstrated variation in histological findings. Similar appearances of myofibril loss and atrophy have been seen, however interstitial fibrosis has been documented in these cases [17 164].

As discussed in section 1.32, metal debris has the potential to disseminate to distant organs. Case et al demonstrated this in post-mortem studies, identifying metal within lymph nodes, bone marrow, liver and the spleen [5]. Unfortunately, the group did not obtain myocardial tissue for assessment. They performed light microscopy, electron microscopy and mass spectrometry.

Light microscopy of lymph nodes demonstrated black metal particles within macrophages and to a lesser extent within extra-cellular spaces. Metal was also seen within mononucleated histiocytes and langerhans giant cells. Areas of necrosis and fibrosis were also seen. Macrophages underwent nuclear change in response to metal debris, and in some cases nuclei were not found at all [5].

Within the liver tissue, metal particles were found in portal tract macrophages and in Kupffer cells, but the concentration was less than that seen in the lymph nodes. The degree of dissemination appeared to correlate with the degree of wear and metal debris production, where higher debris load led to dissemination further afield and in higher concentrations. Certainly, the morphological macrophage response appeared to follow the same trend, in addition necrosis and fibrosis was only seen in the lymph nodes that carried the greatest metal burden.

Necrosis and fibrosis is thought to arise through macrophage activation, which in turn leads to a cytokine response that activates proteases and promotes the release of tissue necrosis factor [214]. In this small series, no evidence of necrosis or fibrosis was seen in the liver or spleen, however it is believed that if the saturation threshold is reached then necrosis is likely to ensue through the same process [5].

Tissue biopsies reported in recent cases of cobalt cardiomyopathy have confirmed cobalt presence within the myocardium [13 165]. See table 1.2. The collective of 21 cases reporting systemic toxicity to metal implants have a mean blood cobalt level of 644 ppb. Five of these cases had either myocardial biopsy as part of their routine care or tissue biopsies at post mortem. Of these, two commented on cobalt presence within myocardial tissues and estimated tissue cobalt loads of 3.85μg/g and 2.5μg/g, with blood cobalt measured at 6521ppb and 644ppb respectively [13 165].

This highlights the extremely elevated blood cobalt levels of patients reporting systemic effects when compared to the general population and the majority of patients living with metal hip implants. However concern exists that milder cardiotoxicity may be common and under-recognized.

1.6 Evaluation of Cardiac Function with Imaging

1.6.1 What is MRI?

Unlike traditional x-ray radiographs or computed tomography (CT), MRI does not use ionizing radiation. During MRI, the patient is placed within the bore of a

powerful magnet and radio waves are passed through a designated area in the patient in a particular sequence of very short pulses. Each pulse leads to a responding pulse of radio waves to be emitted from the patient's tissues. The location from where the signals originated is recorded by a detector within the scanner and processed by the computer. This creates a 2-Dimensional picture representing the predetermined slice/section of the patient [215].

The MRI uses magnets with varying field strengths, commonly ranging from 0.3 to 3.0 Tesla – most use 1.5 Tesla. Diagnostic MRI is based on imaging hydrogen atoms within fat and water molecules inside the patients' tissues. Hydrogen atoms act like small magnets themselves, and when placed in a magnetic field they align themselves to this field. When pulsed radio waves of a particular radiofrequency are directed at the patient, hydrogen ions become disorganised and no longer align with the magnetic field. Subsequently the hydrogen atoms re-establish alignment with the surrounding magnet, and as they do so they emit the absorbed radiofrequency waves. The distribution of the emitted waves is detected and processed by the computer to produce the image. The time taken for the hydrogen atoms to re-establish alignment is called the relaxation time, of which there are two recognised types. The T1 time is the longitudinal relaxation time and the T2 is the transverse relaxation time [215].

The time between radiofrequency pulses (RF) is the repetition time (TR) and the echo time (TE) is the time between the exciting RF pulse and the arrival of the subsequent relaxation emission from the hydrogen atoms. T2 images are achieved when longer TR and TE times are used, whereas T1 is more dependent on shorter TR and TE times [215]. A disadvantage of MRI imaging is the time required to obtain imaging data, and therefore is susceptible to motion artefact.

This is particularly problematic when imaging the chest due to physiological movement associated with breathing and cardiac contractions. To overcome this, patients are asked to breath-hold during imaging sequences. Secondly, the heart changes shape during the cardiac cycle. Electrocardiographic gating may be used during scanning to obtain slice specific images that match various phases of the cardiac cycle

1.6.2 What is Echocardiography?

Also known as ultrasound, provides an image of a slice of the body achieved by directing a narrow bean of high frequency sound waves at the selected area and recording the manner in which sound is reflected back to the transducer. It is operator dependent as the ultra-sonographer uses a hand-held transducer that converts electrical energy into sound waves. Depending on the physical density of the tissues and the velocity of the sound, the beam is reflected back (ECHO) at different strengths, which is detected by the transducer (acoustic impedance). The acoustic impedence varies between tissues and allows the computer to generate live images of the area of interest. ECHO is good for assessing the structure, size and motion of the heart, but does not provide images as detailed as that of MRI [215].

1.6.3 MRI or ECHO?

CMR is well suited to assess ventricular function. First, MRI is non-invasive and the examination process does not affect the cardiac function of the patient.

Second, because of high contrast between blood and myocardial tissue in the MR image, contrast agents are not required. Lastly, MRI allows contiguous sections to be imaged, thus providing 3-dimensional imaging that does not rely on geometric assumptions to determine ventricular dimensions [216].

Global ventricular function refers to the effectiveness of the ventricle as a pump. It is determined by the relationship between the preload, afterload and cardiac contractility.

Preload = the extent of stretch of muscle fibres before contraction, (equivalent to End Diastolic Volume, EDV)

Afterload = the load that muscle fibres in ventricular walls sustain during contraction (equivalent to End Systolic Blood Pressure)

Contractility = intrinsic contractile level of the myocardium (equivalent to Ejection Fraction)

Ejection Fraction (%) = ((EDV – ESV) / EDV) x 100

Assessment of LV function is essential for the diagnosis and management of LV dysfunction in patients with cardiomyopathies, while quantification of LV mass has important prognostic implications as discussed earlier. The interaction between preload, afterload and contractility demonstrates the importance of precise measurements when assessing ventricular function, and the accuracy achieved with MR imaging is considered by most as the gold standard [216] [217]. Figure 1.25.

LV mass as measured by CMR has been validated in animal studies to be more accurate than 2D or 3D ECHO [217]. In addition ECHO suffers because it depends on acoustic windows and operator/user skill. Variable image quality and the

potential for errors in wall thickness measurements (which is dependent on the angle of incidence) lead to inaccurate results with poor reproducibility. Ejection fraction and LV mass are calculated from measurements made only at one position (at the base of the LV), and LV is assumed to have a uniform geometric shape with no regional variation in wall thickness [217]. The formula used to subsequently calculate LV mass and EF assumes an ellipsoid shape for the LV that is not the case in cardiomyopathy. Studies have shown that such assumptions lead to overestimation of the mass when compared to CMR.

Figure 1.25: *Left ventricle short axis stack (multiple axial slices) data set acquired by CMR from which detailed volume and mass measurements can be acquired*

Lastly, inter-reader variability was demonstrated by Hoffmann et al, who set out to analyse the inter-reader agreement of non-contrast and contrast enhanced 2D and 3D ECHO with CMR when measuring LV volumes and EF. Variability between two independent readers reached 28% for non-contrast 3D ECHO,

compared to 4.8% for CMR, when measuring EDV and similar for ESV. The variability in ECHO measurements improved when the studies were contrast enhanced, but did not surpass CMR. The mean variability for CMR measurements of EF was 7.9% compared to 13.6% for non-contrast 3D ECHO. However this difference was eliminated when contrast was used [218]. Figure 1.26a-c.

Figure 1.26a: *Inter-reader variability in the assessment of LV ESV between two readers for non-contrast ECHO, contrast enhanced ECHO and CMR.*

Figure 1.26b: *Inter-reader variability in the assessment of LV EDV between two readers for non-contrast ECHO, contrast enhanced ECHO and CMR.*

Figure 1.26c: *Inter-reader variability in the assessment of LV EF between two readers for non-contrast ECHO, contrast enhanced ECHO and CMR.*

1.6.4 Tissue Mapping Techniques

T1 and T2 values are determined by the molecular status of the water molecules within the tissue, thus characterise the pathologic status of the tissue. In the instance of acute myocardial ischaemia, water is released from within cells and consequently prolongs T1 and T2 values. CMR permits the routine acquisition of quantitative measures of myocardial and blood T1, which are key tissue characteristics, where one can measure biologically important properties of both regional and global myocardium independent of function. This is important because focal or global cardiac disease can reflect the pathophysiological disease process responsible [219].

Native T1 reflects myocardial disease involving the myocyte and interstitium without use of gadolinium based contrast agents. On the other hand the extracellular volume (ECV) fraction after application of gadolinium based

contrast agent offers a direct measure of the size of the extracellular space, reflecting interstitial disease such as fibrosis [219] [220].

Native T1

T1 mapping is a parametric map in which individual voxel's intensity represents the T1 value of the corresponding voxel. T1 value of a specific tissue is defined as the specific time when the longitudinal magnetisation of a proton recovers approximately 63% of its equilibrium value [220]. T1 mapping requires the acquisition of multiple images (at least 6-10) to derive the T1 recovery curve, which is governed by the exponential time constant for MR longitudinal relaxation [219] [220]. Each image that is used to form the final co-registered parametric map is required to be taken at exactly the same time during the cardiac cycle.

Native (non contrast) T1 changes can detect pathologically important processes related to excess water in oedema, protein deposition, and other T1 altering substances such as Iron (haemorrhage or haemochromatosis). Such diseases detected by alteration in T1 are myocardial infarction, myocarditis, amyloidosis or diffuse fibrosis (all high T1), or siderosis (low T1) [219].

One of the limitations of T1 mapping is the effect of cardiac and respiratory motion on co-registration of images. To overcome this a Modified Look and Locker Inversion recovery sequence (MOLLI) was proposed by Messroghli et al [221]. This uses two principles; 1) selective data acquisition at a given time of the cardiac cycle over successive heart beats, and 2) merging of images from three consecutive Inversion Recovery (IR) experiments into one data set, which together generate a single slice T1 map of the myocardium [220].

A restraint to using MOLLI however is the need for prolonged breath holds to achieve a 17-heart beat sequence for a single slice T1 map. This can be achieved in healthy individuals, but can be challenging for those with respiratory compromise or slow heart rates, particularly the elderly patients. Piechnik et al, presented a Shortened MOLLI (ShMOLLI) sequence obtained during a single breath hold over 9 heartbeats [222]. ShMOLLI uses sequential inversion recovery measurements where full recovery of the longitudinal magnetisation between inversion pulses is not achieved. An algorithm is then applied to conditionally analyse the data depending on the T1 value [222]. This technique is as accurate if not better than MOLLI as significant errors are seen when pooling data in the latter method [220 222].

Extracellular Volume (ECV)

The ECV of the myocardium reflects the volume fraction of heart tissue that is not taken by cells. To understand ECV, we need to define the myocardium by two compartments. These include the cellular (dominated by myocyte mass) and the extracellular interstitial (extracellular Matrix, ECM) compartments. Changes within these compartments arise through different disease processes. Expansion of the ECM appears to correlate with a poor outcome in conditions such as diabetes, underpinning the importance of ECV as a prognostic indicator [219 223].

Expansion of the ECM can result in mechanical and electrical dysfunction. Often it is the myocardial collagen fraction that is seen to expand, and some have described band like fibrosis formation within the myocardium. Fibrosis is seen as the final common pathway in several disease processes affecting the heart [219].

Neither T1 mapping nor ECV directly measure the ECM, rather, ECV measures the space the ECM occupies which is a useful surrogate. This has been validated histologically [224], which has shown good correlation between ECV and collagen volume fraction, therefore ECV is considered a CMR biomarker for myocardial fibrosis in the absence of amyloidosis or other conditions that cause myocardial oedema [219].

Metal Deposition and T2*

Fibrosis and cardiomyopathy leading to heart failure was the commonest cause of death in patients with beta thalassaemia major. This was the result of a dependence on blood transfusions, which led to patients receiving approximately 20 times the normal intake of iron and its consequent accumulation within the liver and heart of such patients. Excessive iron deposition within cardiac tissues can lead to premature death secondary to fatal arrhythmias and heart failure [225-227].

Early detection of iron overload was necessary to prevent the onset of cardiomyopathy and heart failure, and thus mortality. The drive for a non-invasive technique to measure myocardial iron led to the development of an optimised T2* CMR technique.

T2* is a CMR relaxation parameter arising principally from local magnetic field inhomogeneities that are increased with cardiac iron deposition [24]. Particulate intracellular iron causes shortening of T2* and can be easily quantifiable. During its inception, Anderson et al, conducted a study of 30 beta-thalassaemic patients undergoing a liver biopsy. They were able to correlate the T2* value with the chemical estimation of liver iron measured from tissue biopsies [23]. By

subsequently scanning 106 subjects with thalassaemia major, they demonstrated that increased myocardial iron (as measured by T2*) correlated with a progressive decline in LVEF [23]. Subsequent validation of cardiac iron with T2* has been demonstrated [24]. Figure 1.27.

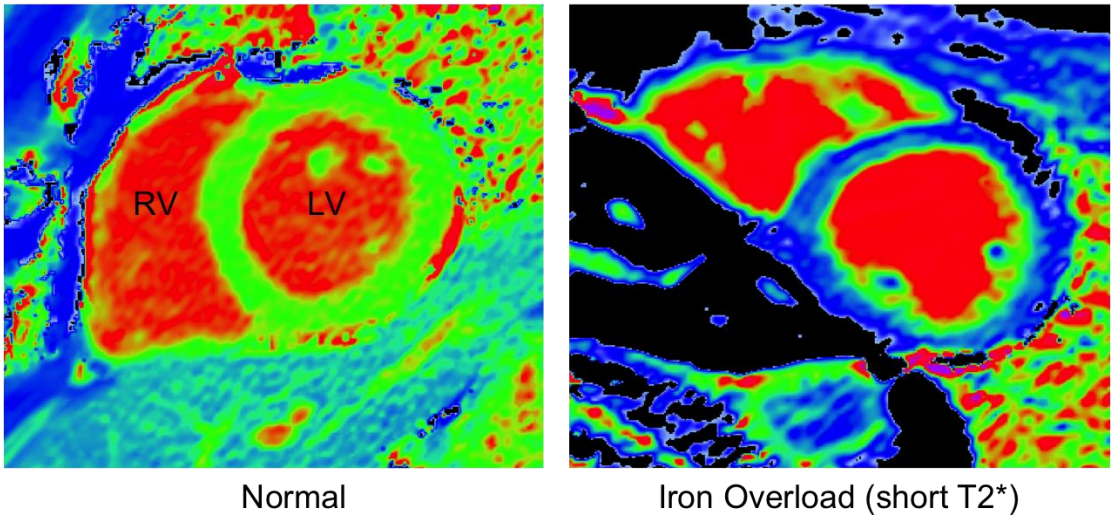

Figure 1.27: *Short Axis 2 chamber view comparing T2* values in a normal myocardium (green walls) vs. a myocardium with Iron overload (blue walls)*

Cardiovascular magnetic resonance (CMR) imaging has revolutionised the management of this particular group of patients by allowing a robust non-invasive method of detecting iron loading [23 227 228]. Figure 1.28.

Figure 1.28: *The advent of T2* for early diagnosis of iron overload has reduced the associated mortality from this condition between 2000-2003* [23]

Iron exhibits ferromagnetic properties and acts like a contrast agent, relaxing water hydrogen, which is detectable as an MR signal. Both cobalt and chromium have magnetic properties and have been proposed as MR contrast agents [229] [230] and should therefore be detectable in vivo using MR T2* quantification.

Parkes et al, created polymer coated cobalt nanoparticles of approximately 3-4nm in diameter, which was successfully detected by MR with relaxitivities similar to that seen with iron oxide [229]. Cobalt particulate size measured from simulator samples of MoM hips ranged from 10nm up to 1μm, and would suggest that metal debris in vivo would have a similar effect on MR relaxitivities [231]. Cobalt is paramagnetic, and chromium is diamagnetic or paramagnetic depending on the oxidation state and this has a direct effect on magnetic susceptibility. Figure 1.29.

Figure 1.29: Particulate debris shape distribution as a function of maximum Feret's diameter (dmax) for a typical MoM sample retrieved from a hip simulator model. Demonstrating the distribution of sizes – majority of which are nanoparticles [231]

1.7 Thesis Rationale

No study has attempted to identify cobalt deposition within hepatic and cardiac tissues using MRI. The number of patients requiring ongoing surveillance for their metal on metal hip justifies the importance of establishing a non-invasive technique. We aim to demonstrate the feasibility of established MRI protocols, in particular T2*, in detecting hepatic and cardiac metal deposition.

In addition, since the majority of reported cases of systemic toxicity involve the heart, we sought to detect and constrain the correlation between blood metal ions and a comprehensive panel of established markers of early cardiotoxicity.

Lastly, the clinical overlap between orthopaedics and medical subspecialties (cardiology) when managing patients with metal on metal hip implants and potential systemic toxicity justifies the need for a multi-disciplinary approach to the clinical management of such patients. Therefore, we also intend to analyse the use of a multi-disciplinary team (MDT) meeting in the discussion and clinical management of patients with metal on metal hip implants.

1.8 Study Hypothesis

Our hypothesis is that there is no discernable effect on cardiac function detectable on MRI and Echocardiography in patients with elevated blood metal ion levels.

In addition, we hypothesise that an MDT meeting is a clinically useful method of managing all aspects of care for patients with MoM hip implants.

CHAPTER 2

CHAPTER 2 CLINICAL DETECTION OF METAL DEPOSITION BY CMR AND VALIDATION OF FINDINGS

2.1 Introduction

With over a million metal-on-metal hips implanted worldwide the need for comprehensive guidance on the management of patients with MoM hip implants is of great importance. Currently the majority of patients implanted have well functioning hips: the chance of developing serious problems has not yet been quantified for all patient groups and implants types. We know that hip resurfacings work well in young men (<55 years of age) with osteoarthritis [232].

It is well accepted that imaging findings influence the decision to revise in patients with well functioning hip replacements, for example osteolysis that is likely to cause impending fracture [144]. The influence of imaging findings of soft tissue abnormalities around MoM hips is yet to be fully understood [131].

Guidance to aid clinicians manage patients with MoM hip implants has been published by various regulatory bodies, including the Medicines and Healthcare Related Products Agency (MHRA, UK), the Food and Drug Administration (FDA, USA) and the Scientific Committee on Emerging and Newly Identified Health Risks (SCENIHR, Europe) [6 8 9]. The decision to revise MoM hips may not be based on a single investigation, particularly since current guidelines have limited detail on the interpretation of MRI findings and clinical symptoms. Some cases are straightforward for most surgeons and decision-making is relatively easy.

However, there are many cases that because of the difficulty of applying guidelines in complex cases, surgeons experience considerable uncertainty with decision-making. This led to the development of an Internet enhanced Multi-Disciplinary Team (iMDT) meeting at the Royal National Orthopaedic Hospital as an extension of the guidance published by the regulatory agencies, with the aim of using surgical experience, tacit knowledge and evidence based current best practice to reduce the uncertainty surrounding the management of MoM hip patients. The team consists of hip revision surgeons, radiologists and nurse coordinators. The referring surgeon who is often based at a different hospital then executes decisions recommended by the iMDT. This method has demonstrated good concordance between the recommendation and referrers [233]. See Chapter 7.

Current guidance recommends a blood metal ion threshold of 7ppb (118nmol/L cobalt or 134.5nmol/L chromium) to track the risk of local soft tissue reactions and the risk of failed resurfacings/total hip arthroplasties, but there are currently no non-invasive tests for the detection of systemic or organ specific toxicity. Confirmation of systemic toxicity has previously been from invasive tissue biopsy or post-mortem.

Magnetic resonance imaging (MRI) using a T2* protocol is the current gold-standard method for detection and quantification of iron deposition in patients with iron overload, and has histological validation [24]. Iron is ferromagnetic and acts like a contrast agent, relaxing water hydrogen, which is detectable as an MRI

signal. Both cobalt and chromium have magnetic properties and have been proposed as MRI contrast agents [229] [230].

A patient treated through the RNOH iMDT was identified at particularly high risk of systemic toxicity. The case history and management of this case is presented here including the experimental application of imaging techniques discussed above and the subsequent validation of the findings.

2.2 Case Presentation

A 44-year-old man presented to our institution via the iMDT with hip pain, a peri-prosthetic mass and scar pigmentation. See figure 2.1. He had initially undergone primary total hip arthroplasty 35 months previously, with a ceramic on ceramic bearing for osteoarthritis.

Figure 2.1: *Scar pigmentation in a patient with highly elevated metal ions*

He had suffered a post-operative hip dislocation within the first week after implantation that was successfully relocated, and subsequently functioned well. See figure 2.2.

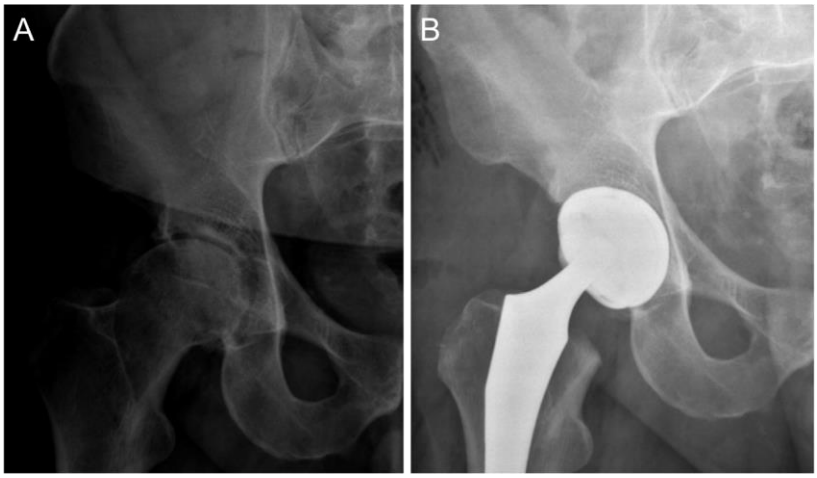

Figure 2.2: *AP radiograph demonstrating (A) the pre-operative native hip suffering osteoarthritis and (B) following total hip arthroplasty with CoC bearing surfaces*

However, 16 months following primary implantation, he complained of pain and stiffness arising from the right hip. A ceramic acetabular liner fracture was diagnosed and he underwent revision surgery to exchange the ceramic head and cup liner to a metal on polyethylene bearing. Figure 2.3.

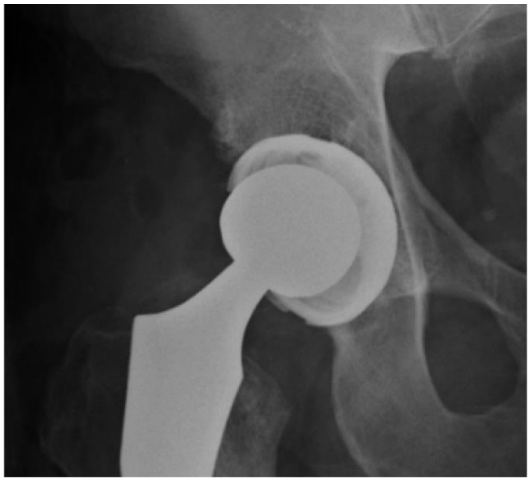

Figure 2.3: *AP radiograph after revision to Metal on Polyethylene bearing, note slight eccentric position of head within the cup*

Four months following his revision to a MoP bearing implant he again complained of increasing pain and stiffness. On this occasion he also described fullness around the hip joint. His attending surgeon performed a repeat revision, describing his finding of a flattened metal head. A revised fresh MoP bearing surface was again implanted. However, despite undergoing a second revision, similar problems arose, with pain, stiffness, swelling and irritable hip movements. Repeat x-ray images revealed rapid destruction of the metal femoral head that appeared flattened and deformed. Figure 2.4.

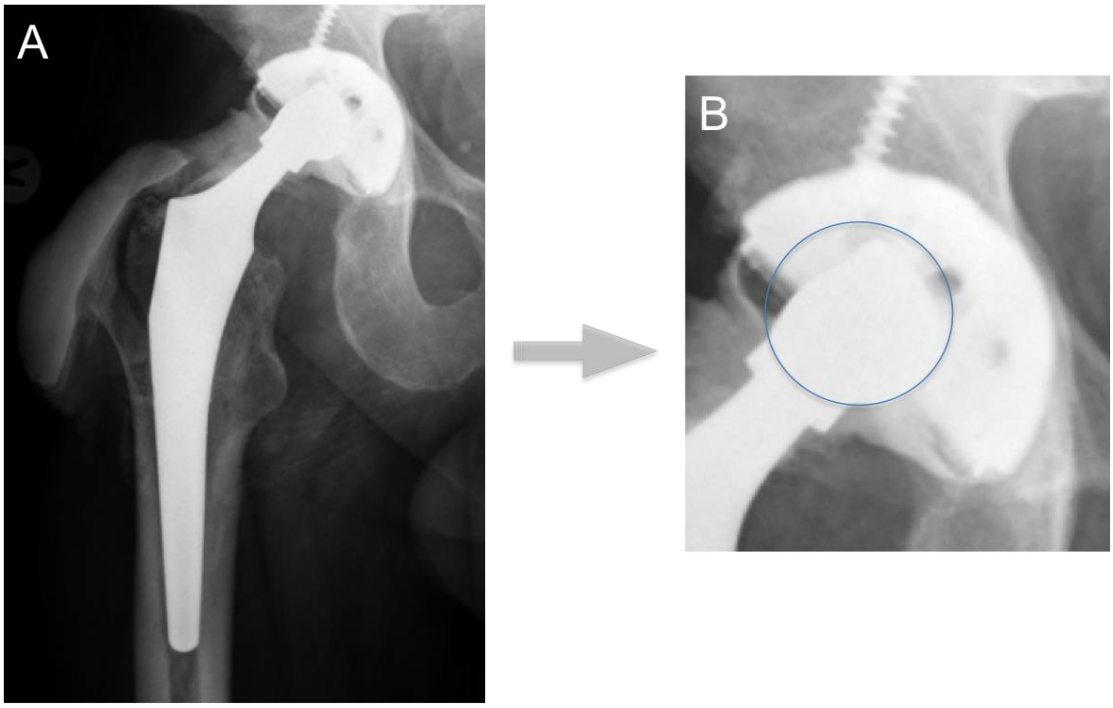

Figure 2.4: *(A) An x-ray arthrogram (injection of contrast agent into the hip joint) revealed a flattened head and contrast extending into the lateral bursa, suggestive of a defect within the abductor attachment to the greater trochanter of the hip; (B) Demonstrates an enlarged view of the femoral head and a superimposed line to demonstrate the expected sphericity should there be no wear of the head*

On presentation to our institution, he was found to have pain on flexion, with irritable movements and a palpable swelling within the trochanteric region. Laboratory investigations revealed extreme blood Cobalt and Chromium levels (587.9ppb and 20.4ppb respectively), with normal inflammatory markers. Urgent re-revision surgery to a new Ceramic on Ceramic bearing hip implant was performed. At surgery we found substantial soft tissue metallosis and a catastrophically worn metal head (made of CoCr alloy). Figures 2.5-2.7. The substantial degree of wear of the femoral head demonstrated is assumed to arise from the residual ceramic particles that have embedded into the plastic liner surface following previous ceramic fracture. The abrasive ceramic particles led to accelerated wear of the femoral head.

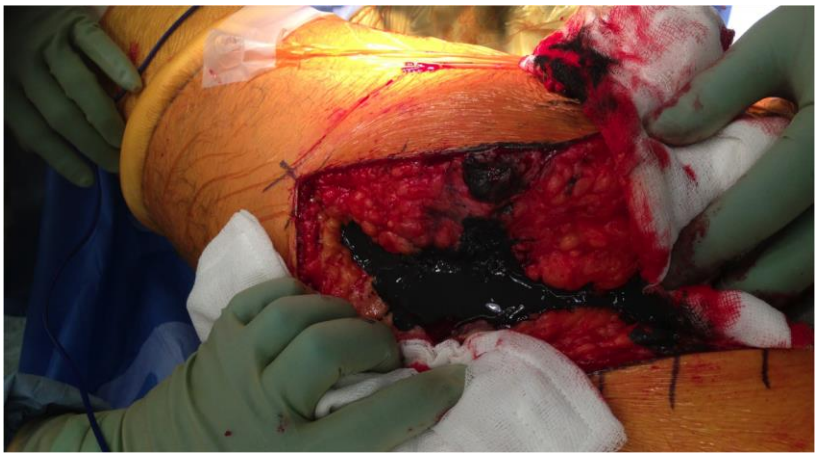

Figure 2.5: *Intra-operative image demonstrates substantial soft tissue metallosis extending from the scar down to the hip joint*

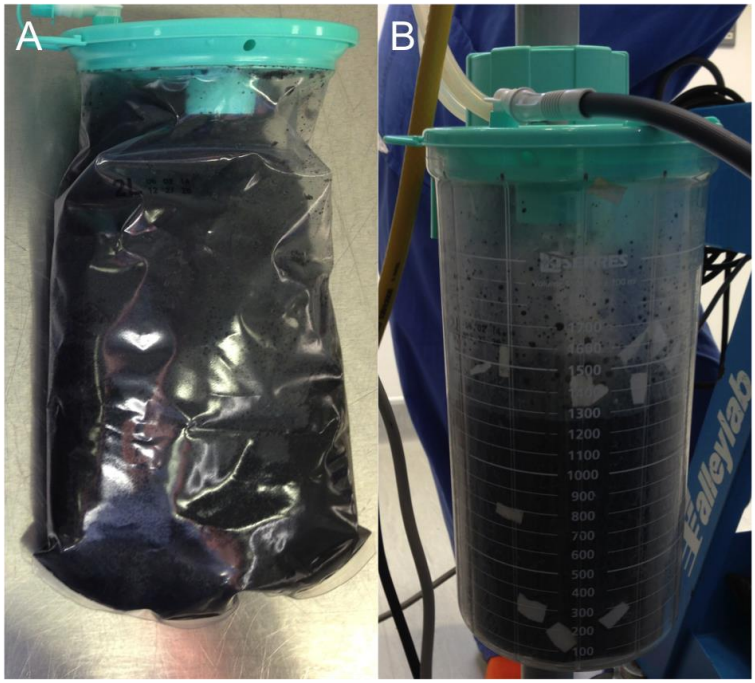

Figure 2.6: *A and B both demonstrate the fluid extracted from the hip joint during revision surgery. The fluid resembled thick oil like material*

Figure 2.7: *The retrieved metal head and plastic cup liner. Substantial deformation of the femoral head can be seen – normally spherical in shape*

His blood ion levels reduced after re-revision surgery but were sufficient to cause concern regarding potential cobalt cardiotoxicity as reported in the literature [12] [13] [152] [153] [156] [157] [167], and he was therefore referred for cardiac assessment. Table 2.1. Of interest only four other cases have been reported with cobalt levels higher than 587.9ppb (table 1.2).

Date	Cobalt PPB	Chromium PPB
Pre-op	587.9	20.4
Jun-14	284.9	16.7
Aug-14	77.0	11.2
Oct-14	23.1	10.4
Dec-14	16.2	10.0
Jan-15	15.6	10.4
Jun-15	8.9	6.9

Table 2.1: Serial whole blood cobalt and chromium levels, before and after revision surgery

2.3 Aim

Based on this case we had heightened concern regarding metal deposition and metal toxicity, and set out to determine whether MRI can non-invasively diagnose tissue deposition of cobalt and chromium. We further set out to validate our findings through tissue sampling.

2.4 Magnetic Resonance Imaging

In light of the numerous case reports published in the literature, our primary concern given the blood metal levels seen in this case was the risk of cardiac toxicity. Cardiac MRI (CMR) is the gold standard for the analysis of cardiac volume and function. The additional T2* protocol has the potential to detect tissue metal deposition. In addition the same CMR protocol can be applied to surrounding structures, namely the liver, for assessment of patients suffering from haemochromatosis.

2.4.1 Imaging Protocol

The patient was referred to the Heart Hospital (University College London Hospitals) cardiac imaging centre, where a CMR scan was performed using a 1.5 Tesla Magnetic Resonance scanner (Avanto, Siemens medical solutions, Erlangen, Germany). The protocol routine includes imaging of the heart and the liver. Conventional volumetric assessment and gadolinium CMR imaging were performed. All acquisitions are obtained during breath holding in expiration.

Following standard survey images, breath-hold cine acquisitions in the ventricular long axis (VLA), short axis, horizontal long axis (HLA) and four-chamber planes are acquired to ensure accurate planning of the left ventricular short axis orientation. From these, a stack of short axis images parallel to the mitral valve and covering the entire heart is acquired.

Pre-contrast, myocardial and liver T2* single breath-hold ECG-gated multi-echo technique were acquired to generate eight (heart) and 12 (liver) images which were displayed as a map. (TR: 2msec, TE 2.59- 18.2 cardiac and minimum 0.99ms liver, slice thickness: 10mm, flip angle: 20°, field of view read/ phase: 400mm/75%). In addition, a T2 (presented as reciprocal, R2) measurement (FerriScan®) was performed through the middle of the liver in the transverse plane. CMR image analysis was performed off-line using commercially available analysis software (CMRTools).

Following the initial study, a further three identical but non-contrast serial scans were performed within a fourteen-month period.

2.4.2 CMR Results

Cardiac volumetric and functional assessments were normal in all studies. The myocardial T2* was also within normal limits ruling out the presence of myocardial ferromagnetic or paramagnetic metal. Table 2.2 and 2.3.

Marker	Value	Range		Indexed to BSA	Value	Range
EDV (ml)	142	159(117-200)		EDVi (ml/m^2)	63	81(64-99)
ESV (ml)	46	54(31-76)		ESVi (ml/m^2)	20	27(17-38)
SV (ml)	96	105(77-133)		SVi (ml/m^2)	43	54(42-66)
EF (%)	68	66(58-75)				
Mass (g)	127	146(108-185)		Massi (g/m^2)	56	75(58-91)

Table 2.2: *Full cardiac volumetric and functional assessment results by CMR April 2014 (Height 170cm; Weight 107kg; BSA 2.25)*

Scan Date	LVEF (%)	EDV (ml)	ESV (ml)	Mass (g)	T2* (ms)
Apr-14	68	142	46	127	29
Oct-14	66	139	47	122	24
Jan-15	60	143	58	129	36
Jun-15	65	145	51	113	27

Table 2.3: *Serial cardiac function and volume values with concurrent T2* values (myocardial T2* Lower limit of normal = 20ms)*

On the other hand the liver was found to have shortened signal decay by T2*, and R2 values at levels usually consistent with liver iron (Fe) overload was seen on all scans, Figure 2.8.

Figure 2.8: *Liver T2* maps. Left panel (A) shows the patient with a low T2* (dark blue), compared to a healthy volunteer shown in the right panel (B) with normal T2* values (orange/red)*

Despite normalizing blood Co and Cr levels over the 16-month period post revision, the first three MRIs suggested worsening liver involvement, with some improvement in the most recent scan. Table 2.4.

Scan Date	Liver T2* (ms)	Blood Co (PPB)	Blood Cr (PPB)
Apr-14	4.2	587.9	20.4
Oct-14	3.3	23.1	10.4
Jan-15	3.0	15.6	10.4
Jun-15	2.9	8.9	6.9

Table 2.4: *Liver T2* values with concurrent blood cobalt and chromium values (Liver T2* lower limit of normal = 6.3ms)*

2.5 Interpretation of Results

The liver T2* values suggest the presence of metal. At these levels, one would suspect the presence of iron, commonly seen in iron overload disorders such as hereditary haemochromatosis (HH). HH is a term used to describe a group of genetic disorders typified by excessive iron absorption, which can lead to progressive accumulation of iron in tissues and organs. The liver and heart are commonly affected. The underlying pathology arises through mutations that lead to a deficiency in Hepcidin. Hepcidin is synthesized by hepatocytes and acts to control plasma iron concentration by binding to and degrading ferroportin, which is the only known cellular iron exporter. In the presence of elevated plasma iron, hepcidin binds to ferroportin to stop both intestinal absorption of iron from enterocytes and iron release from hepatocytes [234].

Four types of HH exist, of which type 1 is most common and is determined by which protein involved in iron homeostasis is affected. Type 1 is divided in to two types. Type 1a affects the HFE gene and leads to a diminished production of hepcidin. The mutation results in a cysteine to tyrosine substitution at amino acid 282, referred to as p.C282Y. There is a high prevalence, however the penetrance of the disease is low. Another known genetic subtype is p.H63D mutation, which does not cause a significant iron overload, but can act as a cofactor in combination with p.C282Y, to lead to phenotypic expression of iron overload. This is known as compound heterozygosity (p.C282Y/p.H63D) or type 1b [234].

Diagnosis of HH is first made by blood biomarkers. This includes iron studies and liver function tests. Serum iron, total iron binding capacity and serum ferritin are commonly measured. An increase in serum ferritin concentration (>400μg/L in men) is suggestive of haemochromatosis.

If HH is suspected from blood results then DNA testing should be performed to investigate for the presence of a HFE gene mutation.

2.5.1 Blood Tests

All routine hematological and biochemical blood tests were normal throughout the follow up period, including liver function tests (ALP 71units/L (NR 40 -129); ALT 21units/L (NR 10 -50)) and ferritin levels (45μg/L; NR 30-400μg/L). Blood Co and Cr were very high and fell with revision, Table 2.1.

2.5.2 Hemochromatosis DNA testing

Restriction enzyme PCR revealed the patient to be HFE compound heterozygous for C282Y/H63D (type 1b), known to cause <5% of cases of hereditary hemochromatosis. With this mutation, iron loading is uncommon without a second co-factor such as alcohol abuse or hepatitis;[235] [236] and has previously always been associated with elevated serum ferritin and transferrin saturation levels (which were normal here). Combined review by hepatology and ferro-hematology teams concluded his abnormal liver MRI results were unlikely to be caused by iron loading despite the mutation.

2.6 Shortened T2*: Iron or Cobalt

In summary thus far, a patient with extremely elevated blood cobalt and chromium levels has changes on liver T2* images that would correspond to elevated liver iron. DNA testing has confirmed that he is a carrier of a gene mutation that classifies him as type 1b for Haemochromatosis. However his blood iron studies and his liver function tests are normal. To understand what was responsible for the abnormal T2* the patient was referred for an ultrasound guided liver biopsy to obtain a tissue sample for histological analysis.

2.6.1 Methods

Preparation of patient liver tissue sample

Liver tissue from the patient was analyzed. Tissue metal contamination avoidance (MCA) technique was used to prepare the sample since there were concerns that the process of fixing and sectioning could contaminate the tissue or alter the distribution and chemistry of any implant-derived wear debris. The sample was snap frozen at the time of sampling from the patient.

Sectioning was performed with quartz-tipped blades, spreading epoxy glue around the sections on the quartz slides and covering with 25 μm thick Kapton (a polyamide film) cut to size using plastic scissors.

Quartz slides were used to reduce the signal from the variable iron background in many regular glass slides. The section was cut at 5μm thickness for haematoxylin and eosin (H&E) staining and an adjacent section cut at 10μm. The cryostat and blade were cleaned with absolute alcohol before processing of the specimens.

Histological examination of the H&E stained sample allowed examination for the presence of metal and its likely location. This also enabled the architecture of the section to be determined so that the area to be mapped by the synchrotron beam could be reliably chosen (because unstained sections were aligned in the beam before analysis).

Synchotron Micro-XRF and Micro-XAS

To determine the exact location and chemical composition (speciation) of metal deposits within the tissue samples, micro-X-ray Fluorescence (μXRF) and micro X-ray Absorption Spectroscopy (μXAS) was performed on beamline I18 at Diamond Light Source (Harwell, UK) [237]. μXRF elemental mapping causes minimal sample damage, is sensitive to very low concentrations, and allows the

samples to be later treated by conventional histology techniques for co-registration. μXAS can then provide details on the speciation. The typical beam size was 4 x 4μm. Figure 2.9.

Figure 2.9: *Typical setup for Xray Fluorescence Spectroscopy. (source www.horiba.com)*

Two-dimensional maps of the elemental distribution in the samples were produced for all patient samples, typically covering a 400 x 400μm region in 4μm steps. The majority of maps were produced using an incident energy of 8 keV, which is sufficient to observe any residual Fe, Cr and Co in the tissue. EXAFS spectroscopy of the metallic deposits was measured at points of interest selected from the XRF map. Figure 2.10.

Figure 2.10: *Atomic model for the X-Ray Fluorescence Analysis method, where energy is emitted on displacment of an electron from the inner electron shell (K). (Source www.fischer-technology.com)*

2.6.2 Results

Light microscopy was used to perform a scout analysis for the presence of black spots typical of metal deposition. In total 4 areas were chosen to be mapped. Two areas were selected based on similarity to the adjacent stained histological slide, and a further two areas were selected based on blackspots visible though the light microscope. Figure 2.11.

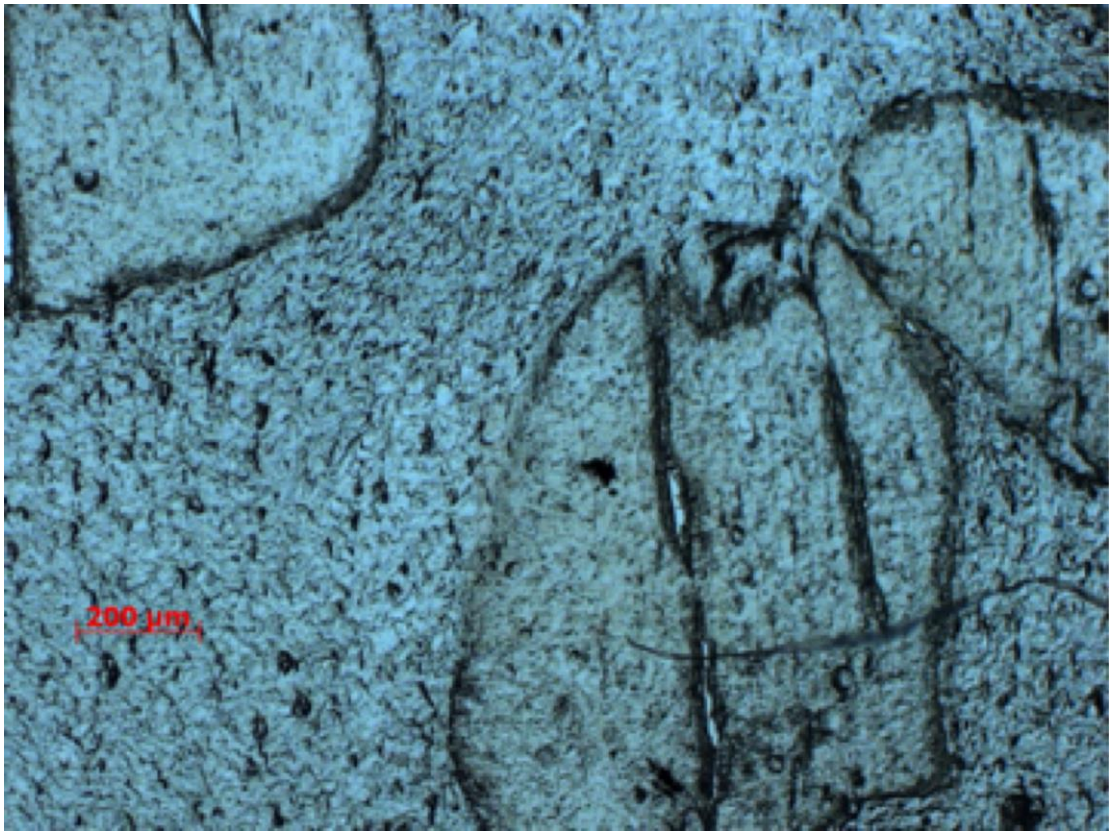

Figure 2.11: *10µm slice of liver tissue viewed under light microscope (x5 magnification)*

XRF was performed on the selected areas. XRF images for cobalt, chromium and calcium were included in the XRF maps as calcium helps to provide an image of the tissue from the XRF data which aids in registration of the images. Due to the concern of iron presence, stainless steel contamination and overlap between the K-beta of iron (energy = 7.059keV) and the K-alpha of Cobalt (6.931keV), XRF maps for iron have been included. Colour blending used in the maps do not represent relative concentrations – i.e. yellow is not a 50% CoCr particle. The colour maps are normalized concentractions – each element concentration is scaled to a 0-1 range and then overlayed. This helps to visually see the mixing of elements in Red, Green and Blue images.

Area 1

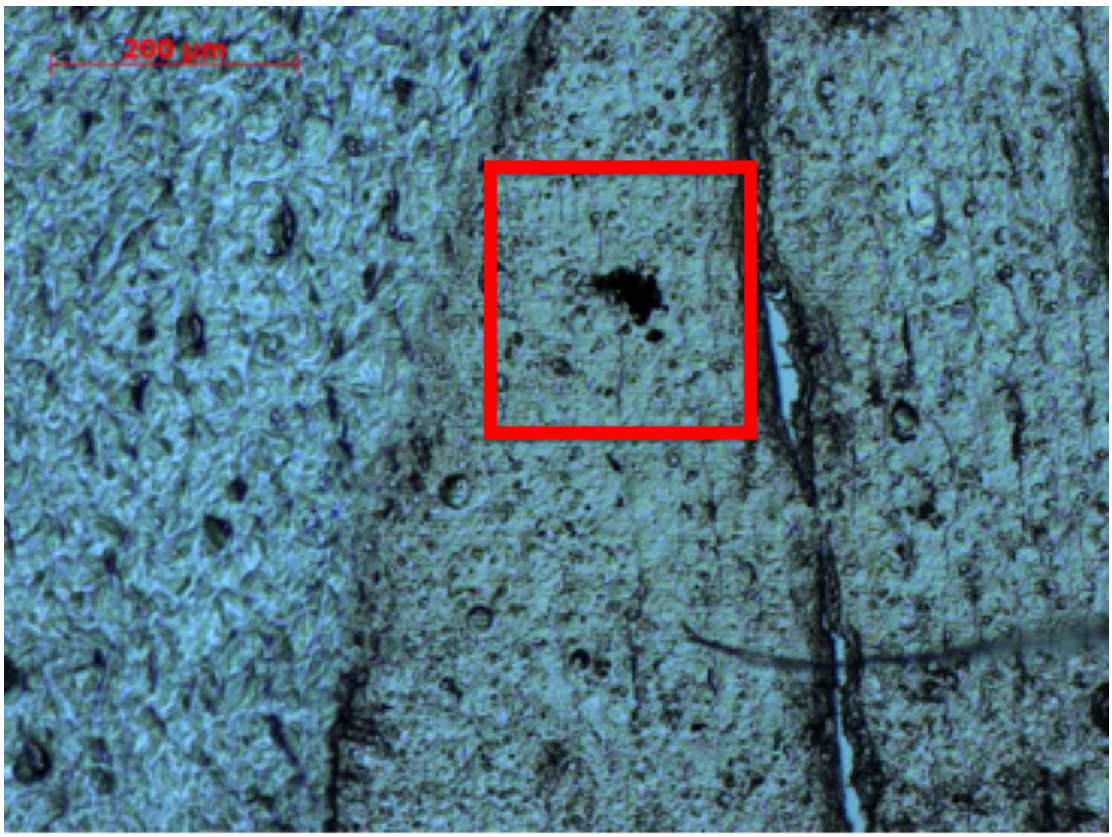

Figure 2.12: *Light microscopy image of area 1.*
A large blackspot can be seen as highlighted.
(x10 magnification)

Area 1 was selected due to a large blackspot suggestive of metal deposition within the liver, figure 2.12. The adjacent corresponding H&E stained sample correlated with this image, demonstrating metal deposits congregated in a small area, with several similar deposits in nearby tissue, figure 2.13.

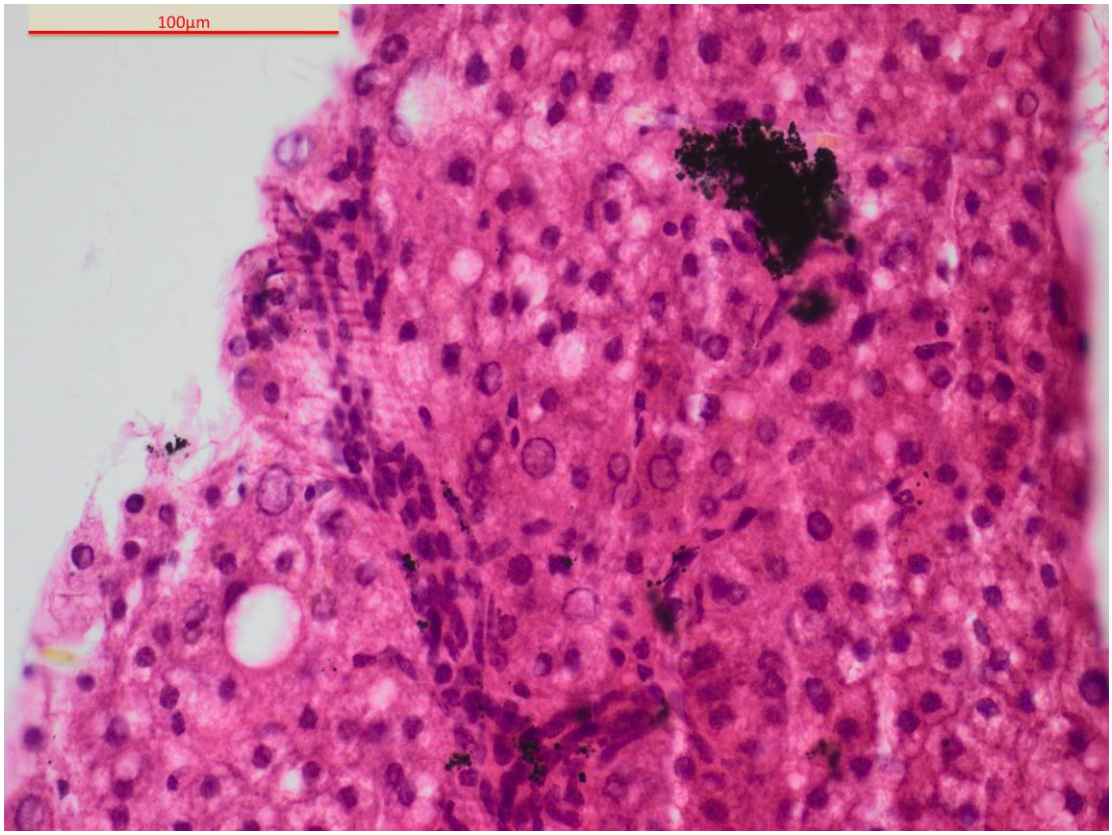

Figure 2.13: *Haemotoxylin and Eosin stained sample – adjacent tissue to area 1 (see figure 2.12). A large blackspot suggestive of metal deposition can be seen, seen to congregate within macrophages. Smaller black deposits can be seen at several other loci. (x20 magnification)*

XRF analysis for area 1 was performed and the output images are demonstrated in figure 2.14. The XRF analysis revealed abundant Co and Cr deposits within the tissue sample. No isolated cobalt or chromium spots were seen; instead the cobalt and chromium deposits are found together indicating CoCr particles. XRF for iron demonstrated no evidence of significant iron deposition, contamination from stainless steel in the sampling process, or a strong iron signal contributing to that of Cobalt due to K-alpha and K-beta overlap as mentioned above. The peak iron signal was 25 times weaker than that of cobalt. Co-registration of the maps visually correlated with the blackspots seen on the microscope image.

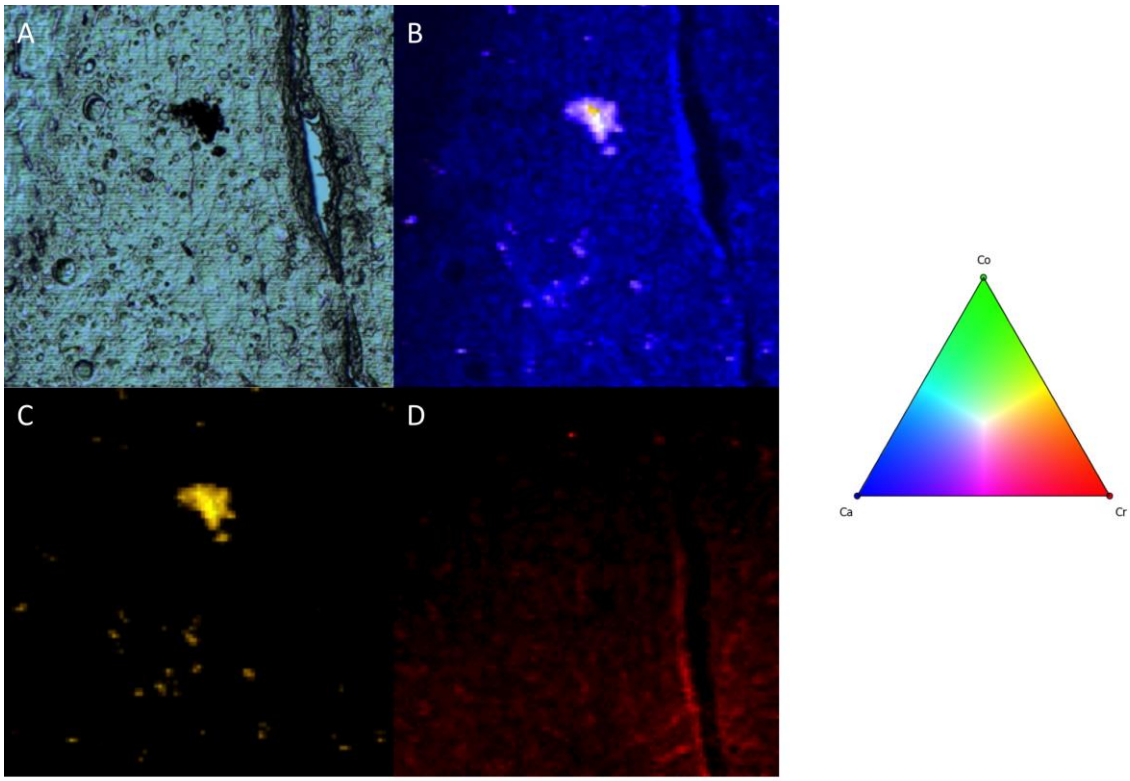

Figure 2.14: *(A) a 10x magnification of the mapped region (area 1), (B) XRF image of Cr, Co and Ca, overlaid. (C) XFF images of Cr and Co – note that there are no isolated Co and Cr deposits. The cobalt and chromium are seen together indicating CoCr particles. (D) XRF image of Fe distribution demonstrating the absence of iron contamination, deposition or Ka/Kb overlap with cobalt.*
(Legend: Colour blending used in the maps)

During XRF analysis the emitted counts measured by the detector were totalled and plotted to assess the correlation between the relative concentrations of cobalt versus chromium. Pearsons correlation coefficient demonstrated a strong correlation between cobalt and chromium with a ratio of 4.47:1 (Co to Cr), r = 0.99. Figure 2.15.

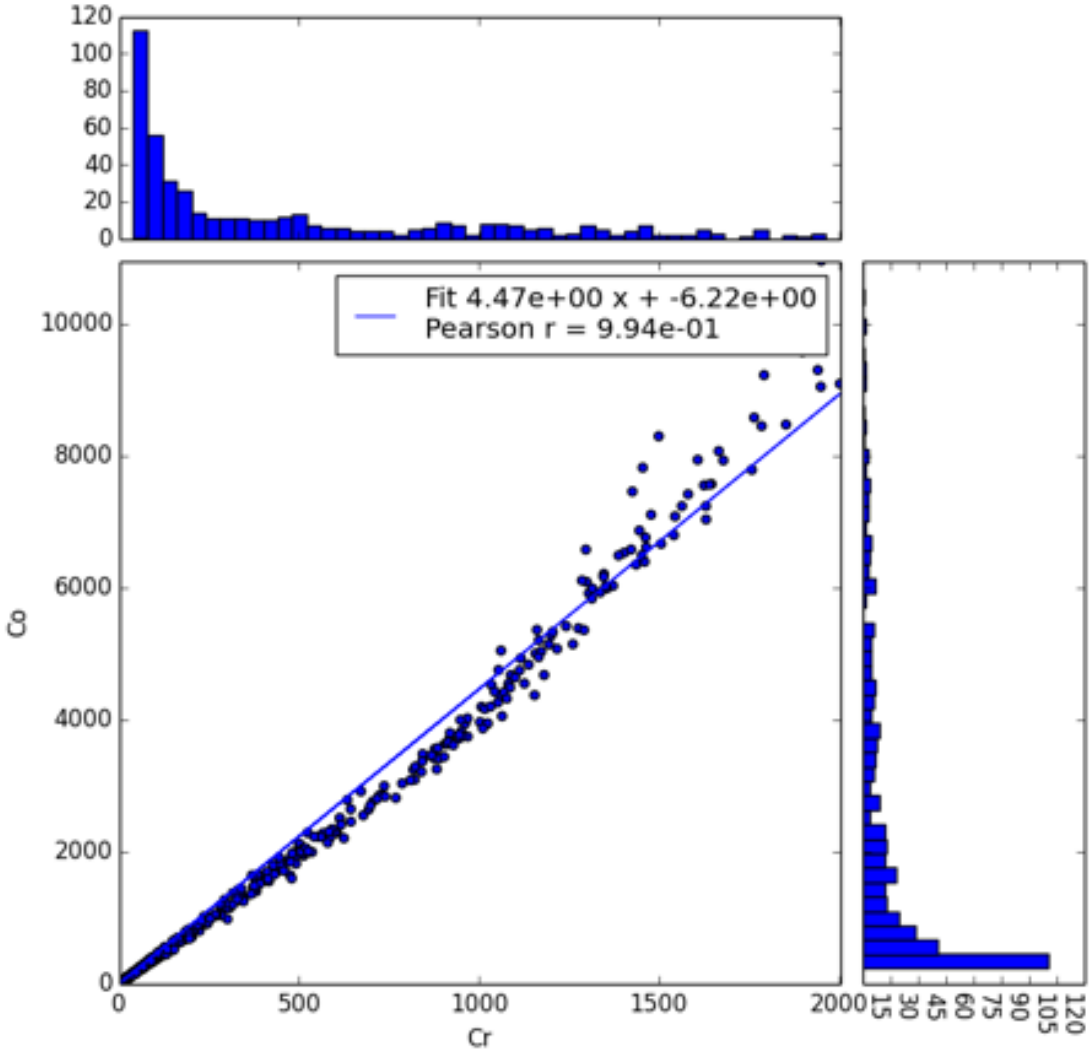

Figure 2.15: *Plot to demonstrate the Co and Cr signals across mapped area 1 are strongly correlated and demonstrate co-localisation between cobalt and chromium with a 4.47:1 ratio of Co to Cr*

Area 2

Area 2 was selected due to small areas suggestive of metal deposition within the liver. The adjacent corresponding H&E stained sample correlated with this image, with several similar deposits within tissue. Figure 2.16.

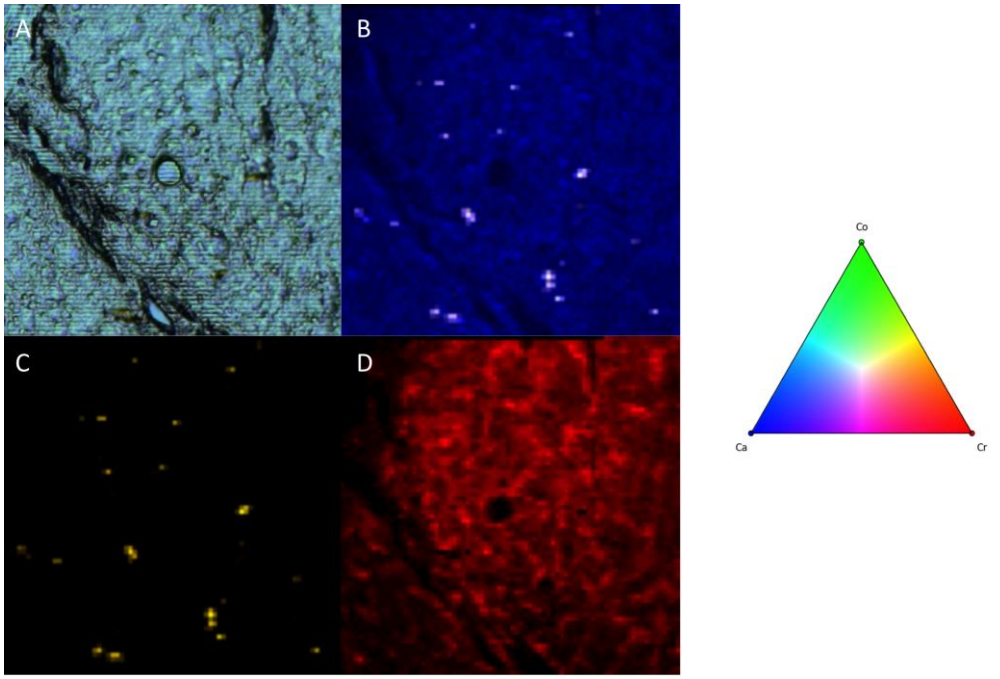

Figure 2.16: *(A) Microscope image of the chosen and subsequently mapped region (area 2); (B) Overlaid XRF images of Cr, Co and Ca where the calcium signal is included to aid registration of the image by helping to demonstrate the underlying tissue from the XRF data; (C) XRF images of Cr and Co, with colour blending to give a yellow signal; (D) XRF image of the iron distribution showing there is no stainless steel contamination, or strong iron signal contributing to the XRF due to Ka and Kb overlap. (Legend - colour blending used in the maps)*

The XRF analysis revealed several small loci of co-registered cobalt and chromium deposits, neither of which were in isolation, suggesting CoCr particle deposition. The peak iron signal detected was 51x lower than the peak Co signal detected from the sample. The signal from the cobalt and chromium were strongly colocalised at a ratio of 4.13:1 as seen in figure 2.17, r=0.997.

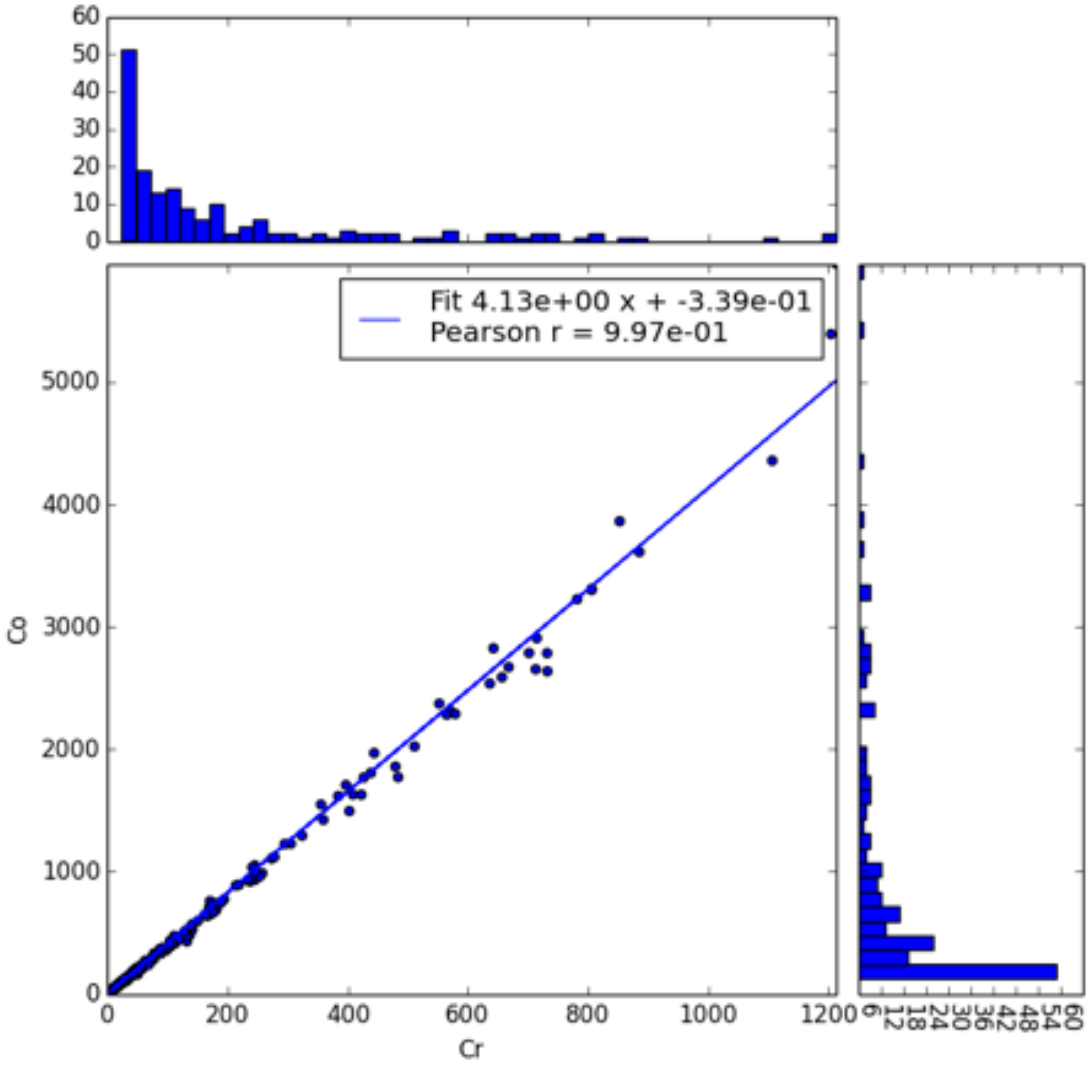

Figure 2.17: *Plot to demonstrate the correlation between cobalt and chromium signal detected from area 2, demonstrating a strong correlation and co-localisation between cobalt and chromium at a ratio of 4.13:1 (Co to Cr)*

Area 3

Area 3 demonstrates a series of small areas typical of metal deposition within the liver. Figure 2.18.

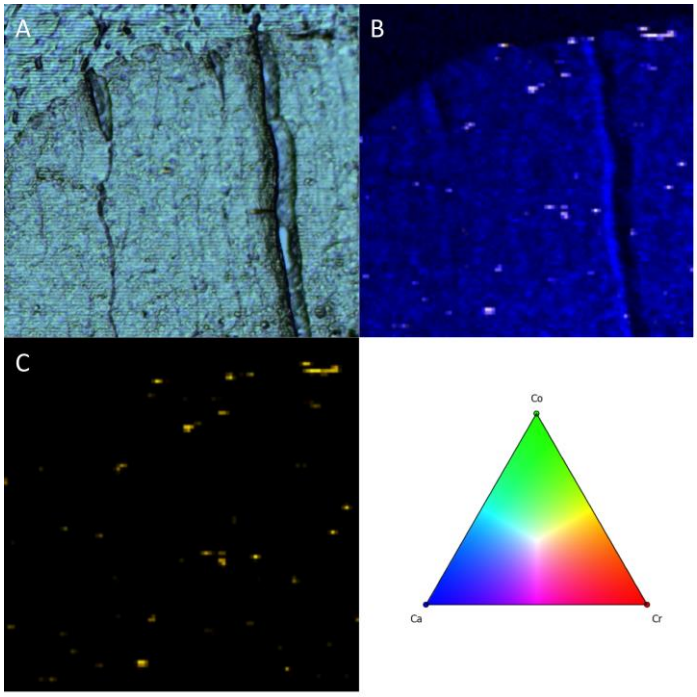

Figure 2.18: *(A) 10x magnification of the mapped region only (area 3); (B) XRF images of Cr, Co and Ca. The calcium signal is included as it helps to provide an image of the tissue from the XRF data which aids in registration of the images; (C) XRF images of Cr, Co – Note that there are no isolated Co or Cr spots. The Co and Cr are found together indicating a CoCr particles.*
(Legend - colour blending used in the maps)

The XRF analysis revealed several small loci of co-registered cobalt and chromium deposits, neither of which were in isolation, suggesting CoCr particle deposition. The signal from the cobalt and chromium were strongly co-localised at a ratio of 4.16:1 as seen in figure 2.19, r=0.997.

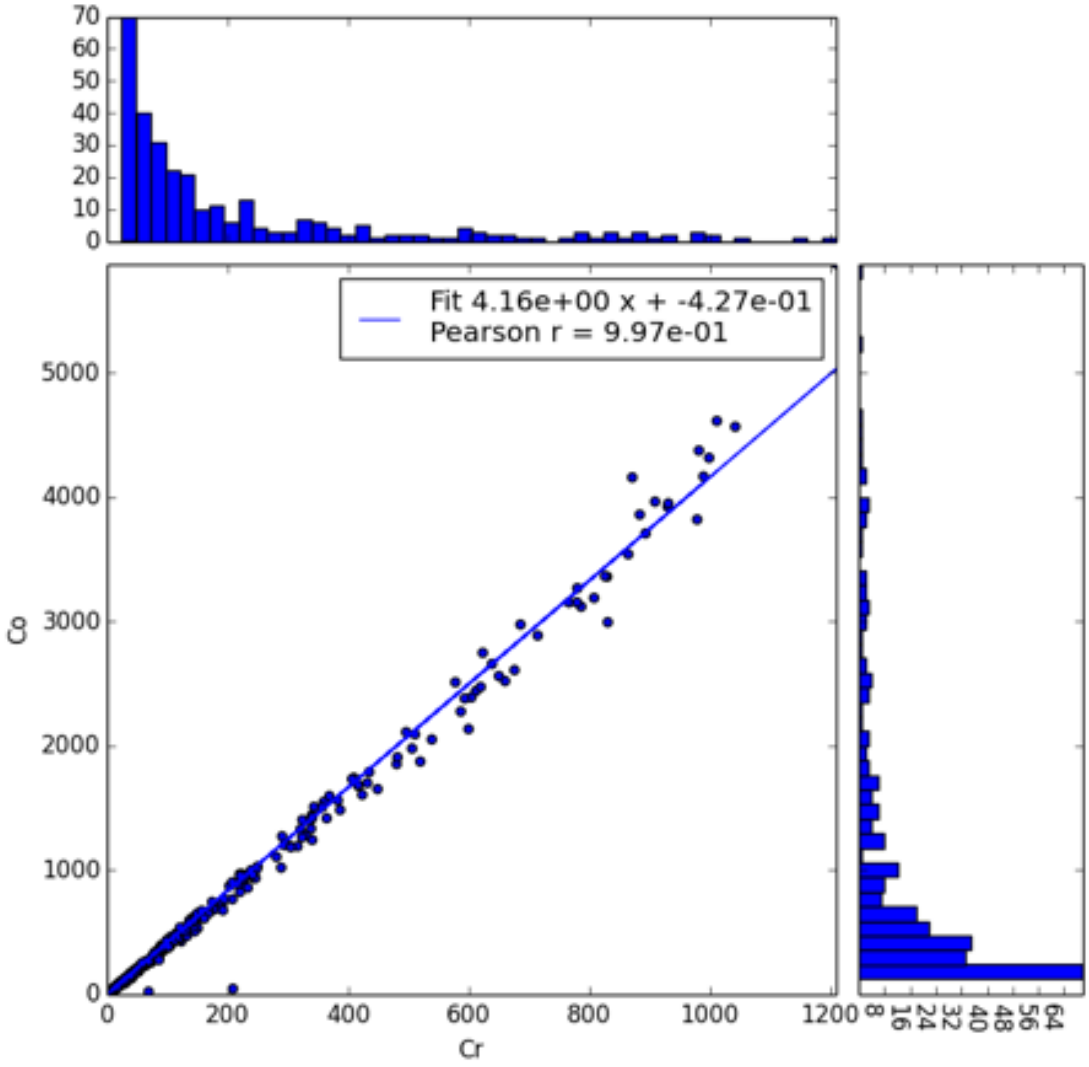

Figure 2.19: *Plot to demonstrate the correlation between cobalt and chromium signal detected from area 3, demonstrating a strong correlation and co-localisation between cobalt and chromium at a ratio of 4.16:1 (Co to Cr)*

Area 4

Area 4 was selected due to a large blackspot suggestive of metal deposition within the tissue. XRF analysis for area 4 was performed and the output images are demonstrated in figure 2.20. The XRF analysis revealed abundant Co and Cr deposits within the tissue sample. No isolated cobalt or chromium spots were

seen; instead, as above, the cobalt and chromium deposits are found together indicating CoCr particles.

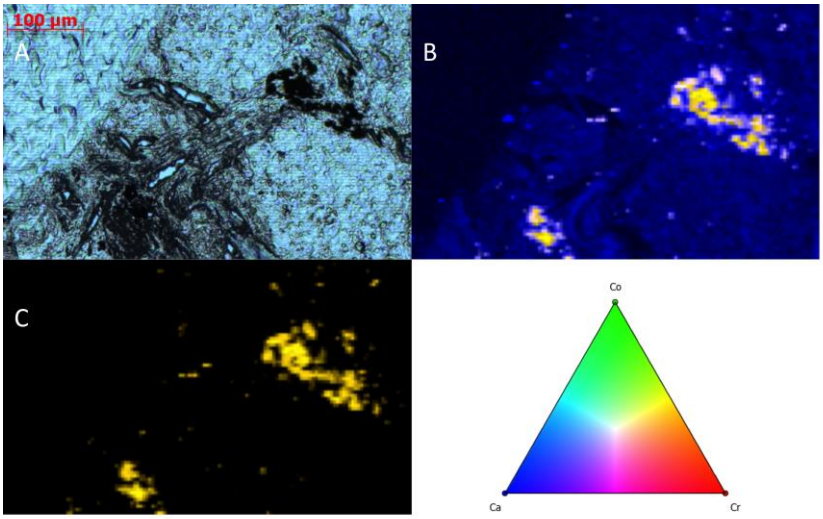

Figure 2.20: *(A) 10x magnification of the mapped region only; (B) XRF images of Cr, Co and Ca. The calcium signal is included as it helps to provide an image of the tissue from the XRF data which aids in registration of the images; (C) XRF images of Cr and Co – Note that there are no isolated Co or Cr spots. The Co and Cr are found together indicating CoCr particles.*
(Legend - colour blending used in the maps)

Correlation between the Cobalt and Chromium signal revealed a strong association between the cobalt and chromium signal showing a 3.97:1 Co to Cr ratio throughout the sample. The cobalt and Chromium signals were co-locatlised suggesting CoCr particles rather than isolated cobalt or chromium, r=0.998. Figure 2.21.

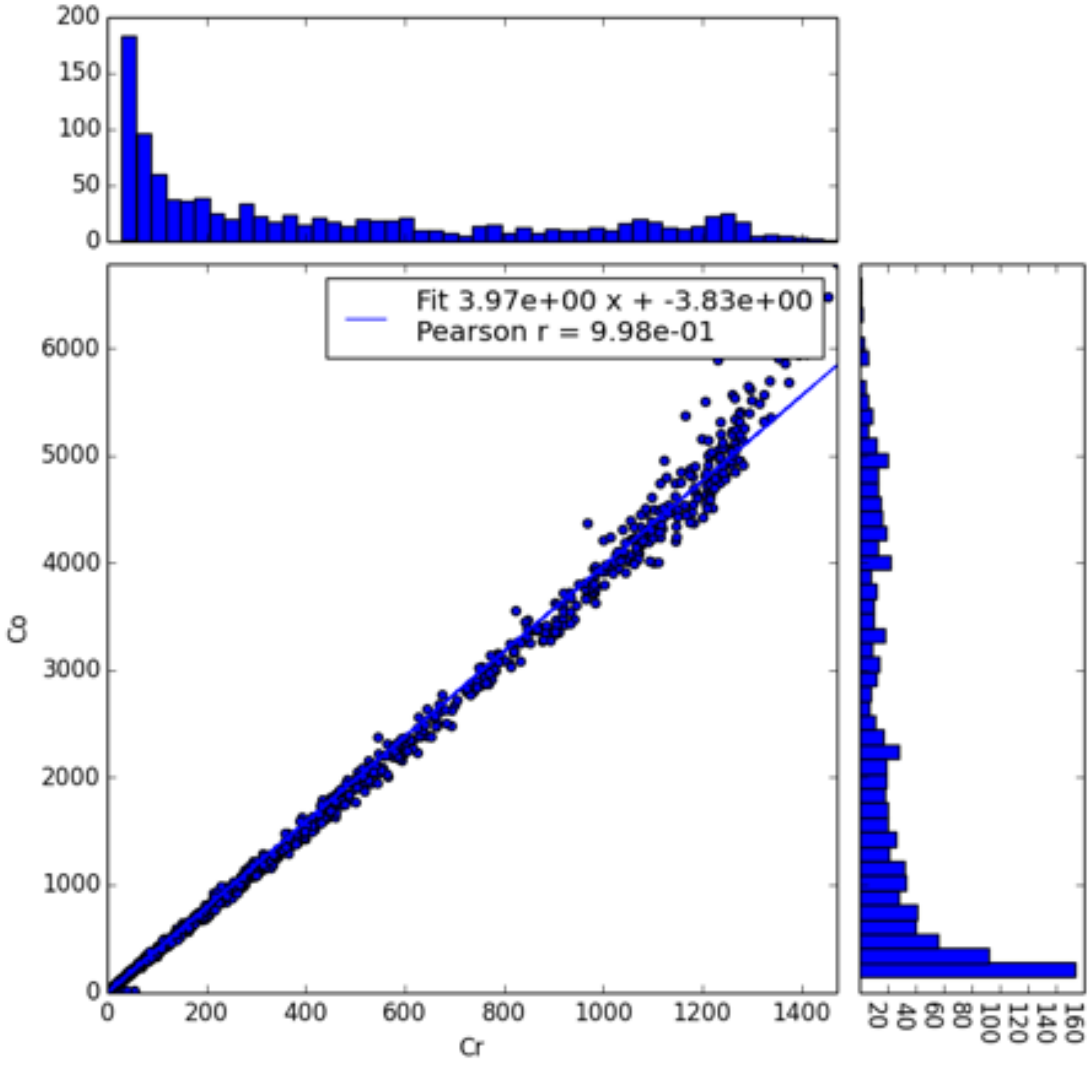

Figure 2.21: *Correlation of Co and Cr in tissue sample (area 4) showing a 3.97:1 ratio of Co to Cr and strong colocalization of the Co and Cr throughout the sample*

2.7 Interpretation of Results

XRF and EXAFS Spectroscopy revealed an abundance of cobalt and chromium within the liver tissue. The cobalt and chromium were highly co-localized. There were no examples of isolated cobalt or chromium indicating that this was particulate debris from the hip.

The particulates were cobalt rich. The observed ratio of cobalt to chromium was approximately 4:1 which is considerably larger than the 2.25:1 ratio found in the source hip metal (ASTM F75 alloy typically Co:Cr 2.25:1) so some loss of Cr has occurred. It has been previously demonstrated that peri-prosthetic hip tissue is chromium rich including isolated chromium particles, which would explain the loss of chromium in the particulates seen in the liver tissue [121] [122].

The spectroscopy scans of the cobalt and chromium spots are consistent with metallic CoCr particles. Chromium phosphate (CrPO4) or oxides as previously observed in the hip tissue samples were not observed here.

2.8 Discussion

This is the first description of MRI using T2* techniques to non-invasively detect and map liver cobalt and chromium. This finding has been validated through tissue sampling and characterization techniques. This patient had extremely elevated blood metal levels from a failed hip prosthesis with wear of the CoCr head. Liver biopsy followed by μXRF and μXAS confirmed CoCr debris in liver macrophages, with no other ferromagnetic material (including iron) deposits found. Serial T2* assessment in this patient suggested clearance from the liver was far slower than from the blood.

More than one million people globally have MoM hip prostheses and are “at-risk” of cobalt and chromium release. There is a high failure rate due to local soft tissue reactions causing pain and pseudotumors in response to metal debris in these patients. Implantation of MoM hips has now all but ceased. Cobalt and

Chromium release may also occur with other types of prostheses, seen here due to ceramic fracture - although improved surgical technique, implant design and materials are making this uncommon. In addition to local complications, there is concern from clinicians and patients alike regarding potential systemic toxicity from the high blood cobalt and chromium. Systemic organ deposition is hard to measure without invasive biopsy, meaning that currently available evidence is not always robust. This uncertainty coupled with medico-legal influences have fuelled patient anxiety, are driving some aspects of management, and highlight the need for non-invasive tests for systemic organ deposition.

This case illustrates that systemic deposition of cobalt and chromium in the liver can occur in subjects with extreme blood levels of metal secondary to failed hip implants, even without blood markers of hepatic abnormality. The absence of liver enzyme disturbance suggests that this patient tolerated the metal at least in the short term. The relationship of liver deposition/sequestration to other organ toxicity (heart, thyroid, spleen etc.) is unknown. The relative proportions of cobalt and chromium suggest progressive particle processing during the transport from the hip to the liver, although this mechanism remains unknown.

MRI tissue characterization using T2* measurement is currently routinely used to detect and quantify iron tissue deposition in the heart and liver in patients suffering haemochromatosis, with the pancreas, pituitary and kidney also potentially quantifiable. These techniques could also be repurposed for non-invasive screening of cobalt and chromium deposition in at-risk patients. To date, only non-specific qualitative abnormalities have been reported on cardiac

MRI scans in patients with biopsy-proven cobalt cardiomyopathy; the reported changes likely reflecting the myocyte response and inflammation rather than deposition. A non-invasive tool for cobalt and chromium organ deposition, if sensitive, would likely influence clinical decision-making. Whether the non-invasive detection as described here works only in extreme cases, or whether liver (or other organ) metal quantification may inform about risk in that or other organs is unknown.

The questions raised by this case surround the potential use of MRI to detect metal deposition within systemic organs. These questions include which patients would be most at risk? Who we should target? And whether a threshold metal ion level is available? At present, we cannot conclusively provide answers to these questions. However, the work set out in the remainder of this thesis will hopefully help us to understand this problem further.

CHAPTER 3

CHAPTER 3 MATERIALS AND METHODS

3.1 Introduction

Metal-on-metal hip implants have the potential to release metal ions upon wear of the component material. Some of the metal ions (e.g. cobalt and chromium) from the metal implant or from the metal wear particles will enter the bloodstream and be deposited / processed by distant organs such as the liver, as demonstrated in chapter 2.

The Food and Drug Administration (FDA, USA) have highlighted systemic toxicity from metal-on-metal hip implants as a cause for concern and recommended that patients with systemic symptoms be assessed. They draw attention to the cardiovascular, neurological, endocrinological (especially thyroid), and renal systems. [9]

A number of cases of suspected toxicity to circulating cobalt and chromium from MoM hip implants, including cardiac toxicity, have been reported [116 151-153 155 156 160]. See table 1.2. The most profound case involves a patient who died from cardiac failure secondary to cardiomyopathy with autopsy proven cobalt deposition within the cardiac tissues [18]. A recent cross sectional health screen [167] and isolated case reports, suggest that raised metal ion levels have the potential to cause cardiomyopathy and cardiac failure [12 152 153]. Such cases have raised public anxiety in the process [238].

Blood metal ions released from metal hip implants are increasingly recognized as a potential cause of local and distant abnormal tissue responses [79], since cobalt and chromium is released into the peri-prosthetic tissues and transported systemically throughout the body [5 64]. Component design and positioning are associated with increased wear and as a result raised metal ion levels [57 83 91-93]. However, a definitive causal link to systemic symptoms still remains to be established [239].

Iron overload disorders affecting the heart or liver represents a significant cause of morbidity in patients suffering primary and secondary haemochromatosis and thalassaemia. Excessive iron deposition within cardiac tissues can lead to premature death secondary to fatal arrhythmias and heart failure due to dilated cardiomyopathy [225-227]. Cardiovascular magnetic resonance (CMR) imaging has revolutionised the management of this particular group of patients by allowing a robust non-invasive method of detecting iron loading [23 227 228].

CMR is the gold-standard quantification of cardiac volumes and function with standardised protocols [240 241]. It allows repeatable scans with excellent spatial and temporal resolution, tissue characterisation using either contrast or non-contrast techniques to detect iron overload, focal scar and fatty infiltration [242]. Cardiac tissue iron is detected as a result of its effects on relaxation times through the interaction of iron with hydrogen nuclei in normal cardiac tissue [23]. Cobalt is a paramagnetic material, containing unpaired electrons allowing it to align in parallel to applied magnetic fields, and therefore is believed to have a similar effect as iron.

As demonstrated in chapter 2, transport and deposition of cobalt and chromium to the liver occurs in the presence of high circulating blood levels. MRI T2* protocols were shown to detect cobalt and chromium within the liver, albeit without clinical comorbidity. Based on published literature it is believed that similar deposition occurs within cardiac tissues in susceptible patients. What is not known is whether this happens in the majority of patients or just a small group of patients.

Given the lack of literature reporting liver toxicity, despite evidence of metal deposition as seen in the case discussed in chapter 2, the decision was made to continue with non-invasive tests alone without invasive tissue biopsies in study subjects. The main reason governing the choice to avoid invasive testing is the high risk of complications associated with obtaining tissue biopsy samples from patients, which would not have gained clearance from ethics boards or have been acceptable to patients.

3.2 Study Objectives

Primary Objective

To establish the effect on cardiac function as a result of metal ion release from metal hip implants as measured by non-invasive imaging and established biomarkers of cardiac toxicity.

Secondary Objectives

To apply novel T2* imaging protocols to assess for the presence of metal deposition within cardiac and liver tissues in a cohort of patients with varying blood metal levels.

3.3 Study Impact

It is estimated that approximately 60,000 patients were implanted with a MoM hip component in the United Kingdom alone, and over one million worldwide. Such a significant number of potentially at risk patients highlights the need to clarify this important question. With the published cases of systemic toxicity, circulating blood metal debris is the source of significant concern amongst patients and surgeons alike.

In addition, the problem of circulating blood metal is not unique to MoM hips. All hip implants have at least one metal component. As in the case described in chapter 2, and other case reports, high blood cobalt levels have arisen after catastrophic failure of a component (e.g. fracture of a ceramic bearing surface) leading to abnormal wear of the implant and release of metal ions into the body. To put this into context, over 80,000 hip implants are inserted annually in the United Kingdom.

3.4 Methods

The research received approval from the Institutional Review Board and Ethics Committee (reference: 14/LO/1722). The study was registered on ClinicalTrials.gov (NCT02331264).

Roles

For this study, I worked with Prof Hart, Prof Moon and Dr Manisty to prepare the design and methods to be employed. From here I applied for study sponsorship

through RNOH, and gained ethics approval following an application through IRAS to the ethics committee. I also applied for and successfully obtained funding from the Gwen Fish Trust and hospital charities. Once approvals and funds were obtained I personally led the recruitment of patients to the study and coordinated slots at the heart hospital for imaging. I supervised each study day and greeted patients. I cannulated each patient to gain vascular access to enable contrast injection and took all blood samples for troponin and BNP testing. A single trained sonographer conducted all ECHO studies and reported these studies whilst blinded to patient grouping. Dr Abdel-gadir and a team of CMR technicians acquired all CMR imaging. Images were stored anonymously and subsequently reported and analysed offline by Dr Abdel Gadir and myself, with Dr Manisty overseeing this process. Patient groupings were not revealed at the time of image reporting to ensure there was no reporting bias. Dr Palla provided statistical support during data handling.

3.4.1 Study Setting

A two-centre collaboration was established. The Royal National Orthopaedic Hospital (RNOH, University College London Hospital) hosted the study and was the base for patient recruitment and processing of the results. Patients were referred for all imaging procedures to be performed at the Heart Hospital (HH, University College London Hospital).

Between October 2014 and November 2015, patients were recruited from specialist outpatient clinics held at the Royal National Orthopaedic Hospital. See

patient recuitment (section 3.4.3 below) for details on how patients were identified and recruited based on inclusion criteria as set out below.

3.4.2 Study Design

In order to achieve the objectives a cross-sectional observational study was designed, Figure 3.1a. This involved the study of patients with MoM hip implants compared to patients with non-MoM hip implants.

Patients were divided into three groups based on prosthesis type and blood metal ion levels. For the non-MoM group, Ceramic on Ceramic (CoC) was chosen over Metal on Polyethylene couplings due to concerns regarding metal debris arising through trunionosis in the latter.

7 parts per billion (ppb) was used as a cut-off point as this represents the UK Medicines and Healthcare products Regulatory Agency (MHRA) recommended threshold above which there may be heightened concern [6].

- Group A: Patients with a CoC bearing implant with normal whole blood metal ion levels
- Group B: Patients with a MoM implant and low whole blood metal ion levels (<7 ppb)
- Group C: Patients with a MoM implant and raised whole blood metal ion levels (≥7ppb)

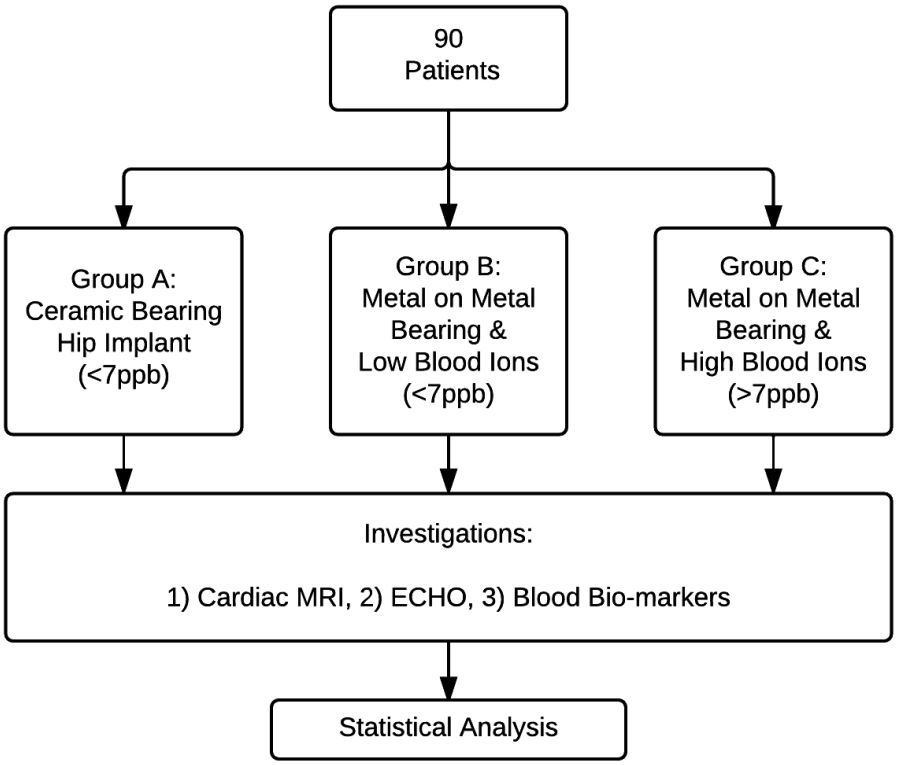

Figure 3.1a: *Study flow diagram highlighting patient groups and study design*

To satisfy our first objective a sub analysis was condcucted after combining groups B and C together to form a two-arm study with all the metal on metal hip patients combined into a single group. The combined group of metal on metal hip patients was then compared to the original group of ceramic on ceramic hip patients (group A). See figure 3.1b.

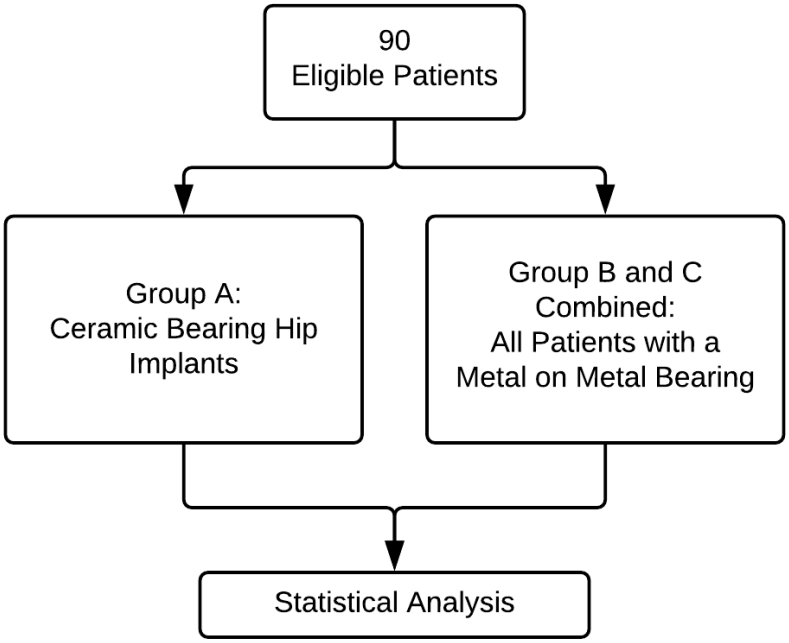

Figure 3.1b: *Subgroup analysis after groups B and C were combined to have all metal on metal hip patients in a single group*

3.4.3 Patient Recruitment

Patients were identified from RNOH clinic databases of patients with hip implants. Data in databases provided details of basic patient demographics, time since implantation and implant type, allowing for the identification of suitable patients. Patients were approached consecutively based on their time for clinic attendance, so long as their suitability was confirmed. Patients were approached during their routine outpatient clinic reviews.

Metal ion blood levels defined selection into MoM groups. Patients with two consecutive blood tests at the appropriate level and less than 10% variation (in

the last 12 months) were included, or those with a blood test at the appropriate level taken in the 3 months prior were included. Blood tests are a part of the patients normal clinical testing, and did not require additional testing.

Patients recruited to the control CoC group were recruited on the assumption that they had low metal ion levels. Formal blood metal ion level testing was performed during the research blood sampling.

Consent

All participants gave written informed consent conforming to the Declaration of Helsinki (fifth revision, 2000).

Consent to enter the study was sought from each participant only after a full explanation had been given, an information leaflet offered and time allowed for consideration. Signed participant consent was obtained on research and ethics committee approved consent forms. The right of the participant to refuse to participate without giving reasons was respected.

After the participant had entered the study, they remained free to receive alternative treatment to that specified in the protocol at any stage if they felt it was in their best interest as advised by the clinician. In these cases the participants remained within the study for the purposes of follow-up and data analysis. All participants were free to withdraw at any time from the study without giving reasons and without prejudice.

The confidentiality of participants taking part in the study was preserved at all times in line with the Data Protection Act 1998.

3.4.4 Inclusion and Exclusion Criteria

Inclusion and exclusion criteria were established based on the expected population that may have been treated with hip replacement surgery. In particular it was felt that patients with metal on metal hip components implanted within 12 months of the proposed study should be excluded due to the described bedding in period where steadily increasing blood ion levels are observed before they are seen to plateau [85] [86]. Only those with primary hip implants were included, and those with revised implants were excluded due to the uncertainty of the remaining implants and the nature of wear particles.

CMR imaging is ECG gated; therefore patients with known cardiac arrhythmias, such as atrial fibrillation, were excluded, as this would affect the imaging obtained from the scanner. Similarly patients with known contra-indications to MRI scanning were excluded. This included claustrophobia, inability to lay supine, and the presence of a pacemaker or other metal implants (brain / eye / ear / chest). Part of the reason here is the risk of artefact if metal is situated near the chest. Lastly, patients were asked whether they suffered any underlying renal disease and previous renal function was reviewed to ensure they were not at risk of deterioration secondary to intravenous gadolinium contrast agent used during scanning (estimated glomerular filtration rate <30mL/min).

Inclusion criteria

- Age over 18 years of age
- Either male or female

- Metal on Metal hip implant (ceramic on ceramic hip implant for patients within control group)
- Implanted greater than 12 months (i.e. beyond the bedding in period of the implant)
- Suitable for MRI scanning (no contraindications for Magnetic scanning - for instance metal implants in eyes/brain/heart, or claustrophobia)
- Consenting to the proposed research activity

Exclusion criteria

- Age below 18 years
- Metal hip implant not MoM (or CoC if part of group A)
- Not suitable to undergo MRI scanning (contra-indications or claustrophobia)
- Revised hip implant
- Atrial Fibrillation
- Poor renal function (eGFR<30)
- Failing to offer consent
- Vulnerable adults

3.5 Blinding

Recruited patients were invited to attend the Heart Hospital for all imaging and blood sampling to be undertaken. An MR technician conducted the MRI image acquisition and an ultra-sonographer undertook the echocardiograms. The

imaging technicians were blinded with regards to patient grouping, to ensure there is no bias when acquiring the clinical and cardiological investigations, particularly in light of the presence or absence of raised blood metal ions.

Acquisition of imaging datasets and subsequent analysis were undertaken separately. Imaging datasets were stored anonymously under a serial number unique to each patient. Patients were numbered consecutively regardless of grouping using CMR001, CMR002, CMR003 etc. Anonymous storage of scans allowed for the images to be analysed without knowledge of grouping and therefore free of bias. Un-blinding was performed only once all images had been reported and the study completed, for the purposes of statistical analysis.

3.6 Study Outcome Measures

To assess the effect of metal ions from hip implants on cardiac function as measured by CMR and ECHO. This involves the assessment of ejection fraction and tissue characterization (with and without intravenous contrast) and the detection of cobalt ion deposition within cardiac and liver tissues using methods described in chapter 2.

3.6.1 Imaging Modalities and Investigations

Patients underwent all imaging, investigations and data collection during a single visit. All data collection was performed at the Heart Hospital, London.

Magnetic Resonance Imaging

Patients underwent CMR at 1·5T (Avanto; Siemens Medical, Erlangen, Germany). Cardiac volumes and ejection fraction were calculated conventionally from short-axis cine images. Figure 3.2.

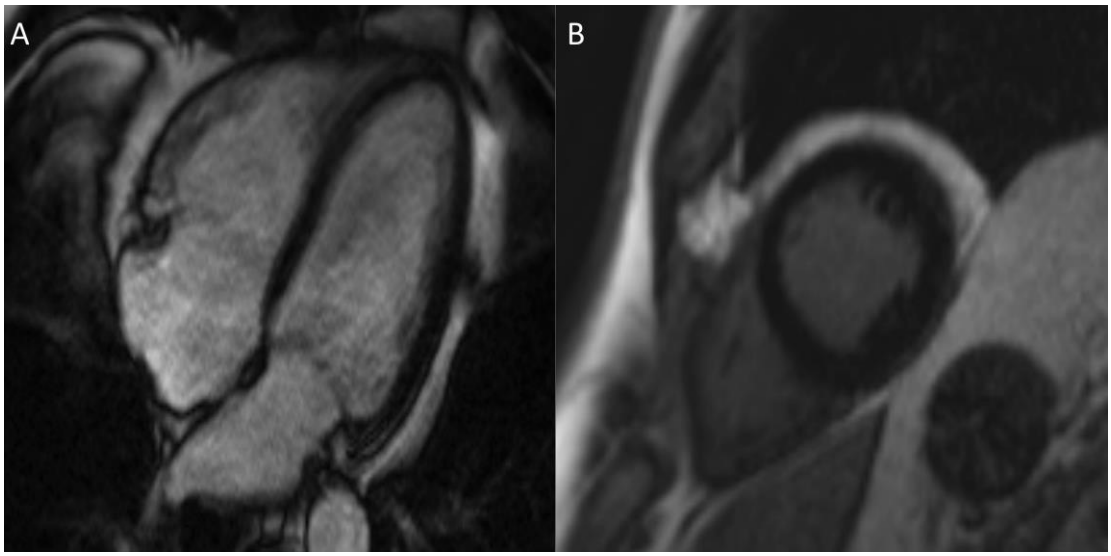

Figure 3.2: *Conventional (A) Long axis 4-chamber cine view, and (B) Short axis mid ventricular cine view used during cardiac volume and ejection fraction calculation.*

Bright blood T2* and pre-contrast T1 mapping of the myocardium and liver were acquired on a mid-left ventricular short axis slice (figure 3.2) and axial mid hepatic slice respectively. As T1 mapping is not fully standardized, two implementations – MOLLI and ShMOLLI sequences were used (Myomaps, Siemens).

Late gadolinium enhancement images were acquired using a motion corrected phase sensitive inversion recovery sequence to identify focal myocardial fibrosis after administering 0·1mmol/kg gadolinium-based contrast (Gadoterate meglumine - Dotarem, Guerbet SA, France). Gadolinium is a paramagnetic element and reduces the T1 time. Thus, T1 weighted sequences are used. The contrast to noise ratio using the inversion recovery principle (IR) effectively

nulls the signal from normal myocardium. The technique used for LGE consists of the acquisition of T1-weighted images after 15 minutes with an adequate inversion time (TI) to null the signal from normal myocardium.

In addition, post contrast injection T1 sequences were repeated for ECV quantification, figure 3.3.

Figure 3.3: *Pre and Post contrast T1 sequences used in the calculation of ECV*

Transthoracic Echocardiography

Echocardiography was performed using a Vivid E9 ultrasound machine (GE Medical, Horten, Norway). Measurements were made according to the British Society of Echocardiography standard protocol [243], including acquisition of standard 2D views, M-mode, spectral tissue Doppler and blood flow

measurements, figure 3.4. Qualitative and quantitative evaluation of chamber size and function is a major component of every echocardiographic examination. Chamber dimensions may be influenced by age, gender and body size and therefore where appropriate, data was indexed to body surface area.

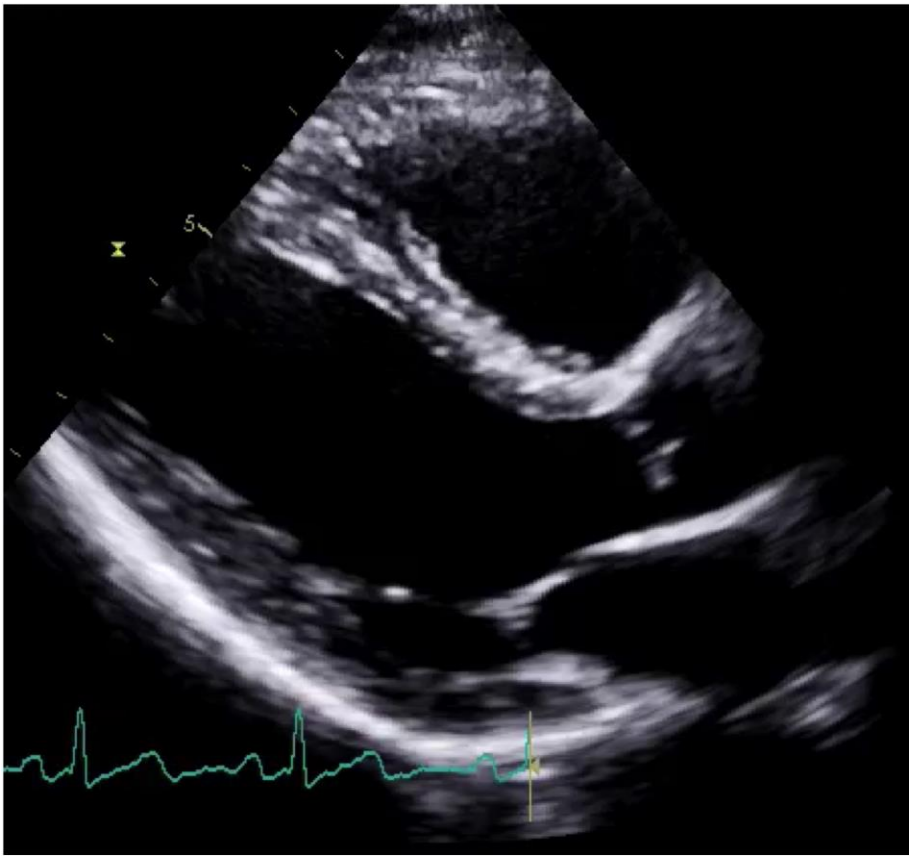

Figure 3.4: *Standard 2D cine view acquired by ECHO, demonstrating the Left Ventricular Outflow Tract (LVOT)*

Blood Biomarkers

Blood sampling was performed prior to patients undergoing CMR for B-type Natriuretic Peptide (BNP), troponin I, and whole blood cobalt and chromium levels. BNP and high sensitivity troponin are the most commonly used biomarkers in cardiology. They cover a range of cardiac processes – troponin

measuring myocyte death, BNP measuring myocyte strain. Both have prognostic significance and are a form of tissue characterisation.

The cardiac Troponin biomarkers, Troponin-I or Troponin-T, are highly specific and sensitive for cardiac injury. Cardiac Troponin provides the information needed for the evaluation of patients who present with possible acute ischemic heart disease. However cardiac troponin can be elevated in the absence of acute ischemic heart disease, such as in cases of congestive cardiac failure (acute or chronic), aortic valve disease, hypertrophic obstructive cardiomyopathy and hypertension [244].

B-type natriuretic peptide is released in response to cardiac stretch. The BNP values are helpful for the detection of congestive heart failure. For BNP, values <100 ng/l make heart failure unlikely with a negative predictive value of 90%. If the value is >500, heart failure is highly likely with a positive predictive value of 90% [244].

Whole blood cobalt and chromium were measured within the same UK reference laboratory to eliminate inter-laboratory variation, using inductively coupled plasma mass spectrometry (ICP-MS).

3.6.2 Outcome measures

Cardiac MRI

- Left Ventricular Ejection Fraction (%)

- End Diastolic Volume (EDV, ml) and EDV indexed (EDVi, ml/m^2)
- End Systolic Volume (ESV, ml) and ESV indexed (ESVi, ml/m^2)
- Stroke Volume (SV, ml) and SV indexed (SVi, ml/m^2)
- Mass (g) and Mass indexed (g/m^2)
- Mitral Annular Plane Systolic Excursion (MAPSE, mm)
- Tricuspid Annular Plane Systolic Excursion (TAPSE, mm)
- Left Atria area indexed (LA Area, cm^2/m^2)
- Right Atria area indexed (RA Area, cm^2/m^2)

MRI Tissue Mapping (Myocardium and Liver)

- T1 – MOLLI and ShMOLLI (ms)
- T2* (Bright Blood, ms)
- Late Gadolinium Enhancement
- Post Contrast T1 – Extra Cellular Volume (ECV)

Transthoracic Echocardiography

- Left Ventricular Ejection Fraction (LVEF, %)
- Left Ventricular End-Systolic Diameter (LVESD, cm)
- Left Ventricular End-Diastolic Diameter (LVEDD, cm)
- Left Atria Area (LA Area, cm^2)
- Right Atria Area (RA Area, cm^2)
- Left Atrial Volume index (LAVi, ml/m^2)
- Tissue Doppler Imaging Left Ventricle (TDI LV, m/s)
- Tissue Doppler Imaging Inter Ventricular Septum (TDI IVS, m/s)
- Tissue Doppler Imaging Right Ventricle (TDI RV, m/s)

- Global Peak Longitudinal Strain (GPLS, %)

Blood Biomarkers

- B-type Natriuretic Peptide
- Troponin I
- Whole Blood Cobalt
- Whole Blood Chromium

3.7 MRI based outcome measures explained

Ejection fraction is the volume of blood ejected from the ventricle during each heartbeat as a fraction of the total volume of blood within the ventricle at the end of diastole. It is an inherent measure of the pumping efficiency of the heart and is an important determinant of the presence and severity of systolic heart failure. The equation for LVEF is:

$$\text{Ejection Fraction (\%)} = ((EDV - ESV) / EDV) \times 100$$

A low ejection fraction is a marker of disease. However, it is important to stratify a measured ejection fraction with normal reference values for the age and sex of each patient, since LV volumes, mass and functions vary over a broad age range in healthy individuals. A cross sectional study of healthy volunteers used CMR to document the normal physiological variation of ejection fraction and other measures from adolescents to late adulthood [245].

Cardiac function, in terms of left ventricular ejection fraction, may be maintained in early cases of dilated cardiomyopathy, however cardiac chamber volume changes may preclude any functional affect. It is therefore important to assess for changes in ventricular volumes at various stages of the cardiac cycle, as these may be a predictor of cardiac disease.

Ventricular stroke volume (SV) is regarded as the volume of blood ejected per beat by the left ventricle into the aorta. This assumes, however, that all the blood leaving the ventricle is ejected into the outflow tract, which is not always the case (such as with atrioventricular valve regurgitation or an interventricular septal defect). Therefore, a more precise definition for SV and one that is used in imaging when assessing ventricular function is the difference between the ventricular end-diastolic volume (EDV) and the end-systolic volume (ESV).

The EDV is the filled volume of the ventricle immediately prior to contraction and the ESV is the residual volume of blood remaining in the ventricle after ejection. In a typical heart, the EDV is about 120 ml of blood and the ESV about 50 ml of blood. The difference between these two volumes, 70 ml, represents the SV. Therefore, any factor that alters either the EDV or the ESV will change SV. Therefore it is important to look at all these factors individually.

Patients with left ventricular (LV) hypertrophy have an increased incidence of cardiac events, including mortality. However, myocardial mass can vary in other disease states such as cardiomyopathy. It can be measured by echocardiography and CMR, however MRI is considered the ideal method for the determination of LV mass because of its high spatial resolution, generally good image quality, and ability to reconstruct the heart's shape in three dimensions. Some of the

structural changes seen in dilated cardiomyopathy, which can be associated with cobalt cardiac toxicity, emphasizes the need to assess for changes in myocardial mass in patients with metal on metal hip implants.

MAPSE (Mitral Annular Plane Systolic Excursion) represents the amount of displacement of the mitral annular plane towards the apex and thus assesses the global change in size of the LV cavity (in the long-axis direction). It can therefore be interpreted as the volume change during systolic ejection. It is closely associated with the left ventricular ejection fraction (LVEF), and has been described in different patient groups with normal or reduced LV function. Reduced long-axis deformation, and therefore MAPSE, results from dysfunctional or stressed longitudinal myofibres due to myocardial ischaemia, fibrosis, or increased wall stress [246].

The average normal value of MAPSE as derived from previous studies ranged between 12 and 15 mm and a value of MAPSE <8 mm was associated with a depressed LVEF (<50%) with a specificity of 82% and a sensitivity of 98%. A mean value for MAPSE of ≥10 mm was linked with preserved EF (≥55%) with a sensitivity of 90 – 92% and a specificity of 87% [246].

Similarly, TAPSE (Tricuspid Annular Plane Systolic Excursion) is a clinically useful measure of global RV function, which has been shown to have prognostic value in patients with right ventricular failure following myocardial infarction and pulmonary hypertension [247]. Normal reference range for TAPSE is between 15 and 20mm.

Given the varying reports in the literature about the degree of cardiotoxicty seen in terms of LVEF and the nature of structural damage seen, it is important to

assess for localised abnormalities. Therefore an assessment of the effect of circulating cobalt and chromium metal ions on MAPSE and TAPSE is undertaken here, and provides a further assessment of longitudinal myocardial function.

The remaining key cardiac measures to assess in terms of volumes and function are the areas of the right and left atria. Atrial enlargement is either the result of elevated atrial pressure or an increase in flow. However, the degree of left atrial enlargement depends on the compliance of the left atrial wall. Patients with fairly high atrial pressures can often have modest enlargement of the left atrium, or vice versa.

The right atrium is usually slightly smaller than the left side, and is largest in the superior inferior extension. To a certain degree the dimensions of the left atrium also influence the size and shape of the right atrium since an enlarged left atrium will "stretch" the right atrium. Enlargement of the right atrium may occur alone or may be combined with enlargement of the left atrium. In any case, atrial enlargement points to a disease process including cardiomyopathy.

To determine whether the atria are enlarged, the area measurement is indexed to body surface area. An indexed area <13 (cm^2/m^2) is considered normal, 13-16 is mildly enlarged, 17-20 is moderately enlarged and >20 is considered severe.

Refer to section 1.6.4 for details of tissue mapping using T1 (MOLLi and ShMOLLi).

Diffuse myocardial fibrosis, such as that seen in non-ischaemic cardiomyopathies, is difficult to distinguish using Late Gadolinium Enhancement since the myocardial signal intensity may be relatively isointense and may appear globally similar to normal tissue. Quantitative measurement of the myocardial tissue longitudinal relaxation time constant (T1) following administration of an extracellular Gadolinium-based contrast agent is sensitive to increased extracellular volume (ECV) associated with diffuse myocardial fibrosis. The ECV is measured as the percent of tissue comprised of extracellular space. ECV has been shown to correlate with collagen volume fraction, which is of interest as a diagnostic tool for non-ischemic cardiomyopathies.

T2* relaxation times can be shortened in the presence of tissue metal deposits. Cardiovascular magnetic resonance (CMR) imaging has revolutionised the management of haemochromatosis patients by allowing a robust non-invasive method of detecting iron loading [23]. Furthermore, this method has been shown to detect cobalt chromium (due to their paramagnetic properties) in chapter 2 of this thesis, and paves the way for a potential non-invasive method for detecting tissue metal deposits in patients with metal implants. This technique was applied to the 90 patients recruited to this study with the aim of detecting metal deposition within the myocardium and liver in patients with blood metal ions measured upto 118ppb.

The concept of LGE is based on the delayed wash in and wash out of gadolinium from tissue that has an increased proportion of extracellular space. Such as in the setting of an acute myocardial infarction, which is caused by cellular necrolysis

and edema, or in chronic infarcted tissue where the fibrous scar tissue consists of increased extracellular space. The increased amount of gadolinium can be demonstrated by T1-weighted imaging after approximately 10 minutes following contrast administration[248].

While LGE was originally developed to image ischaemic scars in acute and chronic ischaemic heart disease, it is also useful when imaging other forms of heart disease, mainly in the diagnosis of cardiomyopathies. Different kinds of cardiomyopathies exhibit different patterns of LGE. Other conditions include myocarditis and amyloidosis [248].

LGE is evaluated qualitatively by visual estimation, establishing a percentage of the thickness of affected myocardium in relation to the global wall, in order to define the extent of LGE. The patterns of enhancement vary according to the underlying disease process. In hypertrophic cardiomyopathy the enhancement tends to be located in the junction points of the RV and the septum, as well as in the subepicardium and mid-wall of the LV. With idiopathic dilated cardiomyopathy most patients will show no enhancement, whereas others may present with mid-wall hyperenhancement [248]. In a study by McCrohon*, et al.*, 13% of the patients with dilated cardiomyopathy and without significant coronary disease in the angiography showed an LGE pattern indistinguishable from that of the patients with IHD [249].

3.7.1 CMR Image Analysis

CMR technicians blinded to study groups performed all image acquisition. Datasets were stored anonymously under a serial number unique to each

patient. Image analysis was subsequently undertaken using standard techniques and dedicated software (CMRtools, Cardiovascular Imaging Solutions, UK) whilst maintaining blinding to group allocations. Un-blinding was performed once all data was acquired and analyzed, with the dataset locked.

Left ventricular (LV) volumes, ejection fraction (EF) and mass were calculated from CMR data using CMRtools. In order to calculate volumes and ejection fraction a ventricular model was used. Long axis 4-chamber and 2-chamber views and a standard short axis stack were selected. The apex was defined and the left ventricular long axis was identified on each stack image. Figure 3.5.

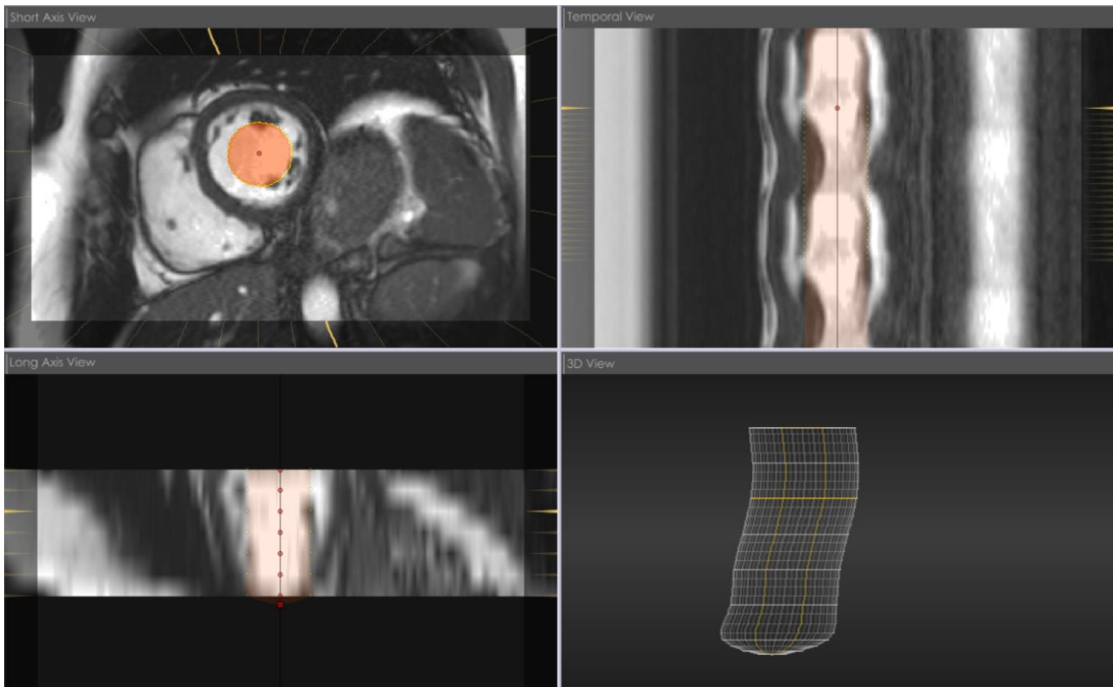

Figure 3.5*: Defining the left ventricular axis (red dot) using CMRtools.*

Once the axis was established, the left ventricular surface was defined during the diastolic phase, taking care to include the entire endocardium. This step was repeated on each individual short axis stack image. Figure 3.6.

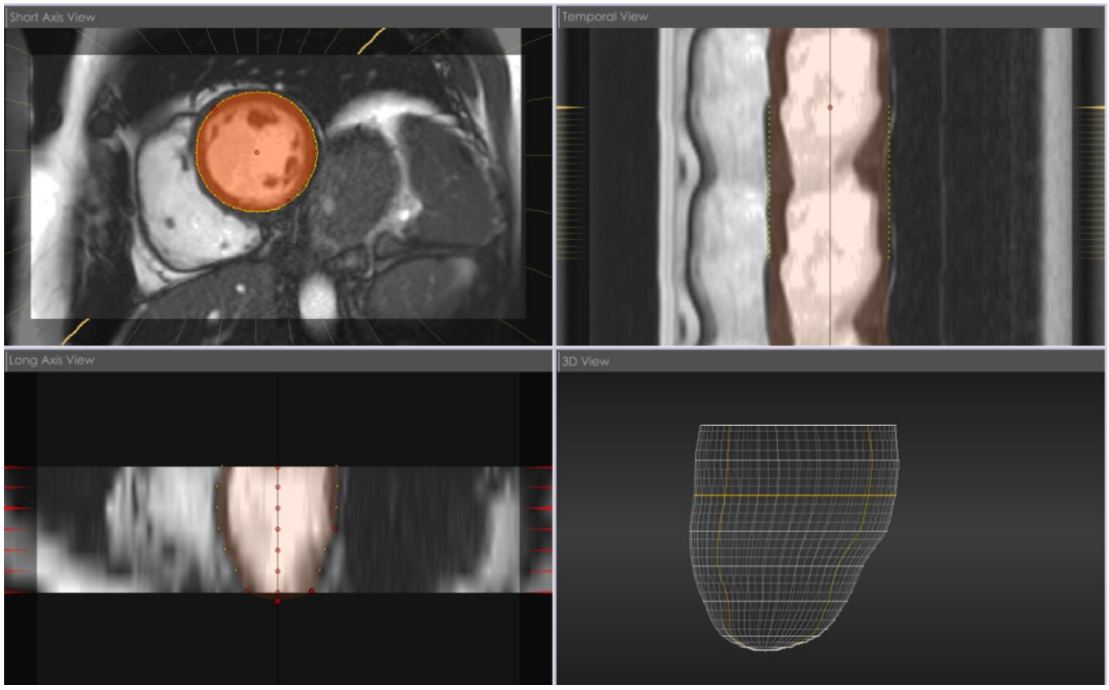

Figure 3.6: *The endocardium was defined during the diastolic phase*

Thresholding methods were used to define the blood pool. Papillary muscles were considered part of the LV myocardium. This stage was relatively subjective. Figure 3.7.

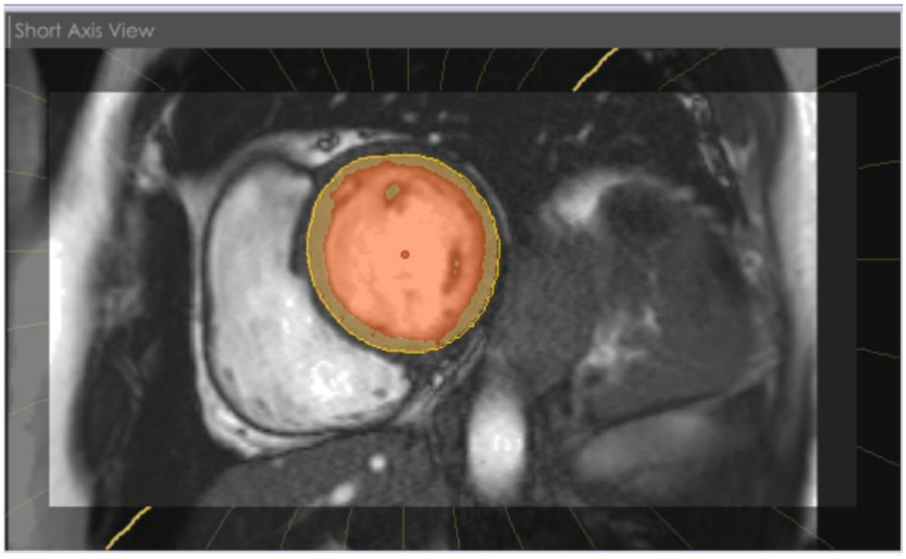

Figure 3.7: *Blood pool thresholding (including papillary muscles)*

Once the blood pool was defined, the valves were identified using markers in both diastolic and systolic phases. These markers were plotted on both the 4-chamber and 2-chamber views. Figure 3.8.

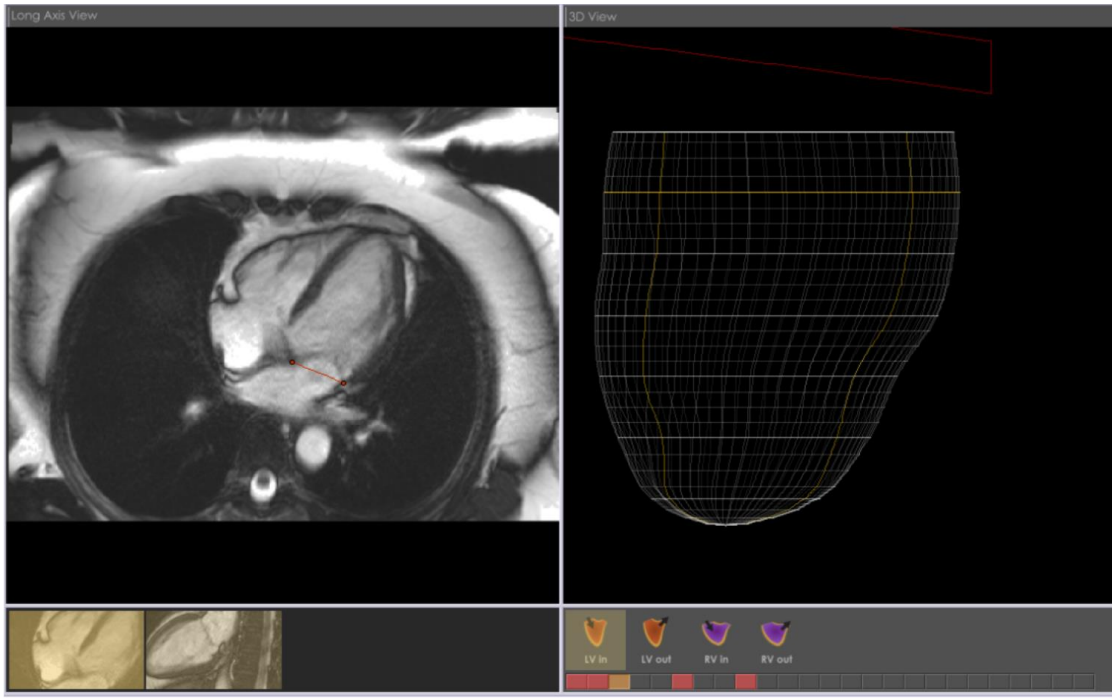

Figure 3.8: *Defining the mitral valve in both diastolic and systolic phases (red markers). This step is repeated in both 4- and 2-chamber views.*

These steps (excluding valve definition) were repeated during the systolic phase in order to establish final volume calculations. With the blood pool and LV endocardium defined, CMRtools calculated systolic and diastolic volumes, and subsequent stroke volumes and LV ejection fractions. Figure 3.9.

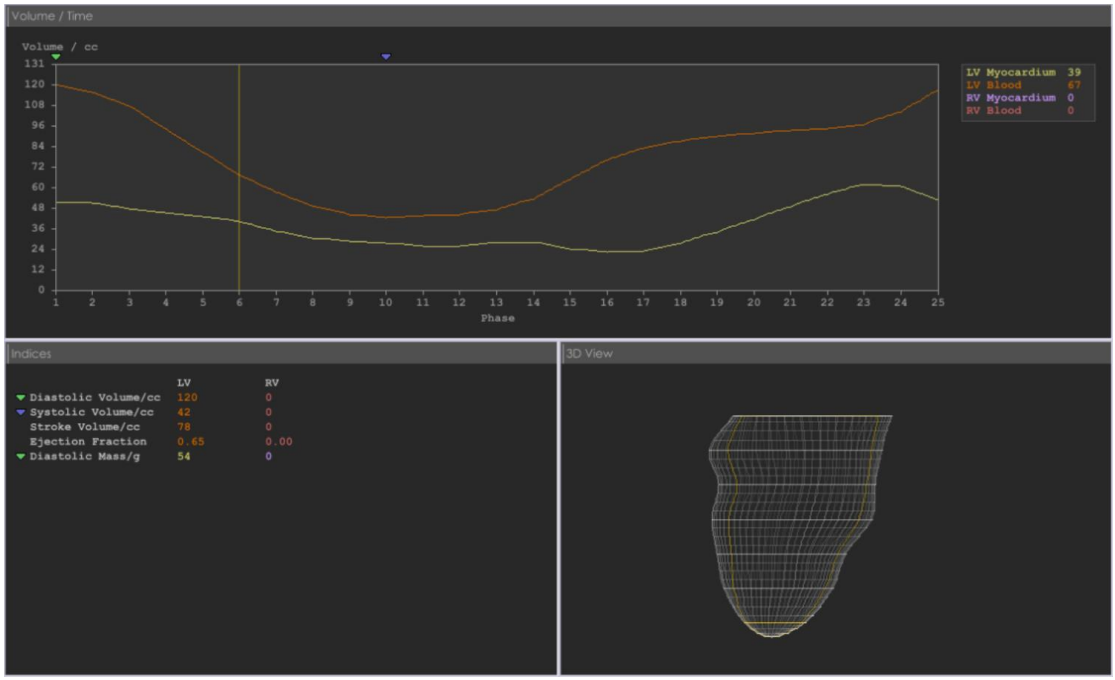

Figure 3.9: *Volume and ejection fraction calculation output from CMRtools*

Atria sizes were determined by mapping the atrial endocardial contours during the end systole stage of the cardiac cycle. The long axis 4-chamber view was used with the descent of the atrio-ventricular valve tracked to ensure maximal descent was selected and therefore maximal volumes of the atria were mapped. Areas mapped were subsequently indexed to body surface area.

For the purposes of calculating myocardial mass, the same steps were repeated, however the surface of the epicardium were mapped in order to calculate myocardial mass versus the blood pool. Volumes were subsequently indexed to body surface area.

In order to determine T2* times, a region of interest (ROI) was manually drawn on the interventricular septum on the mid ventricular short axis image, with care taken to avoid the endo- and epicardial contours to minimize partial voluming

effect. Figure 3.10.

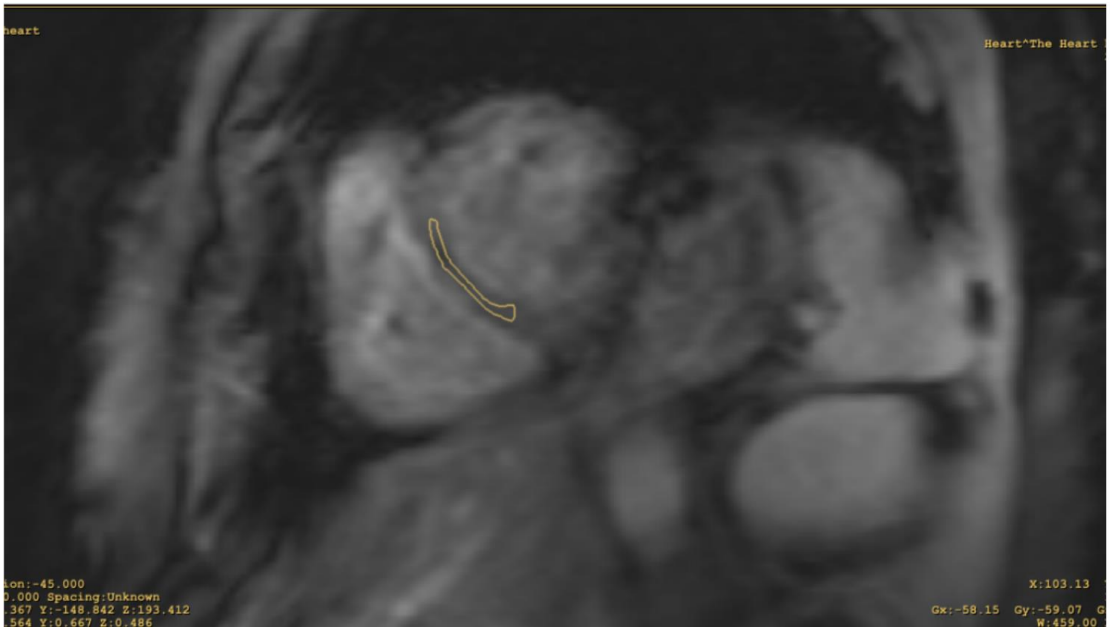

Figure 3.10: *ROI manually drawn on the interventricular septum of the mid ventricular short axis image for the purposes of calculating T2**

This ROI is then automated across all images in the short axis stack, and mean signal intensities are detected from these ROIs for each stack image. Figure 3.11.

SLICE 22						
PHASE	TIMING (ms	MEAN	AREA (mm2	STD	MAX	MIN
1	60.00	154.27	78.28	13.27	186.00	133.0
2	62.00	142.92	78.28	9.99	178.00	120.0
3	65.00	132.68	78.28	8.23	167.00	113.0
4	67.00	120.63	78.28	5.56	156.00	102.0
5	70.00	110.97	78.28	6.36	150.00	95.0
6	72.00	99.37	78.28	6.66	148.00	75.0
7	75.00	90.36	78.28	9.22	139.00	60.0
8	77.00	83.19	78.28	11.54	135.00	51.0

Figure 3.11: *Mean signal intensities calculated from the ROI within the interventricular septum for the purposes of calculating T2**

The T2* output data was then expressed as an exponential decay plot, from which the T2* relaxation time is determined. Figure 3.12.

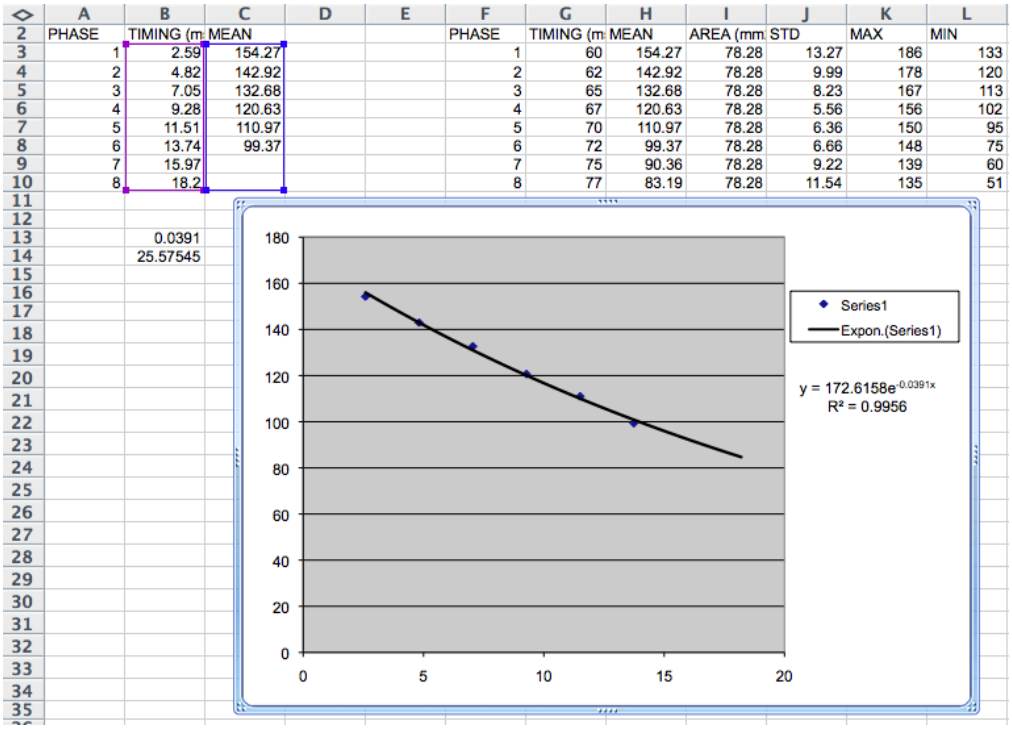

Figure 3.12: *Exponential decay curve plot for the calculation of T2**

Similar ROIs were drawn when calculating Liver T2* values. Care was taken to avoid blood vessels coursing through the liver. Figure 3.13.

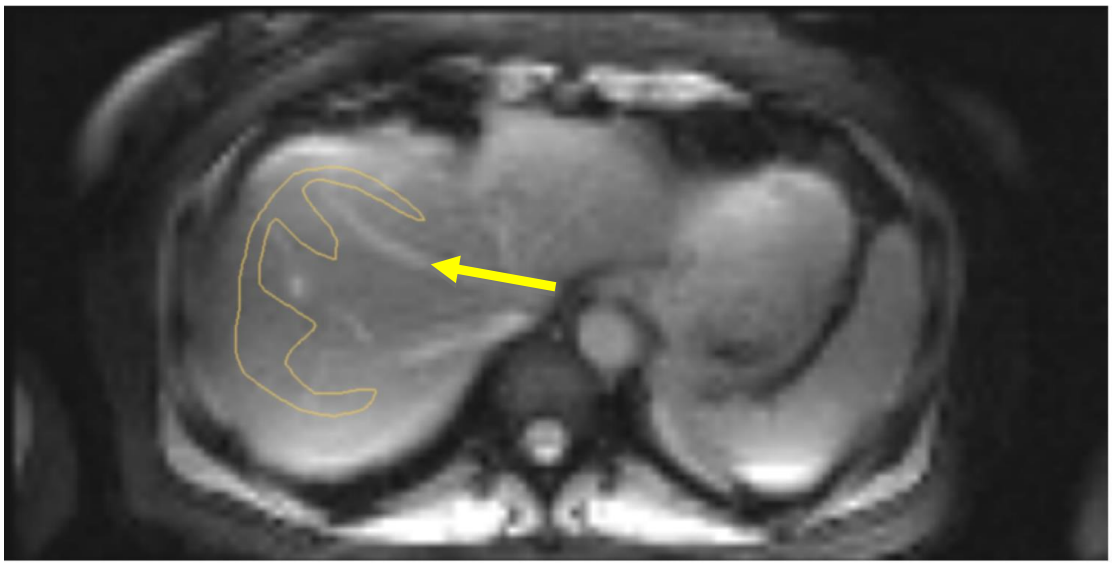

Figure 3.13: *Manually drawn ROI within liver parenchyma (yellow freehand line), avoiding blood vessels (white structure labeled with yellow arrow)*

T1 measurements were calculated similarly to T2*, where a region of interest (ROI) was manually drawn on the interventricular septum on each image, with care taken to avoid the endo- and epicardial contours to minimize partial voluming effect. Both MOLLI and ShMOLLI sequences were used, as T1 mapping is not fully standardized. T1 mapping was performed both pre- and post-contrast. Figure 3.14.

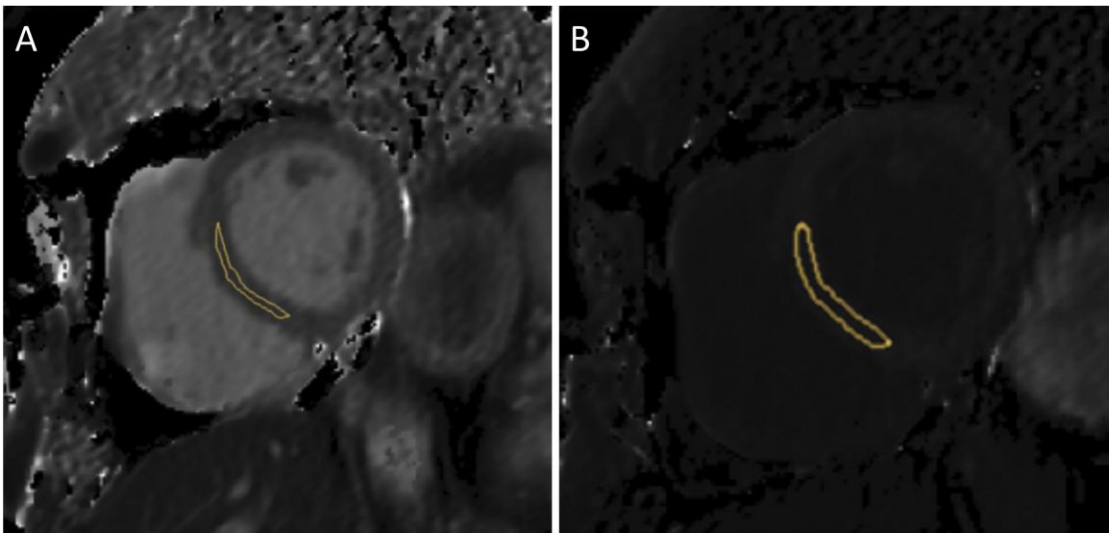

Figure 3.14: *(A) Pre-contrast ShMOLLI and (B) Post-contrast ShMOLLI sequences with ROI drawn on manually*

ECV was calculated using both pre- and post-contrast MOLLI values via a fully automated method that calculates pixel-wise ECV parametric maps [250], based on the standard formulae (figure 3.3):

$$ECV = (1\text{-haematocrit}) * [\Delta R1_{myocardium}] / [\Delta R1_{blood}]$$

(ΔR1 is change in R1 post to pre-contrast, and R1=1/T1).

Post contrast images were manually inspected for the presence of late gadolinium enhancement by visual assessment. This is similar to clinical

practice where LGE is evaluated qualitatively by visual estimation, establishing a percentage of the thickness of infarcted myocardium in relation to the global wall, in order to define the transmural extent of LGE. Quantitative assessments have been reported but can be variable.

3.8 ECHO Outcome measures and Image Analysis

Echocardiographic data was digitally stored for offline analysis with EchoPac dimension software (GE Healthcare, UK). A single ultrasonographer conducted all image acquisition and analysis. The technician was blinded to the group allocations throughout the process.

Conventional analysis of LV structure, systolic and diastolic function including spectral Tissue Doppler parameters were performed according to guidelines, with values averaged over two cardiac cycles. Tissue Doppler parameters for lateral and septal walls were averaged to produce a single marker of systolic longitudinal function.

With echocardiography, a different approach is taken to assess ejection fraction as the percentage of blood ejected from the ventricle during systole in relation to the total end-diastolic volume. Visually left ventricular function is judged on the basis of how much smaller the ventricle becomes during systole. In circumstances of impaired cardiac function, less blood will be ejected and the ejection fraction will fall. Ejection fraction is also a function of ventricular size. When the ventricle is large (in athletes, for instance), ejection fraction will drop. A small systolic reduction in ventricular size (and a relatively low ejection

fraction) will yield a sufficient stroke volume to perfuse the body. Conversely, when the ventricle is small, it will compensate by increasing its contractility. In this condition the ejection fraction will be higher than normal. During conventional echocardiography, left ventricular function is assessed at rest. Therefore the "functional capacity" and contractile reserve of the ventricle is not assessed.

The myocardium has a complex orientation of fibres, which leads to composite contraction in radial, circumferential and longitudinal directions, figure 3.15. Normal and coordinated functioning of these fibres is required for systolic and diastolic function, however this can be affected by various pathologies.

Figure 3.15: *Directions of contraction of myocardium (Adapted from 123sonography)*

There are several methods to measure ejection fraction using echocardiography, however unlike CMR these are reliant on geometric assumptions and can be an over or underestimation.

The first of these is a method called fractional shortening (FS), which does not estimate ejection fraction, rather a percentage size reduction as the equation computes distances rather than volumes.

$$FS = (LVEDD - LVESD)/LVEDD \times 100$$

The Teichholz formula can be used to calculate end diastolic and end systolic volumes from the end diastolic diameter and end systolic diameter respectively, after which ejection fraction can be computed as standard.

$$EDV = 7/(2.4+EDD) \times EDD^3$$

$$ESV = 7/(2.4+ESD) \times ESD^3$$

In addition to geometric assumptions, this method is reliant on adequate views and accurate measurements of diameters in diastole and systole.

An alternative method is the biplane Simpson method, which calculates ventricular volumes by drawing the endocardial outline of the ventricle. Based on the tracing, the system automatically performs a short-axis segmentation from the base to the apex by applying discs of known height and sums up the volume based on the diameter set by the initial segmentation. This is performed in both 4 chamber and 2 chamber views and also in diastolic and systolic cycles to account for the variation in the shape of the ventricle. This method avoids some of the geometric assumptions in the Teichholz formula, however some limitations apply, such as the assumption the discs are circular and the ventricle oval – which is not always the case. Figure 3.16.

Figure 3.16: *Simpson method applies circular discs of known height and diameter, from which ejection fraction can be calculated (adapted from 123sonography)*

Both the Teichholz and Biplane methods are used here and both sets of ejection fraction results are presented, using the ejection fraction formula as follows:

$$EF\ (\%) = (EDV - ESV)/EDV \times 100$$

Left ventricular (LV) size is standardly reported by measurement of the internal diameter in diastole (LVEDD) and systole (LVESD) in patients undergoing echocardiography. It is quickly and easily obtained in the majority of patients and provides important diagnostic and prognostic information. In some conditions, such as cardiomyopathy and valvular heart disease, the LV dimension is important for assessing severity.

Nevertheless, there are limitations of the LV diameter, which may be underestimated if the image plane or the measured diameter is poorly aligned. Variability between readers in terms of where the measure is made can result in inconsistent reporting, particularly if serial assessment is required. Finally, the LV diameter is a relatively crude and simplified assessment of a three-

dimensional structure, which cannot take into account more complex variations in ventricular shape or size.

However, there are particular circumstances where LVEDD alone is an important diagnostic and prognostic measure. Ventricular dilation may be an early marker of disease in patients with dilated cardiomyopathy. Therefore, ventricular dimensions determined by echocardiography continue to contribute to the standard minimum dataset during imaging studies [243].

The left atrium (LA) modulates left ventricular filling and cardiovascular performance by functioning as a reservoir and a conduit for pulmonary venous return and as a "booster" that augments ventricular filling during late ventricular diastole. LA also reflects LV filling pressure and is capable of remodeling (enlarging) in response to its elevation. Ultimately atrial enlargement is either the result of elevated atrial pressure or an increase in flow. However, the degree of atrial enlargement depends on the compliance of the atrial wall. This is why some patients with fairly high atrial pressures have only modest enlargement of the atrium, or vice versa. Myocardial scarring from conditions such as atrial fibrillation can lead to further dilatation. Disproportionate enlargement of the atrium (in relation to the ventricle) may be a pointer to the presence of myocardial disease. If atrial pressure is also high, the inter-atrial septum may be seen to bulge with simultaneous expansion of the left atrial appendage. The atrium may become quite sizeable, especially in mitral stenosis and restrictive cardiomyopathy.

There is a growing body of evidence demonstrating that LA enlargement is an independent marker of adverse outcomes both in primary and secondary cardiovascular prevention [251-253].

Regardless of the cause, it is important to evaluate the atrial dimensions when assessing for cardiac disease. In this section, right and left atrial dimensions are reported and the Left atrial volume is presented indexed to body surface area to account for natural variation.

This echocardiographic technique uses Doppler principles to measure the velocity of myocardial motion. TDI measures only the vector of motion that is parallel to the direction of the ultrasound beam, therefore Pulsed-wave TDI is used to measure peak myocardial velocities and is particularly well suited to the measurement of long-axis ventricular motion because the longitudinally oriented endocardial fibers are parallel to the ultrasound beam in the apical views [254].

To measure longitudinal myocardial velocities, the probe is aligned immediately adjacent to the mitral annulus Figure 3.17. The cardiac cycle is represented by 3 waveforms: (1) Sa, systolic myocardial velocity above the baseline as the annulus descends toward the apex; (2) Ea, early diastolic myocardial relaxation velocity below the baseline as the annulus ascends away from the apex; and (3) Aa, myocardial velocity associated with atrial contraction [254]. Figure 3.18.

Systolic myocardial velocity (Sa) at the lateral mitral annulus is a measure of longitudinal systolic function and is correlated with measurements of LV ejection fraction [254], for this reason results for TDI Sa are reported in this thesis.

Figure 3.17: *Probe alignment adjacent to the mitral annulus and directed for apical views parallel to the longitudinal axis (adapted from Ho et al [254])*

Figure 3.18: *The 3 basic waveforms of tissue Doppler imaging: Sa (systolic myocardial motion), Ea (early diastolic motion), and Aa (atrial contraction) (Adapted from Ho et al [254])*

An additional function of tissue Doppler imaging is the measurement of myocardial strain. Although LV systolic function is commonly defined by ejection fraction (EF), there are numerous technical and hemodynamic limitations to EF, for instance quantitative measurements are subject to endocardial border definition and formulas that make assumptions in geometry of the LV. The EF denotes global LV function and does not convey any regional differences in

function that may exist in patients with various cardiomyopathies. TDI, as discussed earlier in this section, will shed light on this potential issue.

An alternative technique for evaluating the LV uses the concept of strain or strain rate. This technique assesses the mechanics of the myocardium by measuring the relationship between 2 points within the myocardium. When the 2 points move away from each other (myocardial lengthening during diastole), strain values are positive. When the 2 points move toward each other (myocardial shortening during systole), strain is decreased, generating negative strain. Strain and strain rate can be derived from tissue Doppler imaging echocardiography. Using tissue Doppler, which is a form of pulsed Doppler, specific points within the myocardium can be identified. Tracking these Doppler points enables measurement of strain rate. Because Doppler is velocity or distance divided by time, the initial measurement is strain rate. Integrating the strain rate gives strain. LV global longitudinal peak systolic strain (GLPS) takes an average of sectional GLPSs and provides an assessment of global LV systolic function. Normal values of longitudinal strain lie between -20 and -25% [255].

3.9 Study Sample Size

Sample size calculations were based on prior published data. Prentice et al undertook a cross-sectional health screen at a mean of 8 years after surgery in 35 asymptomatic patients who had previously received a metal-on-metal hip resurfacing versus 35 individually age and sex matched asymptomatic patients who had received a conventional hip replacement (non-MoM). Using

Echocardiography they demonstrated that cardiac ejection fraction was 7% lower (mean absolute difference 5%, P = 0.04) and left ventricular end-diastolic diameter was 6% larger (mean difference 2.7 mm, P = 0.007) in the hip-resurfacing group versus those patients who received a conventional hip replacement. [167]

Using the absolute difference in ejection fraction of 5% (and the pooled standard deviation of approximately 8%) between patients with MoM and conventional hip prostheses we set alpha at 0·05 and required a 2:1 sample size ratio between MoM and CoC prostheses, which meant we needed 62 patients with MoM and 31 with CoC to have a power of 80% and to detect a 5% difference (Cohen's delta= 0.63). The MoM group was divided according to blood metal levels using 7ppb [6] as a cut-off (yielding approximately a 1:1:1 ratio overall across 3 groups).

3.10 Statistical Analysis

Pre-specified primary endpoints were EF (by CMR) and T2* measurement. Secondary endpoints included LV end systolic volume indexed, T1 and ECV measurements by CMR; EF and left atrial area indexed and LV long axis function (mean of lateral and septal S' velocities) by echocardiography and blood biomarkers.

The three groups were assessed for matching using chi squared tests (or Fisher's exact tests when the expected counts were <5) for binary variables and ANOVA test for continuous variables.

The distribution of the metal ions was not normal and the group variances highly heterogeneous, hence non-parametric tests on medians were used to compare ion levels between groups. We used parametric and nonparametric tests to establish whether there was a significant difference in the mean and/or median effect on cardiac function between the groups.

The distributions of the cardiac exposure variables in each group appeared normal for outcome variables of interest with the variance usually constant (Bartlett test) hence ANOVA (F test) was conducted for each marker. As the sample sizes were relatively small, a formal test for normality was not conducted but sensitivity analyses by non-parametric tests (comparing the median across groups) were performed to relax the parametric assumption and always confirmed the conclusions obtained for the mean. The presence of significant results at 5% significance level was further assessed dividing the threshold by the number of tests conducted (Bonferroni correction).

Correlations between whole blood metal ion levels and EF and T2* were calculated using Pearson's correlation coefficient (with metal ions log-transformed) and Spearman's correlation coefficient (metal ions on the original scale). The minimum detectable effect size was calculated using Cohen's d [256].

To fulfil the subgroup analysis, the statistical analyses described thus far were repeated for all outcome measures after combining groups B and C together to form a super group of all metal on metal patients compared to group A containing all the ceramic on ceramic hip patients.

All calculations were performed using STATA 14 (Statacorp LP, USA).

3.11 Participants

108 patients were recruited from specialist outpatient clinics held at the Royal National Orthopedic Hospital, from which 90 patients completed the study. Figure 3.19. Baseline patient characteristics are shown in Table 3.1.

Six patients were excluded due to arrythmias (e.g. atrial fibrillation). We could consider the exclusion of these patients a form of selection bias for potentially excluding patients with possible cardiac toxicity. However, of these six patients, four would have been assigned to group A (CoC), and one each to groups B and C, thus relaxing any concerns of selection bias here. Of the other exclusions, five failed to attend, four complained of claustrophobia on the scan day, two were unable to be scanned due to their body habitus and one patient was found to have a metal breast implant (marker for previous radiotherapy). Figure 3.19 details patient progress through the study.

Patients were matched for age and gender across the three groups; Group A (CoC) n=28; age 65·3 ± 8·8 years, 75% female; Group B (low metal) n=33; age 61·9 ± 11·9 years, 64% female; and Group C (high metal) n= 29; 67·6 ± 10·8, 62% female. Mean cobalt levels in groups A, B and C were 0·17 (SD 0.08), 2·47 (SD 1.81) and 30·0 (SD 29.1) ppb respectively.

Overall mean time since implantation to date of scan was slightly shorter within group A as compared to groups B and C (84 ± 33 versus 95 ± 22 versus 107 ± 41 months, F=3·5, p=0·03).

Although not matched for, there were no significant differences between the groups with regards to body mass index, cardiovascular risk factors or medications, see table 3.1.

Figure 3.19: *Study Flow Diagram with patient allocations after recruitment*

Demographic	All patients	Group A	Group B	Group C	p
Sample (n)	90	28	33	29	-
Age (y)	64·9 (SD 10·5)	65·3 (SD 8·80)	61·9 (SD 11·9)	67·6 (SD 10·8)	0·115
Gender (F/M)	60/30	21/7	21/12	18/11	0·525
Years since implantation	8·76 (SD 2·34)	7·86 (SD 2·62)	9·03 (SD 1·87)	9·39 (SD 2·52)	0·041
BMI (kg/m^2)	28	28 (18-38)	28 (20-45)	27 (20-48)	0·929
Diabetes (n; %)	3; 3	1; 4	1; 3	1; 3	0·982
Hypertension (n;%)	32; 36	11; 39	12; 36	9; 31	0·715
Hypercholesterolemia (n,%)	20; 22	9; 32	4; 12	7; 24	0·105
ß Blocker (n; %)	5; 8	2; 7	0	3; 10	0·181
ACE I (n; %)	10; 11	5; 18	3; 9	2; 7	0·326
Thiazide Diuretic (n; %)	8; 9	2; 7	4; 12	2; 7	0·741
Calcium Channel Blocker (n; %)	15; 17	7; 25	4; 12	4; 14	0·289
Aspirin (n; %)	3; 3	1; 4	0	2; 7	0·317
Statin (n; %)	20; 22	9; 32	4; 12	7; 24	0·121
Proton Pump Inhibitor (n; %)	18; 20	8; 29	3; 9	7; 24	0·101
Thyroxine (n; %)	8; 9	4; 14	4; 12	0	0·108
Haemoglobin (g/dL)	14	14·1	14·2	13·6	0·134
Cobalt (ppb; mean, range)	10·9	0·17 (0·10-0·47)	2·47 (0·73-6·97)	30·01 (7·54-118)	<0·0001
Chromium (ppb; mean, range)	7·7	0·74 (0·53-1·42)	2·84 (0·94-10·5)	19·6 (1·71-69·0)	<0·0001

Table 3.1: *Patient demographics by study group*

3.12 Ethical Considerations

This study commenced once ethics approval from the London Westminster National Research Ethics Committee was granted (Reference number: 14/LO/1722, dated 14th October 2014). The study was conducted in accordance with the research governance framework, EU and UK legislations and applicable UK acts. The confidentiality of participants taking part in the study was preserved in line with the Data Protection Act 1998.

Full ethical considerations, management of incidental clinical findings, and written communications are set out in Appendices A-F respectively.

3.13 Resources and Costs

Details of Resources and Costs incurred are detailed in Appendix G.

CHAPTER 4

CHAPTER 4 RESULTS – CMR VOLUMES AND FUNCTION

4.1 Introduction

We have discussed the potential for cobalt toxicity on systemic organs and it has been demonstrated that circulating cobalt from MoM implants cause rare but fatal autopsy-diagnosed cardiac toxicity. The most profound case involves a patient who died from cardiac failure (reduced left ventricular ejection fraction) secondary to cobalt deposition within the cardiac tissues and secondary cardiomyopathy. Several other cases of cardiac toxicity have also been reported, with the common theme seemingly dilated cardiomyopathy and reduced cardiac function. See table 1.2 (chapter 1). A recent health screen used echocardiography to suggest reduced cardiac function is seen in patients with MoM hip implants, even in the absence of elevated blood metal ions (>7ppb). [167] Concern exists that milder cardiotoxicity may be common and under-recognized despite there only being a small number of case reports reporting cardiac toxicity from cobalt arising from metal hip implants. Cardiac MRI is the gold-standard quantification of cardiac volumes and function using standardised protocols. [240] It is an accessible and repeatable study, with excellent inter-observer reliability.

In this chapter, we set out to report the results of Cardiac Ventricular Volumes and Function of three groups of patients as defined in the methods section, Chapter 3.

4.2 Left Ventricular Ejection Fraction

90 patients across three age and gender matched groups, defined by type of hip implant and blood metal ion level, underwent CMR imaging. LVEF was calculated using dedicated cardiac MRI software (CMRtools).

4.2.1 Results

The mean LVEF as determined by CMR did not differ between groups A, B and C, 70·1% ± 5·6 (SD) versus 69·5% ± 6·8 versus 70·6% ± 5·5 respectively, F=0.29, p=0·75. See figure 4.1.

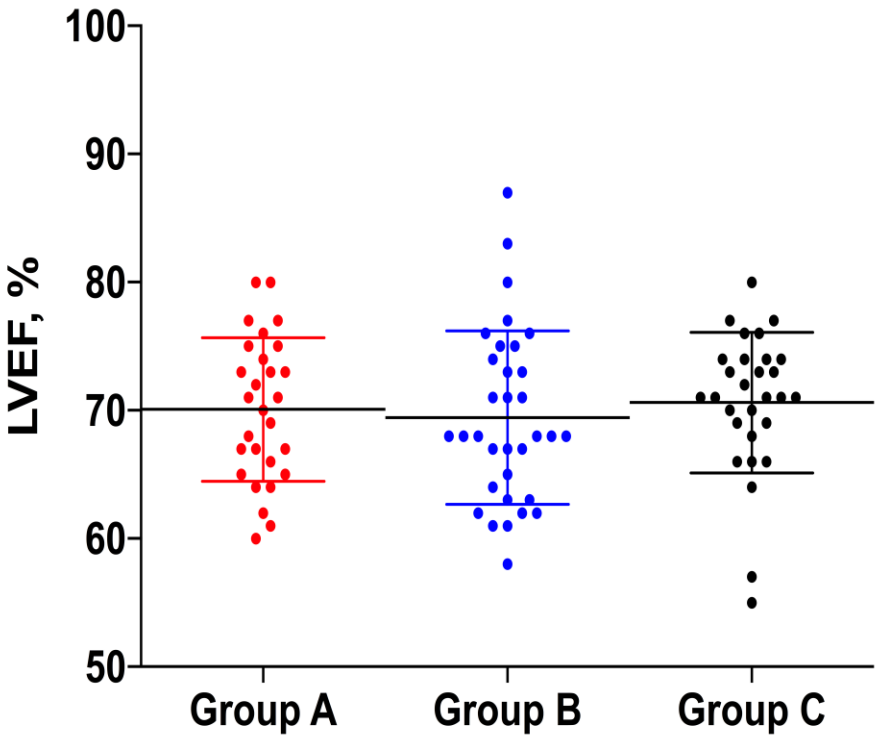

Figure 4.1: *Scatter plot in columns demonstrating LVEF (%) by group, Including the mean (± SD)*

Assessing the variation about the median using non-parametric tests confirmed the results and relaxed the assumptions made by parametric testing. Similarly, groups B and C were combined so that all MoM patients were considered together against the control group A, following which no difference between group means was seen, F=0, p=0.96. See figure 4.2.

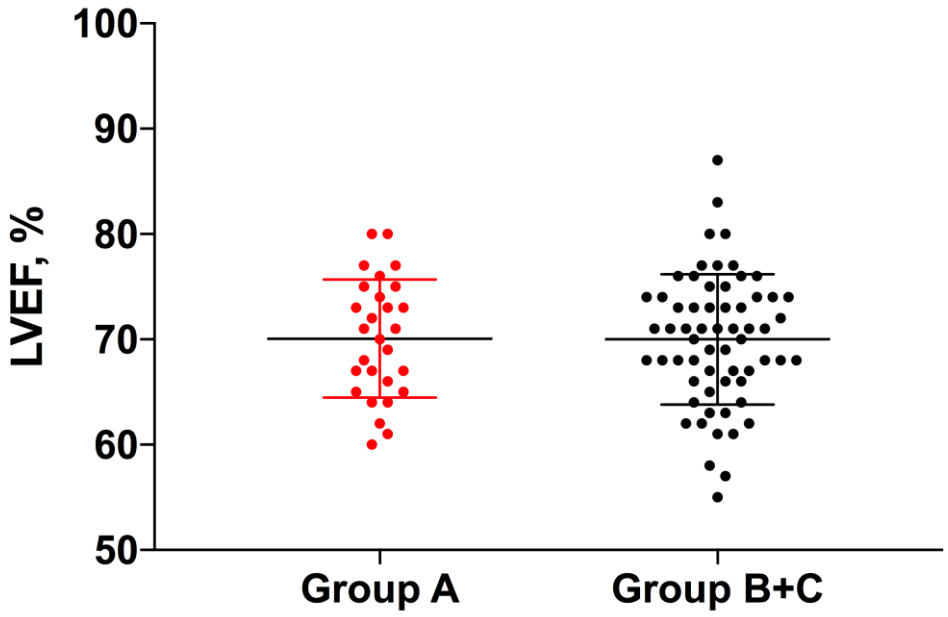

Figure 4.2: *Scatter plot comparing LVEF (%) in the control group (group A) vs. the combined MoM groups (B+C)*

A 'dose response' linear correlation analysis was conducted using Pearson's coefficient to determine whether there was a relationship across groups between blood cobalt or chromium levels and LVEF. There was no significant correlation between blood cobalt levels (Log scale) and LVEF (R=0·022, 95% CI= (-0.185;

0.229), p=0·83), and between blood chromium levels and LVEF (R=0·047, 95% CI= (-0.162; 0.251) p=0·66). Figures 4.3 and 4.4 respectively.

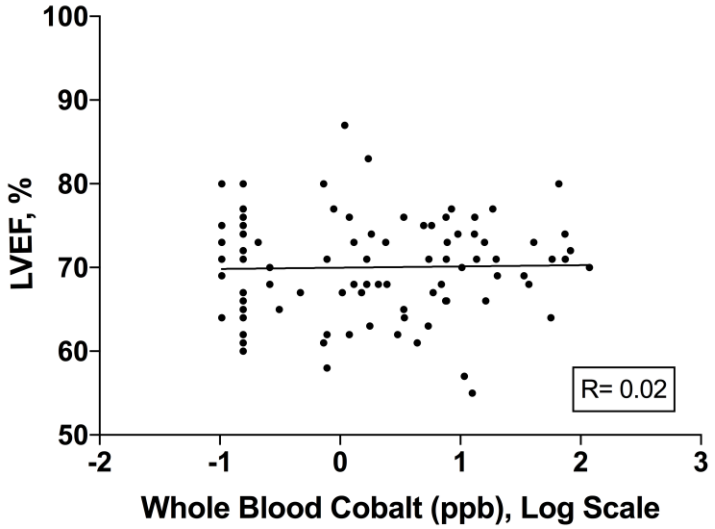

Figure 4.3: *Scatter plot of LVEF vs. whole blood cobalt (log scale)*

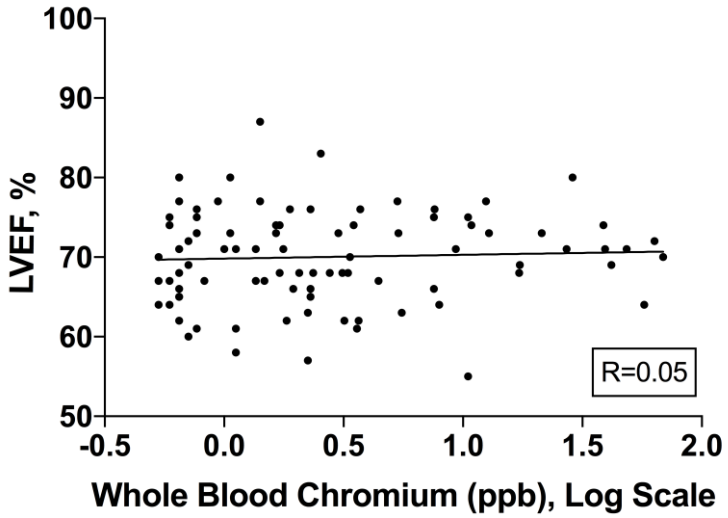

Figure 4.4: *Scatter plot of LVEF vs. whole blood chromium (log scale)*

Whole blood metal levels were non-normally distributed, unlike LVEF, and log-transforms attenuated without circumventing the lack of normality. Hence to avoid this assumption, Spearman's correlation coefficient was also performed

and showed a lack of significant correlation of LVEF against both cobalt and chromium (Cobalt vs. LVEF: rho=0·038, 95% CI= (-0.170;0.243) p=0·72; Chromium vs. LVEF: rho=0·058, 95% CI= (-0.151;0.262), p=0·59).

4.2.2 Summary

Left ventricular ejection fraction did not appear to be affected by circulating blood metal ions in patients with whole blood cobalt levels up to 118ppb. Similarly no blood cobalt or chromium dose effect was seen to suggest a correlation between elevated metal ions and worsening cardiac function.

4.3 Cardiac Volumes

4.3.1 End Diastolic Volume

The mean EDV as determined by CMR between three distinct groups of patients did not significantly differ across groups, 126.57ml ±34.67 (SD) versus 128.88ml ±29.82 versus 128.93ml ±29.33, respectively across groups A, B and C (F= 0.05; p= 0.95). Figure 4.5.

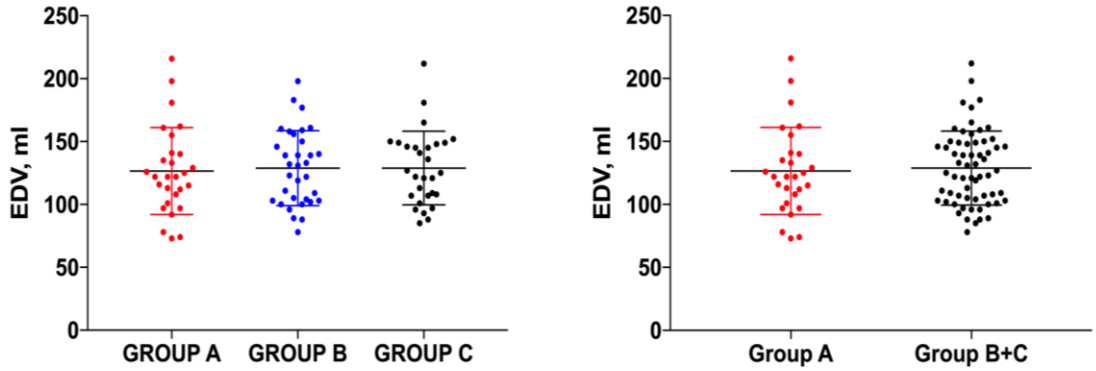

Figure 4.5: *Scatter plots demonstrating the variation in the mean EDV (ml) across a 3-group (left) and 2-group comparison (right)*

Similarly, no difference existed when comparing the mean of the control group (A) with the combined values of the MoM groups (B & C) (t= 0.31; df= 45.21; p= 0.76). Figure 4.5.

There was no significant correlation between blood cobalt levels (Log scale) and EDV (R= -0.03, 95% CI= (-0.23; 0.18), p=0·79), and between blood chromium levels and EDV (R= -0·15, 95% CI= (-0.34; 0.06), p=0·17) using Pearson's coefficient. Figure 4.6.

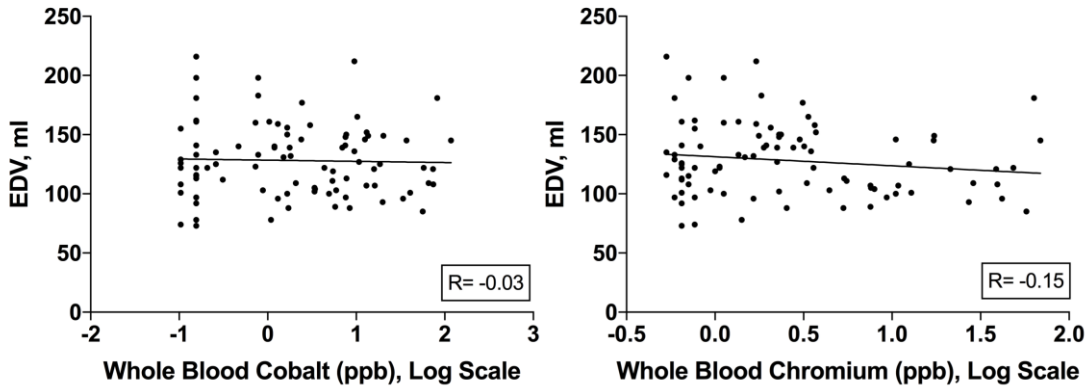

Figure 4.6: *Scatter plots demonstrating correlation coefficients between EDV and whole blood Cobalt (left) and Chromium (right)*

There is natural variation in cardiac volumes in patients of the same age as a result of differences in height and weight amongst the population. To deal with this variation, cardiac volumes can be indexed to body surface area. Repeating the analysis using indexed variables (EDVi) failed to detect a difference in the mean volumes across groups as measured by CMR. The mean EDVi (ml/m^2) for group A was 67.36 ± 15.03 versus 67.12 ± 12.8 and 67.93 ± 10.62 for groups B and C respectively; f= 0.03; p= 0.97. Additionally, there were no differences in EDVi when combining groups B and C compared to group A; t 0.04; df 42.5; p= 0.96. Figure 4.7.

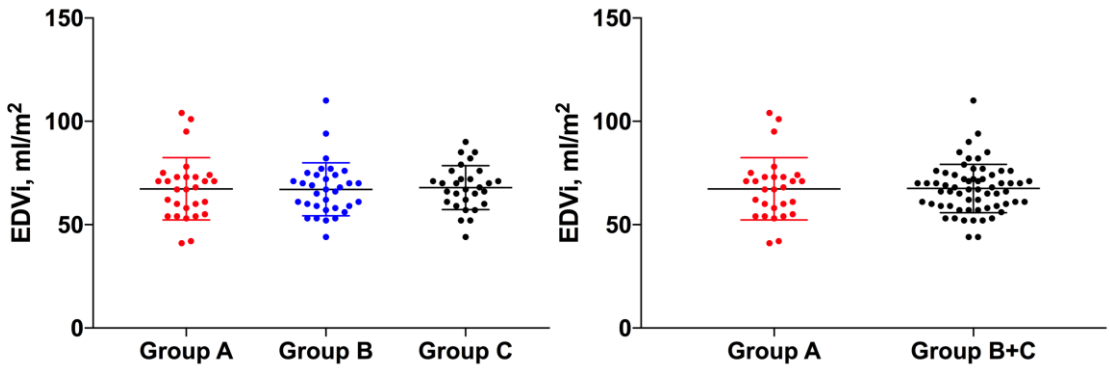

Figure 4.7: *Scatter plots demonstrating variation in mean EDVi values across groups in both a 3-group (left) and 2-group (right) analysis*

Similarly, Pearson's correlation coefficients failed to demonstrate a significant affect of increasing whole blood cobalt or chromium levels versus EDVi volumes (cobalt versus EDVi – R= -0.02, 95% CI= (-0.23; 0.19), p= 0.83; chromium versus EDVi – R= -0.07, 95% CI= (-0.27; 0.14), p= 0.52). Figure 4.8.

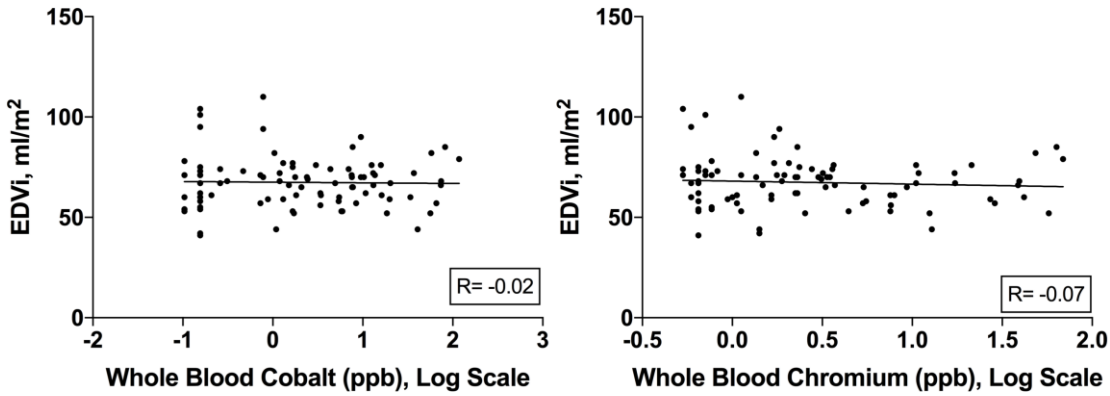

Figure 4.8: *Pearson's correlation coefficients for EDVi versus both whole blood cobalt (left) and chromium (right)*

4.3.2 End Systolic Volume

The mean end systolic volumes (ml) as measured by CMR did not differ between groups (38.57 ± 14.03 (SD) versus 40.48 ± 15.85 versus37.83 ± 11.14 respectively; F= 0.30; p=0.74). Additionally, there were no differences in ESV when combining groups B and C compared to group A (t= 0.21; df= 51.41; p= 0.83). Figure 4.9.

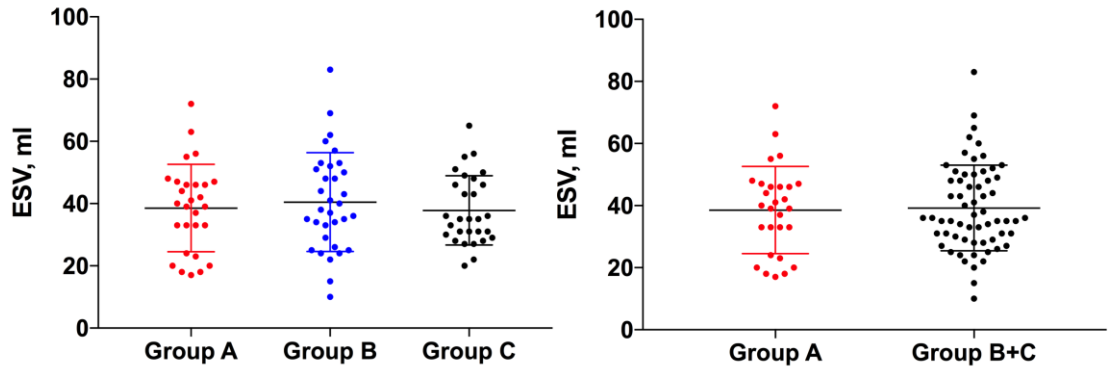

Figure 4.9: *Variation in Mean ESV (±SD) across groups in a 3-group (left) and 2-group (right) comparison.*

No correlation was seen when plotting whole blood cobalt and chromium with ESV respectively (Cobalt – R= -0.06, 95% CI= (-0.27; 0.15), p= 0.56; Chromium – R= -0.15, 95% CI= (-0.34; 0.06), p= 0.16) using Pearson's correlation coefficient. Figure 4.10.

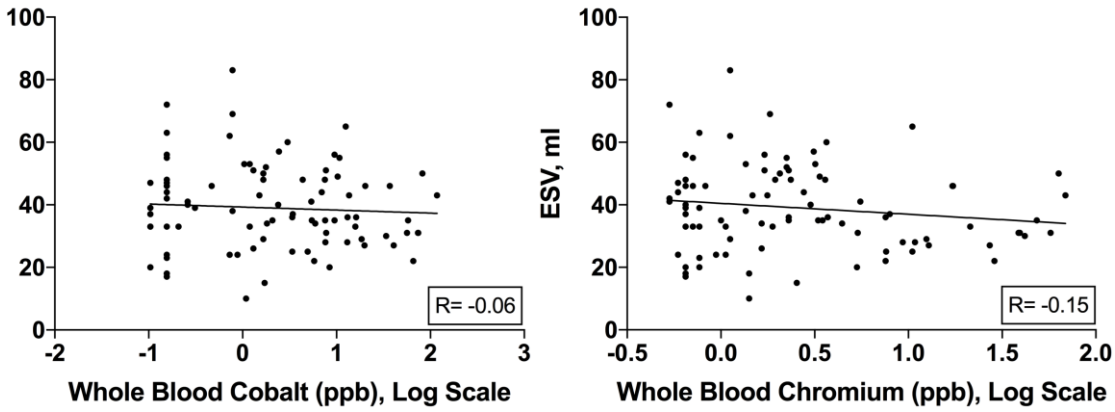

Figure 4.10: *Scatter plots demonstrating the degree of correlation between ESV and Whole Blood Cobalt (left) and Whole Blood Chromium (right)*

ESV was indexed (ESVi) to body surface area and the analysis repeated. This failed to detect a difference across groups using a 3-group comparison (F= 0.15; p=0.86) and a 2-group comparison having combined groups B and C and compared to group A (t= 0.01; df= 54.12; p=0.99). Figure 4.11.

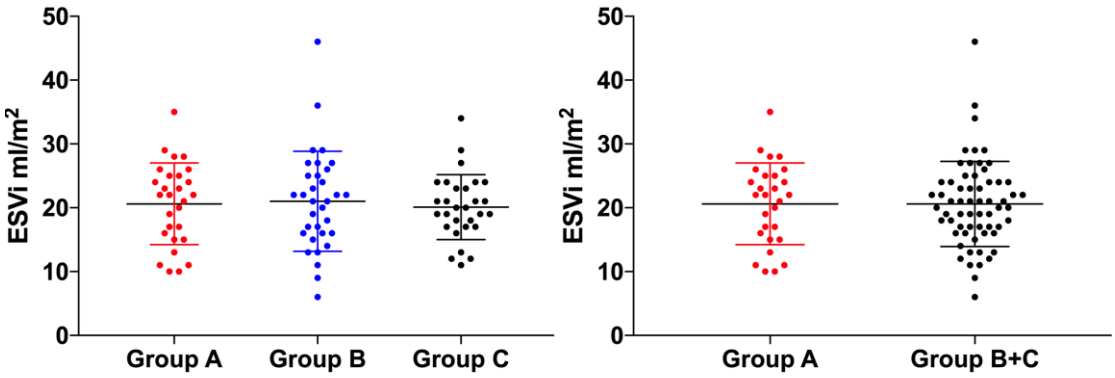

Figure 4.11: *Scatter plot demonstrating ESVi (mean ± SD) across a 3-group (left) and 2-group (right) comparison*

Similarly no significant correlation was seen when comparing whole blood cobalt and chromium with ESVi (Cobalt – R= -0.06, 95% CI= -0.26; 0.15, p= 0.60; Chromium – R= -0.10, 95% CI= -0.30; 0.11, p= 0.37). Figure 4.12.

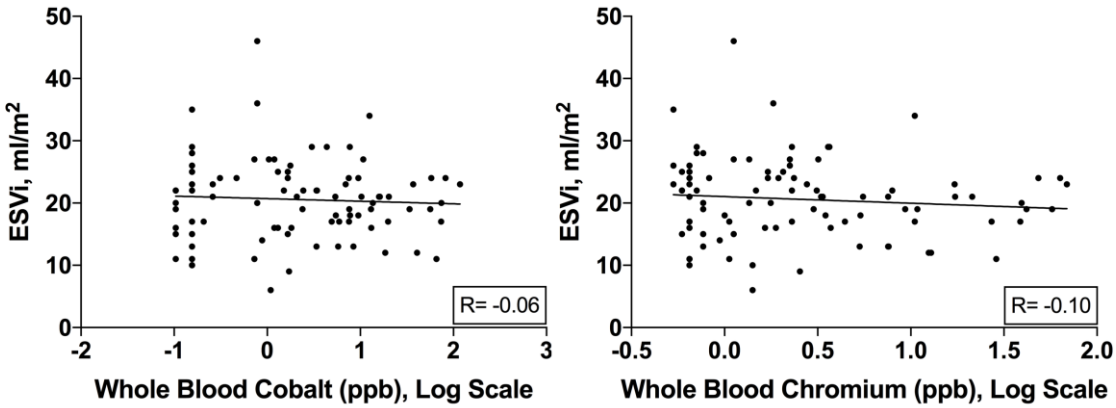

Figure 4.12: *Pearson's correlation coefficient failed to demonstrate a significant correlation between ESVi and Cobalt (left) and Chromium (right)*

4.3.3 Stroke Volume

There was no difference in the mean EDV or ESV across groups (4.3.1 and 4.3.2), however it is necessary to analyse for a difference in the Stroke volume, to which both EDV and ESV contribute.

The mean stroke volume (SV, ml) as determined by CMR was 88.00 ± 23.10 (SD) versus 88.39 ± 16.70 versus 91.10 ± 22.11 across groups A, B and C respectively. No statistical difference was present when comparing the means across groups (F= 0.20; p= 0.82). Additionally, no difference was seen when combining groups B with C and comparing to group A (t= 0.33; df= 44.64; p= 0.74). Figure 4.13.

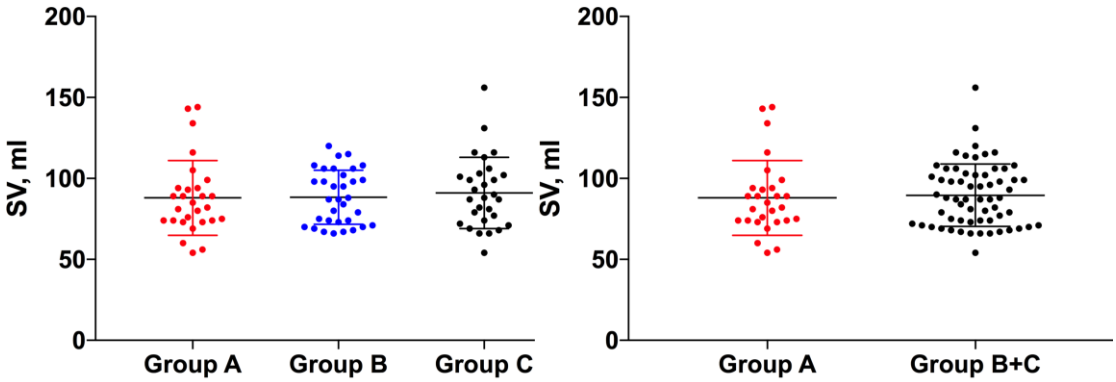

Figure 4.13: *Stroke Volume: Variation of means (*±SD*) across groups using a 3-group (left) analysis and 2-group analysis (right)*

There was no significant correlation between blood cobalt levels (Log scale) and SV (R= -0.002, 95% CI= (-0.21; 0.21), p=0·99), and between blood chromium levels and SV (R= -0.12, 95% CI= (-0.32; 0.09) p=0·26). Figure 4.14.

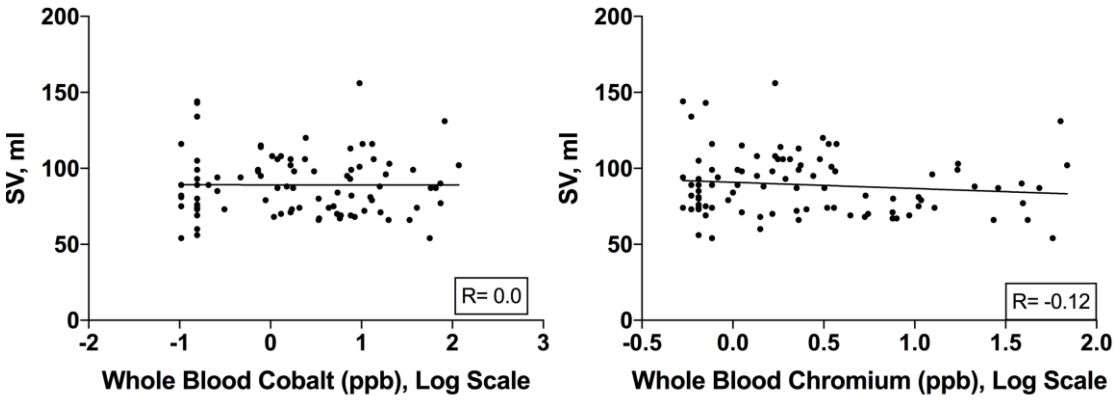

Figure 4.14: *Pearson's Correlation Coefficient computing SV against whole blood cobalt (left) and chromium (right)*

Comparing mean SV indexed (SVi) to body surface area did not reveal a significant difference across groups A, B and C (47.00 ± 10.04 (SD) versus 46.03 ± 6.42 versus 47.90 ± 8.02; F= 0.40, p= 0.67) respectively. Combining groups B and C and comparing to group A did not demonstrate a significant shift in the subsequent means (t= 0.05; df= 40.09; p= 0.96). Figure 4.15. Lastly, no

correlation was seen between SVi and whole blood cobalt or chromium (Cobalt - R= 0.0, 95% CI= -0.21; 0.21, p= 1.0; Chromium – R= -0.04, 95% CI= -0.24; 0.17, p=0.74) respectively. Figure 4.16.

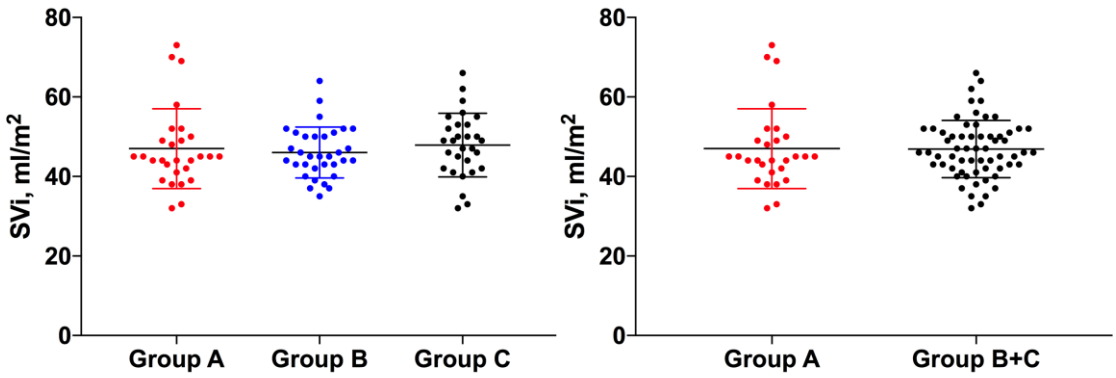

Figure 4.15: *Variation of Means (±SD) of SVi across 3 groups (left) and 2 groups (right)*

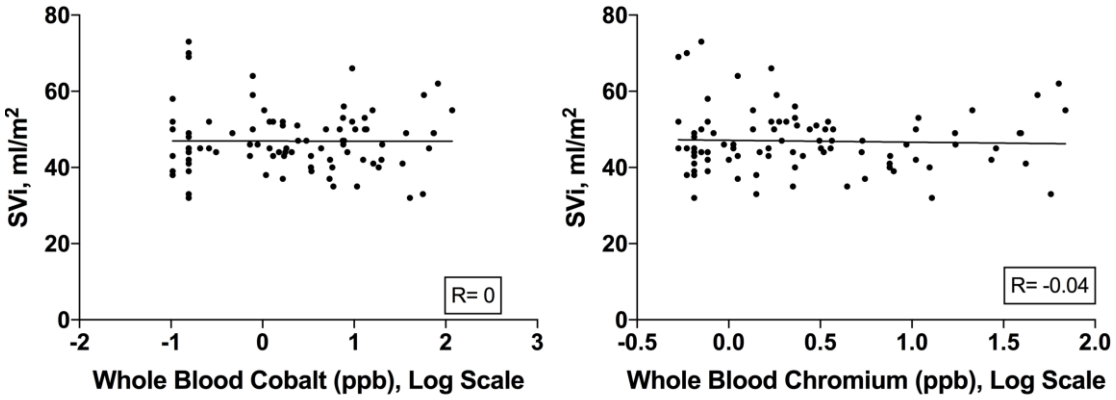

Figure 4.16: *Scatter plots demonstrating correlation between SVi and Cobalt (left) and Chromium (right)*

4.3.4 Summary

No significant detrimental affect on ventricular volumes, including the End Diastolic and End Systolic Volumes and also the Stroke Volume, was demonstrated to result from circulating blood metal ions when compared to patients with non-MoM hip implants. All results were within normal ranges, and

in addition no dose dependent correlation was seen between blood metal ions and ventricular volumes.

4.4 Myocardial Mass

4.4.1 Myocardial Mass Results

Myocardial mass (g) was measured by CMR across three groups of patients defined by implant bearing type and blood metal ion levels. No statistically significant difference was detected between the means of the three groups (101.75 ± 28.20 (SD) versus 107.03 ± 22.96 versus 117.66 ± 35.17 across groups A, B and C respectively; F= 2.25; p= 0.11).

There appeared to be a single outlier with a mass greater than 200g, which subsequently raised the mean myocardial mass of group C. A similar outlier was seen within group A. CMR images for the former patient demonstrated a myocardial mass of 223g with normal biventricular volumes although the presence of marked asymmetrical LV hypertrophy with wall thickness 20mm was seen. This 81-year-old patient had an indexed LV myocardial mass of 97g/m^2, which was 1.3 times the expected normal value (73g/m^2). Other characteristics within the scan indicated amyloidosis, and therefore the changes seen were not attributed to cardiac metal toxicity. The outlier within group A was a 70-year-old male with a myocardial mass of 204g (expected normal = 144g) and an indexed mass of 104g/m^2 (expected normal = 73g/m^2). He was found to have a mildly dilated LV (EDV was 1.3 times normal indexed – 101ml/m^2 versus 75ml/m^2) with eccentric LV hypertrophy. Wall thickness was

normal (up to 10mm), however he had elevated mass (1.4 times average). Figure 4.17.

The myocardial mass measurements were indexed to body surface area, and the analysis repeated, however this did not alter the result with no significant difference seen across the group means (54.43g/m^2 ± 12.60 (SD) versus 55.88 ± 10.31 versus 61.28 ± 11.97 across groups A, B and C respectively; F= 2.80; p= 0.07). Figure 4.18.

Additionally there were no differences in the mean myocardial mass measurements when combining groups B and C and comparing to group A (Mass – t= 1.57; df= 54.49; p= 0.12; Massi – t= 1.43; df= 47.59; p= 0.16).

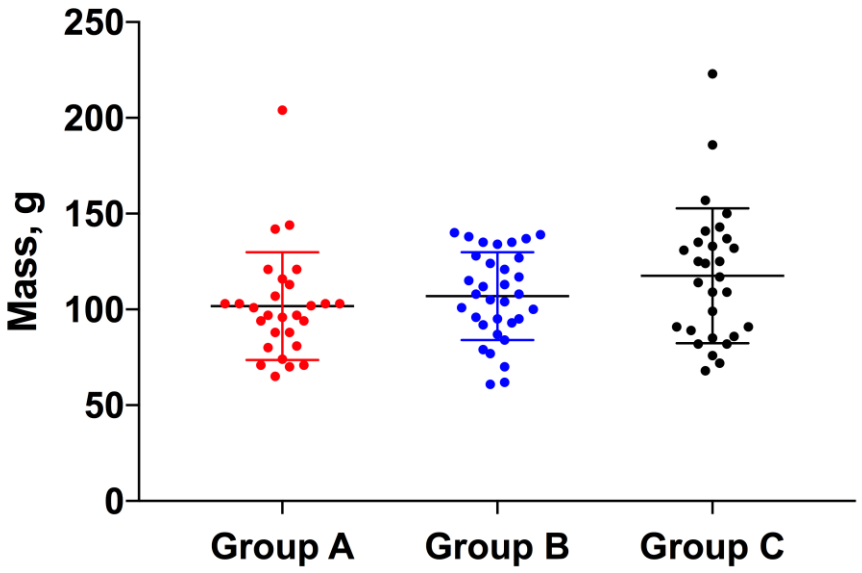

Figure 4.17: *Scatter plots in columns comparing the mean Mass (±SD) for groups A, B and C. The mean for group C is greater than A or B, although not statistically significant.*

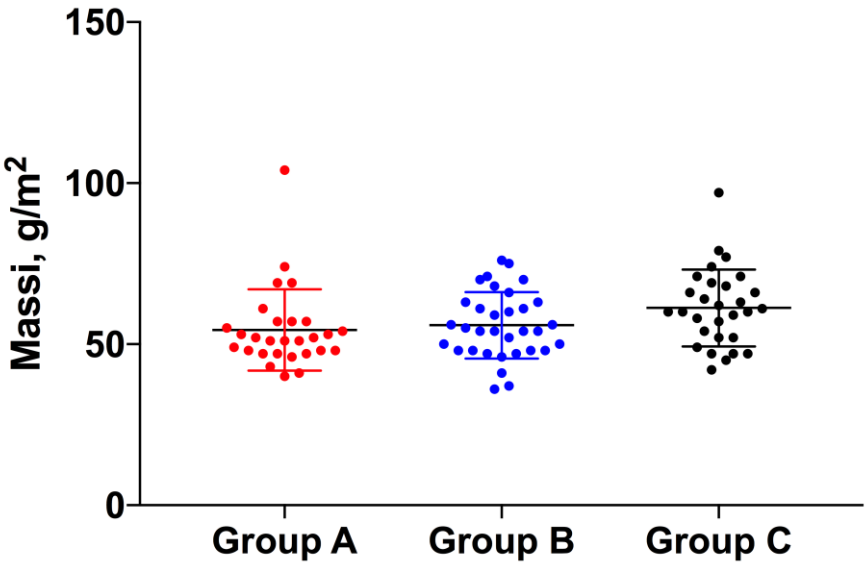

Figure 4.18: *Myocardial mass indexed to body surface area. Scatter plots in columns demonstrating the comparison of means (±SD) across 3 groups.*

Myocardial mass was assessed for a correlation with rising blood cobalt and chromium levels using Pearson's correlation coefficient. No significant correlation was demonstrated for either blood metal type (Cobalt – R=0.15, 95% CI= -0.06; 0.35, p=0.15; Chromium – R= -0.002, 95% CI= -0.21; 0.21, p= 0.99). This analysis was repeated for Massi (indexed), and again no significant correlation was demonstrated against rising cobalt or chromium blood metal ion levels respectively (Massi vs. Cobalt – R= 0.19, 95% CI= -0.02; 0.38, p= 0.08; Massi vs. Chromium – R= 0.08, 95% CI= -0.12; 0.29, p= 0.43). See figures 4.19 and 4.20.

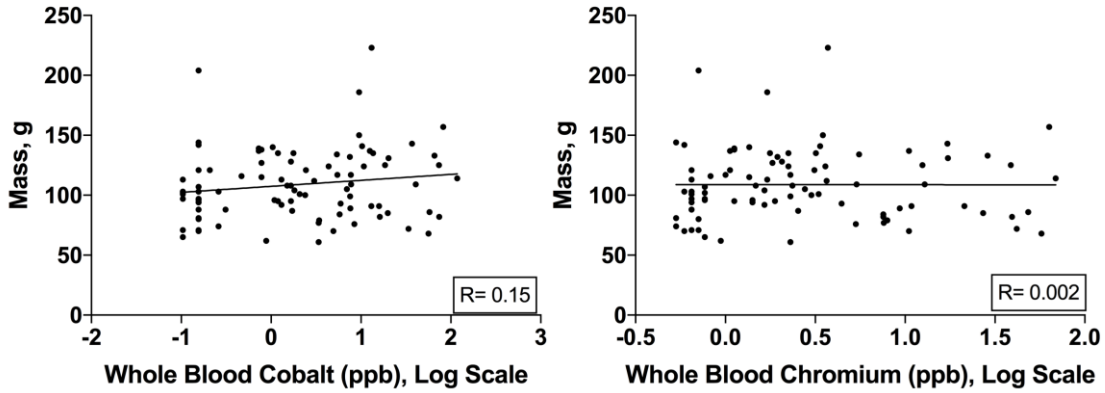

Figure 4.19: *Scatter plots demonstrating the degree of correlation between Mass and Cobalt (left) and Chromium (right)*

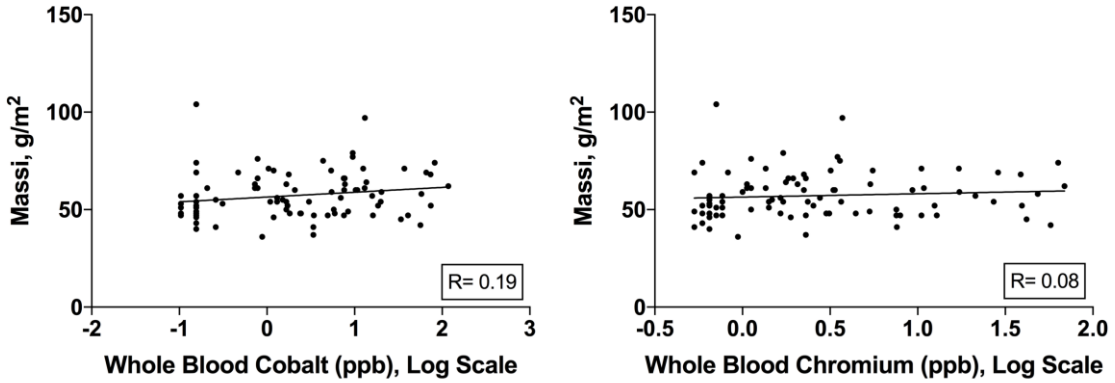

Figure 4.20: *Scatter plots demonstrating the degree of correlation between Massi (indexed) and Cobalt (right) and Chromium (left)*

4.4.2 Summary

No difference was demonstrated in Mass or Massi across groups. Two patients were identified with increased myocardial mass, and belonged to the control group and the high metal ion group respectively, however neither could be attributed to metal disease and in one case a diagnosis amyloidosis was suggested.

4.5 MAPSE and TAPSE

4.5.1 MAPSE Results

The mean MAPSE as measured with CMR did not differ across the three groups A, B and C (12.61mm ± 2.25 (SD) versus 11.98 ± 2.76 versus 12.61 ± 3.14, respectively; F= 0.53, p= 0.59). Additionally, there were no differences in MAPSE when combining groups B and C compared to group A (t= 0.59; df= 67.2; p= 0.56). Figure 4.21.

A patient belonging to group C (high metal ion levels) was found to have good radial systolic function with above-normal ejection fraction (LVEF 76%) but severely reduced longitudinal function (MAPSE 3mm). This is the same 81-year-old patient that was diagnosed with suspected amyloidosis as discussed in the previous section (4.4.1).

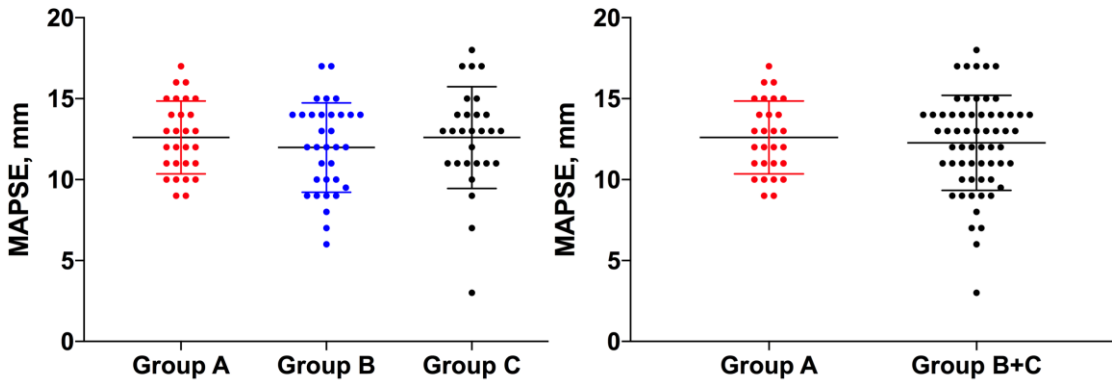

Figure 4.21: *Scatter plots representing MAPSE measurements, demonstrating the variation in the means (±SD) across 3-groups (left) and 2-groups (right)*

An assessment for a correlation between the MAPSE value and the circulating blood metal ion levels were conducted using Pearson's correlation coefficient

against both cobalt and chromium, which were not significant (Cobalt – R= -0.02, 95% CI= -0.23; 0.18, p= 0.83; Chromium – R= -0.08, 95% CI= -0.28; 0.13, p= 0.46). Figure 4.22.

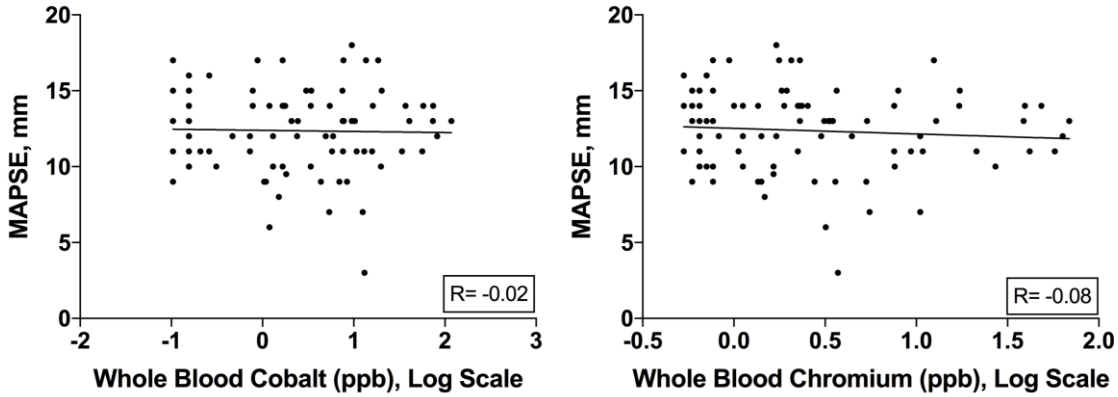

Figure 4.22: *Correlation plots comparing MAPSE (mm) against whole blood cobalt (left) and chromium (right)*

4.5.2 TAPSE Results

The mean TAPSE as measured with CMR did not differ across the three groups A, B and C (22.71mm ± 3.84 (SD) versus 21.79 ± 3.74 versus 23.21 ± 4.04, respectively; F= 1.08, p= 0.34). Additionally, there were no differences in TAPSE when combining groups B and C compared to group A (t= 0.31; df= 53.5; p= 0.76). Figure 4.23.

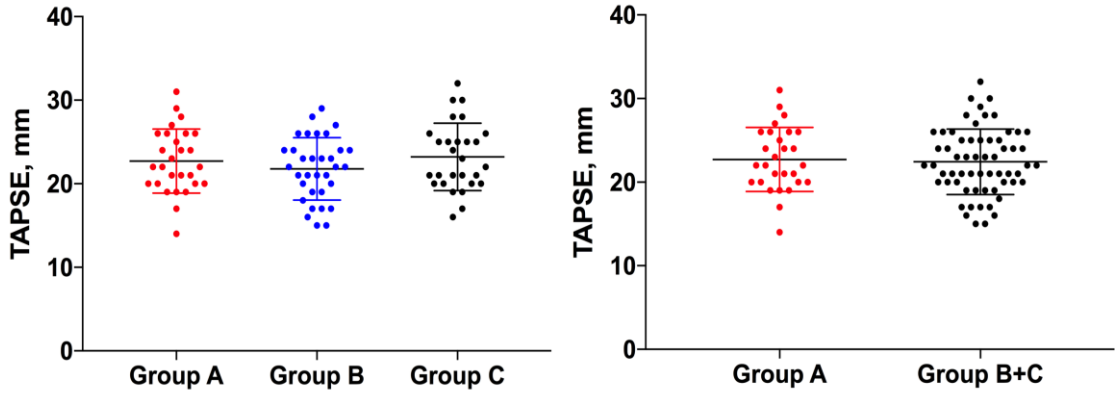

Figure 4.23: *TAPSE - Comparison of group means (±SD) in a 3-group (left) and 2-group analysis*

An assessment for a correlation between the TAPSE value and the circulating blood metal ion levels were conducted using Pearson's correlation coefficient against both cobalt and chromium, which were not significant (Cobalt – R= 0.02, 95% CI= -0.19; 0.23, p= 0.83; Chromium – R= -0.12, 95% CI= -0.32; 0.09, p= 0.28). Figure 4.24.

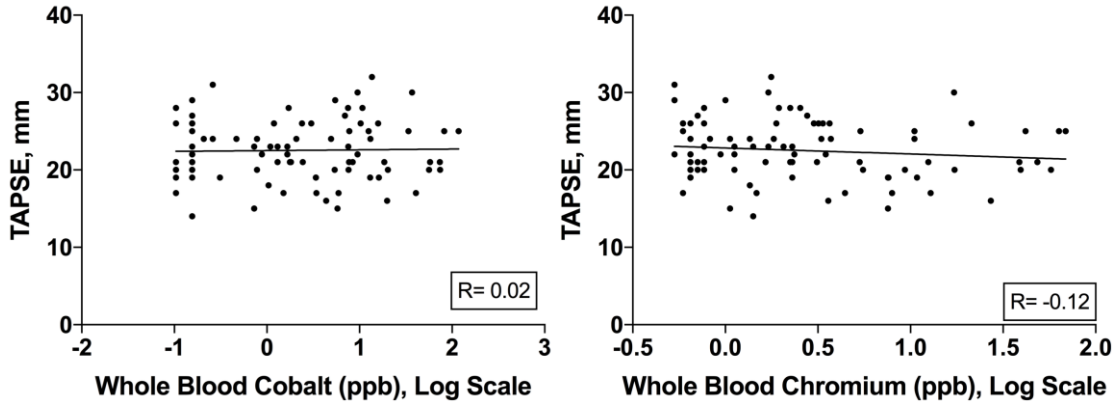

Figure 4.24: *Correlation of TAPSE against whole blood cobalt (left) and whole blood chromium (right)*

4.5.3 Summary

As a marker of longitudinal function that correlates well with ventricular ejection fraction, MAPSE was compared across three groups of patients defined by

implant type and metal ion levels. There was no significant difference in mean MAPSE values across the three groups. Similarly TAPSE is a marker of right ventricular function, which in this setting did not significantly vary across groups with increasing whole blood metal ion levels. No correlation was detected with increasing blood metal levels and deteriorating MAPSE or TAPSE.

4.6 Atrial Size

4.6.1 Left Atrial Area

All left atria area measurements were indexed to body surface area. The mean indexed left atria area measurements did not vary across groups A, B and C (11.56 (cm^2/m^2) ± 2.62 (SD) versus 11.50 ± 1.81 versus 12.62 ± 2.29; F= 2.32; p= 0.10) respectively. Additionally mean left atrial area did not differ when groups B and C were combined and compared to group A (t= 0.83; df= 41.62; p= 0.41).

Pearson's correlation coefficient was used to assess for a correlation between left atrial size and circulating blood cobalt and chromium ions respectively. No significant correlation was seen in either case (Cobalt – R=0.19, 95% CI= -0.03; 0.38, p= 0.08; Chromium – R= 0.17. 95% CI= -0.04; 0.37, p= 0.12). See figure 4.25.

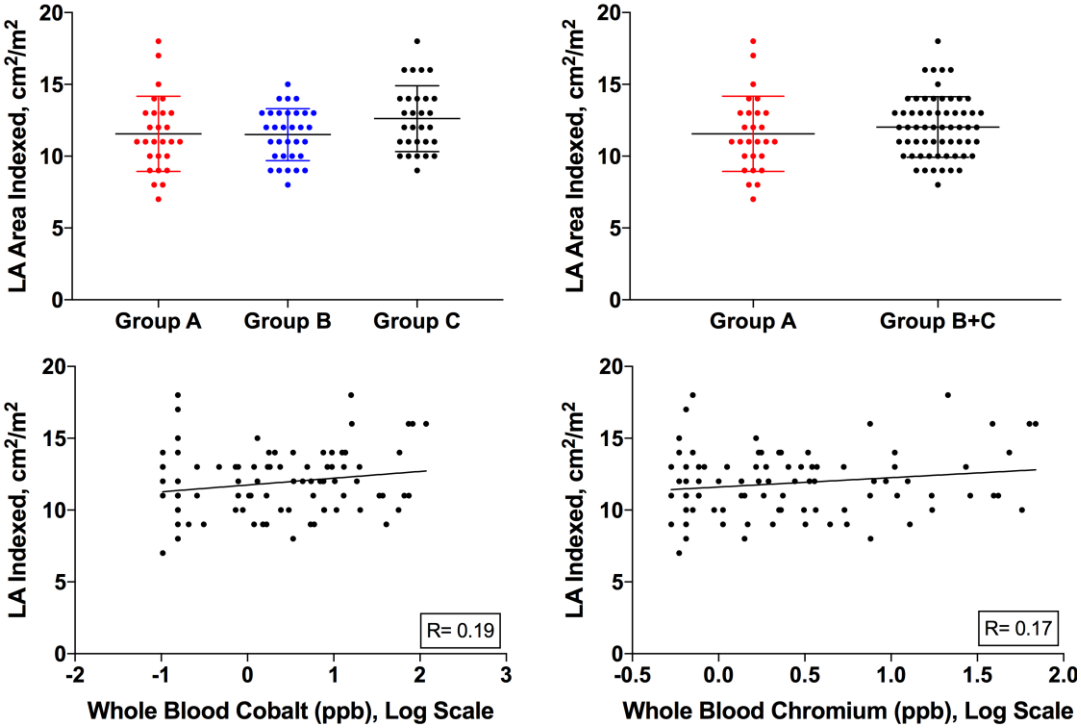

Figure 4.25: *Top left – variation of means across groups. Top right – variation of means when combining groups B and C and comparing to group A. Bottom left – Correlation between blood cobalt and Left atria indexed area. Bottom right – correlation between blood chromium and left atria indexed area.*

4.6.2 Right Atrial Area

The mean indexed right atria area measurements did not differ across groups A, B and C (11.30cm^2/m^2 ± 2.11 (SD) versus 11.06 ±2.27 versus 11.50 ± 1.90; F= 0.32; p= 0.72). Additionally, no difference between the means existed when combining group B with C and comparing to group A (t=0.06; df= 49.95; p= 0.95). An assessment for a correlation between right atrial area (indexed) and blood cobalt and chromium levels was conducted. Increasing cobalt levels did not lead to an increase in the size of the right atria (R= 0.06; 95% CI= -0.15, 0.27; p=0.59). Similarly no correlation was seen between blood chromium and right atria size (R= 0.01; 95% CI= -0.20, 0.22; p=0.91). Figure 4.26.

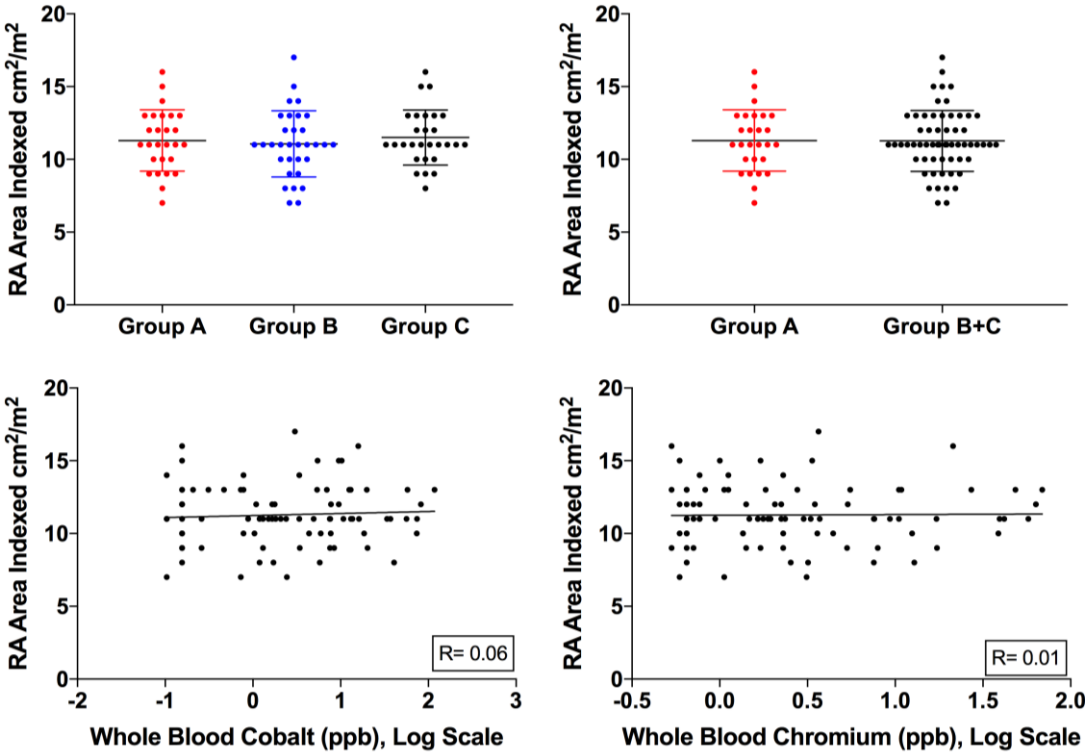

Figure 4.26: *Top left – variation of means across groups. Top right – variation of means when combining groups B and C and comparing to group A. Bottom left - Correlation between blood cobalt and Right atria indexed area. Bottom right – correlation between blood chromium and right atria indexed area.*

4.6.3 Summary

Once indexed for body surface area, no variation was seen in right and left atria sizes as measured by CMR across three groups of patients with varying blood cobalt and chromium levels. No direct correlation was seen between the blood metal level and the size of the atria.

4.7 Discussion

This chapter focused on the effects of metal ions on cardiac volumes and function in three distinct groups of patients defined by their i) hip implant and ii) levels of

circulating blood cobalt and chromium. Using the gold standard imaging technique for volume and function, CMR, a significant change in cardiac function in patients exposed to elevated metal ions was not seen.

Left ventricular ejection fraction is a key determinant of cardiac function and is an important marker for disease. A previous study with a similar sample size documented a 7% reduction in left ventricular ejection fraction (LVEF) in MoM recipients, all with blood levels below 7ppb [167]. If this were a true cardiac toxic effect of being a MoM hip recipient, we would have expected similar if not worse effects here given the much higher degree of blood metal elevation. The Prentice et al study relied on echocardiography for their cardiac volumes and function assessment. Echocardiograhy is subject to inter and intra-observer variability, which may in part have contributed to the results seen.

In this study, no effects were seen in all cardiac volume and functional parameters, including markers of longitudinal function and structural change that may result from cardiac toxicity in the form of cardiomyopathy. There were some cases of dilated atria, however these were seen across all three groups of patients, and are likely a sign of age related changes rather than a response to metal toxicity.

In order to be confident in the findings set out in this chapter, a second imaging modality will be employed to confirm or contest the results. The next chapter will discuss the results from conducting echocardiography for volume and functional assessment of the same three groups of patients as part of a multi-modality assessment.

CHAPTER 5

5.1 Introduction

In chapter 4, cardiac volumes and function as determined by cardiac MRI were presented. This included ventricular and atrial volumes in diastole and systole. From these, the stroke volume and ejection fraction was calculated. Figures 5.1 and 5.2.

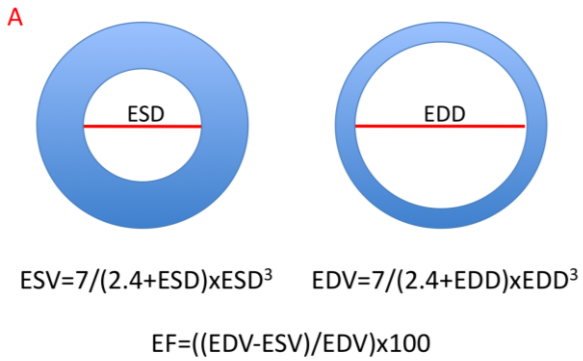

Figure 5.1: *(A) Illustration to demonstrate the Teichholz method for calculation of the LVEF. The End Systolic Diameter (ESD) / End Diastolic Diameter (EDD) are measured at the mid ventricle and the formulae illustrated are used to calculate the LVEF. (B) ECHO image of ventricle diameter measurement*

Figure 5.2: *(A) Illustration of the Simpson method for calculation of the LVEF, which applies circular discs of known height and diameter, from which the ejection fraction is calculated as a fraction of change in height and diameter (B) ECHO image of the application of the simpson method for LVEF calculation*

Additionally, MAPSE and TAPSE were determined, which provide an assessment of longitudinal axes function. No significant difference was demonstrated between groups defined by implant type and metal ion level, to suggest that in most cases elevated blood cobalt and chromium does not have a significant effect on cardiac structure or function.

However, this conclusion relies on a single imaging modality to determine the results. In a previous study undertaken by Prentice et al, echocardiography was used to assess cardiac function in two groups of patients defined by hip implant type, conventional non-MoM versus MoM bearings. The study does report does not specify how many ultrasonographers were involved in acquiring echo data. It is important to state that patients within this study had low metal ion levels. Despite this, they reported a negative effect of circulating metal on cardiac function, where cardiac ejection fraction was 7% lower (mean absolute difference 25%, p= 0.04) and left ventricular end-diastolic diameter was 6% larger (mean difference 2.7 mm, p= 0.007) in the MoM group [167].

Echocardiography is more freely available, cheaper and has relatively few contra-indications when compared to CMR. Despite this, it has a greater inter-observer variability [218]. Given the reassuring findings set out in chapter 4, which contest that of Prentice et al, it is important to confirm the conclusions using a second imaging modality with independent assessment of the same patient cohort. The aim of this is to confirm or discount the results set out in chapter 4, and to afford an additional assessment of the health of the cardiac system in patients with metal hip implants.

5.2 Left Ventricular Ejection Fraction

5.2.1 LVEF – Teichholz Method

The 90 patients presented in chapter 4, distributed across three age and gender matched groups, defined by type of hip implant and blood metal ion level, also underwent echocardiography imaging. LVEF was calculated using dedicated EchoPac dimension software.

The mean LVEF as determined by Teichholz method did not differ between groups A, B and C, 64.88% ± 8.7 (SD) versus 62.03% ± 11.36 versus 62.77% ± 7.47 respectively, F= 0.65, p= 0·53. Figure 5.3.

Assessing the variation about the median using non-parametric tests confirmed the results and relaxed the assumptions made by parametric testing. The median values across the three groups were 66% vs. 63 vs. 62.5, respectively. The box and whiskers plot seen in figure 5.3 demonstrates this.

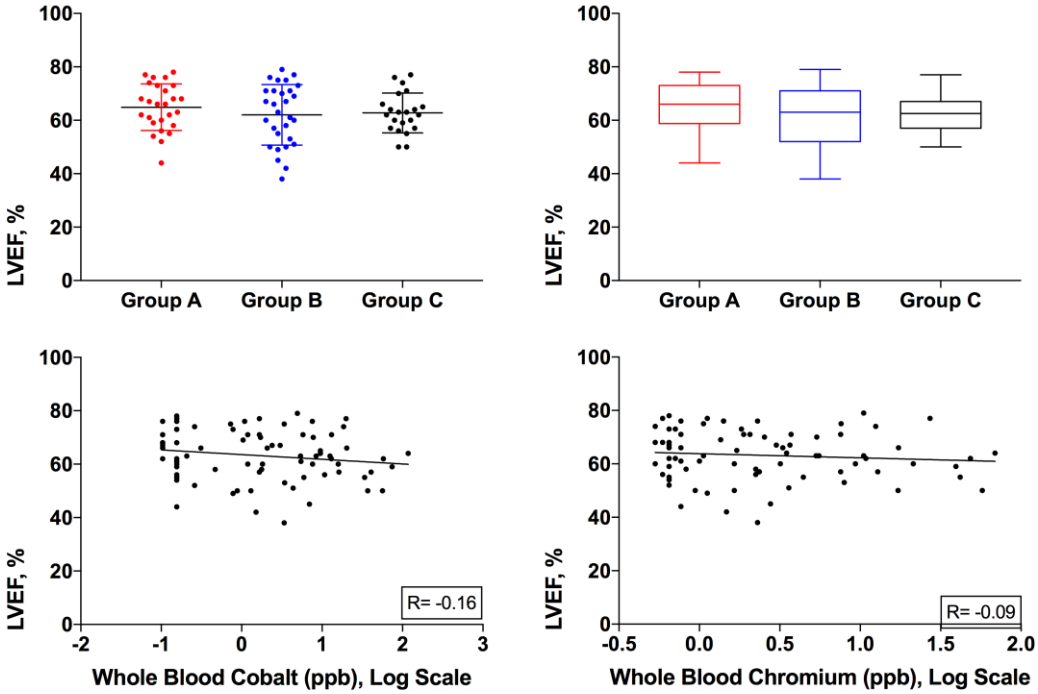

Figure 5.3: *Top left – Scatter plot representing the variation of mean LVEF (Teichholz) across groups; Top right – Box and whisker plot demonstrating variation of median values across groups; Bottom left – Dose Correlation plot of Cobalt vs. LVEF (Teichholz); Bottom right – Dose response plot of Chromium vs. LVEF (teichholz).*

A 'dose response' linear correlation analysis was conducted using Pearson's coefficient to determine whether there was a relationship across groups between blood cobalt and chromium levels and LVEF. There was no significant correlation between blood cobalt levels (Log scale) and LVEF (R= -0.16, 95% CI= (-0.37; 0.13), p= 0·16), and between blood chromium levels and LVEF (R= -0·09, 95% CI= (-0.31; 0.13) p= 0·41). See figure 5.3.

5.2.2 LVEF – Biplane Simpson Method

LVEF as determined by the biplane Simpson method revealed similar results to those calculated by Teichholz method, and similarly little variation was seen in mean values across groups. The difference in the means was not significant, with values of 65.08% ± 85.57 (SD) versus 62.33% ± 7.24 versus 63.15% ± 5.96 for groups A, B and C respectively, F= 1.31, p= 0·28. The median values were close to the mean values and similarly showed little variation across groups (Kruskal-Wallis = 1.58; p= 0.45). See figure 5.4.

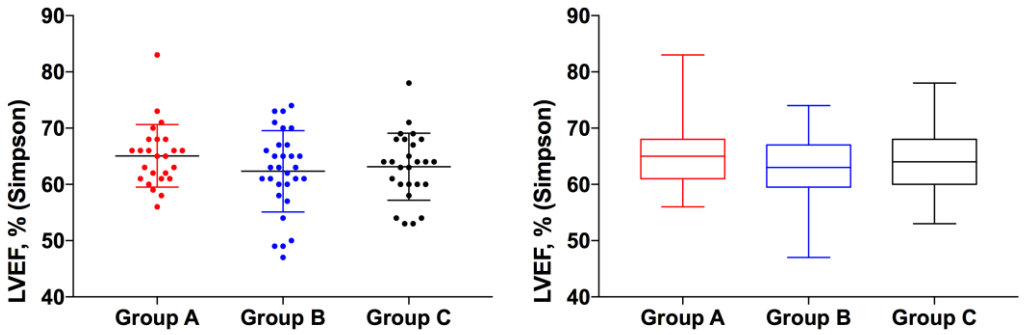

Figure 5.4: *Left – Scatter plot demonstrating the variation about the mean value of LVEF (Simpson) across groups; Right – Bow and Whiskers plot demonstrating the median value and variation across groups*

5.2.3 Summary

Despite the geometric assumptions and the inter-reader variability assumed with echocardiography, both methods for estimating Left Ventricular Ejection Fraction demonstrated no significant variation across groups, with no evidence of a cobalt/chromium dose effect on the measured fraction. Given that these methods use measures of ventricular diameters in both systole and diastole it is

important to assess these measures individually to determine if a difference exists without functional compromise. These measures include Left Ventricular End Diastolic Diameter (LVEDD) and Left Ventricular End Systolic Diameter (LVESD).

5.3 Left Ventricular Dimensions

5.3.1 Left Ventricular End-Diastolic Diameter (LVEDD)

The left ventricular end diastolic diameter was determined by echocardiography for patients across three groups defined by implant type and blood metal levels. The mean LVEDD did not differ across groups using both parametric and non-parametric analysis (4.29cm ± 0.87 (SD) versus 4.55 ± 0.46 versus 4.54 ± 0.6, respectively for groups A, B and C; F= 1.35; p= 0.26). Median diameters were 4.3cm versus 4.7 versus 4.6 respectively (Kruskal-Wallis statistic = 2.55; p= 0.28). Figure 5.5.

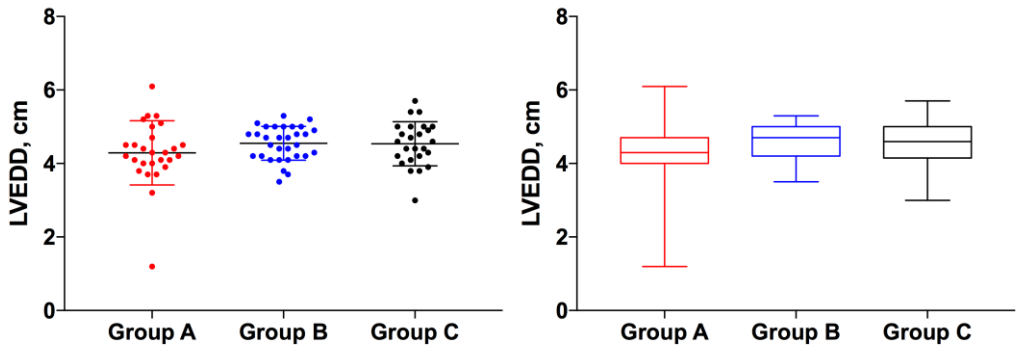

Figure 5.5: *Left – scatter plot in columns defined by groups, demonstrates the variation about the mean (±SD); and Right – Box and whiskers plot demonstrating the variation about the median and max / min values*

A correlation analysis was conducted using Pearson's coefficient to determine whether there was a relationship across groups between blood cobalt and chromium levels and LVEDD as determined by echocardiography. No significant correlation between blood cobalt levels (Log scale) and LVEDD was demonstrated (R= 0.14, 95% CI= -0.08; 0.34, p= 0·22), and between blood chromium levels and LVEDD (R= 0·04, 95% CI= -0.18; 0.25 p= 0·72). Figure 5.6.

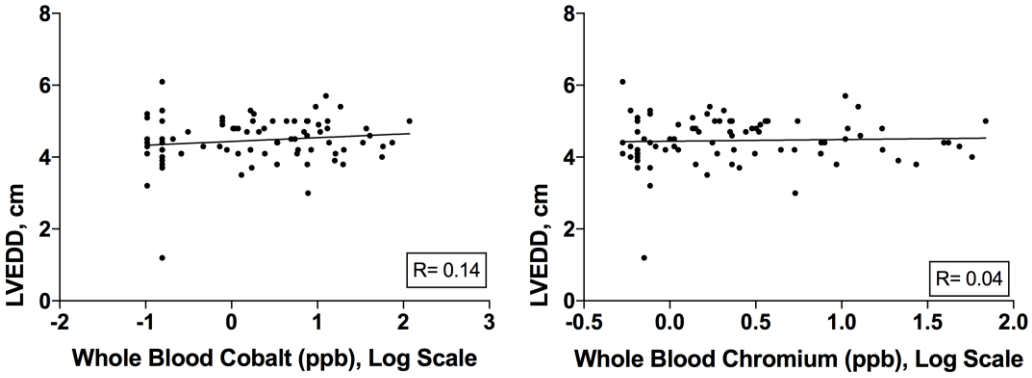

Figure 5.6: *Scatter plots demonstrating the correlation between LVEDD and Cobalt (Left) and Chromium (Right) respectively*

5.3.2 Left Ventricular End-Systolic Diameter

Similar to LVEDD, left ventricular end systolic diameter (LVESD) is measured during echocardiography. The mean values determined across the three groups did not differ significantly (2.76cm ± 0.64 (SD) versus 2.99 ± 0.44 versus 2.99 ± 0.48, respectively across groups A, B and C; F= 1.78; p= 0.18). Similarly, no significant difference was demonstrated when comparing the median values across the three groups (2.75cm versus 3.0 versus 2.95; KW= 3.9; p= 0.14). Figure 5.7.

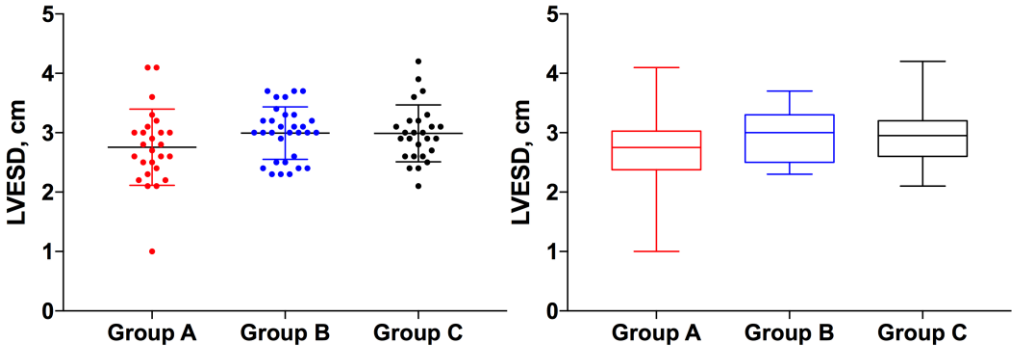

Figure 5.7: *Left – Scatter plot in columns comparing mean LVESD values (±SD) and variation about the mean; Right – Median values plotted using Box and Whiskers demonstrating the max and min values*

Pearson's correlation coefficient was used to determine if elevated cobalt or chromium blood metal ions contributed to increased diameters as measured by echocardiography. No significant correlation was seen to suggest a relationship (LVESD versus Cobalt – R= 0.20, 95% CI= -0.02; 0.40, p= 0.08; versus Chromium – R= 0.07, 95% CI= -0.15; 0.28, p= 0.54). Figure 5.8.

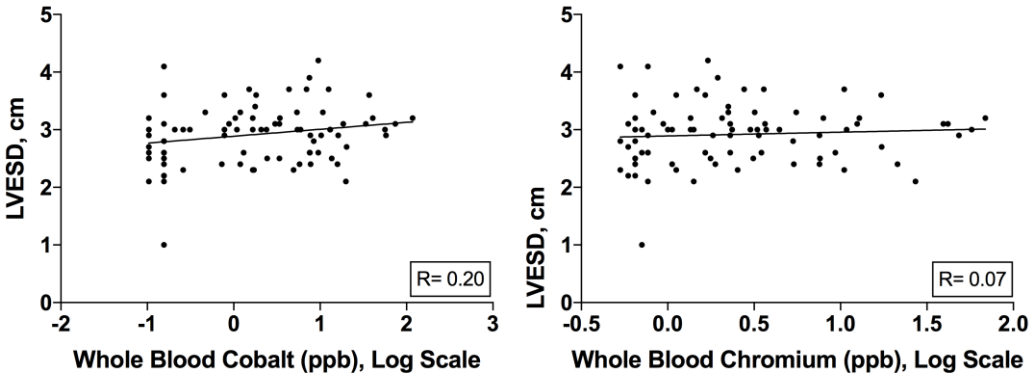

Figure 5.8: *Plots to demonstrate the correlation between LVESD and Blood Cobalt (Left) and Chromium (Right), respectively.*

5.3.3 Summary

No difference in the ventricular diameters has been demonstrated in both the diastolic and systolic periods of the cardiac cycle. This is somewhat expected given the calculated left ventricular ejection fraction results were not significantly different across groups, section 5.2. This represents the absence of left ventricular structural dilatation that would be expected if dilated cardiomyopathy were common in patients exposed to high levels of cobalt or chromium.

5.4 Atrial Dimensions

5.4.1 Right Atrial Area

The mean Right Atrial area measurements across the three groups did not vary significantly (13.81cm^2 ± 4.02 (SD) versus 15.69 ± 3.24 versus 16.10 ± 3.20 respectively; F= 2.37; p= 0.10). Median values were similarly not significantly different across groups (13.6cm^2 versus 15.75 versus 15.45; KW= 3.00; p= 0.22). Additionally, no significant dose response correlation was seen between Right Atrial Area and blood cobalt levels (R= 0.22; 95% CI= -0.02; 0.44; p= 0.07) or blood chromium levels (R= 0.11; 95% CI= -0.14; 0.34; p= 0.40). Figure 5.9.

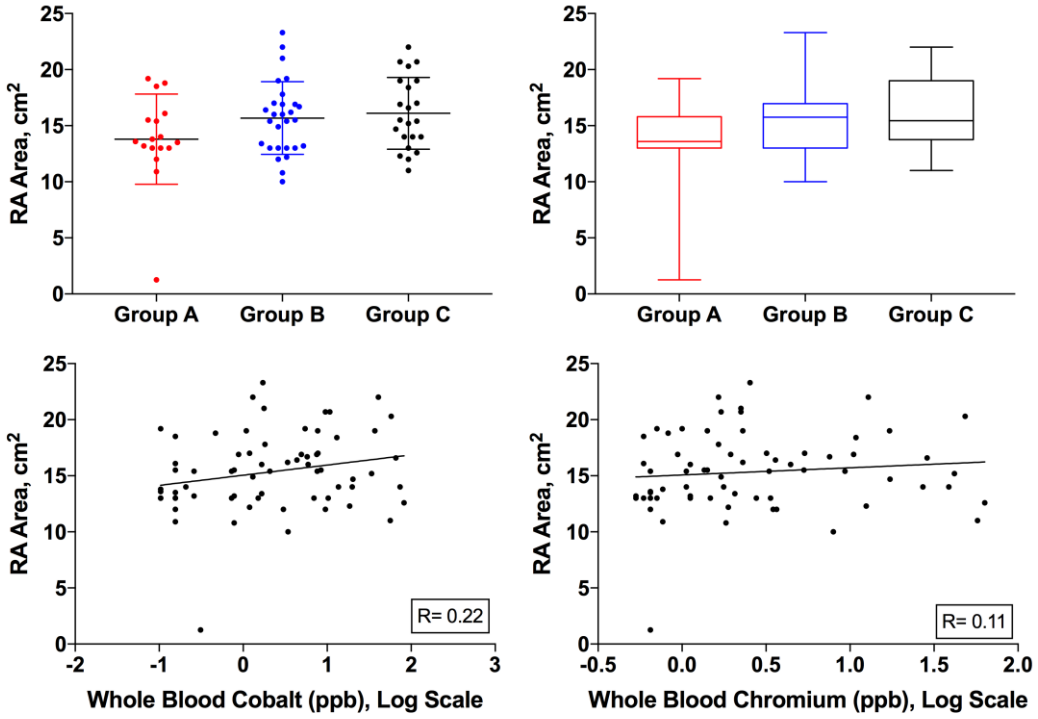

Figure 5.9: *Top left – scatter plot demonstrating the mean value (±SD) across groups; Top right – Box and whiskers plot of median values and spread of values about the median; Bottom left – Plot of correlation between RA Area and Cobalt levels; Bottom right – Correlation between RA Area and Chromium levels*

5.4.2 Left Atrial Area

The left atrial areas mean values were not significantly different across groups (16.20cm^2 ± 3.69 (SD) versus 17.89 ± 4.25 versus 18.98 ± 4.29; F= 3.07; p=0.052; Bartlett's Test p= 0.71). However, the difference between the mean values was close to achieving significance. Non-parametric tests confirmed this result when assessing the difference between the median values (16.45cm^2 versus 17.45 versus 17.75 respectively) confirmed the lack of significance (Kruskal-wallis test = 3.07; p= 0.16). Assessing for a correlation between the blood cobalt level and the left atrial area did demonstrate a positive correlation suggesting a negative

effect (R= 0.23; 95% CI 0.01; 0.42; p= 0.04). This effect was not seen with chromium however (R= 0.11; 95% CI= -0.11; 0.32; p= 0.31). See figure 5.10.

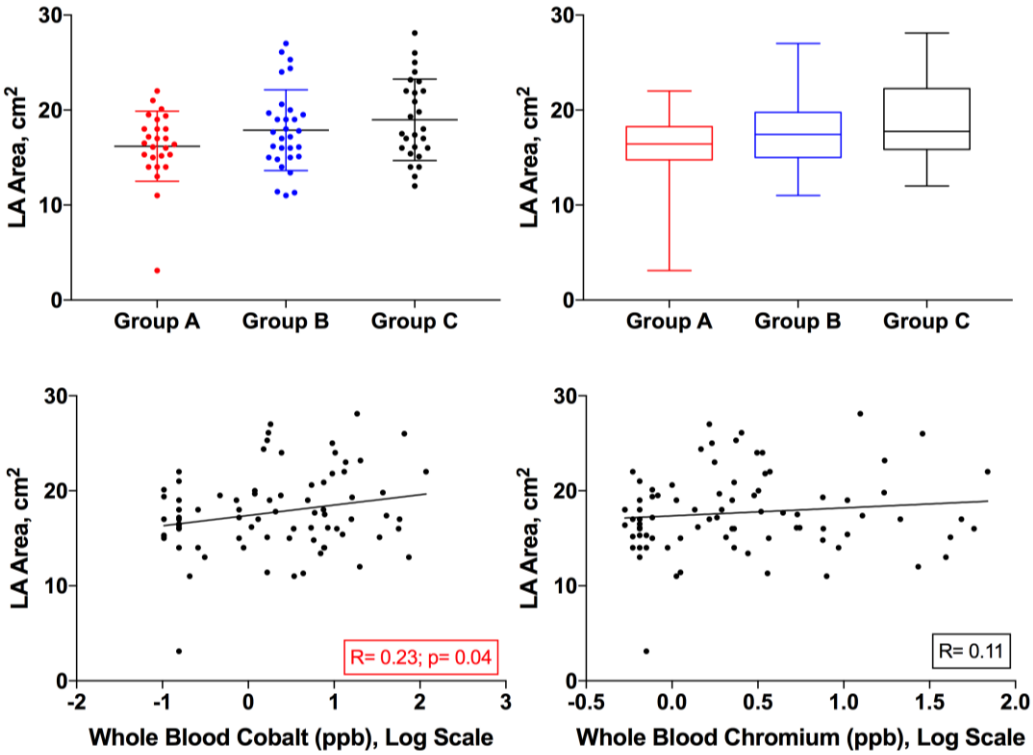

Figure 5.10: *Top left – Scatter plot depicting LA Area across groups with mean (±SD); Top right – Box and whisker plot demonstrating median LA Area values; Bottom left – Scatter plot to demonstrate positive correlation between Cobalt and LA Area; Bottom right – correlation between Chromium and LA Area*

It can be seen from the plots in figure 5.10 that group A included a single outlier that appeared the skew the data and may have resulted in the positive correlation seen with Cobalt. On further review this patient was found to have LA dilatation on CMR images (with a background of mitral regurgitation) and therefore it is likely that the LA Area measured by echocardiography (3.1cm^2) was incorrect, most likely due to poor views.

The analysis was repeated excluding this outlier result with a resulting group A mean of 16.72cm^2 (± 2.6; median 16.5). The ANOVA statistic revealed no difference across the groups (F= 2.23; p= 0.11), however this test assumes

similar standard deviations across groups, which was not the case (Bartlett's test p= 0.03). The correlation coefficient between cobalt and LA Area was no longer significant (R= 0.19; p= 0.09) and chromium was unchanged (R= 0.08; p= 0.49). Figure 5.11.

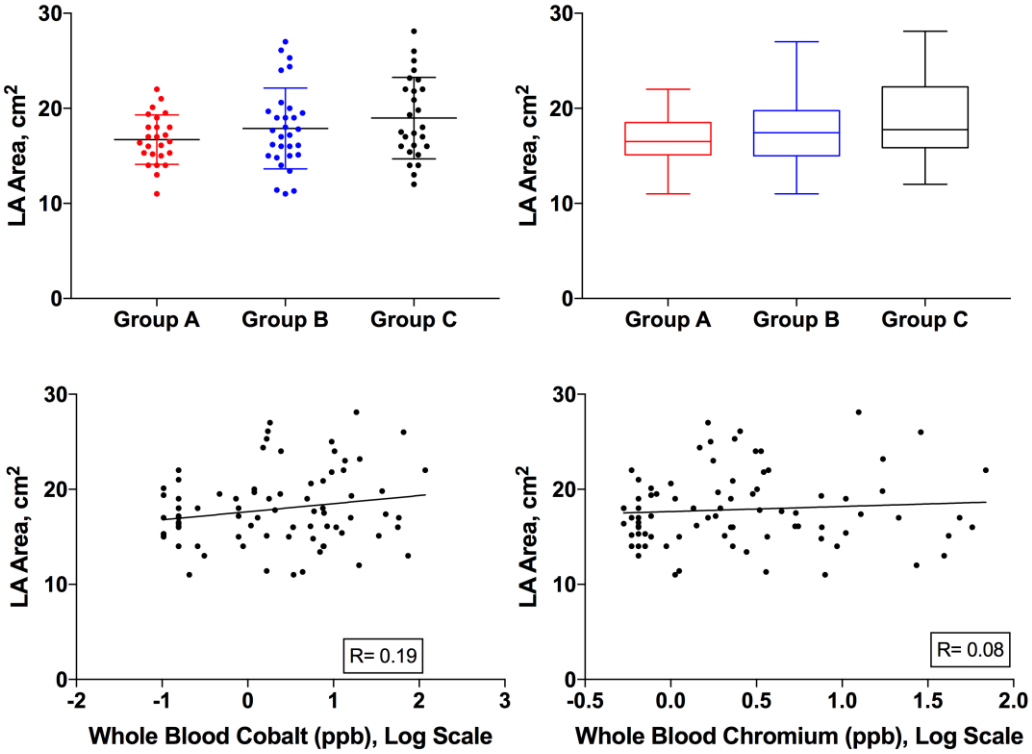

Figure 5.11: *Repeat plots for LA Area once outlier excluded*

5.4.3 Left Atrial Volume indexed

The mean LAVi value did not vary significantly across the three groups (27.02cm^2/m^2 ± 6.39 (SD) versus 28.00 ± 6.80 versus 30.58 ± 7.73; F= 1.67; p= 0.20). Median values for groups A, B and C were 27.5cm^2/m^2 versus 27 versus 31, respectively, and did not differ across groups (KW= 3.20; p= 0.20).

Pearson's correlation coefficient was used to assess for a correlation between measured LAVi and whole blood cobalt and chromium. No correlation was seen

between these two comparisons (Cobalt – R= 0.22; 95% CI= -0.01; 0.43; p= 0.07; Chromium – R= 0.21; 95% CI= -0.02; 0.42; p= 0.08). Figure 5.12.

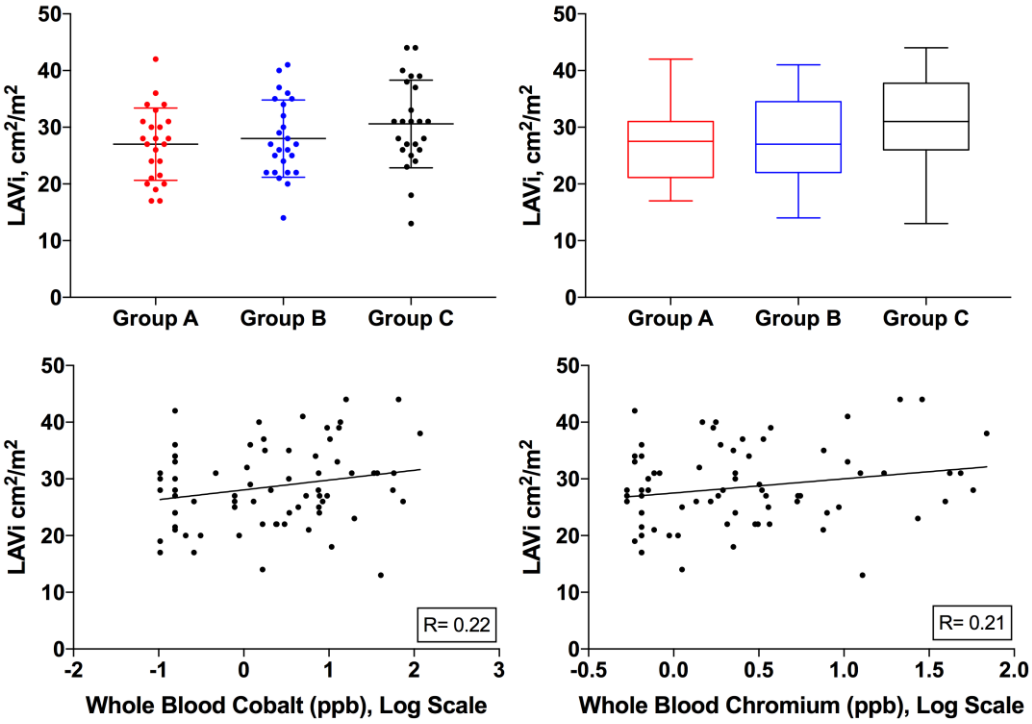

Figure 5.12: *Top left – Scatter plot showing the variation about the mean (±SD); Top right – Median values and associated variation across groups; Bottom left – Correlation between blood cobalt and LAVi; Bottom right – Correaltion between blood cbromium and LAVi*

5.4.4 Summary

This section reported the atrial dimensions measured by echocardiography. Despite the left atrial area demonstrating some positive differences across groups with a significant positive correlation when compared to blood cobalt levels, suggesting a detrimental effect of cobalt, this conclusion was commuted when an apparent outlier was removed from group A. Overall, there was no significant differences in atrial dimensions demonstrated across the three groups.

5.5 Tissue Doppler Imaging

5.5.1 TDI Lateral Wall Left Ventricle

The mean velocity of the lateral wall of the left ventricle did not vary between groups (0.09m/s ± 0.02 (SD) versus 0.08 ± 0.02 versus 0.09 ± 0.02, respectively; F= 1.46; p= 0.24). Similarly, no difference was seen between median velocities (0.09m/s versus 0.08 versus 0.09; KW= 2.98; p= 0.23). The majority of the values in all groups lay within the expected normative range (0.067-0.146)[257].

No correlation existed between Left Ventricular wall velocities versus blood cobalt (R= -0.07; 95% CI= -0.28; 0.15; p= 0.54) or blood chromium (R= -0.08; 95% CI= -0.29; 0.14; p= 0.49). Figure 5.13.

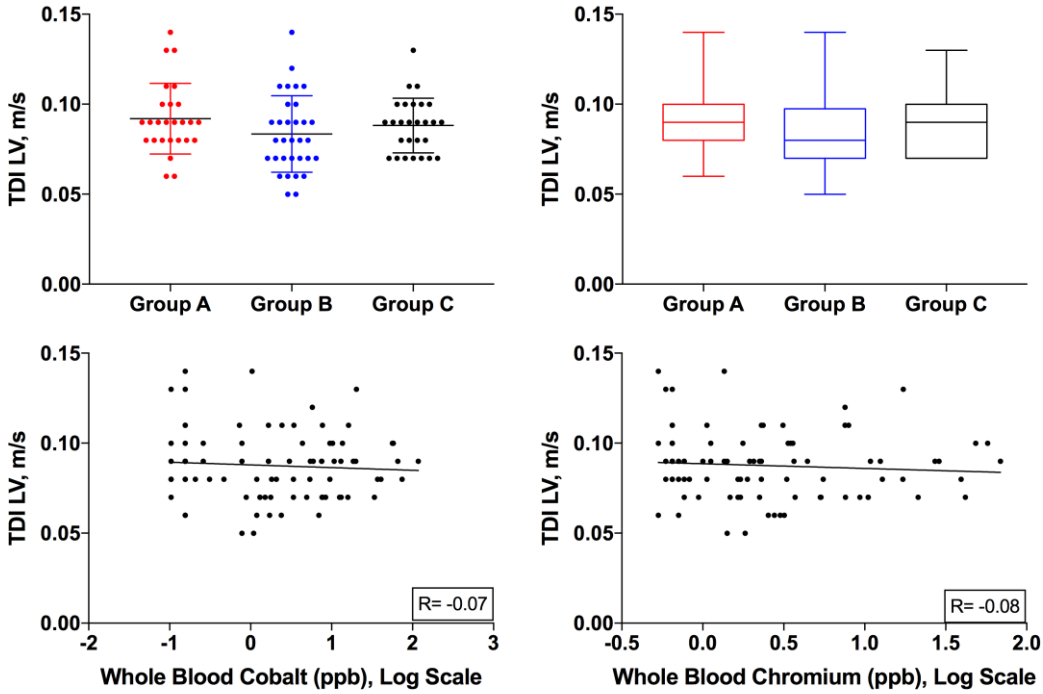

Figure 5.13: *TDI Left Ventricle. Top left - Scatter plot depicting variation about the mean velocities, compared across groups; Top right – median values plotted on a box and whiskers chart with associated max and min values; Bottom left – Plot of correlation between blood cobalt and TDI LV; Bottom right – Plot of correlation between blood chromium and TDI LV*

5.5.2 TDI Inter-Ventricular Septum (IVS)

Mean inter-ventricular septal velocities did not differ across groups A, B and C (0.08m/s ± 0.02 (SD) versus 0.07 ± 0.02 versus 0.08 ± 0.01; F= 1.90; p= 0.16) respectively. Similarly no differences existed between median values (0.08 versus 0.07 versus 0.08; KW= 4.72; p= 0.09).

Pearson's correlation coefficient was used to assess for a correlation between TDI IVS and blood Cobalt levels and also blood Chromium levels, both of which were non-significant (Cobalt – R= -0.13; 95% CI= -0.35; 0.07; p= 0.19; Chromium – R= -0.13; 95% CI= -0.34; 0.08; p= 0.22). Figure 5.14.

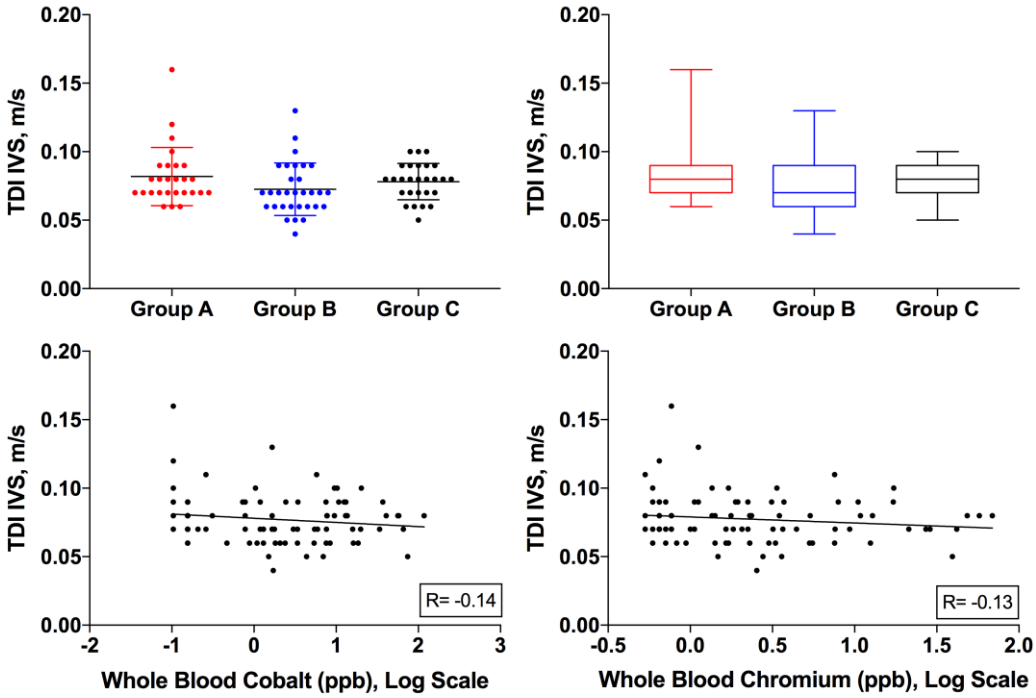

Figure 5.14: *TDI Inter-Ventricular Septum. Top left - Scatter plot depicting variation about the mean velocities, compared across groups; Top right – median values plotted on a box and whiskers chart with associated max and min values; Bottom left – Plot of correlation between blood cobalt and TDI IVS; Bottom right – Plot of correlation between blood chromium and TDI IVS*

5.5.3 TDI Right Ventricle

Tissue Doppler Imaging was also applied to the right ventricle to assess for abnormalities in wall motion. However due to the obtainable views being suboptimal in some patients there were a number of missing datasets (9 versus 4 versus 12 missing from groups A, B and C respectively).

With this in mind, the mean velocities across the three groups differed significantly (0.14m/s ± 0.03 (SD) versus 0.11 ± 0.02 versus 0.12 ± 0.04; F= 5.77; p= 0.005; (Bartlett's Statistic = 4.79; p= 0.09)) to suggest the patients exposed to metal implants had reduced right ventricular velocities compared to the ceramic hip group. To avoid assumptions of normality, median velocities were compared,

which confirmed the parametric test results (KW= 9.7; p= 0.008). Despite this difference, the velocities recorded were within the expected normal range [258]. Despite the differences seen between the group mean and median values, no significant correlations existed between TDI RV and blood cobalt (R= -0.19; 95% CI= -0.41; 0.06; p= 0.14) and also versus blood chromium (R= -0.12; 95% CI= -0.36; 0.13; p= 0.33) to suggest a dose response to metal levels. Figure 5.15.

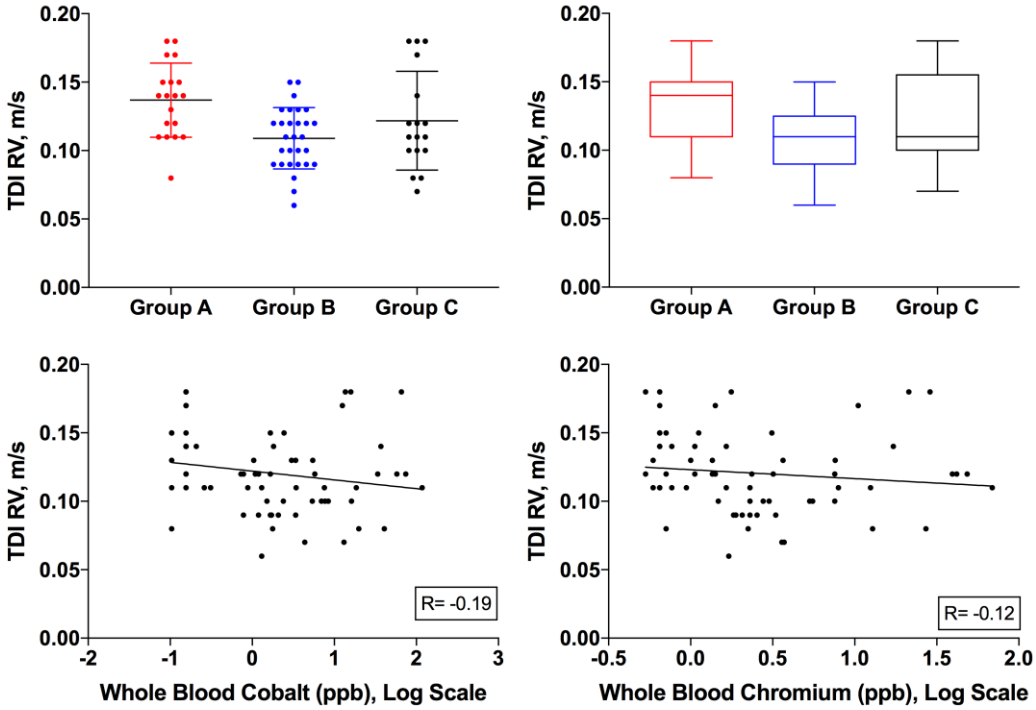

Figure 5.15: *TDI Right Ventricle. Top left - Scatter plot depicting variation about the mean velocities, compared across groups; Top right – median values plotted on a box and whiskers chart with associated max and min values; Bottom left – Plot of correlation between blood cobalt and TDI RV; Bottom right – Plot of correlation between blood chromium and TDI RV*

5.5.4 Summary

In summary, left ventricular and inter-ventricular wall function did not appear to be affected by exposure to blood metal, which correlates well with measurements of LV ejection fraction. A negative effect of blood metal was seen

against right ventricular wall motion velocity, although this did not correlate with blood metal levels. The difficulty with drawing a conclusion from the results for the right ventricle lie in the number of missing datasets that may have skewed the data.

5.6 Global Longitudinal Peak Strain

5.6.1 Results

GLPS was determined by Doppler imaging in all patients, however due to poor obtainable views a number of examinations were suboptimal. Missing data was equivalent across the three groups, with 19 versus 22 versus 19 datasets available for final comparison.

The mean strain recorded across the three groups was not significantly different (-18.86% ± 2.39 (SD) versus -18.48 ± 3.68 versus -18.43 ± 3.93; F= 0.09; p= 0.91). The median values were also similar across groups (-19.1 versus -18.05 versus -19.2; KW= 0.25; p= 0.88). Figure 5.16.

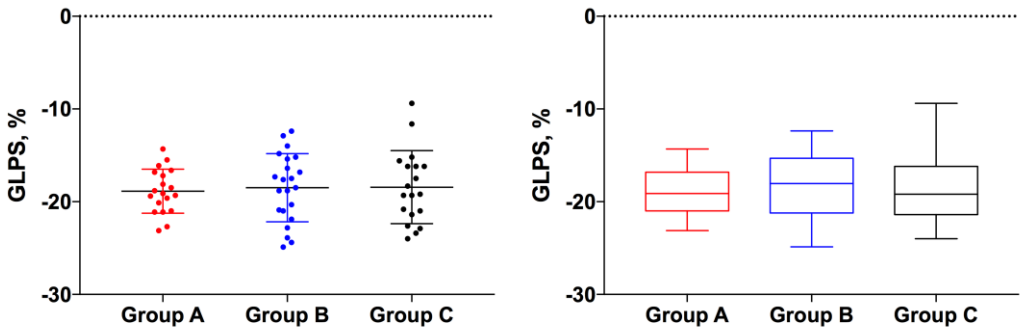

Figure 5.16: *GLPS (%) - Variation about the Mean and Median, presented on a scatter plot and box and whiskers plot respectively.*

Pearson's correlation coefficient was used to assess for a correlation between the recorded GLPS and blood cobalt (R= 0.09; 95% CI= -0.17; 0.33; p= 0.51) and chromium levels (R= 0.01; 95% CI= -0.24; 0.26; p= 0.94), however no significant correlation was seen. Figure 5.17.

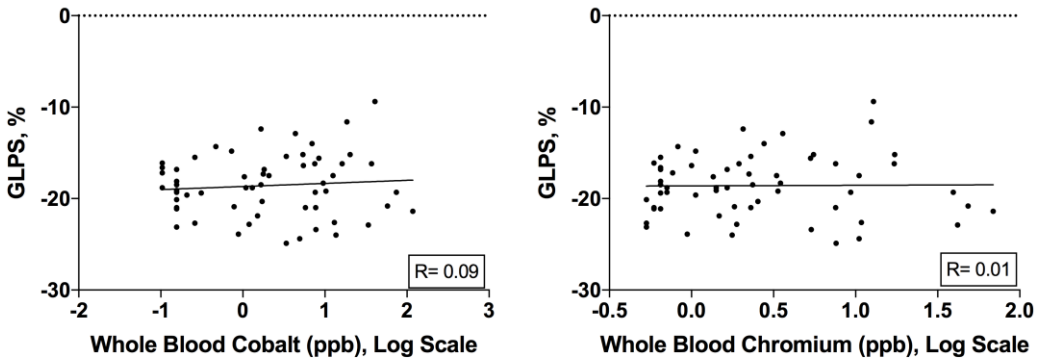

Figure 5.17: *Scatter plots demonstrating the correlation between measured GLPS (%) and whole blood cobalt (left) and chromium (right) levels (log scale ppb)*

5.6.2 Summary

Global longitudinal peak strain was not seen to vary across groups, with the majority of cases falling within normative ranges. No correlation was seen to suggest worsening strain patterns with higher blood cobalt or chromium levels. This result suggests global LV function is unaffected and aligns well with previous assessments of LV function, namely LV ejection fraction.

5.7 Discussion

In this chapter, the results of echocardiographic assessment of 90 patients belonging to three groups defined by implant type and exposure to metal ions of

different levels was presented. Although there are perceived limitations when using echocardiography in comparison to CMR, such as increased inter-observer variability and geometric assumptions, echo offers an ideal confirmation of CMR findings. There are advantages to its use, which include being more freely available compared to CMR, it offers dynamic cardiac assessments and is more acceptable to patients with fewer contra-indications. In addition, echo also offers supplementary tests not seen with CMR such as Doppler assessment of regional wall motion abnormalities and strain.

In summary, left ventricular ejection fraction and dimensions were not negatively affected by exposure to blood cobalt or chromium. This is in line with the results presented in chapter 4 (CMR – volumes and function). There appeared to be a false positive result to suggest left atrial area was greater (dilated) in the metal exposed groups, however after removal of an outlier, no difference was subsequently seen. Right ventricular wall motion velocities measured by tissue Doppler imaging revealed reduced velocity in patients exposed to elevated cobalt and chromium compared to those with ceramic hip implants. Although missing datasets may have contributed to this positive finding.

Overall however, the results from assessment were largely reassuring and corroborated the results seen in chapter 4.

CHAPTER 6

CHAPTER 6 TISSUE CHARACTERISATION

6.1 Introduction

Tissue characterisation entails the use of specific CMR sequences to define the myocardium and liver tissues in terms of cellular and extracellular compartments. It also entails the use of blood biomarkers that reflect the function and morphology of cardiac tissues with respect to certain pathological conditions that can affect the myocardium.

T1 (without contrast) reflects myocardial and liver disease involving the host cells and interstitium without use of gadolinium based contrast agents. On the other hand the extracellular volume (ECV) fraction after application of gadolinium based contrast agent offers a direct measure of the size of the extracellular space, reflecting interstitial disease such as fibrosis.

In addition to these sequences, T2* has been validated for the detection of myocardial and liver iron in diseases such as haemochromatosis. Furthermore, as discussed in chapter 2, T2* can detect the presence of other paramagnetic metals such as cobalt and chromium.

Thus far, elevated circulating blood cobalt and chromium levels have been shown to have little detrimental affects on the myocardial volume, structure and subsequent function of the heart. This has been demonstrated using both CMR and echocardiography, and contradicts the findings in a study by Prentice et al [167]. However, several case reports have reported biopsy / autopsy proven metal deposits within the myocardium, with subsequent associated comorbidity [17] [18] [156] [165].

Despite normal myocardial volumes and function seen thus far in this study, there may still be evidence of sub-clinical tissue pathology and metal deposition. Therefore, these well characterized T1 and T2 sequences were used to assess for underlying tissue pathology in the cohort of patients recruited to this study. Both the myocardium and liver were characterized using both MOLLi and ShMOLLi T1 sequences (pre and post-contrast), followed by T2* and assessment for post contrast Late Gadolinuum Enhancement. ECV was computed once pre and post-contrast T1 values were obtained.

6.2 Results for T1 Mapping

6.2.1 Myocardial MOLLI

Mean T1 times using MOLLI sequences did not significantly vary across the groups (1030.26ms ± 42.47 (SD) versus 10.13.94 ± 33.44 versus 1022.07 ± 36.88; F= 1.39; p= 0.26). In addition, median times were also statistically similar (1036ms versus 1012.5 versus 1022; KW= 2.6; p= 0.27). Figure 6.1.

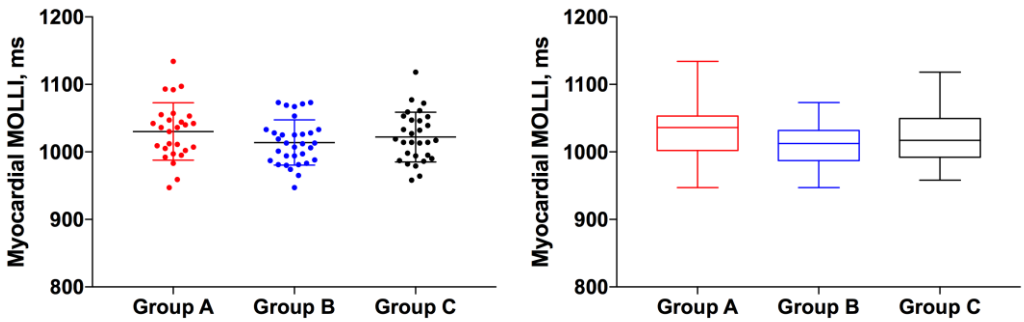

Figure 6.1: *Scatter plot demonstrating the variation about mean MOLLi values across groups (left) and a box and whiskers plot demonstrating the variation about the median (right).*

Rising whole blood cobalt levels did not have a significant effect on the measured T1 time, with a statistically non-significant Pearson's correlation coefficient (R= -0.06; 95% CI= -0.27; 0.15; p= 0.57). There was also a lack of correlation between T1 and blood chromium (R= -0.05; 95% CI= -0.26; 0.16; p= 0.64). Figure 6.2.

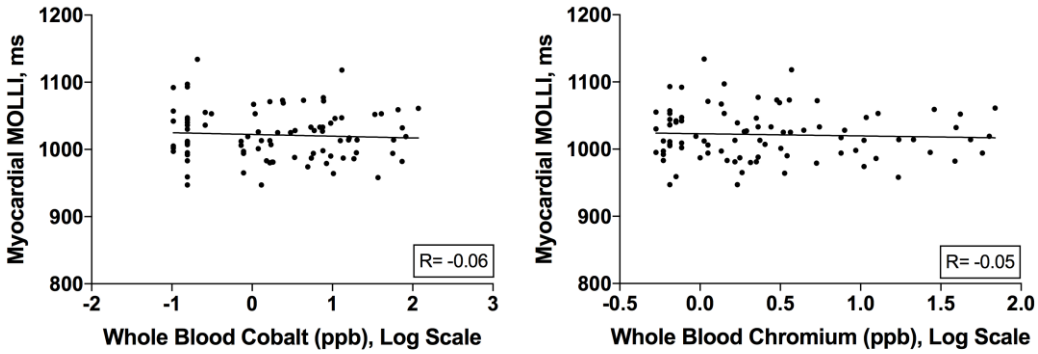

Figure 6.2: *Scatter plots demonstrating Pearson's correlation coefficient between T1 MOLLI and blood cobalt (left) and chromium (right)*

6.2.2 Liver MOLLI

T1 MOLLI times obtained from a mid-hepatic sequence failed to demonstrate a significant difference between the mean values across the three groups (615.60ms ± 71.71 (SD) versus 596.03 ± 77.74 versus 583.71 ± 49.49; F= 1.57; p= 0.21). Similarly, median times were similar across groups (607.5ms versus 584 versus 595.5 respectively; KW= 1.79; p= 0.41). No obvious outliers were identified amongst the three groups. Figure 6.3.

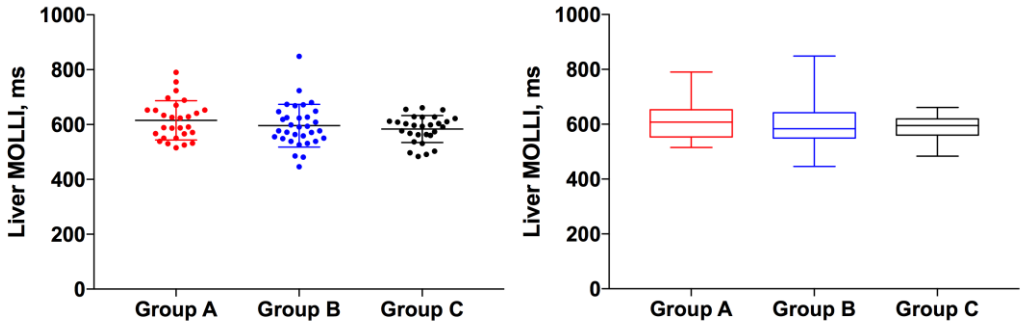

Figure 6.3: *Left – scatter plot demonstrating the mean (±SD) Liver T1 across the three groups; Right – Box and whiskers plot demonstrating the variation about the median Liver T1 value across the three groups*

Pearson's correlation coefficient was used to assess for a significant correlation between the recorded Liver T1 times and the circulating blood cobalt and chromium. Neither revealed a significant correlation, and a slight negative trend was seen in both (Cobalt – R= -0.13; 95% CI= -0.33; 0.08; p= 0.21; Chromium – R= -0.12; 95% CI= -0.32; 0.09; p= 0.25). Figure 6.4.

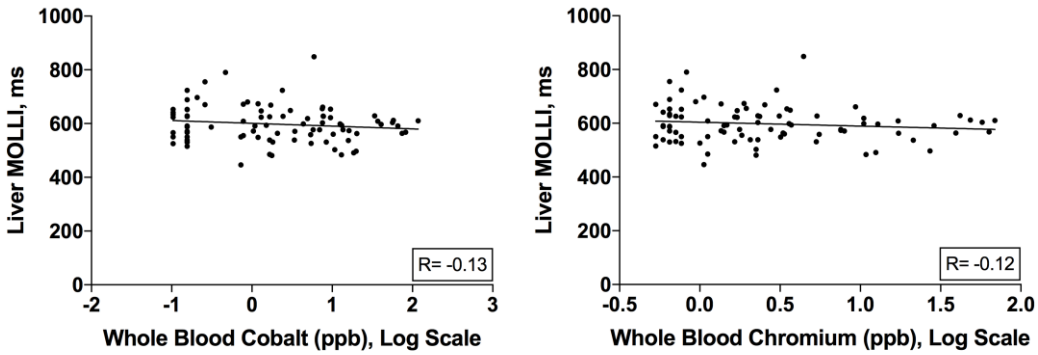

Figure 6.4: *Scatter plots depicting the Pearson's correlation coefficient between Liver T1 (MOLLI) times and blood cobalt (left) and chromium (right)*

6.2.3 Myocardial ShMOLLI

Since T1 mapping is not yet fully standardized, ShMOLLI sequences were also conducted. These sequences re-iterated the findings from the MOLLI sequences.

The mean myocardial T1 ShMOLLI times did not differ across groups (961.18ms ± 30.55 (SD) versus 956.85 ± 29.65 versus 955.61 ± 44.03; F= 0.20; p= 0.82). Median times were also similar across the three groups (959ms versus 953 versus 948 respectively; KW= 1.72; p= 0.42). Figure 6.5.

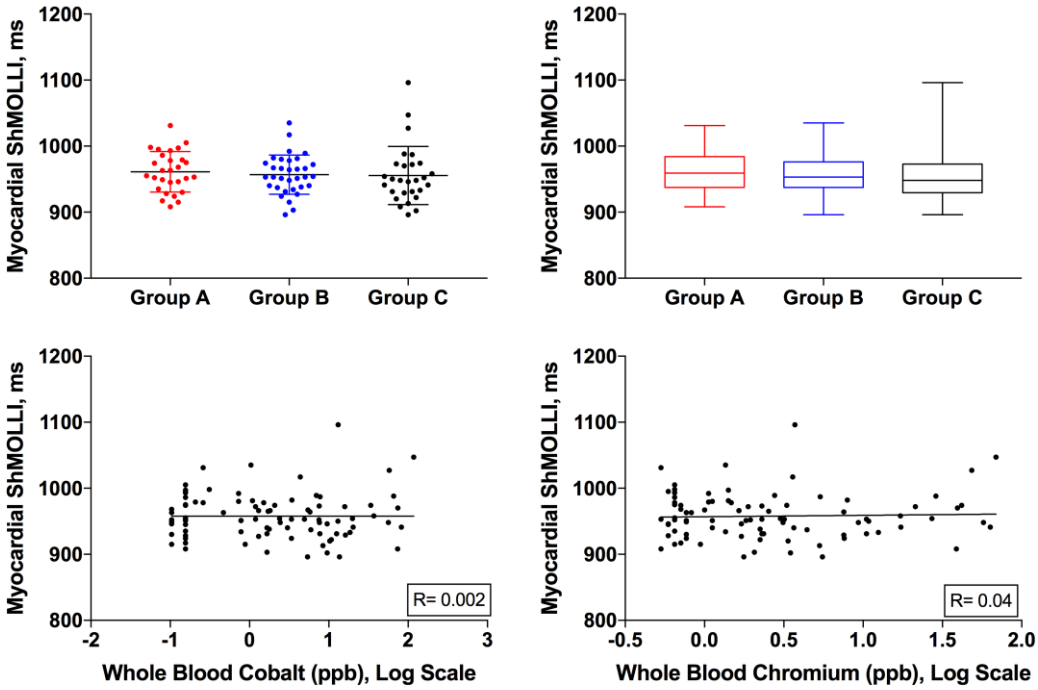

Figure 6.5: *Top left – scatter plot in columns demonstrating the mean value and the associated spread; Top right – Box and whiskers plot of median values and associated spread; Bottom left – scatter plot of correlation coefficient between blood cobalt and T1 ShMOLLI; Bottom right – correlation coefficient between T1 ShMOLLI and blood chromium*

Correlation coefficients were determined between the measured T1 ShMOLLI time and whole blood cobalt (R= 0.002; 95% CI -0.21; 0.21; p= 0.98) and whole blood chromium levels (R= 0.04; 95% CI= -0.17; 0.24; p= 0.74), neither of which had a significant correlation. Figure 6.5.

6.2.4 Liver ShMOLLI

Similar to Liver MOLLI sequences, the mean T1 times using ShMOLLI sequences were not different across the three groups (558.25ms ± 45.88 (SD) versus 538.61 ± 49.97 versus 542.97 ± 45.83 respectively; F= 1.40; p= 0.25). To ensure parametric assumptions were not incorrect, non-parametric tests to compare median T1 values across the groups were also undertaken, and revealed similar median times across the three groups (551ms versus 540 versus 548 respectively; KW= 2.16; p= 0.34). Figure 6.6.

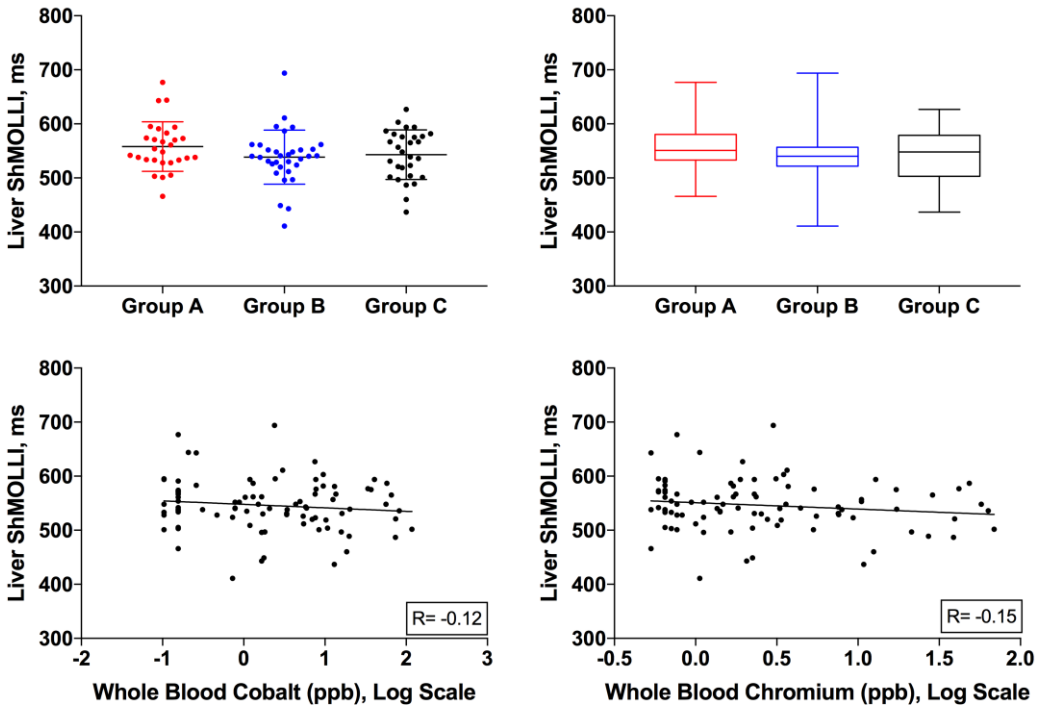

Figure 6.6: *Liver ShMOLLI Top left – scatter plot in columns demonstrating the mean value and the associated spread; Top right – Box and whiskers plot of median values and associated spread; Bottom left – scatter plot of correlation coefficient between blood cobalt and T1 ShMOLLI; Bottom right – correlation coefficient between T1 ShMOLLI and blood chromium*

Correlation coefficients were also non statistically significant when comparing liver T1 ShMOLLI times with blood cobalt (R= -0.12; 95% CI= -0.32; 0.09; p=

0.26) and blood chromium levels (R= -0.15; 95% CI= -0.34; 0.06; p= 0.17). Figure 6.6.

6.2.5 Summary

T1 mapping with both MOLLI and ShMOLLI sequences revealed relaxation times within normal ranges and without variation across groups, suggesting no negative effects of elevated cobalt or chromium on the myocardial and liver cellular and extracellular structure.

6.3 Extra Cellular Volume

6.3.1 Myocardial ECV

The mean ECV fraction did not significantly differ across the three groups of patients studied in this thesis (0.28 ± 0.03 (SD) versus 0.27 ± 0.03 versus 0.29 ± 0.04 respectively; F= 1.28; p= 0.28). Median values were equally similar and relaxed the parametric assumptions regarding the data (0.29 versus 0.27 versus 0.28; KW= 2.44; p= 0.30). Figure 6.7.

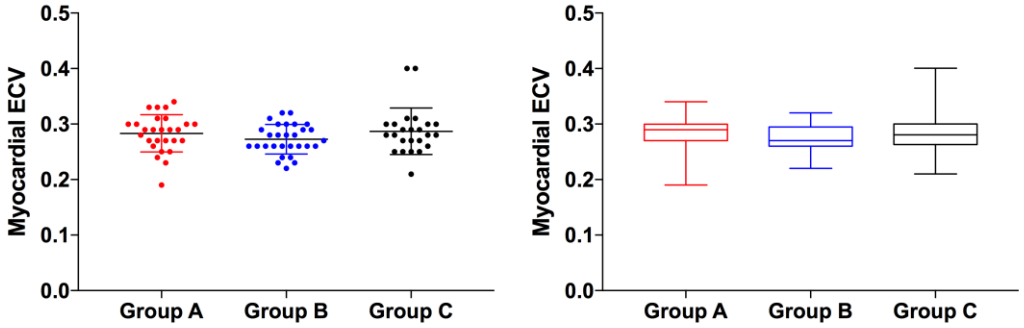

Figure 6.7: *Left – scatter plot of mean ECV (±SD) for each group studied; Right – Box and whiskers plot demonstrating the median value and associated variation*

Pearson's coefficient was used to assess for a significant correlation between the measured myocardial ECV and blood cobalt (R= 0.05; 95% CI= -0.17; 0.27; p= 0.64) and blood chromium levels (R= 0.04; 95% CI= -0.18; 0.26; p= 0.71) respectively. Neither showed a positive correlation to suggest that increasing blood metal levels had a detrimental effect on the extracellular matrix. Figure 6.8.

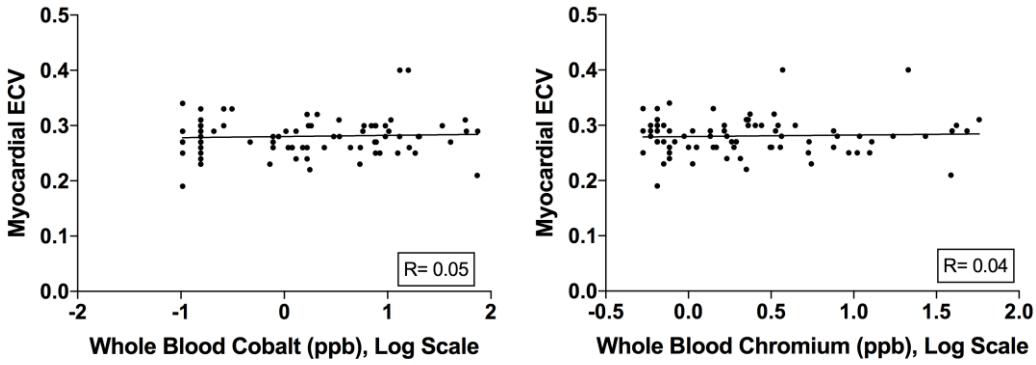

Figure 6.8: *Scatter plots of ECV versus blood cobalt (left) and chromium (right)*

6.3.2 Liver ECV

Liver ECV demonstrated similar findings to myocardial ECV, with little variation of the mean values across the three groups studied here (0.29 ± 0.04 (SD) versus 0.30 ± 0.03 versus 0.30 ± 0.04; F= 0.48; p= 0.62). Median values were also similar across groups (0.28 versus 0.30 versus 0.30; KW= 2.13; p= 0.35). Figure 6.9.

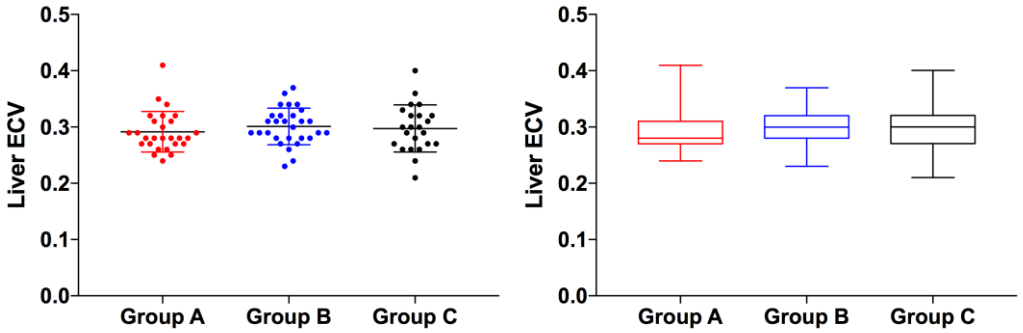

Figure 6.9: *Left - Scatter plot of mean (±SD) for ECV across the three groups studied; Right – Median fractions and associated variation for the three groups studied*

No significant correlations were detected between Liver ECV and circulating blood cobalt (R= 0.05; 95% CI= -0.17; 0.27; p= 0.65) or blood chromium levels (R= 0.006; 95% CI= -0.22; 0.23; p= 0.96). Figure 6.10.

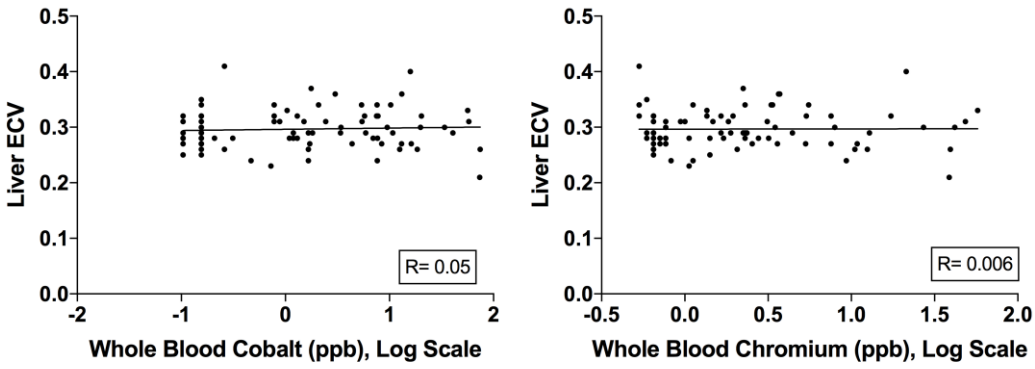

Figure 6.10: *Scatter plots of Liver ECV versus blood cobalt (left) and blood chromium (right)*

6.3.3 Summary

There was no evidence of expanded myocardial ECV to suggest widespread fibrosis of non-ischaemic cardiomyopathy amongst the three groups studied, with no correlation between increasing blood metal levels and ECV to suggest a dose effect. Similarly, the liver ECV did not appear to be expanded, nor did it correlate with an increasing level of blood cobalt or chromium.

6.4 T2*

6.4.1 Myocardial T2*

Normal myocardial T2* values are >20ms. No abnormal T2* values were recorded throughout the 90 patient cohort studied here. Mean values were not significantly different when compared across groups and the variation about the mean was similar throughout (31.48ms ± 4.63 (SD) versus 31.18 ± 5.88 versus 32.37 ± 5.65; F= 0.37; p= 0.69). Figure 6.11.

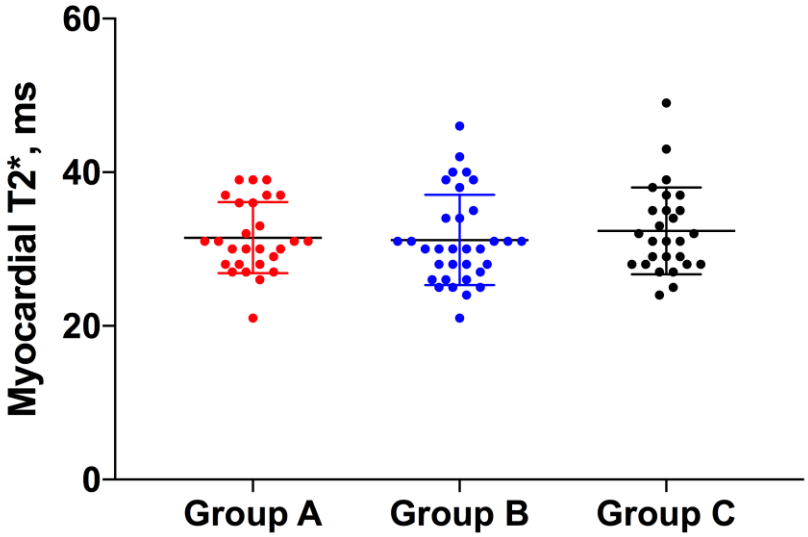

Figure 6.11: *Scatter plot demonstrating the mean myocardial T2* value for each group with variation about the mean (±SD)*

To relax the parametric assumptions without testing for normal distribution (small sample sizes), the median values for each group was compared using the Kruskal-Wallis statistic and no significant difference was demonstrated (31 versus 30 versus 31; KW= 0.87; p= 0.65). Figure 6.12.

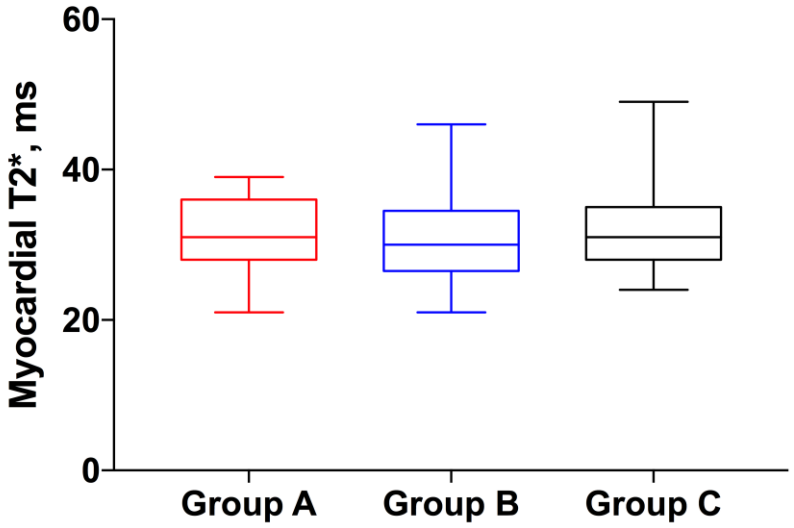

Figure 6.12: *Median myocardial T2* value and associated min-max values across the three groups studied*

Pearson's coefficient was used to assess for an underlying correlation between the recorded T2* value and the circulating blood cobalt (R= 0.11; 95% CI= -0.10; 0.31; p= 0.32) and blood chromium level (R= 0.06; 95% CI -0.15; 0.27; p= 0.55). Neither combination demonstrated a significant correlation to suggest increasing metal deposition with shortened T2* values. Figure 6.13.

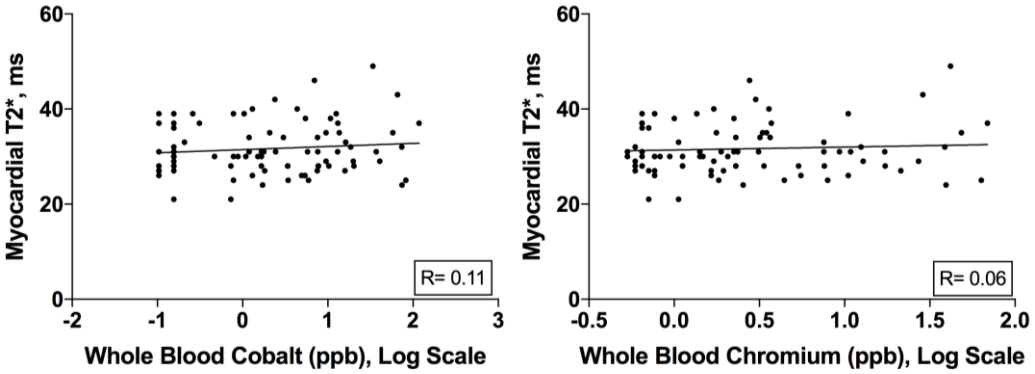

Figure 6.13: *Scatter plots demonstrating correlation between myocardial T2* and circulating blood cobalt (left) and chromium (right)*

6.4.2 Liver T2*

The lower limit of normal for the liver T2* time is 6.3ms. The mean T2* times for groups A, B and C did not vary significantly between groups (25.49ms ± 4.48 (SD) versus 25.96 ± 6.65 versus 24.69 ± 4.96; F= 0.40; p= 0.67). Median values were also statistically similar (25.65 versus 27 versus 25.7; KW= 1.43; p= 0.49). Figure 6.14.

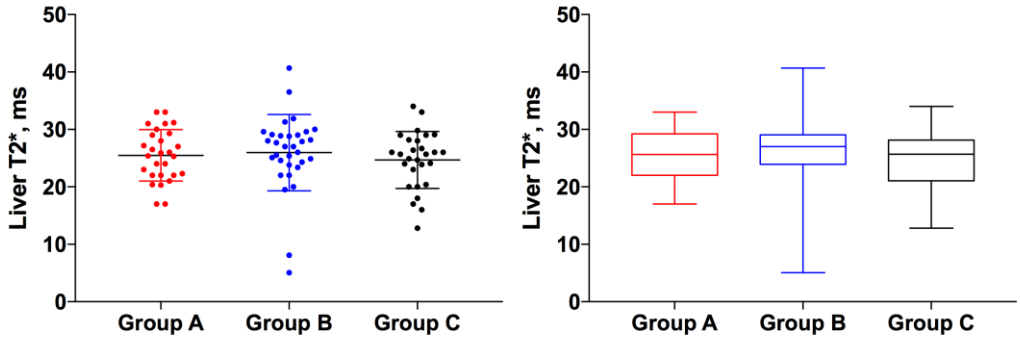

Figure 6.14: *Left – scatter plot of Liver T2* times for each group with mean (±SD) values and associated spread; Right – Median Liver T2* times for each group. NB: Group B has a minimum value within the abnormal range*

Of note, two patients belonging to group B appeared to have shortened Liver T2* times, of which one was deemed abnormal. The T2* recorded for this 45 year old patient was 5.05ms. This man had relatively normal circulating blood metal ions (cobalt 1.77ppb and chromium 2.24ppb). On review of his CMR findings he was found to have low hepatic T2* and low T1 (ShMOLLI 449ms – lower end of normal) values suggesting the presence of iron or metal ions. Myocardial T2* (31ms) was normal. His biventricular myocardial sizes and function (ejection fraction 63%) were within normal range. No late gadolinium enhancement was seen to suggest focal fibrosis or scar. This patient underwent further investigation beyond this study and was diagnosed with hereditary haemochromatosis.

Pearson's coefficient was used to assess for a correlation between the Liver T2* times and the circulating blood cobalt and chromium levels. No significant correlation was demonstrated with either comparison (cobalt – R= -0.02; 95% CI= -0.23; 0.19; p= 0.83; chromium – R= -0.03; 95% CI= -0.24; 0.18; p= 0.79). This

was without exclusion of the patient found to have hereditary haemochromatosis. See figure 6.15.

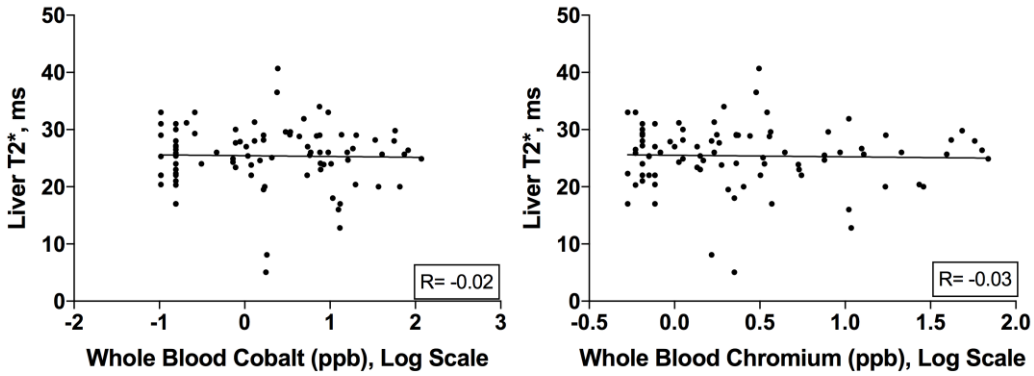

Figure 6.15: *Scatter plot demonstrating correlation coefficient between Liver T2* and Cobalt (left) and Chromium (right)*

6.4.3 Summary

T2* sequences are currently used to non-invasively detect tissue deposition of iron in haemochromatosis patients and has the potential to offer similar uses in the detection of cobalt and chromium as seen in chapter 2. In this series of 90 patients with a range of blood metal levels rising to 118ppb, no cases of abnormally reduced T2* times were seen to suggest myocardial or liver deposition of cobalt or chromium.

6.5 Late Gadolinium Enhancement

6.5.1 LGE Results

There were a small number of patients from each group that were identified as having late gadolinium enhancement. No patients demonstrated changes suggestive of cardiomyopathy.

Two patients in group A demonstrated midwall/subepicardial LGE within the basal inferolateral wall, which is of a non-ischaemic distribution, and its relevance was unknown. Both cases were deemed to represent scarring from prior myocarditis. Both patients had otherwise normal myocardial volumes and function.

Within group B two patients had subendocardial scars within the distal mid-wall of the left ventricle that likely demonstrated small coronary embolic events or previous myocarditis. A further 35-year-old patient with an otherwise normal cardiac MRI was found to have mid-wall septal fibrosis, the significance of which was unclear. This patient was referred for repeat scanning at 12 months to re-assess the scar.

Two patients within group C demonstrated similar basal inferolateral subepicardial late gadolinium enhancement in a non-ischaemic distribution, likely to demonstrate previous myocarditis. Myocardial volumes and functions in these two patients were otherwise normal. A third patient, 81 years of age, demonstrated widespread patchy mid-wall and subendocardial late gadolinium enhancement (most marked in the basal and inferolateral segments) typical of amyloidosis, which he was later diagnosed with. A 70 year old male patient

demonstrated evidence of prior infarction in the circumflex territory with transmural infarction in the basal inferolateral segment and subendocardial infarction in the mid inferolateral and basal segments.

6.5.2 Summary

Ultimately, no patients across the three groups demonstrated changes suggestive of dilated cardiomyopathy or other changes thought to arise from metal tissue loading. However, the cases of basal enhancement in non-ischaemic patterns did not have definitive diagnoses.

6.6 Blood Biomarkers

6.6.1 Cardiac Troponin

The normal range for cardiac troponin lies between 0-14ng/L. The group mean values did not differ significantly when compared using an ANOVA analysis (7.38 ± 6.9 (SD) versus 7.16 ± 4.99 versus 8.62 ± 10.17 respectively for groups A, B and C; F= 0.27; p= 0.77). To relax the parametric assumptions, the median values were also compared between the three groups with no significant difference demonstrated (4 versus 6 versus 4.5 respectively; KW 1.06; p= 0.59). Cardiac troponin was also compared to circulating blood cobalt (R= 0.03; 95% CI= -0.20; 0.26; p= 0.80) and chromium (R= -0.03; 95% CI= -0.26; 0.20; p= 0.79) using

Pearson's correlation coefficient. No significant correlations were seen. Figure 6.16.

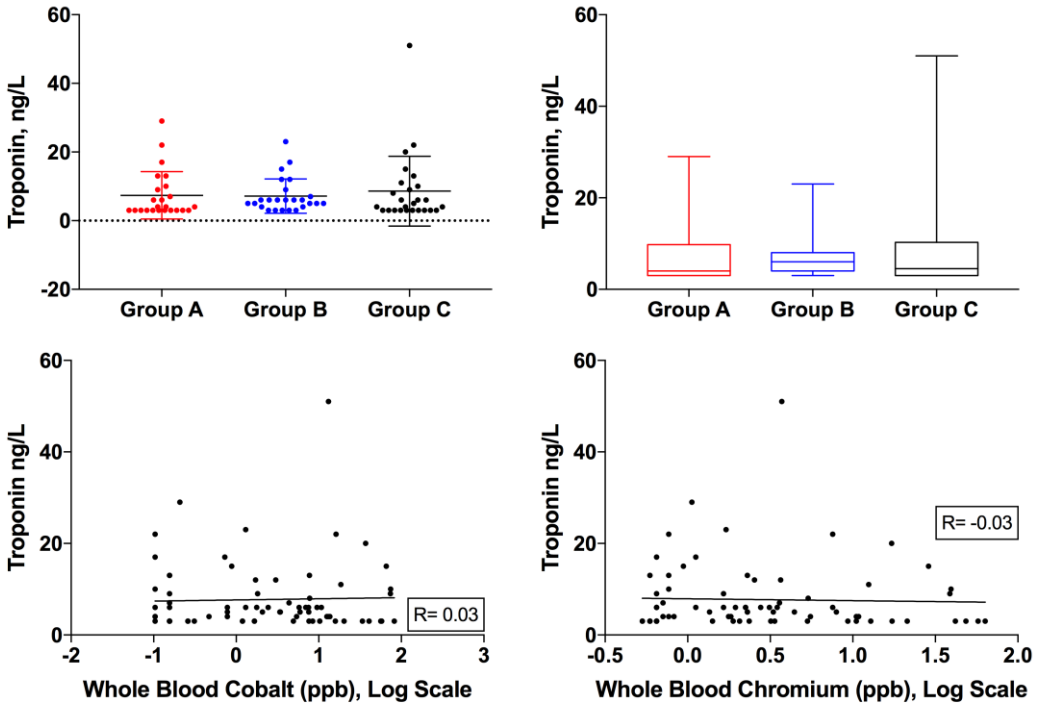

Figure 6.16: *Top left – scatter plot demonstrating group means and associated variation (SD); Top right – Box nd whiskers plot of group median values including min/max values; Bottom left – Scatter plot of correlation between Cardiac Troponin and blood cobalt; Bottom right – Scatter plot of correlation between Cardiac Troponin and blood chromium*

6.6.2 B-type Natriuretic Peptide

The normal range for B-type natriuretic peptide (BNP) is <47 µmol/L. The mean values across the three groups studied here were not statistically different (11.39 ± 10.08 (SD) versus 10.54 ± 7.88 versus 24.85 ± 61.32 fo groups A, B and C respectively; F= 1.21; p= 0.30; Bartlett's statistic = 106.7; p< 0.001). However despite the ANOVA analysis proving non-significant, which assumes similar standard deviations, this was not the case. Group C had a single patient with a BNP value of 322 µmol/L, which elevated the group mean considerably. This

patient was diagnosed with hypertrophic obstructive cardiomyopathy (unrelated to metal disease) that explained the elevated BNP. Therefore the ANOVA was repeated with this value excluded, and remained statistically not significant (F= 0.46; p= 0.64). Similarly no significant difference was seen between the three groups using non-parametric testing (7 versus 7.5 versus 10.5 for groups A, B and C respectively; KW= 4.50; p= 0.11).

No correlation was evident between blood BNP and blood cobalt (R= 0.20; 95% CI= -0.02; 0.41; p= 0.08) or blood chromium levels (R= 0.19; 95% CI= -0.04; 0.40; p= 0.10) using Pearson's correlation coefficient. Figure 6.17.

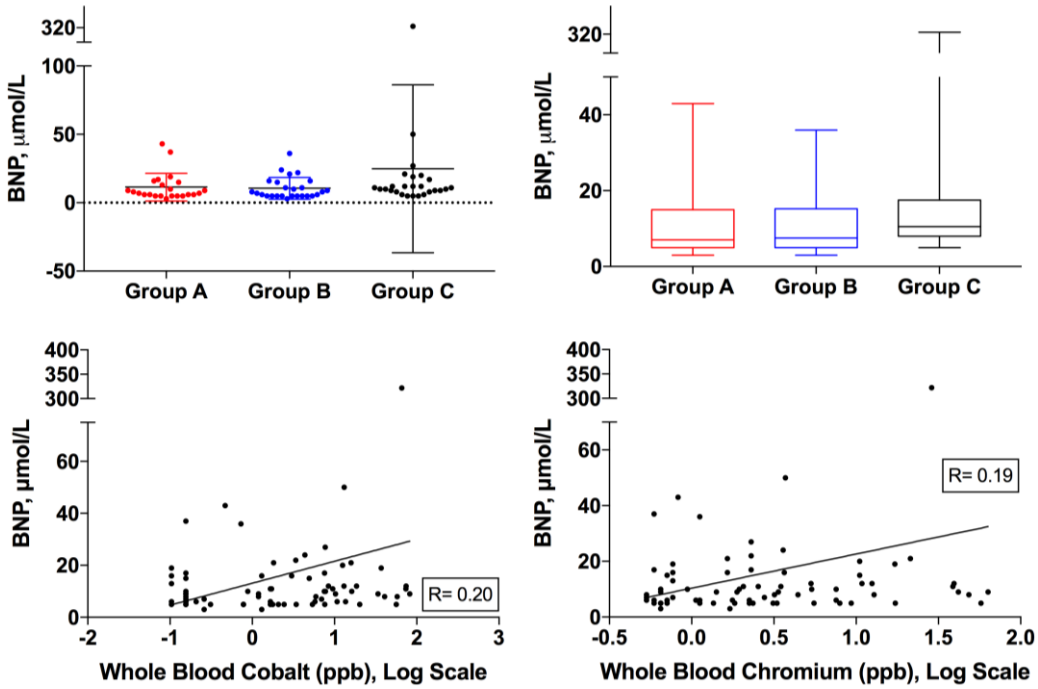

Figure 6.17: *Top left – scatter plot demonstrating group means and associated variation (SD); Top right – Box nd whiskers plot of group median values including min/max values; Bottom left – Scatter plot of correlation between BNP and blood cobalt; Bottom right – Scatter plot of correlation between BNP and blood chromium*

6.6.3 Summary

Blood biomarkers were aligned to the general results seen throughout this thesis, which suggest no significant effect of circulating metal ions on cardiac health in this cohort of patients.

6.7 Discussion

It has previously been suggested that the pathophysiology of cobalt cardiotoxicity consists of cobalt interference with cardiac myocyte oxygen uptake, and transmembrane transport system disruption[74]. Histopathological findings in cobalt-related cardiac toxicity include myofibrillar hypertrophy, interstitial fibrosis, and muscle fiber degeneration. What is unknown is whether this process occurs in the majority of patients that have been exposed to cobalt and chromium, and therefore should be expected to some extent in all patients.

T1 mapping techniques including ECV and late gadolinium enhancement all revealed similar results across the three groups of patients recruited to this study, with blood metal levels rising to 118ppb. T2* times were also within normal range for the majority of patients. The findings suggest that tissue metal loading within the myocardium and liver is not common, and subsequent pathophysiological changes are not seen.

Blood biomarkers, which are sensitive for tissue strain and myocyte death, also demonstrated healthy results in the majority of patients.

Overall the results suggest that little change is seen on a cellular basis within the majority of patients with varying levels of blood cobalt and chromium.

CHAPTER 7

CHAPTER 7 ANALYSIS OF MDT APPLICATION OF RESULTS

Surgeons in the UK refer to the MHRA guidelines for advice and guidance when managing patients with MoM hip implants. However, the most recent updated guidance (2017) fails to mention actions that should be taken in cases of possible systemic toxicity [259]. The US FDA however does specify that patients should be assessed for clinical signs of metal toxicity, and that this should be conducted in collaboration with the patients medical physicians [9].

These regulatory agencies state the current evidence is lacking with regards to systemic toxicity, but that reports highlight a potential link. In that regard the results presented in this thesis go someway to reassure clinicians and patients. This is still an evolving problem and likely to change. In the meantime, surgeons are still seeking guidance on how best to tackle their clinical concerns, which introduces the idea of a multi-disciplinary approach in collaboration with medical specialists.

7.1 Application of this work

The concept of the work conducted in this thesis brings together several disciplines to question what is practically speaking an orthopaedic concern. However, given the very nature of adverse reactions to metal debris and its potential to affect not only the local tissues surrounding the hip implant, but also distant tissues and visceral organs, it is believed these patients may best be served through a multi-disciplinary approach. This would make sense when considering cases of systemic cardiotoxicity in particular, where cardiology

specialists would be best placed to advise on the clinical scenario and interpret the results of particular investigations.

Therefore, from a clinical perspective, the results from this thesis would best serve clinicians involved in multi-disciplinary management of patients with MoM hip implants. At the Royal National Orthopaedic Hospital we set in motion a dedicated tertiary referral Internet enhanced Multi-Disciplinary Team (iMDT) to advise on the management of patients with such hip implants.

The aim of this chapter is to review the activities and outcomes from this iMDT approach in order to understand further how a collaborative multi-disciplinary approach bringing together evidence such as results from this thesis can impact the management of patients with MoM hip implants including those suspected of having systemic toxicity.

7.1.1 Background to the iMDT

In 2012 the UK National Health Service spent approximately £124.5 million on hip revision surgery (10,466 cases at a cost of £11,897 per case) [232] [260]. This was anticipated to increase in line with the increasing rates of hip revision surgery; with revision hip surgery increasing 50% in 5years up until 2012 [232]. However in reality the NJR has reported a gradual reduction in the number of revisions performed annually, figure 7.1. The 14th Annual report of the NJR listed a total of 7,933 revision hip procedures in 2016, down from 10,466 in 2012 [261]. A more

recent cost analysis demonstrated increased costs for elective revision surgery at £13,110, which would equate to an annual cost of £104 million in 2016.

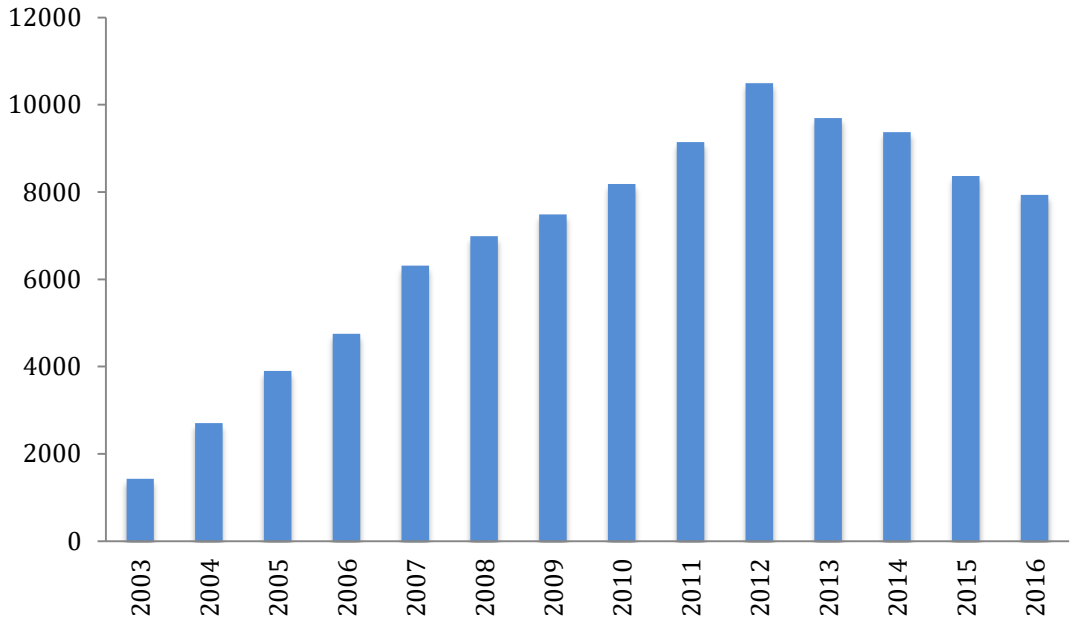

Figure 7.1: *Graph to demonstrate the number of revision cases recorded with the UK NJR and the temporal changes*

Interestingly, ARMD was the reported cause for revision in 11% of the total revision cases reported within the NJR to be undergoing a single stage revision (equivalent to 7361 cases). This would equate to a cost of £96.5 million to pay for all MoM revisions upto 2016. It is not known how many were revised for potential systemic toxicity, however it is assumed a small proportion of these will have been revised for systemic toxicity concerns.

There are additional economic losses to patients and the society [260], as well as an impact on the wellbeing of patients and a mortality rate of 2.5% in the first post-operative year [262]. Therefore, the decision regarding the need to revise a hip implant is never taken lightly. With over a million MoM hips implanted worldwide the need for comprehensive guidance on the management of these patients' remains of great importance. Currently the majority of patients

implanted have well functioning hips, and it is currently estimated that 80% of primary MoM implants remain in situ [263]. We know that hip resurfacings work well in young men (<55 years of age) with osteoarthritis [232], however it is a concern that patients can be asymptomatic despite having devastating complications from ARMD that may require revision surgery [264]. The chance of developing serious problems is yet to be risk stratified for all patient groups and implant types. In particular there are currently no robust thresholds for performing ARMD revision surgery [263].

It is well accepted that imaging findings influence the decision to revise in patients with well functioning hip replacements, for example osteolysis that is likely to cause impending fracture [144]. The influence of imaging findings of soft tissue abnormalities around MoM hips is yet to be fully understood [131]. The decision to revise MoM hips may not be based on a single investigation, particularly since current guidelines have limited detail on the interpretation of MRI findings and clinical symptoms, a scenario that is slowly changing with increasing literature to support certain positions.

Some cases are straightforward for most surgeons and decision-making is relatively easy. However, there are many cases that because of the lack of guidelines or the difficulty of applying guidelines in complex cases, surgeons experience considerable uncertainty with decision-making. For this reason some would argue for complex, if not all, MoM revision cases to be undertaken in specialist centres.

The patient group with potential systemic toxicity highlights a particular subgroup of patients that may be aymptomatic from the hip implant but may report other non-specific symptoms related to circulating metal ions. These

patients may not present through normal referral pathways and therefore it is up to all clinicians to maintain a level of vigilance for this concern. The work presented within this thesis is one of reassurance, however it highlights the need for a collaborative multi-disciplinary approach, in this case between orthopaedic surgeons, cardiologists and imaging specialists.

To help execute such decisions and in particular to help interpret clinical results we developed an Internet enhanced Multi-Disciplinary Team (iMDT) meeting in a tertiary referral centre. This acts as an extension of the guidance published by the regulatory agencies, with the aim of using surgical experience, tacit knowledge and evidence based current best practice to reduce the uncertainty surrounding the management of MoM hip patients. The referring surgeon who is often based at a different hospital then executes decisions recommended by the iMDT if it was deemed acceptable to the patient.

Hypothesis

By analyzing the activities and outcomes from this MDT approach we can understand further the impact of the results presented in this thesis. We hypothesise that an MDT meeting is a clinically useful method of managing the care recommendations for patients with MoM hip implants.

7.2 The iMDT method

The iMDT was set up in order to help interpret latest evidence and guidance from regulatory agencies like the MHRA when understanding baseline

investigations. A set of definitions was developed that have enabled a standardised approach to managing patients. The reliance on any one test or any one result as key to patient management was not advocated, instead an all-encompassing review of all available results was preferred. Additionally the use of an algorithm alone was avoided. This approach was based on the success of MDT meetings in other areas of medicine [265].

7.2.1 Patients

A review of the first 2 years worth of patients referred to and discussed through the iMDT was undertaken. From August 2012 through to July 2014, the iMDT had discussed 215 patients with 266 implants (51 bilateral). In total, there were 342 discussions when we add up those requiring more than one discussion.

This includes 101 females and 84 males, with an overall median age of 62 (26-90) years. This includes 132 Hip Resurfacing Arthroplasty (HRA) and 104 Total Hip Arthroplasty (THA). The remaining 30 cases were problematic revised MoM hip implants and these have been excluded from the analysis.

7.2.2 iMDT setup and Method

Patients were referred to our tertiary referral centre via a secure, online portal used to collect demographic and clinical data according to specific referral data requirements (http://www.rnoh.nhs.uk/clinical-services/joint-reconstruction-hip/painful-metal-metal-hip-replacements). The United Kingdom Image

Exchange Portal (IEP, http://www.image-exchange.co.uk/) permitted transfer of all imaging.

Cases were discussed at weekly meetings with clinical and basic science faculty in attendance. The team included four revision hip arthroplasty surgeons, two musculoskeletal radiologists (one present at each meeting), an arthroplasty nurse practitioner (coordinator), and an arthroplasty physiotherapy practitioner. A consultant cardiologist and neurologist provided specialist medical opinions for patients with suspected systemic toxicity.

This system does not require patient attendance since the referring surgeon collects clinical and imaging data, which is transferred using a secure online portal. See figure 7.2 and 7.3. IMDT methods include a systematic approach to each case, starting with history, Oxford Hip Score (validated for assessment of hip symptoms [266]), examination and basic investigations including x-ray and blood tests. The panel refers to current best practice guidelines US FDA and UK MHRA to provide an evidence-based recommendation that is returned to the referring surgeon to consider in the management of the patient at their local unit.

The resources required, in addition to the staff listed above include a secure online webpage that enables online referrals, access to the IEP, a conference room with a projector and a secure laptop for storage of patient database and referral forms / outcome forms, Dictaphones and secretarial support for maintaining up to date correspondence for MDT work. A formal cost analysis to include an assessment of resources and staff time was not formally undertaken.

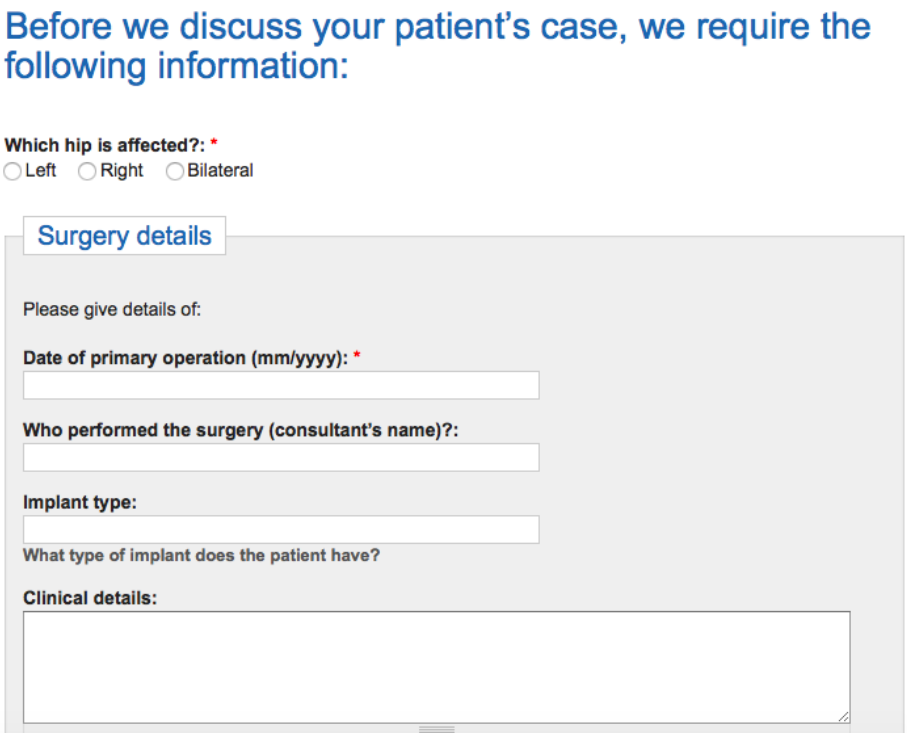

Figure 7.2: *Image demonstrating the online referral form and the core data required for each referral – details of the primary surgery including implant details and patients current clinical picture.*

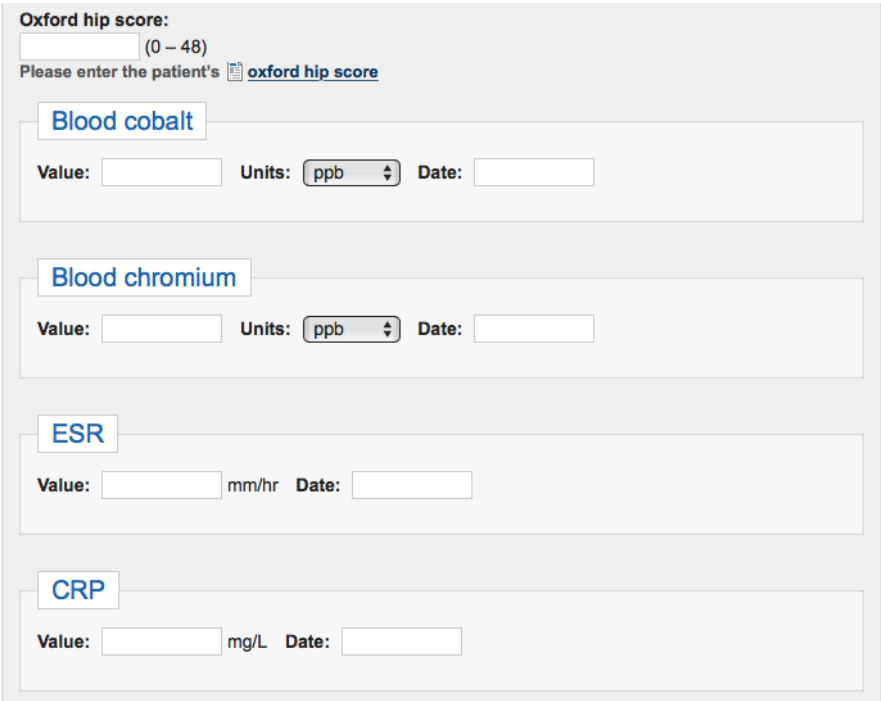

Figure 7.3: *Image demonstrating the online referral form and the core data required for each referral – here it requests the patient reported outcome measure (OHS) and blood test values.*

7.2.3 Risk Stratification of implants

The MHRA categorises implants broadly by femoral head size (threshold at 36mm) and design including hip resurfacing arthroplasty (HRA) or MoM total hip arthroplasty (THA). We further categorised each current generation implant, which based upon our experience we considered as low, medium or high risk using joint registry and regulatory recall data [6 7 232 267 268], See Chapter 1, Table 1.1.

7.2.4 Interpretation of Baseline investigations

Oxford Hip Score

As a validated tool for assessing symptoms arising from the hip, the Oxford Hip Score (OHS) gives a useful snapshot of the symptoms suffered by the patient and their functional limitation. Our threshold for defining a hip as symptomatic is an OHS of <42 out of a total of 48 [266].

Blood metal ion levels

The MHRA have recommended a whole blood cobalt level of greater than 7 ppb as the threshold beyond which concern for soft tissue reactions exists, a level with good specificity however poor sensitivity [82].

Inflammatory blood markers

The threshold level for C-Reactive Protein (CRP) of >10mg/l is considered where prosthetic joint infection is a concern [269]. These patients require needle aspiration of the joint and culture of the fluid obtained.

Radiographs

Radiographs were analysed for features that may indicate an underlying cause for pain or the potential for implant failure. These include patient, surgeon and implant related features. See Table 7.1.

Cause	Radiographic Feature
Patient	Osteolysis/Bone Resorption
	Component Migration (Serial images)
	Gender (i.e. HRA in elderly female patient)
Surgeon	Offset (ischiofemoral impingment)
	Inclination (>50 degrees)
	Version (deviation from 20degrees anteversion)
	Oversized implants or size Mismatched implants
	Impingement
Implant	Mix and Match of manufacture implants
	High Risk implants

Table 7.1: *Table demonstrating radiographic features that should be identified when investigating a patient with a MoM hip implant.*

MARS MRI

All MRI scans were reported by one of two musculoskeletal radiologists working within the MDT team. MARS MRI is the preferred cross sectional imaging tool. We recorded the presence or absence and subsequent grade of soft tissue lesions (pseudotumours) [131], abductor muscle atrophy [270], muscle oedema, muscle tendon avulsion, and bony abnormalities including osteolysis and fracture.

Soft tissue lesions

Soft tissue lesions or pseudotumours were assessed according to the parameters described in a previously published classification system [131]. See table 7.2 and figure 7.4.

Type	Wall	Contents	Shape
1	Thin-walled	Fluid-like: hypointense on T1, hyperintense on T2	Flat, with walls mainly in apposition
2A	Thick-walled or irregular	Fluid-like: hypointense on T1, hyperintense on T2	Not flat, with >50% of the walls not in apposition
2B	Thick-walled or irregular	Atypical fluid: hyperintense on T1, variable on T2	Any shape
3	Solid Throughout	Mixed Signal	Any shape

Table 7.2: *Pseudotumour classification system as published by Hart et al* [131]

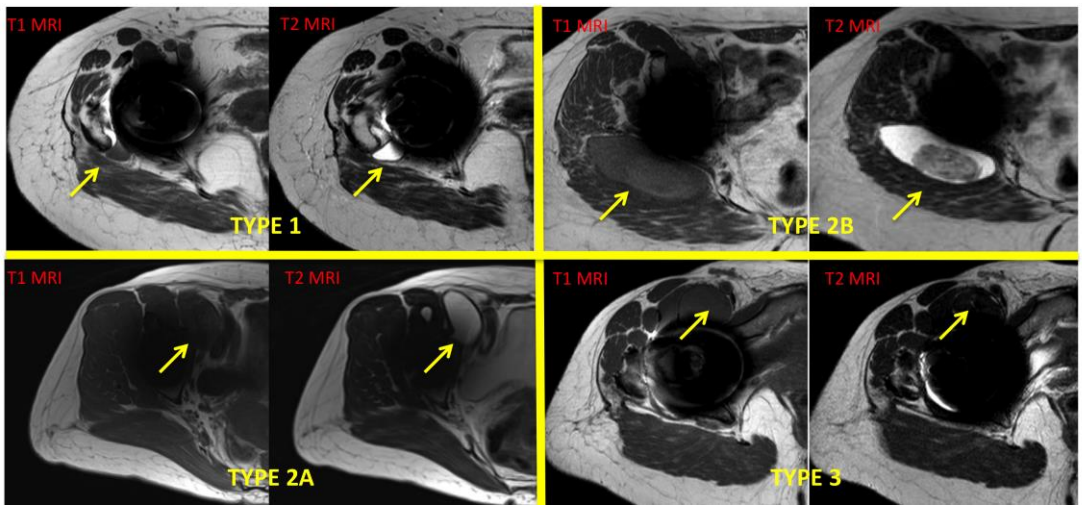

Figure 7.4: *Axial T1 and T2 MRI images demonstrating increasing grades of pseudotumour in MoM hip patients. (Top left) demonstrates grade 1, (Bottom left) grade 2A, (Top right) grade 2B and (Bottom right) grade 3. Soft tissue lesions of interest are highlighted by the arrows*

Muscle atrophy

Muscle atrophy was defined as the decrease in volume and appearance of fatty change, according to the grading system proposed by Pfirrmann et al [270]. See table 7.3 and figure 7.5. In cases of incomplete atrophy (e.g. anterior half of

gluteus medius), reference is made to the surgical approach used at time of implantation.

Grade	Description of Muscle Atrophy (T1 weighted MRI)
0	No intramuscular fat present
1	Some fat streaks present
2	Fat evident, but there is less fat than muscle
3	Equal amounts of fat and muscle tissue
4	More fat than muscle tissue

Table 7.3: *Description of the Pfirrmann muscle atrophy grading system when reporting T1 weighted MRI images* [270]

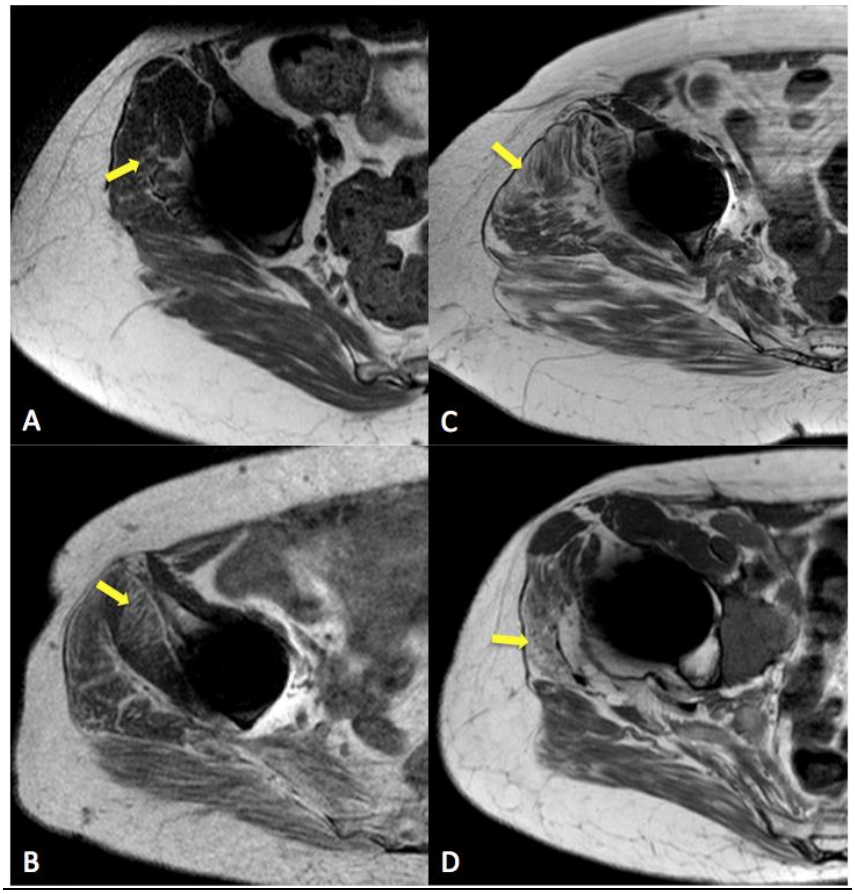

Figure 7.5: *Axial MRI images demonstrating increasing grades of muscle atrophy in MoM hip patients. (A) demonstrates grade 1, (B) grade 2, (C) grade 3 and (D) grade 4. Areas of significant atrophy are highlighted by the arrows*

Non-hip Related Pain

Referred pain from the spine to the hip can be difficult to differentiate from true hip pain. In these cases local anaesthetic injection into the hip joint is advised. A positive analgesic effect would be diagnostic of hip pain [271] [272].

Supplementary Investigations

SPECT-CT (single photon emission tomography-computed tomography) was reserved for patients with unexplained pain after baseline testing. SPECT has superior contrast resolution compared to conventional bone scan and its coupling with CT allows integration of mechanical and metabolic imaging data, and therefore the ability to identify loosening or infection specific to either the femoral or acetabular component [273].

7.2.5 Differential Diagnosis

A diagnosis is sought for each patient where the possible diagnoses align themselves with those presented by Liddle et al [144]. These included conventional failure (impingement, mal-position, and infection), synovitis, soft tissue destruction (cystic pseudotumour or muscle atrophy), bony destruction (osteolysis) and solid pseudotumour. In cases where systemic toxicity was a concern, then this was stated and the patient referred for further specialist review.

7.2.6 Final iMDT Recommendation

Following discussion by the iMDT panel, a recommendation is provided with an appropriate rationale justifying the decision. The outcomes given to patients fall into three categories: Monitoring, Further Investigation or Revision surgery. This decision is fed back to the treating surgeon, who then undertakes the care of the patient as they best see fit.

7.3 Clinical Usefulness of iMDT

One measure of the usefulness of this novel iMDT approach is the assessment of whether the iMDT recommendation was actually fulfilled by the referring surgeon, see figure 7.6. This information was obtained by survey of referring surgeons, and review of clinical notes. Concordance between the recommendation from the iMDT and the actual treatment undertaken by the patient was seen as a postive result. On the other hand, discordance was seen as a negative result and the reasons for this were analysed in greater detail.

Figure 7.6: *Study flow diagram demonstrating cases considered and the assessment of concordance.*

A Pearson Chi Square test was used to perform this comparison, where $p<0.05$ was considered statistically significant. All calculations were performed using STATA 14 (Statacorp LP, USA).

7.4 Results

Of the 266 hips in 215 patients, 30 were revised MoM hip implants and were excluded from further analysis. 236 hips were included in the study. Referrals

were received from 67 surgeons from 40 units across the UK. Median time since implantation was 91 months (24-240), figure 7.7. Table 7.4 demonstrates the frequency of implant types discussed categorized by their risk profile.

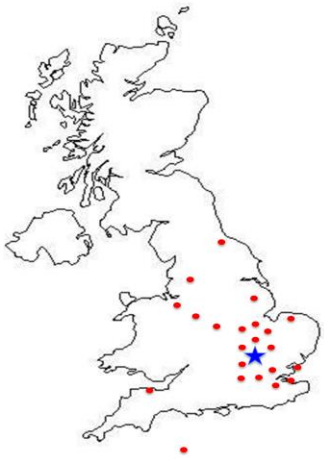

Figure 7.7: *Ilustration to demonstrate the number of units across the UK (including channel islands) from where referrals were received. Each red dot demonstrates a referring unit, of which 21 units were from within the M25 in London. The Blue star represents the location of RNOH.*

Risk	Hip Resurfacing Arthroplasty (HRA)	N	Total Hip Arthroplasty (THA)	N
Low	BHR	86	Small head THA (<36mm)	2
	ReCap	9		
Medium	Cormet	20	Birmingham Mid-Head	7
	Magnum	2	Resection	
	Conserve Plus	-		
High	Adept	1	All large head THA	82
	Durom	4	(≥ 36mm)	
	Mitch	-		
	ASR	10	ASR XL	13

Table 7.4: *Table demonstrating the frequency with which different hip implant types were discussed in the iMDT, categorized by their risk profile.*
BHR = Birmingham Hip Resurfacing, ASR = Articular Surface Replacement

7.4.1 Baseline investigations

The median OHS for the cohort was 35(4-48). The number of patients with individual hips classified as symptomatic (OHS <42) was 165 (70%). The

median whole blood cobalt was 3.54ppb (0.18-161.46) and chromium 3.17ppb (0.20-100.67). The number of patients with blood cobalt ion levels over the MHRA threshold of 7ppb was 64 (34.6%, excluding bilateral cases). Median CRP was 3 (1-235) mg/l.

7.4.2 Specialist Investigations

57 hips underwent aseptic needle aspiration. Three cases were culture positive for staphylococcus hominis (n=1), and staphylococcus aureus (n=2). These patients were treated for prosthetic joint infection.

MARS MRI scanning revealed the proportion of hips with abductor muscle atrophy to be 92 (39%) when it is considered that significant muscle atrophy was grade 2 or above. Of the 92 cases 31 (34%) suffered Gluteus Minimus atrophy alone, 10 (11%) suffered Gluteus Medius alone and 51 (55%) suffered both Gluteus Medius and Minimus atrophy together.

The proportion of hips with evidence of a pseudotumour on imaging was 34% (80 hips). The most common grade of pseudotumour seen in this cohort was type-2B (56 cases, 70%) of the total number of pseudotumours seen. Type-1 pseudotumours were seen in 15 hips (19%), type-2A in 6 (8%) and the solid type-3 pseudotumours was seen in 3 (4% of the total number of pseudotumours identified on scanning).

SPECT-CT was used to aid diagnosis in 9 patients (12 hips). All hips were investigated using SPECT-CT for unexplained pain. Loosening of the stem was identified in 2 patients, where increased uptake was detected on the scans, and

both of which were recommended revision surgery. In 4 patients the spine was identified as the cause of pain with sacro-iliac joint arthropathy (n=2), T12 facet arthropathy (n=1), and multilevel end-plate arthropathy (n=1). The cause of pain remained unexplained in the remaining patients. In total, a diagnosis was identified in 50% of hips with unexplained pain.

7.4.3 Concerns of Systemic Toxicity

Six patients (seven hips) with highly elevated metal ions were referred for assessment for systemic toxicity. Median time since implantation was 83 (48–108) months and median blood cobalt level was 27.3(11.4–130.9) ppb. Cardiological review included assessment by a consultant cardiologist involving a comprehensive history, electrocardiogram and cardiac MRI, which is the gold-standard quantification of cardiac volumes and function with standardised protocols [240 241].

Neurological review included comprehensive history and neurological examination by a consultant neurologist.

No patients were found to demonstrate systemic effects of raised blood metal ions.

7.4.4 Clinical Usefulness

Patients were either recommended for monitoring, further investigation or revision surgery.

Of 236 hips, 148 (62.7%) hips were recommended for monitoring, 30 (12.7%) hips were advised further investigations and the remaining 58 (24.6%) hips were recommended further surgery. See figure 7.5.

The MDT final decision was reached after a single discussion in 161 (68.2%) cases. However, the remaining cases required two discussions (49; 20.8%), three discussions (21; 8.9%) and four discussions (5; 2.1%) until a final recommendation was made. Multiple discussions were required in order for specialist tests recommended by the MDT to be undertaken and the results reviewed prior to a final recommendation being given.

The actual outcome undertaken by the referring surgeon after receiving the MDT recommendation was then analysed. In 6 cases the outcome is unknown. However 149 (63.1%) cases are under monitoring at the time of review, 25 (10.6%) cases were undergoing further investigations, and 56 (23.7%) cases have been recommended revision surgery by the treating surgeon.

Since the referring surgeon treats the patient, the recommendation from the MDT is a guide to their management, and pragmatically, it is believed to be open to interpretation. Concordance was seen in 211 cases (91.7%; out of 230, excluding 6 cases with unknown outcome) and discordance was seen in 19 cases (8.3%). Pearsons chi squared test was used to assess the concordance between the recommendation from the MDT and the actual outcome undertaken by the treating surgeon. The association between the two was significant (Pearson Chi Square Test = 302.6 (df = 6), $p<0.05$).

The rationale for the discordance in the 19 cases seen was broadly based on the following reasons: patient choice (n=6), symptomatic change (n=8), further investigation indicated (n=3) and other diagnoses suggested (n=2). See figure 7.8.

Figure 7.8: *Flow diagram demonstrating the frequency and reasons for discordance between the MDT recommendation and the actual management by the treating surgeon.*

Patient choices and preferences are an important part of managing their care. This explained the 6 cases (out of 19 (32%)) where discordance between the MDT recommendation and the actual management was secondary to patient choice. In one case, the patient had other medical issues that precluded significant revision surgery. Revision was declined in 2 cases, and further investigations were declined in another 2 cases on the basis that the patients were not keen on revision surgery. Lastly one patient had requested revision due to a subjective feeling of worsening of their symptoms.

A change in symptoms was also a reason for discordance between MDT recommendations and actual outcomes, where symptoms had improved in 3 cases, deteriorated in 3 cases and were deemed stable in 2 cases. In 3 cases, surgeons had opted for further testing after clinical review, and alternative diagnosis had a bearing on management in the remaining 2 cases.

7.5 Discussion

The use of an iMDT is an effective tool in the management of patients with problematic MoM hip arthroplasties due to the feasibility of the methods employed, the concordance between recommendation and actual management, and therefore the reduction of uncertainty. The significant level of concordance (91.7%) between the recommendation made and the treating surgeons final management demonstrates the effectiveness of this method in reducing uncertainty amongst surgeons, and from this we infer that this may improve patient management. This is believed to be the first use of such an approach in

orthopaedic arthroplasty surgery, and it is believed that this approach reduces the need for revision surgery where only 24.6% of cases were recommended this course of action. Although without long-term outcome studies the true clinical impact is not yet known. The novelty of this approach is highlighted further by its effective use of telemedicine where patients can be referred via secure online platforms by their treating surgeon, thus precluding the need for patient attendance at the tertiary referral centre.

A decision to revise a hip replacement can be very subjective, so much so that the consulting surgeons attitude on any one-day may influence their decision. It is hoped that a panel approach, such as with an MDT, would reduce the subjectivity of decision-making and provide a more balanced approach. Despite this, it is known that interventions published by a regulator can change human behaviour, a phenomenon described previously in economic models [274]. The Lucas Critique described that regulatory intervention irreversibly changes the decision making process. It is therefore assumed that the same would apply to healthcare. The UK regulatory agency (MHRA) was the first to issue management guidelines on all MoM hips in 2010. This was followed by guidance from the FDA in 2012, and more recently by the European regulatory bodies (SCENIHR). This guidance is essential to simplify decision-making. However, in the case of MoM hips this can be too simplistic and difficult to interpret in cases that do not confine to the description in the guidelines, leading to potentially unnecessary revision surgery, and therefore cost to the health service and harm to the patients.

The advantages of guidelines are that they can help decision making, improve uniformity in actions and ultimately improve outcomes for patients by reducing unnecessary deviation from best practice. The disadvantages however include the variation in interpretation, blind practise and failing to identify new situations that may arise. A further disadvantage is the inhibition of innovation in management [275]. What is clear however is that guidelines are most appropriate for situations where there is little patient variation and a strong evidence base. Both of which are lacking when it comes to the long-term outcomes of patients with MoM hip implants.

With respect to MoM hip patients, those with severe symptoms, soft tissue masses and elevated metal ions clearly need revision surgery, however on the other hand those that are asymptomatic, with non-elevated metal ions and minimal soft tissue changes can unmistakably be managed conservatively. However a large proportion of patients fall in the middle of this spectrum, where a wide variation in clinical, biochemical and radiological pathology exists. It is this group that is the most challenging to manage based on current evidence and guidance.

The MDT panel uses details regarding the patients concerns and expectations, current evidence based knowledge, and regulatory guidance when providing opinions. The key purposes of the MDT team are to reduce uncertainty in who should be revised, when they should be revised and how. The underlying principles include the belief that MDT discussion ensures higher quality decision-making and improved outcomes, based on the ability of a panel of experts to pool knowledge and experience in providing a balanced viewpoint.

The most important feature of this arrangement however, is that a panel of experts can offer their combined tacit knowledge and experience of hip revision surgery when making recommendations, which cannot be emphasised in any written guidance. With a high level of concordance between the MDT recommendation and the actual management undertaken by the referring surgeon suggests a significant level of agreement on both sides that goes some way to validate the recommendations being given.

There are improvements that can be considered when considering the MDT process. First and foremost, it is a resource heavy process for considering patient management. Despite the cost of running an MDT has not been considered here, it is important to ensure the whole process is as cost effective as possible. Gore et al, demonstrated that the average cost for discussion of a new patient in a cancer MDT was £415 [276]. This highlights the need to consider whether all MoM patients should be discussed in an MDT. It may be that some simple cases can be managed through an algorithm approach, leaving the more complex cases for discussion within the MDT format. To counter that concept, one could argue that comprehensive evidence does not yet exist to ensure that all aspects of patient management can be dictated within an algorithm. To ensure there is an adequate triage service to rule out cases that are not appropriate for discussion or that lack certain clinical information, an online scoring system that enables automatic triage can be considered.

There are of course additional benefits of the MDT other than the discussion relating to the management of individual patients. These include its role as an educational forum, a catalyst for ideas for research and audit, identification and

verification of the suitability of patients for clinical trials and a quality assurance process [276].

MDT meetings are widely established in the National Health Service (UK), where the Department of Health has endorsed them as the core model for managing chronic diseases and cancer. It is believed that MDTs lead to superior outcomes for patients [277-279]. The effectiveness of multidisciplinary team approaches in orthopaedics has been reported in a limited number of cases [280-282], however these are distinct from an MDT meeting composed of an expert panel. Currently MDT meetings are only commonly seen in orthopaedic sarcoma units, as recommended by the British Sarcoma Group [283].

The RNOH iMDT is likely to be the first team focusing on painful hip arthroplasty and revision surgery. Since its inception we have run weekly meetings and have received referrals from over 40 units across the UK, highlighting the scale of the problem. As part of this process we have developed an algorithm that we follow for all patients, as described within our methods. The recommendations from the MDT are accompanied by a decision rationale. Decisions are constantly audited to allow for reflective practice. The concordance of the referring surgeons in following through the recommendation of the MDT would suggest the agreement and the suitability of the plan for the patient and surgeon alike.

The limitation of this study is that there is no true measure of effect on patient outcomes. This can only truly be measured by way of a randomised control trial

comparing outcomes of patients treated through an MDT with those treated without, i.e. normal care.

7.6 Conclusion

Collaborative research highlights the need for collaborative management of patients with complex medical concerns. In cases where systemic toxicity is a concern, guidance is lacking, and therefore a multidisciplinary approach is advised in order to help manage these patients in line with the most up to date information that is available. In this case, 6 patients were referred to medical specialists for further assessment using the latest medical technologies to aid their clinical review.

We advocate the use of a multi-disciplinary approach for the management of patients with problematic MoM hips. Such an approach combines the tacit knowledge of an expert panel, regulatory guidance and up to date evidence in order to improve decision-making amongst surgeons by reducing uncertainty in decision-making, and therefore unnecessary revision surgery.

CHAPTER 8

CHAPTER 8 DISCUSSION AND CONCLUSION

8.1 Discussion

This study investigated the effects of metal ions on cardiac function in three distinct groups of patients defined by their i) hip implant and ii) levels of circulating blood cobalt. Two independent cardiac imaging techniques (including the gold standard, cardiac MRI) were used to assess cardiac volumes and function, to characterize the cardiac and liver tissues, and applied novel T2* sequences to assess for evidence of myocardial or liver tissue metal deposition. In addition to the assessment of systemic toxicity, this thesis also explored how current evidence and guidance is interpreted when managing patients with MoM hip implants. This involved the analysis of the workings and outcomes from a Multi-Disciplinary Team approach to patient care. The justification for this was based on the clinical dilemmas faced by surgeons on a daily basis and the need for a collaborative approach to patient care, particularly in cases where systemic toxicity is suspected and the apparent lack of published guidance.

The basis of this thesis centred on a single extreme clinical case of a patient with a failed hip with blod metal ions measured at 587ppb. This case was investigated for systemic effects and T2* sequences demonstrated metal loading within the liver, confirmed as cobalt chromium following liver biopsy and micro X-ray Fuoroesence. Subsequent to this case, 90 patients with varying levels of blood metal were recruited to this study, which in summary failed to find a significant change in cardiac volumes and function in patients exposed to elevated metal ions.

Recently, there has been increasing concern regarding the effects of systemic cobalt and chromium toxicity in patients with MoM hip implants. Although the evidence for toxicity is limited, anxiety is fuelled by increasing numbers of case reports of end-organ damage and mortality.[11] Table 1.2 (chapter 1). Cobalt is a trace metal element, and is a key constituent of cobalamin (vitamin B12), and therefore an essential component of normal cellular metabolism. High levels can lead to cellular apoptosis, necrosis and oxidative DNA damage [16]. Historically, industrial exposure highlighted cobalt toxicity as a clinical concern, similar to cases of iatrogenic toxicity that followed treatment of patients with anaemia using cobalt-chloride tablets [284]. A recognized event occurred when cobalt had been used in a foam-stabilising agent in the beer industry, which led to an increase in low-output cardiomyopathy that subsequently resolved when cobalt was removed from the manufacturing process [73 74]. The recent cases described in patients with metal on metal hip implants have increased in frequency since the re-introduction of the bearing in the late 1990's, and has been associated with a rise in reports of metal-related local adverse events. The increased recognition of local and systemic adverse events associated with the release of cobalt ions and nanoparticles placed the spotlight on metal on metal total hip arthroplasties (THA) and hip resurfacing arthroplasties (HRA).

In June 2012, the United Kingdom's Medicines and Healthcare Products Regulatory Agency (MHRA) published guidance that recommended annual lifetime orthopaedic follow-up and measurement of blood cobalt and chromium ions, for all patients with MoM arthroplasties[6]. The European advisory committee, the Scientific Committee on Emerging and Newly Identified Heath

Risks, released similar supporting statements in September 2014 [285]. The United States Food and Drug Administration (FDA) also acknowledged the risk of cobalt toxicity and its associated signs and symptoms in its advice to surgeons [9]. The FDA took the additional step to advise surgeons of the need to assess patients for systemic toxicity as follows "A thorough physical examination should be performed by the patient's health care team, which include primary medical physicians and/or specialists, with particular focus on cardiovascular, neurological, endocrinological (especially thyroid), and renal systems". This alone highlights the need for a collaborative multi-disciplinary approach. Their advice stops short of advising the type of investigations that may be required to investigate patients further. Similarly, the American Association of Hip and Knee Surgeons and the American Association of Orthopaedic Surgeons (AAOS) have issued similar advisory statements on metal-related adverse reactions; although they note that most patients have well functioning implants [286].

A recent study suggested a higher incidence of first hospitalisation due to heart failure among a group of male patients with ASR XL metal-on-metal (MoM) hip implants when compared with a similar group who had received a metal-on-polyethylene (MoP) implant. The study was a retrospective cohort study conducted using data held in the Australian Government Department of Veterans' Affairs health claims database on patients who received conventional total hip arthroplasties (THA) between 1 January 2004 and 31 December 2012 as treatment for osteoarthritis [287].

A total of 4019 people were included in the study; 3.0% received an ASR XL prosthesis, compared to 8.8% that received an alternative MoM prostheses and 88.2% with a MoP prosthesis. Men with ASR XL prostheses had a higher

incidence of hospitalisation for heart failure after their hip replacement procedure compared with men who had MoP prostheses (15.9% compared to 7.6% respectively). The rate of being hospitalised for heart failure in men was more than three times higher for ASR XL compared to MoP prostheses (hazard ratio = 3.21; 95% CI= 1.59;6.47). There was no evidence of a difference in rate of being hospitalised for heart failure between the other MoM prostheses compared with MoP prostheses in men. No difference in heart failure hospitalisation rates was found for women between the prostheses types. Several limitations arose in this study; for instance the number of patients receiving the ASR XL implant identified as high risk consisted of 121 patients, which is considered small in a study investigating outcomes that are considered low frequency; secondly the patient cohort had a median age of 82 years, which is considerably older than the median age of traditional metal on metal hip recipients, making the generalisability of the conclusion difficult; lastly no data on cobalt or chromium blood levels was available, which again poses difficulties when attributing increased heart failure risk to metal toxicity. Regardless, the Therapeutic Goods Administration (TGA, Australian Government) highlighted this potential concerning link between the ASR XL Metal on Metal hip implant and increased risk of heart failure in elderly men, and advise clinicians to consider monitoring patients for early signs of heart failure through clinical examination and imaging including echocardiogram, especially if there are additional risk factors [288].

The findings in the Gillam et al study demonstrate changes in line with those of Prentice et al, which demonstrated a cardiac ejection fraction that was 7% lower (mean absolute difference 5%; P= 0.04) and left ventricular end-diastolic diameter that was 6% larger (mean difference 2.7 mm; P= 0.007) in the hip

resurfacing group versus those patients who received a conventional non metal on metal hip replacement. It is important to note that the median blood cobalt level in the metal hip group was 1.75ppb (Interquartile range= 1.11 to 6.11) [167]. One could extrapolate that patients with higher blood cobalt levels would be expected to have inferior cardiac volumes and function, however there is no evidence to suggest this. Since this was not the case, it may be argued that this study is limited by less rigorous methodology having used echocardiography, which has a higher inter-observer variability compared to cardiac MRI that may account for the disparity against the findings reported in this thesis [218].

Proving a negative is always difficult. The size of this study (powered to detect a medium to large effect) limited the possibility to directly adjust for confounders when performing statistical testing. However this study used both CMR and echocardiography with meticulous trial design; it was ensured that the pre-specified recruitment number was achieved; data acquisition was conducted in a dedicated cardiac imaging center separate from the recruiting center; and imaging analysis was conducted completely blinded to study groups (both during acquisition and analysis) until all results were reported.

Besides the lack of functional or structural effects seen in the patients examined in this thesis, tissue mapping techniques also failed to identify any demonstrable scarring, fibrosis or metal deposition in the cardiac or liver tissues. Although iron (Fe) can be detected in heart and liver using T2*, and although CoCr (co-localized) can be detected in the liver (as demonstrated in chapter 2), T2* was negative in all subsequent cases.

The lack of demonstrable tissue deposition in the 90 patients may lie with differences in the physical chemistry of cobalt ions compared to cobalt and chromium in combination. Cobalt and chromium exhibit different magnetic properties to iron, and thus a limitation in this study becomes the relative sensitivity of the T2* test to assess metallic deposition in the cardiac muscle. From a purely elemental standpoint, cobalt and iron are both considered ferromagnetic, whereas chromium is paramagnetic yielding different physical phenomena and behavior in the static field [74]. Clearly, they are different from diamagnetic water and thus generate susceptibility artifact when placed in the same tissue voxel. The physical chemistry, however, is different when cobalt chromium molecules are combined. If corrosion processes occur, oxidative molecular states of chromium could generate paramagnetic particles like elemental cobalt or iron.

We know from previous studies that the tissue surrounding metal on metal hips contains a variety of metal species, including cobalt in a metallic state. However, in all the patients where there were significant amounts of metal in the tissue Cr(III)PO4 was the most abundant and no Cr(VI) was observed. The depletion of cobalt within the immediate periprosthetic tissues is of clinical relevance in that elevated blood concentrations of cobalt and chromium very probably cannot be assigned to particulate matter in the bloodstream [121].

However, examination of the fluorescence signal showed that the metal in the liver tissue was always co-localised and had a ratio of cobalt to chromium of approximately 4:1, which is higher than the composition of the MoM hip (ASTM F75). It is possible that the metal particulate debris is depleted of chromium, especially since Cr(III)PO4 was highly abundant in periprosthetic tissues.

The case described in chapter 2 may be unusual in that the elevated blood metal ions followed a ceramic fracture and subsequent catastrophic abrasive wear of the metal femoral head. Given this is not typical for most patients with metal on metal hips, it may highlight that particulate debris can spread to distant organs. From this we can conclude that T2* techniques can detect the ferromagnetic cobalt debris in its metal state, but may not be sensitive enough to detect ionic cobalt or chromium that arises from corrosion commonly seen in most metal on metal hip recipients. The flipside to this argument is that deposition is not occurring in the majority of patients, and therefore there is no tissue metal present to reduce the T2* times. This is unlikely however, since there were no cases of abnormal T1 mapping or ECV to suggest underlying myocardial or liver tissue pathology that would be expected with metal deposition. In other words, T2* should be considered a candidate biomarker which, if it had been different between the groups would have indicated the biological process of deposition.

Systemic toxicity occurs through diffusion and transport of soluble cobalt ions generated in the peri-articular space, or the transport of metal wear particles through the lymphatic and vascular system with subsequent deposition at remote sites. If deposition is occurring, as reported by twenty-one cases (table 1.2; chapter 1), the pathophysiology is still uncertain. The pathophysiology behind a possible link between elevated blood cobalt and cardiac toxicity is unclear. Suggested theories include cobalt interference with cardiac myocyte oxygen uptake, and transmembrane transport system disruption. Histopathological findings in cobalt-related cardiac toxicity include myofibrillar

hypertrophy, interstitial fibrosis, and muscle fiber degeneration.[73] However, calcified fibrils or other deposits within myofibrils are often absent, differentiating cobalt-induced cardiomyopathy from other aetiologies.[14] Such mechanisms can be considered the cause of the fibrosis and structural changes seen in the cobalt cardiomyopathy cases reported in the literature.

It has been postulated that cobalt-related cardiac toxicity is due to additional predisposing factors; including poor nutrition and excess alcohol intake seen in the Quebec beer drinkers cobalt cardiomyopathy epidemic (where foam stabilizer contained ten times the usual quantity of cobalt).[73] Case reports in MoM hips of recent years mainly had extremely elevated blood cobalt levels (>100ppb). National surveillance programmes now mean that such patients are likely to have had revision surgery by now, with presumed reduction in their risk of systemic toxicity.

With the lack of functional consequences, demonstrated by complementary and independent imaging modalities (CMR and echocardiography), two blood biomarkers and the lack of positive T2* findings, although not definitive, the results are reassuring.

Based on these findings, it can be concluded that individual reports of heart failure reported within case reports (mainly extreme ion levels) are not likely to be the tip of an iceberg of unrecognized epidemic of occult metal on metal hip related community heart failure.

However, given the magnitude of reported clinical sequelae of cardiac toxicity in cases with extremely elevated metal ion levels (>300ppb), we would argue that cardiac imaging should be mandated if such levels are identified, until further

research sheds light on potential cardiotoxicity at extremely elevated levels of metal ions.

Our findings are particularly useful for both regulators and individual surgeons when it comes to advising the treatment of patients with MoM hip implants. Until definitive guidance is produced, it is up to surgeons to interpret current guidance, which is vague in certain parts particularly when recommending management for systemic toxicity. For this reason we also looked at the work and outcomes from a collaborative MDT meeting that aids surgeons in deciding how to manage patients with MoM hip implants. This approach brings together all specialties, including medical physicians and interprets current guidance on a case-by-case basis. Our analysis of this approach revealed a successful and highly acceptable method that enjoyed upto 92% concordance between the recommendation from the MDT and the actual treatment undertaken by the referring surgeon. Such an approach interprets the latest evidence, such as the findings from the cardiac studies performed in this thesis.

In the United States, MoM articulations were used in approximately 35% of hip arthroplasties in 2006, but usage has since declined rapidly worldwide [1]. The increased level of clinical vigilance has shown that adverse events are more common than previously thought [130], and patients may develop, potentially, systemic symptoms [14]. This is not limited to only MoM articulations, but also other component parts of modular THAs with standard MoP or CoC bearings may be implicated [97].

The development of systemic cobalt toxicity from hip arthroplasty appears to be very rare. Only 21 cases have been reported, ten involving metal on metal

articulations. However, it is estimated that one million metal on metal hip arthroplasties had been performed in the United States and 60 000 in the United Kingdom [14]. We believe these findings offer reassurance to over one million patients worldwide with MoM hip implants and will support clinicians caring for such patients, and in the meantime we continue to advocate the use of MDT meetings to aid decision making. Further work is needed, particularly from large volume linkage studies currently underway internationally.

8.2 Conclusions

At the outset, this thesis hypothesized that no consistent discernable effect on cardiac function is detectable on Cardiac MRI and Echocardiography in patients with raised blood cobalt ion levels. At the conclusion of this study, this hypothesis was proved correct, since no functional or structural abnormalities were detected in patients with increasing blood cobalt and chromium levels.

Additionally, the application of novel T2* techniques did not reveal any further cases of metal deposition within the myocardium or liver.

We advocate the use of a multi-disciplinary approach for the management of patients with problematic MoM hips and for the consideration of cardiac imaging in cases of extremely elevated metal ion levels (>100ppb).

8.3 Further Work

The conclusion set out here contradicts the findings of two recent studies, admittedly both with less rigorous trial design. In all accounts this multi-modality study of well matched patient groups was ultimately a small study, despite being powered to detect a medium to large difference in ejection fraction of 5%, and therefore larger studies are required to confirm the findings set out in this thesis. This would include large-scale registry linkage studies of patients with exposure to metal on metal hip implants and heart failure diagnosis.

Further work would be required to assess the true sensitivity of T2* for the detection of cobalt and chromium within tissue, and to assess whether T2* is sensitive to metallic particles or their oxidized forms.

Fluid obtained from hip aspiration or at the time of revision hip surgery can be a potential source of metal debris from hip implants. This fluid may serve to help determine whether MRI techniques such as T2* can detect the presence of cobalt / chromium once placed within an MRI suitable phantom. Ultimately, further work is needed to assess the utility of T2* MRI as a screening tool in at-risk patients with metal on metal hip prostheses.

Certain sub groups of patients were not studied in this thesis. There is concern surrounding the release of corrosion products from the trunion at the head stem junction of the femoral component of hip replacements. In particular this would apply to patients with MoP bearing surfaces or those with double taper modular

neck stems. Repeating the analysis to incorporate a MoP group would be important as this would provide an additional comparator to the MoM group.

Table 1.2 demonstarted several cases of cardiomyopathy second to ceramic fracture and subsequent revision to MoP bearing surface. These patients may be more susceptible to cardiotoxicity in part due to the extremely elevated blood metal levels that result. This highlights a potential group of patients that require further assessment with the methods described in this thesis.

The results demonstrated here are largely negative, and fail to support a reported link between metal ion exposure (up to 118ppb) and cardiotoxicity. Based on the clinical reports of cardiotoxicity further work would be critical to look for cardiotoxicity in those patients with levels well above 100ppb, particulary with levels above 300ppb, since this link may have been missed with the patient cohort described in this thesis.

Further analysis of the MDT would be required to understand its true value, and to assess where improvements could be made. Its true value would only be understood by way of a direct comparison of decisions made with or without an MDT and the impact on the patient outcome. This would ideally be through a randomized control trial. Assessing for unnecessary variation in patient management and whether MDT discussions reduce such variation is an important endpoint.

Cost effectiveness in today's health service is critical and therefore a qualitative analysis of the contribution of each panel member is mandated to ensure their presence and therefore the affiliated cost of their time is justified. An analysis of

those patients that required multiple discussions would be important to help improve the cost effectiveness of the MDT by reducing duplication and ensuring that time spent discussing such patients was necessary. An assessment of whether an algorithm could be developed in order to triage the cases that need to be discussed over those that are considered more straightforward.

BIBLIOGRAPHY

BIBLIOGRAPHY

1. Bozic KJ, Kurtz S, Lau E, et al. The epidemiology of bearing surface usage in total hip arthroplasty in the United States. *The Journal of bone and joint surgery American volume* 2009;91(7):1614-20. doi: 10.2106/JBJS.H.01220
2. Hart AJ, Sabah S, Henckel J, et al. The painful metal-on-metal hip resurfacing. *The Journal of bone and joint surgery British volume* 2009;91(6):738-44. doi: 10.1302/0301-620X.91B6.21682
3. Pandit H, Glyn-Jones S, McLardy-Smith P, et al. Pseudotumours associated with metal-on-metal hip resurfacings. *The Journal of bone and joint surgery British volume* 2008;90(7):847-51. doi: 10.1302/0301-620X.90B7.20213
4. Schaffer AW, Pilger A, Engelhardt C, et al. Increased blood cobalt and chromium after total hip replacement. *J Toxicol Clin Toxicol* 1999;37(7):839-44.
5. Case CP, Langkamer VG, James C, et al. Widespread dissemination of metal debris from implants. *The Journal of bone and joint surgery British volume* 1994;76(5):701-12.
6. Medical Device Alert: All metal-on-metal (MoM) hip replacements (MDA/2012/036). http://www.mhra.gov.uk/ (accessed 01/03/16).
7. Food and Drug Administration, USA - Metal-on-Metal Hip Implants: Recalls http://www.fda.gov/ [Available from: http://www.fda.gov/ accessed 01/03/2016).
8. Epstein M, Emri I, Hartemann P, et al. The safety of Metal-on-Metal joint replacements with a particular focus on hip implants. October 2014; (1). http://ec.europa.eu/health/scientific_committees/ (accessed 01/03/16).
9. Food and Drug Administration, USA - Metal-on-Metal Hip Implants: Advice for Surgeons http://www.fda.gov/ [Available from: http://www.fda.gov/ accessed 01/03/16).
10. 12th Annual Report 2015 - National Joint Registry for England, Wales and Northern Ireland 2015 [14/05/2016]. Available from: www.njrcentre.org.uk accessed 14/05/2016.
11. Bradberry SM, Wilkinson JM, Ferner RE. Systemic toxicity related to metal hip prostheses. *Clin Toxicol (Phila)* 2014;52(8):837-47. doi: 10.3109/15563650.2014.944977
12. Machado C, Appelbe A, Wood R. Arthroprosthetic cobaltism and cardiomyopathy. *Heart Lung Circ* 2012;21(11):759-60. doi: 10.1016/j.hlc.2012.03.013 [published Online First: 2012/04/24]
13. Zywiel MG, Brandt JM, Overgaard CB, et al. Fatal cardiomyopathy after revision total hip replacement for fracture of a ceramic liner. *The bone & joint journal* 2013;95-B(1):31-7. doi: 10.1302/0301-620X.95B1.30060
14. Cheung AC, Banerjee S, Cherian JJ, et al. Systemic cobalt toxicity from total hip arthroplasties: review of a rare condition Part 1 - history, mechanism, measurements, and pathophysiology. *The bone & joint journal* 2016;98-B(1):6-13. doi: 10.1302/0301-620X.98B1.36374
15. Samar HY, Doyle M, Williams RB, et al. Novel Use of Cardiac Magnetic Resonance Imaging for the Diagnosis of Cobalt Cardiomyopathy. *JACC Cardiovasc Imaging* 2015;8(10):1231-2. doi: 10.1016/j.jcmg.2014.12.016

16. Zywiel MG, Cherian JJ, Banerjee S, et al. Systemic cobalt toxicity from total hip arthroplasties: review of a rare condition Part 2. measurement, risk factors, and step-wise approach to treatment. *Bone Joint J* 2016;98-B(1):14-20. doi: 10.1302/0301-620X.98B1.36712
17. Khan AH, Verma R, Bajpai A, et al. Unusual case of congestive heart failure: cardiac magnetic resonance imaging and histopathologic findings in cobalt cardiomyopathy. *Circulation Cardiovascular imaging* 2015;8(6) doi: 10.1161/CIRCIMAGING.115.003352
18. Gilbert CJ, Cheung A, Butany J, et al. Hip pain and heart failure: the missing link. *Can J Cardiol* 2013;29(5):639 e1-2. doi: 10.1016/j.cjca.2012.10.015
19. Urban RM, Jacobs JJ, Tomlinson MJ, et al. Dissemination of wear particles to the liver, spleen, and abdominal lymph nodes of patients with hip or knee replacement. *The Journal of bone and joint surgery American volume* 2000;82(4):457-76.
20. NICOR. National Heart Failulre Audit 2016 [updated 06/10/2015. Available from: https://www.ucl.ac.uk/nicor/audits/heartfailure accessed 07/03/2016.
21. Wilkinson N, Pantopoulos K. IRP1 regulates erythropoiesis and systemic iron homeostasis by controlling HIF2alpha mRNA translation. *Blood* 2013;122(9):1658-68. doi: 10.1182/blood-2013-03-492454
22. Graves S, Gillam MH, Pratt N, et al. Heart Failure after ASR XL Metal-on-Metal Hip Replacements in Men. American Academy of Orthopaedic Surgeons. Orlando, Florida, USA, 2016.
23. Anderson LJ, Holden S, Davis B, et al. Cardiovascular T2-star (T2*) magnetic resonance for the early diagnosis of myocardial iron overload. *Eur Heart J* 2001;22(23):2171-9. [published Online First: 2002/03/27]
24. Carpenter JP, He T, Kirk P, et al. On T2* magnetic resonance and cardiac iron. *Circulation* 2011;123(14):1519-28. doi: 10.1161/CIRCULATIONAHA.110.007641
25. Jenkins PJ, Clement ND, Hamilton DF, et al. Predicting the cost-effectiveness of total hip and knee replacement: a health economic analysis. *The bone & joint journal* 2013;95-B(1):115-21. doi: 10.1302/0301-620X.95B1.29835
26. Learmonth ID, Young C, Rorabeck C. The operation of the century: total hip replacement. *Lancet* 2007;370(9597):1508-19. doi: 10.1016/S0140-6736(07)60457-7
27. Kluzek S, Newton JL, Arden NK. Is osteoarthritis a metabolic disorder? *Br Med Bull* 2015;115(1):111-21. doi: 10.1093/bmb/ldv028
28. Pereira D, Peleteiro B, Araujo J, et al. The effect of osteoarthritis definition on prevalence and incidence estimates: a systematic review. *Osteoarthritis Cartilage* 2011;19(11):1270-85. doi: 10.1016/j.joca.2011.08.009
29. Suri P, Morgenroth DC, Hunter DJ. Epidemiology of osteoarthritis and associated comorbidities. *PM R* 2012;4(5 Suppl):S10-9. doi: 10.1016/j.pmrj.2012.01.007
30. Hip fracture: management https://www.nice.org.uk/guidance/cg1242014 [updated 01/03/2014. Available from: https://www.nice.org.uk/guidance/cg124 accessed 01/09/2016.
31. Swarup I, Lee YY, Movilla P, et al. Common factors associated with osteonecrosis of the femoral head in young patients requiring total hip arthroplasty. *Hip international : the journal of clinical and experimental*

research on hip pathology and therapy 2015;25(3):232-6. doi: 10.5301/hipint.5000225
32. Zalavras CG, Lieberman JR. Osteonecrosis of the femoral head: evaluation and treatment. *The Journal of the American Academy of Orthopaedic Surgeons* 2014;22(7):455-64. doi: 10.5435/JAAOS-22-07-455
33. Smith-Petersen MN. Evolution of mould arthroplasty of the hip joint. *The Journal of bone and joint surgery British volume* 1948;30B(1):59-75.
34. Mahalingam K, Reidy D. Smith-Petersen vitallium mould arthroplasty: a 45-year follow-up. *The Journal of bone and joint surgery British volume* 1996;78(3):496-7.
35. Wiles P. The surgery of the osteoarthritic hip. *Br J Surg* 1958;45(193):488-97.
36. Judet J, Judet R. The use of an artificial femoral head for arthroplasty of the hip joint. *The Journal of bone and joint surgery British volume* 1950;32-B(2):166-73.
37. Pridie KH. The problem of the broken Judet prosthesis. *The Journal of bone and joint surgery British volume* 1955;37-B(2):224-7.
38. Devas MB. Arthroplasty of the hip: a review of 110 cup and replacement arthroplasties. *The Journal of bone and joint surgery British volume* 1954;36-B(4):561-6.
39. Shepherd MM. A review of 650 hip arthroplasty operations. *The Journal of bone and joint surgery British volume* 1954;36-B(4):567-77.
40. McKee GK, Watson-Farrar J. Replacement of arthritic hips by the McKee-Farrar prosthesis. *The Journal of bone and joint surgery British volume* 1966;48(2):245-59.
41. Charnley J. Anchorage of the femoral head prosthesis to the shaft of the femur. *The Journal of bone and joint surgery British volume* 1960;42-B:28-30.
42. Charnley J. The Bonding of Prostheses to Bone by Cement. *The Journal of bone and joint surgery British volume* 1964;46:518-29.
43. Charnley J. The long-term results of low-friction arthroplasty of the hip performed as a primary intervention. *The Journal of bone and joint surgery British volume* 1972;54(1):61-76.
44. Charnley J. Surgery of the hip-joint: present and future developments. *Br Med J* 1960;1(5176):821-6.
45. Freeman MA, Bradley GW. ICLH surface replacement of the hip. An analysis of the first 10 years. *The Journal of bone and joint surgery British volume* 1983;65(4):405-11.
46. Freeman MA, Cameron HU, Brown GC. Cemented double cup arthroplasty of the hip: a 5 year experience with the ICLH prosthesis. *Clinical orthopaedics and related research* 1978(134):45-52.
47. Howie DW, Cain CM, Cornish BL. Pseudo-abscess of the psoas bursa in failed double-cup arthroplasty of the hip. *The Journal of bone and joint surgery British volume* 1991;73(1):29-32.
48. August AC, Aldam CH, Pynsent PB. The McKee-Farrar hip arthroplasty. A long-term study. *The Journal of bone and joint surgery British volume* 1986;68(4):520-7.
49. Ball ST, Le Duff MJ, Amstutz HC. Early results of conversion of a failed femoral component in hip resurfacing arthroplasty. *The Journal of bone and joint surgery American volume* 2007;89(4):735-41. doi: 10.2106/JBJS.F.00708

50. Fisher J, Jin Z, Tipper J, et al. Tribology of alternative bearings. *Clinical orthopaedics and related research* 2006;453:25-34. doi: 10.1097/01.blo.0000238871.07604.49
51. Weber BG. [Metal-metal total prosthesis of the hip joint: back to the future]. *Z Orthop Ihre Grenzgeb* 1992;130(4):306-9. doi: 10.1055/s-2008-1039623
52. Amstutz HC, Thomas BJ, Jinnah R, et al. Treatment of primary osteoarthritis of the hip. A comparison of total joint and surface replacement arthroplasty. *The Journal of bone and joint surgery American volume* 1984;66(2):228-41.
53. McMinn D, Treacy R, Lin K, et al. Metal on metal surface replacement of the hip. Experience of the McMinn prothesis. *Clinical orthopaedics and related research* 1996(329 Suppl):S89-98.
54. Pollard TC, Baker RP, Eastaugh-Waring SJ, et al. Treatment of the young active patient with osteoarthritis of the hip. A five- to seven-year comparison of hybrid total hip arthroplasty and metal-on-metal resurfacing. *The Journal of bone and joint surgery British volume* 2006;88(5):592-600. doi: 10.1302/0301-620X.88B5.17354
55. Daniel J, Pynsent PB, McMinn DJ. Metal-on-metal resurfacing of the hip in patients under the age of 55 years with osteoarthritis. *The Journal of bone and joint surgery British volume* 2004;86(2):177-84.
56. Treacy RB, McBryde CW, Shears E, et al. Birmingham hip resurfacing: a minimum follow-up of ten years. *The Journal of bone and joint surgery British volume* 2011;93(1):27-33. doi: 10.1302/0301-620X.93B1.24134
57. De Haan R, Pattyn C, Gill HS, et al. Correlation between inclination of the acetabular component and metal ion levels in metal-on-metal hip resurfacing replacement. *The Journal of bone and joint surgery British volume* 2008;90(10):1291-7. doi: 10.1302/0301-620X.90B10.20533
58. Ollivere B, Darrah C, Barker T, et al. Early clinical failure of the Birmingham metal-on-metal hip resurfacing is associated with metallosis and soft-tissue necrosis. *The Journal of bone and joint surgery British volume* 2009;91(8):1025-30. doi: 10.1302/0301-620X.91B8.21701
59. Clarke MT, Lee PT, Arora A, et al. Levels of metal ions after small- and large-diameter metal-on-metal hip arthroplasty. *The Journal of bone and joint surgery British volume* 2003;85(6):913-7.
60. Freeman MA. Some anatomical and mechanical considerations relevant to the surface replacement of the femoral head. *Clinical orthopaedics and related research* 1978(134):19-24.
61. Loughead JM, Starks I, Chesney D, et al. Removal of acetabular bone in resurfacing arthroplasty of the hip: a comparison with hybrid total hip arthroplasty. *The Journal of bone and joint surgery British volume* 2006;88(1):31-4. doi: 10.1302/0301-620X.88B1.16764
62. Jameson SS, Langton DJ, Nargol AV. Articular surface replacement of the hip: a prospective single-surgeon series. *The Journal of bone and joint surgery British volume* 2010;92(1):28-37. doi: 10.1302/0301-620X.92B1.22769
63. Navarro M, Michiardi A, Castano O, et al. Biomaterials in orthopaedics. *J R Soc Interface* 2008;5(27):1137-58. doi: 10.1098/rsif.2008.0151
64. Merritt K, Brown SA. Release of hexavalent chromium from corrosion of stainless steel and cobalt-chromium alloys. *Journal of biomedical materials research* 1995;29(5):627-33. doi: 10.1002/jbm.820290510

65. Wooley PH, Nasser S, Fitzgerald RH, Jr. The immune response to implant materials in humans. *Clinical orthopaedics and related research* 1996(326):63-70.
66. Simonsen LO, Harbak H, Bennekou P. Cobalt metabolism and toxicology--a brief update. *Sci Total Environ* 2012;432:210-5. doi: 10.1016/j.scitotenv.2012.06.009
67. Schirrmacher UO. Case of cobalt poisoning. *Br Med J* 1967;1(5539):544-5.
68. Peters K, Unger RE, Barth S, et al. Induction of apoptosis in human microvascular endothelial cells by divalent cobalt ions. Evidence for integrin-mediated signaling via the cytoskeleton. *J Mater Sci Mater Med* 2001;12(10-12):955-8.
69. Zou W, Yan M, Xu W, et al. Cobalt chloride induces PC12 cells apoptosis through reactive oxygen species and accompanied by AP-1 activation. *J Neurosci Res* 2001;64(6):646-53. doi: 10.1002/jnr.1118
70. Catelas I, Petit A, Vali H, et al. Quantitative analysis of macrophage apoptosis vs. necrosis induced by cobalt and chromium ions in vitro. *Biomaterials* 2005;26(15):2441-53. doi: 10.1016/j.biomaterials.2004.08.004
71. Alarifi S, Ali D, Y AO, et al. Oxidative stress contributes to cobalt oxide nanoparticles-induced cytotoxicity and DNA damage in human hepatocarcinoma cells. *Int J Nanomedicine* 2013;8:189-99. doi: 10.2147/IJN.S37924
72. Harris RM, Williams TD, Hodges NJ, et al. Reactive oxygen species and oxidative DNA damage mediate the cytotoxicity of tungsten-nickel-cobalt alloys in vitro. *Toxicol Appl Pharmacol* 2011;250(1):19-28. doi: 10.1016/j.taap.2010.09.020
73. Alexander CS. Cobalt-beer cardiomyopathy. A clinical and pathologic study of twenty-eight cases. *Am J Med* 1972;53(4):395-417.
74. Barceloux DG. Cobalt. *J Toxicol Clin Toxicol* 1999;37(2):201-6.
75. Anderson RA. Chromium as an essential nutrient for humans. *Regul Toxicol Pharmacol* 1997;26(1 Pt 2):S35-41. doi: 10.1006/rtph.1997.1136
76. Barceloux DG. Chromium. *J Toxicol Clin Toxicol* 1999;37(2):173-94.
77. Coleman RF, Herrington J, Scales JT. Concentration of wear products in hair, blood, and urine after total hip replacement. *Br Med J* 1973;1(5852):527-9.
78. Brodner W, Bitzan P, Meisinger V, et al. Elevated serum cobalt with metal-on-metal articulating surfaces. *The Journal of bone and joint surgery British volume* 1997;79(2):316-21.
79. Jacobs JJ, Skipor AK, Patterson LM, et al. Metal release in patients who have had a primary total hip arthroplasty. A prospective, controlled, longitudinal study. *The Journal of bone and joint surgery American volume* 1998;80(10):1447-58.
80. MacDonald SJ, McCalden RW, Chess DG, et al. Metal-on-metal versus polyethylene in hip arthroplasty: a randomized clinical trial. *Clinical orthopaedics and related research* 2003(406):282-96. doi: 10.1097/01.blo.0000043066.62337.9d
81. Jacobs JJ, Skipor AK, Doorn PF, et al. Cobalt and chromium concentrations in patients with metal on metal total hip replacements. *Clinical orthopaedics and related research* 1996(329 Suppl):S256-63.

82. Hart AJ, Sabah SA, Bandi AS, et al. Sensitivity and specificity of blood cobalt and chromium metal ions for predicting failure of metal-on-metal hip replacement. *The Journal of bone and joint surgery British volume* 2011;93(10):1308-13. doi: 10.1302/0301-620X.93B10.26249
83. Langton DJ, Sprowson AP, Joyce TJ, et al. Blood metal ion concentrations after hip resurfacing arthroplasty: a comparative study of articular surface replacement and Birmingham Hip Resurfacing arthroplasties. *The Journal of bone and joint surgery British volume* 2009;91(10):1287-95. doi: 10.1302/0301-620X.91B10.22308
84. Daniel J, Ziaee H, Pradhan C, et al. Blood and urine metal ion levels in young and active patients after Birmingham hip resurfacing arthroplasty: four-year results of a prospective longitudinal study. *The Journal of bone and joint surgery British volume* 2007;89(2):169-73. doi: 10.1302/0301-620X.89B2.18519
85. Daniel J, Ziaee H, Pradhan C, et al. Six-year results of a prospective study of metal ion levels in young patients with metal-on-metal hip resurfacings. *The Journal of bone and joint surgery British volume* 2009;91(2):176-9. doi: 10.1302/0301-620X.91B2.21654
86. Jacobs JJ, Skipor AK, Campbell PA, et al. Can metal levels be used to monitor metal-on-metal hip arthroplasties? *The Journal of arthroplasty* 2004;19(8 Suppl 3):59-65.
87. Ball ST, Severns D, Linn M, et al. What happens to serum metal ion levels after a metal-on-metal bearing is removed? *The Journal of arthroplasty* 2013;28(8 Suppl):53-5. doi: 10.1016/j.arth.2013.06.040
88. Ebreo D, Khan A, El-Meligy M, et al. Metal ion levels decrease after revision for metallosis arising from large-diameter metal-on-metal hip arthroplasty. *Acta Orthop Belg* 2011;77(6):777-81.
89. Amstutz HC CP, Dorey FJ, Johnson AJ, Skipor AK, Jacobs JJ. Do ion concentrations after metal-on-metal hip resurfacing increase over time? A prospective study. *Journal of Arthroplasty* 2013;28(4):695-700. doi: 10.1016/j.arth.2012.07.040 [published Online First: 2012 Nov 2]
90. Berry DJ, Abdel MP, Callaghan JJ, et al. What are the current clinical issues in wear and tribocorrosion? *Clinical orthopaedics and related research* 2014;472(12):3659-64. doi: 10.1007/s11999-014-3610-1
91. Langton DJ, Jameson SS, Joyce TJ, et al. The effect of component size and orientation on the concentrations of metal ions after resurfacing arthroplasty of the hip. *The Journal of bone and joint surgery British volume* 2008;90(9):1143-51. doi: 10.1302/0301-620X.90B9.20785
92. Hart AJ, Skinner JA, Henckel J, et al. Insufficient acetabular version increases blood metal ion levels after metal-on-metal hip resurfacing. *Clinical orthopaedics and related research* 2011;469(9):2590-7. doi: 10.1007/s11999-011-1930-y
93. Matthies AK, Henckel J, Cro S, et al. Predicting wear and blood metal ion levels in metal-on-metal hip resurfacing. *Journal of orthopaedic research : official publication of the Orthopaedic Research Society* 2013 doi: 10.1002/jor.22459
94. Grammatopoulos G, Pandit H, Glyn-Jones S, et al. Optimal acetabular orientation for hip resurfacing. *The Journal of bone and joint surgery British volume* 2010;92(8):1072-8. doi: 10.1302/0301-620X.92B8.24194

95. Underwood RJ, Zografos A, Sayles RS, et al. Edge loading in metal-on-metal hips: low clearance is a new risk factor. *Proc Inst Mech Eng H* 2012;226(3):217-26.
96. Shimmin AJ, Walter WL, Esposito C. The influence of the size of the component on the outcome of resurfacing arthroplasty of the hip: a review of the literature. *The Journal of bone and joint surgery British volume* 2010;92(4):469-76. doi: 10.1302/0301-620X.92B4.22967
97. Cooper HJ, Della Valle CJ, Berger RA, et al. Corrosion at the head-neck taper as a cause for adverse local tissue reactions after total hip arthroplasty. *The Journal of bone and joint surgery American volume* 2012;94(18):1655-61.
98. Gill IP, Webb J, Sloan K, et al. Corrosion at the neck-stem junction as a cause of metal ion release and pseudotumour formation. *The Journal of bone and joint surgery British volume* 2012;94(7):895-900. doi: 10.1302/0301-620X.94B7.29122
99. Dangles CJ, Altstetter CJ. Failure of the modular neck in a total hip arthroplasty. *The Journal of arthroplasty* 2010;25(7):1169 e5-7. doi: 10.1016/j.arth.2009.07.015
100. Langton DJ, Sidaginamale R, Lord JK, et al. Taper junction failure in large-diameter metal-on-metal bearings. *Bone Joint Res* 2012;1(4):56-63. doi: 10.1302/2046-3758.14.2000047
101. Effect of Increased Frictional Torque on the Fretting Corrosion Behaviour of the Large Diameter Femoral Head; 2013 2013. Orthopaedic Proceedings, Bone and Joint Journal.
102. Panagiotidou A, Meswania J, Osman K, et al. The effect of frictional torque and bending moment on corrosion at the taper interface : an in vitro study. *The bone & joint journal* 2015;97-B(4):463-72. doi: 10.1302/0301-620X.97B4.34800
103. Keegan GM, Learmonth ID, Case CP. Orthopaedic metals and their potential toxicity in the arthroplasty patient: A review of current knowledge and future strategies. *The Journal of bone and joint surgery British volume* 2007;89(5):567-73. doi: 10.1302/0301-620X.89B5.18903
104. Keegan GM, Learmonth ID, Case CP. A systematic comparison of the actual, potential, and theoretical health effects of cobalt and chromium exposures from industry and surgical implants. *Crit Rev Toxicol* 2008;38(8):645-74. doi: 10.1080/10408440701845534
105. Papis E, Gornati R, Prati M, et al. Gene expression in nanotoxicology research: analysis by differential display in BALB3T3 fibroblasts exposed to cobalt particles and ions. *Toxicol Lett* 2007;170(3):185-92. doi: 10.1016/j.toxlet.2007.03.005
106. Newton AW, Ranganath L, Armstrong C, et al. Differential distribution of cobalt, chromium, and nickel between whole blood, plasma and urine in patients after metal-on-metal (MoM) hip arthroplasty. *Journal of orthopaedic research : official publication of the Orthopaedic Research Society* 2012;30(10):1640-6. doi: 10.1002/jor.22107
107. Afolaranmi GA, Akbar M, Brewer J, et al. Distribution of metal released from cobalt-chromium alloy orthopaedic wear particles implanted into air pouches in mice. *J Biomed Mater Res A* 2012;100(6):1529-38. doi: 10.1002/jbm.a.34091 [published Online First: 2012/03/16]

108. Rae T. The toxicity of metals used in orthopaedic prostheses. An experimental study using cultured human synovial fibroblasts. *The Journal of bone and joint surgery British volume* 1981;63-B(3):435-40.
109. Yang SJ, Pyen J, Lee I, et al. Cobalt chloride-induced apoptosis and extracellular signal-regulated protein kinase 1/2 activation in rat C6 glioma cells. *J Biochem Mol Biol* 2004;37(4):480-6.
110. Papageorgiou I, Brown C, Schins R, et al. The effect of nano- and micron-sized particles of cobalt-chromium alloy on human fibroblasts in vitro. *Biomaterials* 2007;28(19):2946-58. doi: 10.1016/j.biomaterials.2007.02.034
111. Papageorgiou I, Yin Z, Ladon D, et al. Genotoxic effects of particles of surgical cobalt chrome alloy on human cells of different age in vitro. *Mutat Res* 2007;619(1-2):45-58. doi: 10.1016/j.mrfmmm.2007.01.008
112. Rae T. A study on the effects of particulate metals of orthopaedic interest on murine macrophages in vitro. *The Journal of bone and joint surgery British volume* 1975;57(4):444-50.
113. Allen MJ, Myer BJ, Millett PJ, et al. The effects of particulate cobalt, chromium and cobalt-chromium alloy on human osteoblast-like cells in vitro. *The Journal of bone and joint surgery British volume* 1997;79(3):475-82.
114. Kwon YM, Xia Z, Glyn-Jones S, et al. Dose-dependent cytotoxicity of clinically relevant cobalt nanoparticles and ions on macrophages in vitro. *Biomed Mater* 2009;4(2):025018. doi: 10.1088/1748-6041/4/2/025018 [published Online First: 2009/04/08]
115. Wang G, Hazra TK, Mitra S, et al. Mitochondrial DNA damage and a hypoxic response are induced by CoCl(2) in rat neuronal PC12 cells. *Nucleic Acids Res* 2000;28(10):2135-40.
116. Rizzetti MC, Liberini P, Zarattini G, et al. Loss of sight and sound. Could it be the hip? *Lancet* 2009;373(9668):1052. doi: 10.1016/S0140-6736(09)60490-6
117. De Smet K, De Haan R, Calistri A, et al. Metal ion measurement as a diagnostic tool to identify problems with metal-on-metal hip resurfacing. *The Journal of bone and joint surgery American volume* 2008;90 Suppl 4:202-8. doi: 10.2106/JBJS.H.00672
118. Langton DJ, Jameson SS, Joyce TJ, et al. Early failure of metal-on-metal bearings in hip resurfacing and large-diameter total hip replacement: A consequence of excess wear. *The Journal of bone and joint surgery British volume* 2010;92(1):38-46. doi: 10.1302/0301-620X.92B1.22770
119. Davda K, Lali FV, Sampson B, et al. An analysis of metal ion levels in the joint fluid of symptomatic patients with metal-on-metal hip replacements. *The Journal of bone and joint surgery British volume* 2011;93(6):738-45. doi: 10.1302/0301-620X.93B6.25804
120. Hart AJ, Quinn PD, Lali F, et al. Cobalt from metal-on-metal hip replacements may be the clinically relevant active agent responsible for periprosthetic tissue reactions. *Acta Biomater* 2012;8(10):3865-73. doi: 10.1016/j.actbio.2012.05.003 [published Online First: 2012/06/13]
121. Hart AJ, Quinn PD, Sampson B, et al. The chemical form of metallic debris in tissues surrounding metal-on-metal hips with unexplained failure. *Acta*

Biomater 2010;6(11):4439-46. doi: 10.1016/j.actbio.2010.06.006 [published Online First: 2010/06/15]
122. Goode AE, Perkins JM, Sandison A, et al. Chemical speciation of nanoparticles surrounding metal-on-metal hips. *Chem Commun (Camb)* 2012;48(67):8335-7. doi: 10.1039/c2cc33016d [published Online First: 2012/07/18]
123. Toms AP, Smith-Bateman C, Malcolm PN, et al. Optimization of metal artefact reduction (MAR) sequences for MRI of total hip prostheses. *Clin Radiol* 2010;65(6):447-52. doi: 10.1016/j.crad.2009.12.014 [published Online First: 2010/05/11]
124. Nawabi DH, Hayter CL, Su EP, et al. Magnetic resonance imaging findings in symptomatic versus asymptomatic subjects following metal-on-metal hip resurfacing arthroplasty. *The Journal of bone and joint surgery American volume* 2013;95(10):895-902. doi: 10.2106/JBJS.K.01476
125. Siddiqui IA, Sabah SA, Satchithananda K, et al. A comparison of the diagnostic accuracy of MARS MRI and ultrasound of the painful metal-on-metal hip arthroplasty. *Acta orthopaedica* 2014 doi: 10.3109/17453674.2014.908345
126. Garbuz DS, Hargreaves BA, Duncan CP, et al. The John Charnley Award: Diagnostic accuracy of MRI versus ultrasound for detecting pseudotumors in asymptomatic metal-on-metal THA. *Clinical orthopaedics and related research* 2014;472(2):417-23. doi: 10.1007/s11999-013-3181-6
127. Hayter CL, Koff MF, Shah P, et al. MRI after arthroplasty: comparison of MAVRIC and conventional fast spin-echo techniques. *AJR Am J Roentgenol* 2011;197(3):W405-11. doi: 10.2214/AJR.11.6659
128. Robinson E, Henckel J, Sabah S, et al. Cross-sectional imaging of metal-on-metal hip arthroplasties. *Acta orthopaedica* 2014:1-8. doi: 10.3109/17453674.2014.964618
129. Kwon YM, Ostlere SJ, McLardy-Smith P, et al. "Asymptomatic" pseudotumors after metal-on-metal hip resurfacing arthroplasty: prevalence and metal ion study. *The Journal of arthroplasty* 2011;26(4):511-8. doi: 10.1016/j.arth.2010.05.030
130. Bosker BH, Ettema HB, Boomsma MF, et al. High incidence of pseudotumour formation after large-diameter metal-on-metal total hip replacement: a prospective cohort study. *The Journal of bone and joint surgery British volume* 2012;94(6):755-61. doi: 10.1302/0301-620X.94B6.28373
131. Hart AJ, Satchithananda K, Liddle AD, et al. Pseudotumors in association with well-functioning metal-on-metal hip prostheses: a case-control study using three-dimensional computed tomography and magnetic resonance imaging. *The Journal of bone and joint surgery American volume* 2012;94(4):317-25. doi: 10.2106/JBJS.J.01508
132. Canadian Hip Resurfacing Study G. A survey on the prevalence of pseudotumors with metal-on-metal hip resurfacing in Canadian academic centers. *The Journal of bone and joint surgery American volume* 2011;93 Suppl 2:118-21. doi: 10.2106/JBJS.J.01848 [published Online First: 2011/05/14]
133. Almousa SA, Greidanus NV, Masri BA, et al. The Natural History of Inflammatory Pseudotumors in Asymptomatic Patients After Metal-on-metal Hip Arthroplasty. *Clinical orthopaedics and related research*

2013;471(12):3814-21. doi: 10.1007/s11999-013-2944-4 [published Online First: 2013/03/29]
134. Ebreo D, Bell PJ, Arshad H, et al. Serial magnetic resonance imaging of metal-on-metal total hip replacements. Follow-up of a cohort of 28 mm Ultima TPS THRs. *The bone & joint journal* 2013;95-B(8):1035-9. doi: 10.1302/0301-620X.95B8.31377 [published Online First: 2013/08/03]
135. van der Weegen W, Brakel K, Horn RJ, et al. Asymptomatic pseudotumours after metal-on-metal hip resurfacing show little change within one year. *The bone & joint journal* 2013;95-B(12):1626-31. doi: 10.1302/0301-620X.95B12.32248 [published Online First: 2013/12/03]
136. Willert HG, Buchhorn GH, Fayyazi A, et al. Metal-on-metal bearings and hypersensitivity in patients with artificial hip joints. A clinical and histomorphological study. *The Journal of bone and joint surgery American volume* 2005;87(1):28-36. doi: 10.2106/JBJS.A.02039pp
137. Delaunay C, Petit I, Learmonth ID, et al. Metal-on-metal bearings total hip arthroplasty: the cobalt and chromium ions release concern. *Orthop Traumatol Surg Res* 2010;96(8):894-904. doi: 10.1016/j.otsr.2010.05.008 [published Online First: 2010/09/14]
138. Kwon YM, Thomas P, Summer B, et al. Lymphocyte proliferation responses in patients with pseudotumors following metal-on-metal hip resurfacing arthroplasty. *Journal of orthopaedic research : official publication of the Orthopaedic Research Society* 2010;28(4):444-50. doi: 10.1002/jor.21015
139. Bisseling P, de Wit BW, Hol AM, et al. Similar incidence of periprosthetic fluid collections after ceramic-on-polyethylene total hip arthroplasties and metal-on-metal resurfacing arthroplasties: results of a screening metal artefact reduction sequence-MRI study. *The bone & joint journal* 2015;97-B(9):1175-82. doi: 10.1302/0301-620X.97B9.35247
140. Hing CB, Young DA, Dalziel RE, et al. Narrowing of the neck in resurfacing arthroplasty of the hip: a radiological study. *The Journal of bone and joint surgery British volume* 2007;89(8):1019-24. doi: 10.1302/0301-620X.89B8.18830
141. Chen Z, Pandit H, Taylor A, et al. Metal-on-metal hip resurfacings--a radiological perspective. *Eur Radiol* 2011;21(3):485-91. doi: 10.1007/s00330-010-1946-9
142. Kanaji A, Caicedo MS, Virdi AS, et al. Co-Cr-Mo alloy particles induce tumor necrosis factor alpha production in MLO-Y4 osteocytes: a role for osteocytes in particle-induced inflammation. *Bone* 2009;45(3):528-33. doi: 10.1016/j.bone.2009.05.020
143. Andrews RE, Shah KM, Wilkinson JM, et al. Effects of cobalt and chromium ions at clinically equivalent concentrations after metal-on-metal hip replacement on human osteoblasts and osteoclasts: implications for skeletal health. *Bone* 2011;49(4):717-23. doi: 10.1016/j.bone.2011.06.007
144. Liddle AD, Satchithananda K, Henckel J, et al. Revision of metal-on-metal hip arthroplasty in a tertiary center: a prospective study of 39 hips with between 1 and 4 years of follow-up. *Acta orthopaedica* 2013;84(3):237-45. doi: 10.3109/17453674.2013.797313 [published Online First: 2013/04/30]

145. Toms AP, Marshall TJ, Cahir J, et al. MRI of early symptomatic metal-on-metal total hip arthroplasty: a retrospective review of radiological findings in 20 hips. *Clin Radiol* 2008;63(1):49-58. doi: 10.1016/j.crad.2007.07.012 [published Online First: 2007/12/11]
146. Hayter CL, Gold SL, Koff MF, et al. MRI findings in painful metal-on-metal hip arthroplasty. *AJR Am J Roentgenol* 2012;199(4):884-93. doi: 10.2214/AJR.11.8203 [published Online First: 2012/09/22]
147. Sabah SA, Mitchell AW, Henckel J, et al. Magnetic resonance imaging findings in painful metal-on-metal hips: a prospective study. *The Journal of arthroplasty* 2011;26(1):71-6, 76 e1-2. doi: 10.1016/j.arth.2009.11.008 [published Online First: 2010/02/13]
148. Berber R, Khoo M, Cook E, et al. Muscle atrophy and metal-on-metal hip implants. *Acta orthopaedica* 2015:1-7. doi: 10.3109/17453674.2015.1006981
149. Grimaldi A, Richardson C, Stanton W, et al. The association between degenerative hip joint pathology and size of the gluteus medius, gluteus minimus and piriformis muscles. *Man Ther* 2009;14(6):605-10. doi: 10.1016/j.math.2009.07.004
150. Leikin JB, Karydes HC, Whiteley PM, et al. Outpatient toxicology clinic experience of patients with hip implants. *Clin Toxicol (Phila)* 2013;51(4):230-6. doi: 10.3109/15563650.2013.768343
151. Steens W, von Foerster G, Katzer A. Severe cobalt poisoning with loss of sight after ceramic-metal pairing in a hip--a case report. *Acta orthopaedica* 2006;77(5):830-2. doi: 10.1080/17453670610013079
152. Tower SS. Arthroprosthetic cobaltism: neurological and cardiac manifestations in two patients with metal-on-metal arthroplasty: a case report. *The Journal of bone and joint surgery American volume* 2010;92(17):2847-51. doi: 10.2106/JBJS.J.00125
153. Tower SS. Arthroprosthetic cobaltism associated with metal on metal hip implants. *Bmj* 2012;344:e430. doi: 10.1136/bmj.e430
154. Pazzaglia UE, Apostoli P, Congiu T, et al. Cobalt, chromium and molybdenum ions kinetics in the human body: data gained from a total hip replacement with massive third body wear of the head and neuropathy by cobalt intoxication. *Archives of orthopaedic and traumatic surgery Archiv fur orthopadische und Unfall-Chirurgie* 2011;131(9):1299-308. doi: 10.1007/s00402-011-1268-7 [published Online First: 2011/02/08]
155. Ikeda T, Takahashi K, Kabata T, et al. Polyneuropathy caused by cobalt-chromium metallosis after total hip replacement. *Muscle Nerve* 2010;42(1):140-3. doi: 10.1002/mus.21638
156. Oldenburg M, Wegner R, Baur X. Severe cobalt intoxication due to prosthesis wear in repeated total hip arthroplasty. *The Journal of arthroplasty* 2009;24(5):825 e15-20. doi: 10.1016/j.arth.2008.07.017
157. Pelclova D, Sklensky M, Janicek P, et al. Severe cobalt intoxication following hip replacement revision: clinical features and outcome. *Clin Toxicol (Phila)* 2012;50(4):262-5. doi: 10.3109/15563650.2012.670244
158. Apel W, Stark D, Stark A, et al. Cobalt-chromium toxic retinopathy case study. *Doc Ophthalmol* 2013;126(1):69-78. doi: 10.1007/s10633-012-9356-8

159. Ng SK, Ebneter A, Gilhotra JS. Hip-implant related chorio-retinal cobalt toxicity. *Indian J Ophthalmol* 2013;61(1):35-7. doi: 10.4103/0301-4738.105053
160. Mao X, Wong AA, Crawford RW. Cobalt toxicity--an emerging clinical problem in patients with metal-on-metal hip prostheses? *Med J Aust* 2011;194(12):649-51.
161. Giampreti A, Lonati D, Ragghianti B, et al. N-Acetyl-Cysteine as Effective and Safe Chelating Agent in Metal-on-Metal Hip-Implanted Patients: Two Cases. *Case Rep Orthop* 2016;2016:8682737. doi: 10.1155/2016/8682737
162. Allen LA, Ambardekar AV, Devaraj KM, et al. Clinical problem-solving. Missing elements of the history. *N Engl J Med* 2014;370(6):559-66. doi: 10.1056/NEJMcps1213196
163. Dahms K, Sharkova Y, Heitland P, et al. Cobalt intoxication diagnosed with the help of Dr House. *Lancet* 2014;383(9916):574. doi: 10.1016/S0140-6736(14)60037-4
164. Mosier BA, Maynard L, Sotereanos NG, et al. Progressive Cardiomyopathy in a Patient With Elevated Cobalt Ion Levels and Bilateral Metal-on-Metal Hip Arthroplasties. *Am J Orthop (Belle Mead NJ)* 2016;45(3):E132-5.
165. Fox KA, Phillips TM, Yanta JH, et al. Fatal cobalt toxicity after total hip arthroplasty revision for fractured ceramic components. *Clin Toxicol (Phila)* 2016;54(9):874-77. doi: 10.1080/15563650.2016.1214274
166. van Lingen CP, Ettema HB, Timmer JR, et al. Clinical manifestations in ten patients with asymptomatic metal-on-metal hip arthroplasty with very high cobalt levels. *Hip international : the journal of clinical and experimental research on hip pathology and therapy* 2013;23(5):441-4. doi: 10.5301/hipint.5000054 [published Online First: 2013/07/03]
167. Prentice JR, Clark MJ, Hoggard N, et al. Metal-on-metal hip prostheses and systemic health: a cross-sectional association study 8 years after implantation. *PLoS One* 2013;8(6):e66186. doi: 10.1371/journal.pone.0066186 [published Online First: 2013/06/14]
168. Linna A, Oksa P, Groundstroem K, et al. Exposure to cobalt in the production of cobalt and cobalt compounds and its effect on the heart. *Occup Environ Med* 2004;61(11):877-85. doi: 10.1136/oem.2003.009605 [published Online First: 2004/10/13]
169. Kesteloot H, Roelandt J, Willems J, et al. An enquiry into the role of cobalt in the heart disease of chronic beer drinkers. *Circulation* 1968;37(5):854-64. [published Online First: 1968/05/01]
170. Jordan C, Whitman RD, Harbut M, et al. Memory deficits in workers suffering from hard metal disease. *Toxicol Lett* 1990;54(2-3):241-3. [published Online First: 1990/12/01]
171. Meecham HM, Humphrey P. Industrial exposure to cobalt causing optic atrophy and nerve deafness: a case report. *J Neurol Neurosurg Psychiatry* 1991;54(4):374-5. [published Online First: 1991/04/01]
172. Catalani S, Rizzetti MC, Padovani A, et al. Neurotoxicity of cobalt. *Hum Exp Toxicol* 2012;31(5):421-37. doi: 10.1177/0960327111414280 [published Online First: 2011/07/07]
173. Licht A, Oliver M, Rachmilewitz EA. Optic atrophy following treatment with cobalt chloride in a patient with pancytopenia and hypercellular marrow. *Isr J Med Sci* 1972;8(1):61-6. [published Online First: 1972/01/01]

174. Travacio M, Polo JM, Llesuy S. Chromium (VI) induces oxidative stress in the mouse brain. *Toxicology* 2001;162(2):139-48. [published Online First: 2001/05/05]
175. Cartwright GE. The relationship of copper, cobalt, and other trace elements to hemopoiesis. *Am J Clin Nutr* 1955;3(1):11-9. [published Online First: 1955/01/01]
176. Brock T, Stopford W. Bioaccessibility of metals in human health risk assessment: evaluating risk from exposure to cobalt compounds. *J Environ Monit* 2003;5(4):71N-76N. [published Online First: 2003/09/02]
177. Kriss JP, Carnes WH, Gross RT. Hypothyroidism and thyroid hyperplasia in patients treated with cobalt. *J Am Med Assoc* 1955;157(2):117-21. [published Online First: 1955/01/08]
178. Prescott E, Netterstrom B, Faber J, et al. Effect of occupational exposure to cobalt blue dyes on the thyroid volume and function of female plate painters. *Scand J Work Environ Health* 1992;18(2):101-4. [published Online First: 1992/04/01]
179. Lantin AC, Mallants A, Vermeulen J, et al. Absence of adverse effect on thyroid function and red blood cells in a population of workers exposed to cobalt compounds. *Toxicol Lett* 2011;201(1):42-6. doi: 10.1016/j.toxlet.2010.12.003 [published Online First: 2010/12/25]
180. Quinteros FA, Poliandri AH, Machiavelli LI, et al. In vivo and in vitro effects of chromium VI on anterior pituitary hormone release and cell viability. *Toxicol Appl Pharmacol* 2007;218(1):79-87. doi: 10.1016/j.taap.2006.10.017 [published Online First: 2006/12/05]
181. Quinteros FA, Machiavelli LI, Miler EA, et al. Mechanisms of chromium (VI)-induced apoptosis in anterior pituitary cells. *Toxicology* 2008;249(2-3):109-15. doi: 10.1016/j.tox.2008.04.012 [published Online First: 2008/06/13]
182. Polyzois I, Nikolopoulos D, Michos I, et al. Local and systemic toxicity of nanoscale debris particles in total hip arthroplasty. *J Appl Toxicol* 2012;32(4):255-69. doi: 10.1002/jat.2729 [published Online First: 2012/02/14]
183. Ziaee H, Daniel J, Datta AK, et al. Transplacental transfer of cobalt and chromium in patients with metal-on-metal hip arthroplasty: a controlled study. *The Journal of bone and joint surgery British volume* 2007;89(3):301-5. doi: 10.1302/0301-620X.89B3.18520 [published Online First: 2007/03/16]
184. Fritzsche J, Borisch C, Schaefer C. Case report: High chromium and cobalt levels in a pregnant patient with bilateral metal-on-metal hip arthroplasties. *Clinical orthopaedics and related research* 2012;470(8):2325-31. doi: 10.1007/s11999-012-2398-0 [published Online First: 2012/06/14]
185. Brodner W, Grohs JG, Bancher-Todesca D, et al. Does the placenta inhibit the passage of chromium and cobalt after metal-on-metal total hip arthroplasty? *The Journal of arthroplasty* 2004;19(8 Suppl 3):102-6. [published Online First: 2004/12/04]
186. Cobb AG, Schmalzreid TP. The clinical significance of metal ion release from cobalt-chromium metal-on-metal hip joint arthroplasty. *Proc Inst Mech Eng H* 2006;220(2):385-98. [published Online First: 2006/05/04]

187. Gilani SH, Alibhai Y. Teratogenicity of metals to chick embryos. *J Toxicol Environ Health* 1990;30(1):23-31. doi: 10.1080/15287399009531407 [published Online First: 1990/05/01]
188. Kanojia RK, Junaid M, Murthy RC. Chromium induced teratogenicity in female rat. *Toxicol Lett* 1996;89(3):207-13. [published Online First: 1996/12/31]
189. Trivedi B, Saxena DK, Murthy RC, et al. Embryotoxicity and fetotoxicity of orally administered hexavalent chromium in mice. *Reprod Toxicol* 1989;3(4):275-8. [published Online First: 1989/01/01]
190. Kasirsky G, Gautieri RF, Mann DE, Jr. Inhibition of cortisone-induced cleft palate in mice by cobaltous chloride. *J Pharm Sci* 1967;56(10):1330-2. [published Online First: 1967/10/01]
191. Wedeen RP, Qian LF. Chromium-induced kidney disease. *Environ Health Perspect* 1991;92:71-4. [published Online First: 1991/05/01]
192. Marker M, Grubl A, Riedl O, et al. Metal-on-metal hip implants: do they impair renal function in the long-term? A 10-year follow-up study. *Archives of orthopaedic and traumatic surgery Archiv fur orthopadische und Unfall-Chirurgie* 2008;128(9):915-9. doi: 10.1007/s00402-007-0466-9 [published Online First: 2007/10/18]
193. Corradi M, Daniel J, Ziaee H, et al. Early markers of nephrotoxicity in patients with metal-on-metal hip arthroplasty. *Clinical orthopaedics and related research* 2011;469(6):1651-9. doi: 10.1007/s11999-010-1682-0 [published Online First: 2010/11/26]
194. Daniel J, Ziaee H, Pradhan C, et al. Renal clearance of cobalt in relation to the use of metal-on-metal bearings in hip arthroplasty. *The Journal of bone and joint surgery American volume* 2010;92(4):840-5. doi: 10.2106/JBJS.H.01821 [published Online First: 2010/04/03]
195. Kurosaki K, Nakamura T, Mukai T, et al. Unusual findings in a fatal case of poisoning with chromate compounds. *Forensic Sci Int* 1995;75(1):57-65. [published Online First: 1995/08/28]
196. Lin CC, Wu ML, Yang CC, et al. Acute severe chromium poisoning after dermal exposure to hexavalent chromium. *J Chin Med Assoc* 2009;72(4):219-21. doi: 10.1016/S1726-4901(09)70059-0 [published Online First: 2009/04/18]
197. Hallab N, Merritt K, Jacobs JJ. Metal sensitivity in patients with orthopaedic implants. *The Journal of bone and joint surgery American volume* 2001;83-A(3):428-36. [published Online First: 2001/03/27]
198. Hallab NJ. Lymphocyte transformation testing for quantifying metal-implant-related hypersensitivity responses. *Dermatitis* 2004;15(2):82-90. [published Online First: 2004/10/12]
199. Atanaskova Mesinkovska N, Tellez A, Molina L, et al. The effect of patch testing on surgical practices and outcomes in orthopedic patients with metal implants. *Arch Dermatol* 2012;148(6):687-93. doi: 10.1001/archdermatol.2011.2561 [published Online First: 2012/02/22]
200. Gill HS, Grammatopoulos G, Adshead S, et al. Molecular and immune toxicity of CoCr nanoparticles in MoM hip arthroplasty. *Trends Mol Med* 2012;18(3):145-55. doi: 10.1016/j.molmed.2011.12.002 [published Online First: 2012/01/17]

201. Colognato R, Bonelli A, Ponti J, et al. Comparative genotoxicity of cobalt nanoparticles and ions on human peripheral leukocytes in vitro. *Mutagenesis* 2008;23(5):377-82. doi: 10.1093/mutage/gen024 [published Online First: 2008/05/28]
202. Messer RL, Bishop S, Lucas LC. Effects of metallic ion toxicity on human gingival fibroblasts morphology. *Biomaterials* 1999;20(18):1647-57. [published Online First: 1999/09/30]
203. Akbar M, Brewer JM, Grant MH. Effect of chromium and cobalt ions on primary human lymphocytes in vitro. *J Immunotoxicol* 2011;8(2):140-9. doi: 10.3109/1547691X.2011.553845 [published Online First: 2011/03/31]
204. Ladon D, Doherty A, Newson R, et al. Changes in metal levels and chromosome aberrations in the peripheral blood of patients after metal-on-metal hip arthroplasty. *The Journal of arthroplasty* 2004;19(8 Suppl 3):78-83. [published Online First: 2004/12/04]
205. Dunstan E, Ladon D, Whittingham-Jones P, et al. Chromosomal aberrations in the peripheral blood of patients with metal-on-metal hip bearings. *The Journal of bone and joint surgery American volume* 2008;90(3):517-22. doi: 10.2106/JBJS.F.01435 [published Online First: 2008/03/04]
206. Elliott P. Cardiomyopathy. Diagnosis and management of dilated cardiomyopathy. *Heart* 2000;84(1):106-12.
207. Japp AG, Gulati A, Cook SA, et al. The Diagnosis and Evaluation of Dilated Cardiomyopathy. *J Am Coll Cardiol* 2016;67(25):2996-3010. doi: 10.1016/j.jacc.2016.03.590
208. Luk A, Ahn E, Soor GS, et al. Dilated cardiomyopathy: a review. *J Clin Pathol* 2009;62(3):219-25. doi: 10.1136/jcp.2008.060731
209. Grogan M, Redfield MM, Bailey KR, et al. Long-term outcome of patients with biopsy-proved myocarditis: comparison with idiopathic dilated cardiomyopathy. *J Am Coll Cardiol* 1995;26(1):80-4.
210. Raghow R. An 'Omics' Perspective on Cardiomyopathies and Heart Failure. *Trends Mol Med* 2016;22(9):813-27. doi: 10.1016/j.molmed.2016.07.007
211. Fauchier L, Babuty D, Poret P, et al. Comparison of long-term outcome of alcoholic and idiopathic dilated cardiomyopathy. *Eur Heart J* 2000;21(4):306-14. doi: 10.1053/euhj.1999.1761
212. Gulati A, Ismail TF, Jabbour A, et al. Clinical utility and prognostic value of left atrial volume assessment by cardiovascular magnetic resonance in non-ischaemic dilated cardiomyopathy. *Eur J Heart Fail* 2013;15(6):660-70. doi: 10.1093/eurjhf/hft019
213. Centeno JA, Pestaner JP, Mullick FG, et al. An analytical comparison of cobalt cardiomyopathy and idiopathic dilated cardiomyopathy. *Biol Trace Elem Res* 1996;55(1-2):21-30.
214. Galante JO, Lemons J, Spector M, et al. The biologic effects of implant materials. *Journal of orthopaedic research : official publication of the Orthopaedic Research Society* 1991;9(5):760-75. doi: 10.1002/jor.1100090516
215. Novelline R. Squire's Fundamentals of Radiology. In: Novelline R, ed. Squire's Fundamentals of Radiology. Sixth ed. Harvard University Press: Harvard University Press 2004.

216. Pattynama PM, De Roos A, Van der Wall EE, et al. Evaluation of cardiac function with magnetic resonance imaging. *Am Heart J* 1994;128(3):595-607.
217. Alfakih K, Reid S, Jones T, et al. Assessment of ventricular function and mass by cardiac magnetic resonance imaging. *Eur Radiol* 2004;14(10):1813-22. doi: 10.1007/s00330-004-2387-0
218. Hoffmann R, Barletta G, von Bardeleben S, et al. Analysis of left ventricular volumes and function: a multicenter comparison of cardiac magnetic resonance imaging, cine ventriculography, and unenhanced and contrast-enhanced two-dimensional and three-dimensional echocardiography. *J Am Soc Echocardiogr* 2014;27(3):292-301. doi: 10.1016/j.echo.2013.12.005
219. Moon JC, Messroghli DR, Kellman P, et al. Myocardial T1 mapping and extracellular volume quantification: a Society for Cardiovascular Magnetic Resonance (SCMR) and CMR Working Group of the European Society of Cardiology consensus statement. *J Cardiovasc Magn Reson* 2013;15:92. doi: 10.1186/1532-429X-15-92
220. Hwang SH, Choi BW. Advanced Cardiac MR Imaging for Myocardial Characterization and Quantification: T1 Mapping. *Korean Circ J* 2013;43(1):1-6. doi: 10.4070/kcj.2013.43.1.1
221. Messroghli DR, Radjenovic A, Kozerke S, et al. Modified Look-Locker inversion recovery (MOLLI) for high-resolution T1 mapping of the heart. *Magn Reson Med* 2004;52(1):141-6. doi: 10.1002/mrm.20110
222. Piechnik SK, Ferreira VM, Dall'Armellina E, et al. Shortened Modified Look-Locker Inversion recovery (ShMOLLI) for clinical myocardial T1-mapping at 1.5 and 3 T within a 9 heartbeat breathhold. *J Cardiovasc Magn Reson* 2010;12:69. doi: 10.1186/1532-429X-12-69
223. Wong TC, Piehler KM, Kang IA, et al. Myocardial extracellular volume fraction quantified by cardiovascular magnetic resonance is increased in diabetes and associated with mortality and incident heart failure admission. *Eur Heart J* 2014;35(10):657-64. doi: 10.1093/eurheartj/eht193
224. Miller CA, Naish JH, Bishop P, et al. Comprehensive validation of cardiovascular magnetic resonance techniques for the assessment of myocardial extracellular volume. *Circulation Cardiovascular imaging* 2013;6(3):373-83. doi: 10.1161/CIRCIMAGING.112.000192
225. Baur LH. Early detection of iron overload in the heart: a key role for MRI! *Int J Cardiovasc Imaging* 2009;25(8):789-90. doi: 10.1007/s10554-009-9538-y [published Online First: 2009/11/26]
226. Chu WC, Au WY, Lam WW. MRI of cardiac iron overload. *J Magn Reson Imaging* 2012;36(5):1052-9. doi: 10.1002/jmri.23628 [published Online First: 2012/10/24]
227. Gulati V, Harikrishnan P, Palaniswamy C, et al. Cardiac Involvement in Hemochromatosis. *Cardiol Rev* 2014;22(2):56-68. doi: 10.1097/CRD.0b013e3182a67805 [published Online First: 2014/02/08]
228. Pepe A, Positano V, Santarelli MF, et al. Multislice multiecho T2* cardiovascular magnetic resonance for detection of the heterogeneous distribution of myocardial iron overload. *J Magn Reson Imaging*

2006;23(5):662-8. doi: 10.1002/jmri.20566 [published Online First: 2006/03/29]
229. Parkes LM, Hodgson R, Lu le T, et al. Cobalt nanoparticles as a novel magnetic resonance contrast agent--relaxivities at 1.5 and 3 Tesla. *Contrast Media Mol Imaging* 2008;3(4):150-6. doi: 10.1002/cmmi.241
230. Runge VM, Foster MA, Clanton JA, et al. Contrast enhancement of magnetic resonance images by chromium EDTA: an experimental study. *Radiology* 1984;152(1):123-6. doi: 10.1148/radiology.152.1.6427845
231. Billi F, Benya P, Kavanaugh A, et al. The John Charnley Award: an accurate and extremely sensitive method to separate, display, and characterize wear debris: part 2: metal and ceramic particles. *Clinical orthopaedics and related research* 2012;470(2):339-50. doi: 10.1007/s11999-011-2058-9
232. Porter M, Borroff M, Gregg P, et al. 10th Annual Report 2013 - National Joint Registry for England, Wales, and Northern Ireland, 2013.
233. Berber R, Pappas Y, Khoo M, et al. A New Approach to Managing Patients with Problematic Metal Hip Implants: The Use of an Internet-Enhanced Multidisciplinary Team Meeting: AAOS Exhibit Selection. *The Journal of bone and joint surgery American volume* 2015;97(4):e20. doi: 10.2106/JBJS.N.00973
234. Rombout-Sestrienkova E, van Kraaij MG, Koek GH. How we manage patients with hereditary haemochromatosis. *Br J Haematol* 2016;175(5):759-70. doi: 10.1111/bjh.14376
235. Gurrin LC, Bertalli NA, Dalton GW, et al. HFE C282Y/H63D compound heterozygotes are at low risk of hemochromatosis-related morbidity. *Hepatology* 2009;50(1):94-101. doi: 10.1002/hep.22972
236. de Valk B, Witlox RS, van der Schouw YT, et al. Biochemical expression of heterozygous hereditary hemochromatosis. *Eur J Intern Med* 2000;11(6):317-21.
237. Mosselmans JF, Quinn PD, Dent AJ, et al. I18--the microfocus spectroscopy beamline at the Diamond Light Source. *J Synchrotron Radiat* 2009;16(Pt 6):818-24. doi: 10.1107/S0909049509032282
238. Cohen D. How safe are metal-on-metal hip implants? *Bmj* 2012;344:e1410. doi: 10.1136/bmj.e1410 [published Online First: 2012/03/01]
239. Devlin JJ, Pomerleau AC, Brent J, et al. Clinical features, testing, and management of patients with suspected prosthetic hip-associated cobalt toxicity: a systematic review of cases. *J Med Toxicol* 2013;9(4):405-15. doi: 10.1007/s13181-013-0320-0 [published Online First: 2013/11/14]
240. Hundley WG, Bluemke D, Bogaert JG, et al. Society for Cardiovascular Magnetic Resonance guidelines for reporting cardiovascular magnetic resonance examinations. *J Cardiovasc Magn Reson* 2009;11:5. doi: 10.1186/1532-429X-11-5 [published Online First: 2009/03/05]
241. Kramer CM, Barkhausen J, Flamm SD, et al. Standardized cardiovascular magnetic resonance (CMR) protocols 2013 update. *J Cardiovasc Magn Reson* 2013;15:91. doi: 10.1186/1532-429X-15-91 [published Online First: 2013/10/10]
242. Quarta G, Sado DM, Moon JC. Cardiomyopathies: focus on cardiovascular magnetic resonance. *Br J Radiol* 2011;84 Spec No 3:S296-305. doi: 10.1259/bjr/67212179 [published Online First: 2012/06/29]

243. Wharton G, Steeds R, Allen J, et al. A minimum dataset for a standard adult transthoracic echocardiogram: a guideline protocol from the British Society of Echocardiography. *Echo Res Pract* 2015;2(1):G9-G24. doi: 10.1530/ERP-14-0079
244. Jaffe AS, Babuin L, Apple FS. Biomarkers in acute cardiac disease: the present and the future. *J Am Coll Cardiol* 2006;48(1):1-11. doi: 10.1016/j.jacc.2006.02.056
245. Cain PA, Ahl R, Hedstrom E, et al. Age and gender specific normal values of left ventricular mass, volume and function for gradient echo magnetic resonance imaging: a cross sectional study. *BMC Med Imaging* 2009;9:2. doi: 10.1186/1471-2342-9-2
246. Hu K, Liu D, Herrmann S, et al. Clinical implication of mitral annular plane systolic excursion for patients with cardiovascular disease. *Eur Heart J Cardiovasc Imaging* 2013;14(3):205-12. doi: 10.1093/ehjci/jes240
247. Schmid E, Hilberath JN, Blumenstock G, et al. Tricuspid annular plane systolic excursion (TAPSE) predicts poor outcome in patients undergoing acute pulmonary embolectomy. *Heart Lung Vessel* 2015;7(2):151-8.
248. Doltra A, Amundsen BH, Gebker R, et al. Emerging concepts for myocardial late gadolinium enhancement MRI. *Curr Cardiol Rev* 2013;9(3):185-90.
249. McCrohon JA, Moon JC, Prasad SK, et al. Differentiation of heart failure related to dilated cardiomyopathy and coronary artery disease using gadolinium-enhanced cardiovascular magnetic resonance. *Circulation* 2003;108(1):54-9. doi: 10.1161/01.CIR.0000078641.19365.4C
250. Kellman P, Wilson JR, Xue H, et al. Extracellular volume fraction mapping in the myocardium, part 1: evaluation of an automated method. *J Cardiovasc Magn Reson* 2012;14:63. doi: 10.1186/1532-429X-14-63
251. Leung DY, Chi C, Allman C, et al. Prognostic implications of left atrial volume index in patients in sinus rhythm. *Am J Cardiol* 2010;105(11):1635-9. doi: 10.1016/j.amjcard.2010.01.027
252. Bombelli M, Facchetti R, Cuspidi C, et al. Prognostic significance of left atrial enlargement in a general population: results of the PAMELA study. *Hypertension* 2014;64(6):1205-11. doi: 10.1161/HYPERTENSIONAHA.114.03975
253. Sakaguchi E, Yamada A, Sugimoto K, et al. Prognostic value of left atrial volume index in patents with first acute myocardial infarction. *Eur J Echocardiogr* 2011;12(6):440-4. doi: 10.1093/ejechocard/jer058
254. Ho CY, Solomon SD. A clinician's guide to tissue Doppler imaging. *Circulation* 2006;113(10):e396-8. doi: 10.1161/CIRCULATIONAHA.105.579268
255. Feigenbaum H, Mastouri R, Sawada S. A practical approach to using strain echocardiography to evaluate the left ventricle. *Circ J* 2012;76(7):1550-5.
256. Cohen J. Statistical power analysis for the behavioural sciences. 2nd edition ed. Hillsdale, NJ: Routledge 1988.
257. Chahal NS, Lim TK, Jain P, et al. Normative reference values for the tissue Doppler imaging parameters of left ventricular function: a population-based study. *Eur J Echocardiogr* 2010;11(1):51-6. doi: 10.1093/ejechocard/jep164
258. Shojaeifard M, Esmaeilzadeh M, Maleki M, et al. Normal reference values of tissue Doppler imaging parameters for right ventricular function in young

adults: a population based study. *Res Cardiovasc Med* 2013;2(4):160-6. doi: 10.5812/cardiovascmed.9843
259. MDA/2017/018 - all metal-on-metal (MoM) hip replacements: updated advice for follow-up of patients. https://www.gov.uk/drug-device-alerts/all-metal-on-metal-mom-hip-replacements-updated-advice-for-follow-up-of-patients (accessed 01/04/2018).
260. Vanhegan IS, Malik AK, Jayakumar P, et al. A financial analysis of revision hip arthroplasty: the economic burden in relation to the national tariff. *The Journal of bone and joint surgery British volume* 2012;94(5):619-23. doi: 10.1302/0301-620X.94B5.27073
261. 14th Annual Report 2017 - National Joint Registry for England, Wales and Northern Ireland 2017 [Available from: http://www.njrcentre.org.uk/ accessed 01/04/2018.
262. Choi HR, Beecher B, Bedair H. Mortality after septic versus aseptic revision total hip arthroplasty: a matched-cohort study. *The Journal of arthroplasty* 2013;28(8 Suppl):56-8. doi: 10.1016/j.arth.2013.02.041
263. Matharu GS, Eskelinen A, Judge A, et al. Revision surgery of metal-on-metal hip arthroplasties for adverse reactions to metal debris. *Acta orthopaedica* 2018:1-11. doi: 10.1080/17453674.2018.1440455
264. Kwon YM, Liow MH, Dimitriou D, et al. What Is the Natural History of "Asymptomatic" Pseudotumours in Metal-on-Metal Hip Arthroplasty? Minimum 4-Year Metal Artifact Reduction Sequence Magnetic Resonance Imaging Longitudinal Study. *The Journal of arthroplasty* 2016;31(9 Suppl):121-6. doi: 10.1016/j.arth.2016.02.070
265. Kesson EM, Allardice GM, George WD, et al. Effects of multidisciplinary team working on breast cancer survival: retrospective, comparative, interventional cohort study of 13 722 women. *Bmj* 2012;344:e2718. doi: 10.1136/bmj.e2718
266. Keurentjes JC, Van Tol FR, Fiocco M, et al. Patient acceptable symptom states after totalhip or knee replacement at mid-term follow-up: Thresholds of the Oxford hip and knee scores. *Bone Joint Res* 2014;3(1):7-13. doi: 10.1302/2046-3758.31.2000141
267. Lennard N, Haque F, Cacou C. Medical Device Alert: ADEPT® 12/14 modular head (Finsbury Orthopaedics Ltd). 2013 12/03/13. http://www.mhra.gov.uk/home/groups/dts-bs/documents/medicaldevicealert/con249629.pdf (accessed 08/09/14).
268. Lennard N, McManus J, Cacou C. Medical Device Alert: MITCH TRH acetabular cups/MITCH TRH modular heads (Finsbury Orthopaedics) when implanted with uncemented Accolade femoral
stems (Stryker Orthopaedics) Medicines and Healthcare Products Regulatory Agency: Medicines and Healthcare Products Regulatory Agency; 2012 [updated 08/09/14. Available from: http://www.codp.org.uk/documents/con149604.pdf accessed 08/09/14 2014.
269. Della Valle CJ, Sporer SM, Jacobs JJ, et al. Preoperative testing for sepsis before revision total knee arthroplasty. *The Journal of arthroplasty* 2007;22(6 Suppl 2):90-3. doi: 10.1016/j.arth.2007.04.013
270. Pfirrmann CW, Notzli HP, Dora C, et al. Abductor tendons and muscles assessed at MR imaging after total hip arthroplasty in asymptomatic and

symptomatic patients. *Radiology* 2005;235(3):969-76. doi: 10.1148/radiol.2353040403 [published Online First: 2005/04/30]
271. Pateder DB, Hungerford MW. Use of fluoroscopically guided intra-articular hip injection in differentiating the pain source in concomitant hip and lumbar spine arthritis. *Am J Orthop (Belle Mead NJ)* 2007;36(11):591-3.
272. Deshmukh AJ, Thakur RR, Goyal A, et al. Accuracy of diagnostic injection in differentiating source of atypical hip pain. *The Journal of arthroplasty* 2010;25(6 Suppl):129-33. doi: 10.1016/j.arth.2010.04.015
273. Tam HH, Bhaludin B, Rahman F, et al. SPECT-CT in total hip arthroplasty. *Clin Radiol* 2014;69(1):82-95. doi: 10.1016/j.crad.2013.08.003
274. Lucas R. Econometric Policy Evaluation: A Critique. (The Phillips Curve and Labor Markets). New York: American Elsevier 1976:19-46.
275. Hale AR, Swuste P. Safety Rules: Procedural freedom or action constraints. *Safety Science* 1998;29(1):163-77.
276. De Ieso PB CJ, Letsa I, Schick U, Nandhabalan M, Frentzas S, Gore ME. A study of the decision outcomes and financial costs of multidisciplinary team meetings (MDMs) in oncology. *British Journal of Cancer* 2013;109(9):2295-300. doi: 10.1038/bjc.2013.586
277. Wagner EH. Effective teamwork and quality of care. *Med Care* 2004;42(11):1037-9.
278. Blazeby JM, Wilson L, Metcalfe C, et al. Analysis of clinical decision-making in multi-disciplinary cancer teams. *Ann Oncol* 2006;17(3):457-60. doi: 10.1093/annonc/mdj102
279. Mickan SM. Evaluating the effectiveness of health care teams. *Aust Health Rev* 2005;29(2):211-7.
280. Campello M, Ziemke G, Hiebert R, et al. Implementation of a multidisciplinary program for active duty personnel seeking care for low back pain in a U.S. Navy Medical Center: a feasibility study. *Mil Med* 2012;177(9):1075-80.
281. Rosati M, Lisanti M, Baluganti A, et al. A multidisciplinary approach and surgical tips in major amputations of diabetic patients. *Musculoskelet Surg* 2012;96(3):191-7. doi: 10.1007/s12306-012-0215-2
282. Bauer S, Bouldouyre MA, Oufella A, et al. Impact of a multidisciplinary staff meeting on the quality of antibiotherapy prescription for bone and joint infections in orthopedic surgery. *Med Mal Infect* 2012;42(12):603-7. doi: 10.1016/j.medmal.2012.09.005
283. Grimer R, Judson I, Peake D, et al. Guidelines for the management of soft tissue sarcomas. *Sarcoma* 2010;2010:506182. doi: 10.1155/2010/506182
284. Gardner FH. The use of cobaltous chloride in the anemia associated with chronic renal disease. *J Lab Clin Med* 1953;41(1):56-64.
285. Hannemann F, Hartmann A, Schmitt J, et al. European multidisciplinary consensus statement on the use and monitoring of metal-on-metal bearings for total hip replacement and hip resurfacing. *Orthop Traumatol Surg Res* 2013;99(3):263-71. doi: 10.1016/j.otsr.2013.01.005 [published Online First: 2013/03/20]
286. Kwon YM, Lombardi AV, Jacobs JJ, et al. Risk stratification algorithm for management of patients with metal-on-metal hip arthroplasty: consensus statement of the American Association of Hip and Knee Surgeons, the

American Academy of Orthopaedic Surgeons, and the Hip Society. *The Journal of bone and joint surgery American volume* 2014;96(1):e4. doi: 10.2106/JBJS.M.00160
287. Gillam MH, Pratt NL, Inacio MC, et al. Heart failure after conventional metal-on-metal hip replacements. *Acta orthopaedica* 2016:1-9. doi: 10.1080/17453674.2016.1246276
288. Alert - TGA advice regarding potential association with heart failure: Therapeutic Goods Administration: Australian Government Department of Health; 2016 [Available from: https://www.tga.gov.au/alert/asr-xl-total-hip-replacements accessed 27/12/2016 2016.

APPENDIX

APPENDIX A

Ethical Considerations

Ethics approval was awarded by the London Westminster National Research Ethics Committee (Reference number: 14/LO/1722, dated 14th October 2014). Continued in Appendix A.

The study sponsor was the Royal National Orthopaedic Hospital NHS Trust, Appendix B. The sponsor and other regulatory bodies ensured adherence to GCP and the NHS Research Governance Framework for Health and Social Care (2nd edition).

The main ethical concerns within this study involved:

- The collection of confidential patient information
- Storage of confidential patient data
- Use of non-ionising imaging (MRI)
- Diagnosis of incidental cardiac / extra cardiac pathology
- Imaging costs will be met by a charity and not the NHS
- Patients inconvenienced by travel costs and time

The data being stored is that collected during routine clinical care, including demographic data, clinical details such as primary diagnosis, surgical procedures and investigations performed and associated results (blood tests

and imaging). Patients were allocated an ID number thus removing any identifiable details and maintaining confidentiality. There were no foreseen legal issues. The data was hosted on a secure NHS server, using protections currently in use within the RNOH Trust. Those with access were required to hold an NHS contract, thus binding them to NHS data protection protocols. Password protected computers were held in an access controlled building.

Magnetic resonance imaging has no proven side effects and is an imaging modality without ionising radiation. All patients prior to CMR scanning complete an MRI specific safety questionnaire, designed to identify patients at risk such as those with sensitive metal implants.

Claustrophobia is a well-recognized condition and the rate of refusing a scan for this reason is less than 1%. There is also a small risk of detecting an undiagnosed abnormality during MRI scanning (estimated at less than 0.1% of cases). If abnormalities were detected, participants were referred to the appropriate medical specialty after discussion with the patient.

A potential benefit from participation includes the early recognition of cardiac toxicity caused by metal ions released from a metal hip replacement, and referral for treatment if required. Since the cardiac MRI / Echocardiogram will be overseen by cardiologists at the Heart hospital, any identified pathology (expected or incidental) will be relayed to the patient with appropriate advice and referred to the patients GP.

Incidental Clinical Findings

An ethical consideration that required particular attention was the potential to make incidental findings when using in depth cross sectional imaging. A protocol detailing how these would be managed was put into place. This depended on the type of incidental finding, with two essential categories.

Incidental cardiac findings: if an incidental finding of a cardiac pathology was identified then the patient would be informed. Subsequently the patient's general practitioner would be informed and a request made for formal referral to the cardiology team at the Heart Hospital in London for review by the senior cardiology team involved in the project. The cadiology team was best placed to offer advice, guidance and ultimately treatment for the patient if this was required.

Non-cardiac findings: Similar proceedings would be undertaken for non-cardiac incidental findings, however in this case it was not possible to treat the patient within the department, and instead the general practitioner would be advised on how to proceed including recommendations for whom to refer the patient.

Written Communications

As part of the ethical considerations and application process, standardised paperwork was prepared and approved by the ethics committee. The purpose of this paperwork was for improved communications with patients and their general practitioners.

These included the following:

- Patient invitation letter (Appendix C)
- Patient information sheet (Appendix D)
- Patient Consent Form (Appendix E)
- General Practitioner Letter (Appendix F)

NHS
Health Research Authority
NRES Committee London - Westminster
Level 3, Block B,
Whitefriars
Lewins Mead
Bristol
BS1 2NT
Telephone: 01173421336

09 October 2014

Prof Alister Hart
Royal National Orthopaedic Hospital
Brockley Hill
Stanmore, Middlesex
HA7 4LP

Dear Prof Hart

Study title:	**Cardiac assessment of patients with Hip Implants**
REC reference:	**14/LO/1722**
Protocol number:	**1**
IRAS project ID:	**157144**

Thank you for your letter of 8 October, responding to the Proportionate Review Sub-Committee's request for changes to the documentation for the above study.

The revised documentation has been reviewed and approved by the sub-committee.

We plan to publish your research summary wording for the above study on the NRES website, together with your contact details, unless you expressly withhold permission to do so. Publication will be no earlier than three months from the date of this favourable opinion letter. Should you wish to provide a substitute contact point, require further information, or wish to withhold permission to publish, please contact the REC Manager Miss Lidia Gonzalez, nrescommittee.london-westminster@nhs.net.

Confirmation of ethical opinion

On behalf of the Committee, I am pleased to confirm a favourable ethical opinion for the above research on the basis described in the application form, protocol and supporting documentation as revised.

Conditions of the favourable opinion

The favourable opinion is subject to the following conditions being met prior to the start of the study.

You should notify the REC in writing once all conditions have been met (except for site

approvals from host organisations) and provide copies of any revised documentation with updated version numbers. The REC will acknowledge receipt and provide a final list of the approved documentation for the study, which can be made available to host organisations to facilitate their permission for the study. Failure to provide the final versions to the REC may cause delay in obtaining permissions.

Management permission or approval must be obtained from each host organisation prior to the start of the study at the site concerned.

Management permission ("R&D approval") should be sought from all NHS organisations involved in the study in accordance with NHS research governance arrangements.

Guidance on applying for NHS permission for research is available in the Integrated Research Application System or at http://www.rdforum.nhs.uk.

Where a NHS organisation's role in the study is limited to identifying and referring potential participants to research sites ("participant identification centre"), guidance should be sought from the R&D office on the information it requires to give permission for this activity.

For non-NHS sites, site management permission should be obtained in accordance with the procedures of the relevant host organisation.

Sponsors are not required to notify the Committee of approvals from host organisations.

Registration of Clinical Trials

All clinical trials (defined as the first four categories on the IRAS filter page) must be registered on a publically accessible database within 6 weeks of recruitment of the first participant (for medical device studies, within the timeline determined by the current registration and publication trees).

There is no requirement to separately notify the REC but you should do so at the earliest opportunity e.g. when submitting an amendment. We will audit the registration details as part of the annual progress reporting process.

To ensure transparency in research, we strongly recommend that all research is registered but for non-clinical trials this is not currently mandatory.

If a sponsor wishes to contest the need for registration they should contact Catherine Blewett (catherineblewett@nhs.net), the HRA does not, however, expect exceptions to be made. Guidance on where to register is provided within IRAS.

It is the responsibility of the sponsor to ensure that all the conditions are complied with before the start of the study or its initiation at a particular site (as applicable).

Ethical review of research sites

The favourable opinion applies to all NHS sites taking part in the study, subject to management permission being obtained from the NHS/HSC R&D office prior to the start of the study (see "Conditions of the favourable opinion" above).

Approved documents

The documents reviewed and approved by the Committee are:

Document	*Version*	*Date*
Covering letter on headed paper [Cover Letter - Response to Provisional Opinion]		03 October 2014
IRAS Checklist XML [Checklist_03102014]		03 October 2014
Other [Revised Participant information sheet (PIS)]	Version 3	30 September 2014
Other [Revised - Participant consent form]	Version 3	30 September 2014
Other [Revised - Letters of invitation to participant]	Version 3	30 September 2014
Other [Revised - GP/consultant information sheets or letters]	Version 3	30 September 2014
REC Application Form [REC_Form_10092014]		10 September 2014
Research protocol or project proposal [Protocol]	2	08 September 2014
Summary CV for Chief Investigator (CI) [CI CV]		

Statement of compliance

The Committee is constituted in accordance with the Governance Arrangements for Research Ethics Committees and complies fully with the Standard Operating Procedures for Research Ethics Committees in the UK.

After ethical review

Reporting requirements

The attached document "After ethical review – guidance for researchers" gives detailed guidance on reporting requirements for studies with a favourable opinion, including:

- Notifying substantial amendments
- Adding new sites and investigators
- Notification of serious breaches of the protocol
- Progress and safety reports
- Notifying the end of the study

The HRA website also provides guidance on these topics, which is updated in the light of changes in reporting requirements or procedures.

Feedback

You are invited to give your view of the service that you have received from the National Research Ethics Service and the application procedure. If you wish to make your views known please use the feedback form available on the HRA website:
http://www.hra.nhs.uk/about-the-hra/governance/quality-assurance

We are pleased to welcome researchers and R & D staff at our NRES committee members' training days – see details at http://www.hra.nhs.uk/hra-training/

14/LO/1722	Please quote this number on all correspondence

With the Committee's best wishes for the success of this project.

Yours sincerely

[redacted]

Chair
Mr Robert Goldstein

Email: nrescommittee.london-westminster@nhs.net

Enclosures: *"After ethical review – guidance for researchers"*

Copy to: *Iva Hauptmannova, Royal National Orthopaedic Hospital R&D Department*

APPENDIX B

Royal National Orthopaedic Hospital NHS
NHS Trust

R&D Office
% UCL-IOMS
RNOH, Brockley Hill
Stanmore HA7 4LP
Tel: 020 8909 5529
Fax: 020 8909 5273
E-mail: [illegible]

NHS R&D Management Approval Letter for Research

To: Alister Hart, John Skinner and Reshid Berber

From: Ufedo Miachi

Date: 12/11/2014

Project Title: Cardiac assessment of patients with Hip Implants

REC Ref: 14/LO/1722

R&D Ref. 14.024

Sponsor: Royal National Orthopaedic Hospital NHS Trust

I am writing on behalf of the Royal National Orthopaedic Hospital NHS Trust Stanmore, to inform you that the above named project has been approved by the Trust and may now proceed.

To maintain this approval, the following conditions must be met:

1. All staff involved in the running of this study must adhere to Trust and Research Governance Framework requirements.

2. As Chief/Principal Investigator you are required to formally advise the R&D Office of **ANY** changes to the project including:
   - Any changes to the status of the project, e.g. abandoned, completed etc
   - Any changes to the protocol – however minor.
   - Any changes to the funding arrangements.

3. The Chief/Principal Investigator is also required to:
   - Notify the R&D, in a timely fashion, any Serious Adverse Events relating to the Research and the appropriate urgent safety measures taken in line with ICH GCP requirements.
   - Ensure that the R&D Office has copies of all annual and final progress reports.
   - Ensure that annual progress report forms are submitted to REC, which has given a favourable opinion.
   - Ensure all researchers involved in the project hold the necessary expertise required and have Honorary Contracts should they need to.
   - Ensure adequate and accurate reporting and monitoring of said project.

- Co-operate with all internal Trust monitoring and auditing procedures.

4. Because it is a statutory requirement to submit annual reports, this approval will automatically lapse if no annual report on this study is received at the R&D office, 14 months from the date of this letter. If you need help on how to prepare your annual report, please contact the R&D Office at the address on this letter.

Yours sincerely,

[redacted]

Research Management and Governance Lead
Research and Innovation Centre

APPENDIX C

PARTICIPANT INVITATION LETTER

STUDY TITLE: CARDIAC ASSESSMENT OF PATIENTS WITH HIP IMPLANTS

Date : <<insert>>

Dear
<<Insert Participant address>>

You are invited to take part in the study because you have a hip implant suitable for the aims of this research.

Recently there has been heightened concern regarding patients with metal hip replacements, which have the potential to release metal (cobalt and chromium) in to the body. We wish to investigate whether this can affect the heart.

Please read the enclosed Patient Information Sheet for full details on this study. You do not have to take part in the study; equally, if you decide to take part, you do have the option to withdraw at any point during the research.

The study will involve an ECG, an ultrasound of the heart (Echocardiogram) and a MRI scan of the Heart.

Chief Investigator:	Prof Alister Hart
Principle Investigator:	Mr Reshid Berber

Please find enclosed a copy of the patient information sheet and consent form for this study.

If you agree to take part we will happily provide you with the results of the study if you request, however we will inform your GP of you participation in this study and of any abnormal results that require attention.

Please sign consent form and return in the stamped addressed envelope if you agree to take part in the study.

Thank you.

Yours Sincerely,

APPENDIX D

Patient Information Sheet

Cardiac Assessment of Patients with Metal Implants Study

Version 3, 30.09.14

We would like to invite you to participate in a study looking into if some people develop heart problems with metal hip implants.

How common are heart problems following metal implants?
There are only a handful of international reports that describe effects on the heart due to the release of metal substances from a hip implant. This is despite an estimated 1.5 million patients who have had a metal on metal hip implanted.

Why did I have a specific type of metal implant?
The type that you had implanted was thought to be the longest lasting at the time of your operation.

Is the type of metal important?
All metal implants release substances from their surfaces. In most cases the amount of material is invisible to the human eye but in some cases the material is responsible for a reaction that may have an impact on the hearts function. To learn whether the heart is affected we need to look in greater detail at the function of the heart in patients with metal hip implants.

What is known from other studies on metal implants?
Other studies have suggested that metal substances released from metal implants can be found throughout the body. One study in particular has suggested that patients with metal hips have a negative yet not apparent impact on the heart. This has not been confirmed in other studies.

Why Me?
You have been invited because you have a hip implant and would be suitable for this research study.

How can I help the research?
There are two possible reasons why we have contacted you:

1) You have a metal hip implant and your blood test suggests you have raised metal levels in your circulation, and we would like to analyse your heart. Alternatively you have a metal hip implant but your blood metal levels are not raised, and you have been asked to participate as part of a comparison group.
To do this we would like to have a heart specialist ask you questions about your medical history, examine you, and undertake a series of specialist tests to look at your heart in detail.

2) You have a different (ceramic) hip implant, and you have been asked to participate as part of a comparison group.

What tests will we conduct?
We will conduct various tests, which will help our understanding of whether your heart has been affected by your hip implant. We will look at previous blood samples that you have had taken in the clinic. A cardiologist (heart doctor) will then review you to undertake a series of tests including an electric tracing of your heart (ECG), an Ultrasound scan and an MRI scan of your heart.

An ECG is a simple test to record information about your heartbeat and the rhythm of your heart by measuring the electrical signals that cause your heart to beat. During the test, a number of wires are connected to your arms, legs and chest by sticky pads and these pick up the electrical signals. This takes up to 5 minutes.

An ultrasound (Echocardiogram) uses sound waves to build up a detailed picture of your heart. It is similar to the ultrasound scan used in pregnancy, which involves a probe and some lubricating jelly placed on your chest, and can take up to 20 minutes.

A cardiac MRI scan is a non-invasive test that uses an MRI machine to create magnetic and radio waves to create clear pictures showing the inside of your heart. An MRI scan does not use radiation, and can take up to 30 minutes. You lie on a bed, which then moves inside a tunnel-shaped scanner. The scanner is open at both ends.

Where will the tests be undertaken?
You will be asked to attend the Heart Hospital in London, where all the tests will be carried out in a single visit. The Heart Hospital can be found at the following address: 16-18 Westmoreland St, London W1G 8PH

How do I get to the Heart Hospital?
By bus:
Portland Place - no's 88, C2
Marylebone Road - no's 18, 27, 30
Oxford Street (Bond Street Station) - no's 7, 8, 10, 25, 55, 73, 98, 176
By Tube:
Bond Street (Central / Jubilee Lines)
Regents Park (Bakerloo Line)
Baker Street (Bakerloo / Circle / Hammersmith & City / Jubilee / Metropolitan Lines)
Please note:
Ramp access is available
Very limited on-street car parking available
National Rail Enquiries: 08457 48 49 50
London Travel Information: 020 7222 1234

Will my travel costs be reimbursed?
Yes we can help with this, please ask a member of the team about this, and keep a copy of your receipts. We will provide up to £50 towards your travel and parking costs.

What are the Risks and Benefits of Taking Part?
The risk of taking part is low, and involves sitting through an MRI scan. The benefit of this research is that the results you provide will further the understanding of whether the heart is affected by the metal substances released by hip implants.

Will my records be kept confidential?
We adhere to the rules of the ethics committee, which insists on compliance with national guidelines for "Good Clinical Practice" and includes confidential storage of records under the Data Protection Act.

Will my GP be told about my participation in this study?
Yes we will inform them that you are taking part in this study, if there are any findings that require attention we will refer you to your GP for further management. Although we do not expect to find anything of concern.

What will happen if I do not take part in this study?
Participation in this study is your choice. If you should decide not to participate then please be reassured that this will not affect your usual care.

What will happen to any samples I give?

The tests we will perform are related to metal levels within your blood and also related to heart and kidney function. You would have already had these tests performed in your usual clinic. No samples will be stored for future use. Only the research team will have access to the results of these tests.

What will happen to the results of the research study?
Your individual results from the heart tests will be analysed and stored. Once the study has been completed the group results will be analysed and the findings of this research will be published in medical journals and presented at medical conferences. You will not be identified in any report/publication. If requested, we will happily provide you with the results of your investigations.

Who is organising and funding the research?
The research is being conducted at the Royal National Orthopaedic Hospital in collaboration with The Heart Hospital, University College London.

Who has reviewed the study?
All research in the NHS is looked at by an independent group of people, called a Research Ethics Committee, to protect your interests. This study has been reviewed and given favourable opinion by Westminster, London Research Ethics Committee.

Who should I approach if I am unhappy with the study?
Patient Advice and Liaison Service via pals@rnoh.nhs.uk or 020 8

Who do I contact for general information about research?
You can contact the R&D office via research@rnoh.nhs.uk or 0208.

Who do I contact for specific information about this research project?
Please do not hesitate to contact us if you have any further questions. If you are happy about the information provided and to participate in this study, please sign the consent form and return it to your surgeon.

Study Chief Investigator: Professor Alister Hart
Study Principle Investigator: Mr Reshid Berber

APPENDIX E

Patient Identification Number for this trial: 0xx-CMR-xx

CONSENT FORM

Title of Project:

Cardiac Assessment of Patients with hip Implants

Please initial

1. I confirm that I have read and understand the information sheet dated 30/09/14 for the above study and have had the opportunity to ask questions.

2. I understand that my participation is voluntary and that I am free to withdraw at any time, without giving any reason, without my medical care or legal rights being affected.

3. I understand that sections of any of my medical notes may be looked at by responsible individuals working in the medical field or from regulatory authorities where it is relevant to my taking part in research. I give permission for these individuals to have access to my records.

4. I agree to take part in the above study.

5. I consent to my GP being informed of my participation within this study.

6. I consent to my results from the investigations undertaken as part of this study being forwarded to my GP.

_____	_____	_____
Name of Study participant	Date	Signature
_____	_____	_____
Name of person taking consent Signature	Date	Signature

1 for patient; 1 for research site file; 1 (original) to be kept in medical notes

APPENDIX F

GP LETTER

STUDY TITLE: CARDIAC ASSESSMENT OF PATIENTS WITH HIP IMPLANTS

Date : <<insert>>

Dear Dr
<<Insert GP address>>

Your patient, _____(date of birth:), has consented to take part in the above study.

They were invited to take part in the study because they have a hip implant suitable for the aims of this research.

No study has attempted to identify cobalt deposition within cardiac tissue using cardiac MRI. We therefore aim to detect cobalt deposition in the cardiac tissue of patients with metal hip implants and markedly raised cobalt blood ion levels. If detected, we aim to assess whether this had any clinical effect on cardiac function. Your patient may have been invited as part of the metal hip implant group or as part of a control group. Your patient has the option to withdraw at any point during the research. The study will involve an ECG, an Echocardiogram and a cardiac MRI.

Chief Investigator: Prof Alister Hart
Principle Investigator: Mr Reshid Berber

Please find enclosed a copy of the patient information sheet for this study.

We will happily provide an update of the patients progress on request, however you will be contacted regardless in the instance that a concerning finding is seen on the patients imaging.

Kind regards,

Resources and Costs

The resources required to conduct this research are centred around the specialist cardiac investigations. These include use of the Cardiac MRI facilities at the Heart Hospital (UCL) with radiographer support, and Echocardiography facilities with technician support required to perform ECHOcardiograms at the Heart Hospital (UCL). In addition blood testing facilities (including venesection equipment and blood testing bottles) are required at both the Heart Hospital (full blood count) and the Royal National Orthopaedic Hospital (cobalt and chromium tests).

The cost of conducting the research was calculated as follows:

- Cost of CMR including radiographer support (extra hours) and ECHO technician at the Heart Hospital (£200 per participant): £18,000
- Out of hours support (heart hospital staff time): £2,745
- Blood testing (Full Blood Count - £6.00 per test, Cobalt and chromium - £25 per test): £2,790
- Patient travel cost to the Heart Hospital (as this is not their usual clinic, they are entitled to claim their travel cost to the Heart Hospital): £1,030
- Study sponsorship (required under the Research Governance Framework): £1,500

A successful application was made for a research grant, kindly awarded by the Orthopaedic Trust Research Charity – Gwen Fish Trust. The grant of £11,000 was matched by a charitable donation from the Heart Hospital. In addition to this the RNOH Hospital Charity awarded a further donation of £4,500 in order to offer compensation to participants for their travel costs to the Heart Hospital and for the blood sampling costs. Total funding granted by the above organizations was £26,500, and adequately covered the estimated costs of the study. With respect to this, care was taken to act resourcefully to limit waste and reduce additional costs.